A Comprehensive Soil Characteristics Study and Finite Element Modeling of Soil-Structure Behavior in Tuzla Area

Danial Lakayan

Submitted to the
Institute of Graduate Studies and Research
in partial fulfillment of the requirements for the Degree of

Master of Science
in
Civil Engineering

Eastern Mediterranean University
June 2012
Gazimağusa, North Cyprus

Approval of the Institute of Graduate Studies and Research

Prof. Dr. Elvan Yılmaz
Director

I certify that this thesis satisfies the requirements as a thesis for the degree of Master of Science in Civil Engineering.

Asst. Prof. Dr. Mürude Çelikağ
Chair, Department of Civil Engineering

We certify that we have read this thesis and that in our opinion it is fully adequate in scope and quality as a thesis for the degree of Master of Science in Civil Engineering.

Asst. Prof. Dr. Huriye Bilsel
Supervisor

Examining Committee

1. Assoc. Prof. Dr. Zalihe Sezai

2. Asst. Prof. Dr. Huriye Bilsel

3. Asst. Prof. Dr. Mehmet Metin Kunt

ABSTRACT

Determination of soil characteristics is important for the design of foundations. The magnitude of settlement, bearing capacity, heave and various other engineering behaviors should be experimentally determined or initially predicted from models, before the design of structures. In order to assess the available in situ and experimental data and to model soil-structure interaction for local soils, Tuzla is chosen as the study area, which is the most disputable area in North Cyprus, regarding the soil formations and soil-structure interactions.

The study consists of four phases: collection of all the available in situ and laboratory data and deriving soil profiles for each parcel in the area; using well known correlations to predict engineering parameters; finite element modeling of the soil-structure interaction and establishing a mathematical model for settlement. A database of the engineering parameters of soils in Tuzla area is formed based on 43 boreholes, and in situ and laboratory experimental data available. Borelogs were plotted and the soil profiles for each parcel of the Tuzla area, and water table profile for the entire area were obtained using RockWare. The SPT-N values were used to correlate with the engineering parameters, including the shear strength parameters and the bearing capacity using the methods available in NovoSPT. The bearing capacity was determined from the available correlations in the software as well as manually using well known methods, such as Burland and Burbidge (1985) and Bowels and Meyerhof (1976) correlations.

In the soil-structure interaction part of the thesis, square mat foundations were modeled in different sizes, and placed at varying depths in the soil profile for the worst borehole location of BH-24 in Parcel No. XXIV 50 W2 Finite element method is implemented by

PLAXIS 2D for the axis-symmetric case and using Mohr-Coulomb criterion. Elastic settlements and consolidation settlements at different time intervals, up to 50 years were studied. It was concluded that the bearing capacity should only be found in relation to consolidation settlement in the region.

In the final phase, an exponential relationship is proposed for the prediction of total settlements for this specific location based on bearing capacity, foundation size, depth, and time. To generalize this relationship for the whole area, further research is required using all the borehole data and the profiles of the other parcels in the region.

Keywords: SPT correlations, Bearing capacity, Settlement, Soil-structure interaction.

ÖZ

Zemin karakteristiğinin ve davranışının önceden tesbiti temel tasarımı için önemlidir. Zeminlerin yapılar altında olabilecek oturma miktarı, taşıma gücü, şişme ve diğer mühendislik özellikleri laboratuvarda çalışılmalı veya modeller kullanılarak binaların tasarımından önce ön tesbit yapılmalıdır. Bu araştırmanın ilk aşamasında Jeoloji ve Maden Dairesi, ve Doğu Akdeniz Üniversitesi'nde Geoteknik Ana Bilim Dalında tamamlanmış tez çalışmalarından elde edilen sondaj datasından ve zemin parametrelerinden Tuzla bölgesi için bir veri tabanı oluşturulmuştur. Bu veri tabanı 43 sondaj logunun GPS koordinatları, zemin katmanlarının sınıflandırılması, bölgenin topoğrafik haritası, ve yeraltı su seviyesi derinliklerini içermektedir. Bölgede bulunan 13 parselin zemin profilleri RockWare yazılımı kullanılarak elde edilmiştir. SPT sonuçları kullanılarak, NovoSPT yazılımındaki empirik yaklaşımlarla zemin parametreleri elde edilmiştir. Bu parametreler ve sondaj loglarından en kötü sonuçların bulunduğu parsel için farklı boyutlarda radye temelin davranışı zamana bağlı olarak PLAXIS yazılımı kullanılarak modellenmiştir.

Çalışma dört aşamada yapılmıştır: Birinci aşama data toplanması ve sondaj loglarının ve zemin profillerinin elde edilmesini içerir. Ayrıca yeraltı su seviyesi profili de bu aşamada belirlenmiştir. İkinci aşama NovoSPT yazılımından zemin parametrelerinin elde edilmesini içerir. 43 sondaj lokasyonu için tüm korelasyon sonuçları ve Jeoloji ve Maden Dairesi'nden elde edilen laboratuvar deney sonuçları toparlanmış ve istatistiki bir çalışma ile deneysel sonuçlarla korelasyonlardan elde edilenler karşılaştırılmıştır. Çalışmanın üçüncü aşaması elde edilen verilerle en kötü sondaj lokasyonunda kare radye temelin zemin-yapı etkileşiminin bir sonlu elemanlar yazılımı olan PLAXIS'le modellenmesini içerir. Sonlu elemanlar yöntemi ile farklı radye boyutları, temel derinlikleri için elastik ve

zamana bağlı konsolidasyon oturmaları çalışılmış ve oturmaya bağlı zemin emniyet gerilmesi değerleri literatürde bulunan bazı analitik yöntemlerle karşılaştırılmıştır. Bu yöntemler arasında sonlu elemanlardan elde edilen sonuçlara en yakın değerleri Burland and Burbidge (1985)'in verdiği tesbit edilmiştir.

Tezin son aşamasında ise MATLAB yazılımı kullanılarak toplam oturma için taşıma gücü, temel boyutu, derinliği ve zamana bağlı olan bir eksponansiyel denklem elde edilmiştir. Bu denklem sadece bir lokasyon için elde edildiğinden, tüm bölge zeminleri için genelleme yapılamaz. Bu çalışmanın devamı olarak, daha kapsamlı bir araştırma programında irdelenecektir.

Anahtar Kelimeler: Zemin karakteristiği, SPT, Sonlu elemanlar yöntemi, Oturmalar

To

my parents,

family

and friends

ACKNOWLEDGEMENTS

I would like to express my deep appreciation to my supervisor Asst. Prof. Dr. Huriye Bilsel for her inspiration and guidance throughout this work. This thesis would not have been possible without her support. I would also like to thank the examining committee members, Assoc. Prof. Dr. Zalihe Sezai and Asst. Prof. Dr. Mehmet Metin Kunt for taking time to review my thesis.

I want to express my sincerest gratitude to my family for their support, unending love and patience during my study.

I would also like to thanks to other staff members of the Department of Civil Engineering for their help.

I would like to express my gratitude to the Department of Geology and Mining, Ministry of Interior, North Cyprus for giving us permission to use the data of their soil investigation survey in Tuzla, and to Mr. Yıldız Gövsa for his technical support in the geodetic part of my thesis.

Finally, I would like to give my heartfelt thanks to my always comrade Tamanna for her support and understanding during my study.

TABLE OF CONTENTS

LIST OF TABLES

LIST OF FIGURES

LIST OF SYMBOLS

Symbol	Meaning
Latin symbols	
N	SPT below count
BH-1	Boreholes Number
XXIV 41 E2	Parcel Number
2D	Two dimentional
3D	Three dimentional
SPT	Standard penetration test
FEM	Finite element method
C_N	Over burden pressure
C_E	Energy ratio factor
C_B	Borehole diameter factor
C_R	Rod length factor
C_S	Sampling method factor
E_S	Young modulus
S_u	Undrained shear strength
V_s	Shear wave velocity
G	Shear modulus
q	Bearing capacity
q_{all}	allowable bearing capacity
q_u	ultimate bearing capacity
FS	factor of safety
N_c,N_q,N_γ	Bearing capacity factors
F_{cs}, F_{qs}, $F_{\gamma s}$	shape factors
F_{cd}, F_{qd}, $F_{\gamma d}$	Depth factors
c	Cohesion
B	Width of foundation
L	Lenght of foundation
D_f	Depth of foundation

Symbol	Meaning
k	Permeability
t	Time
Pa	Atmospheric pressure (100 kN/m^2)
S_T	Tolerable settlement
e	Void ratio
N1(60)	Corrected Nvalue
PI	Placticity index
Greec symbols	
φ	Friction angle
γ	Soil unit weight
γ_d	Dry soil unit weight
γ_s	Saturated unit weight
γ_w	Water unit weight
ψ	Dilatancy angle
ν	Piossan ratio
σ_v	Total vertical stress
β	Angular distortion
ω	Water content
Unified soil classification system symbols	
GW	Well-graded gravels; gravel–sandmixtures (few or no fines).
GP	Poorly graded gravels; gravel–sand mixtures (few or no fines).
GM	Silty gravels; gravel–sand–silt mixtures.
GC	Clayey gravels; gravel–sand–clay mixtures.
SW	Well-graded sands;gravelly sands (few or no fines).
SP	Poorly graded sands; gravelly sands (few or no fines).
SM	Silty sands; sand–silt mixtures.
SC	Clayey sands; sand–clay mixtures.
ML	Inorganic silts; very fine sands; rock flour; silty or clayey fine sands.
CL	Inorganic clays (low to medium plasticity); gravelly clays; sandy clays; silty clays; lean clays.
OL	Organic silts; organic silty clays (low plasticity)

Symbol	Meaning
CH	Inorganic clays (high plasticity); fat clays
MH	Inorganic silts; micaceous or diatomaceous fine sandy or silt
Others	
LS	Lime stone
SS	Sand stone

Chapter 1

INTRODUCTION

Cyprus, is the third largest island in the Mediterranean Sea, with a surface area of 9251 km^2. Based on the geological evolution and emplacement, Cyprus includes six different zones which are: Troodos or the Troodos Ophiolite, North Cyprus (Kyrenia), Mamonia Zone or Mamonia Complex, South Cyprus, Mesaoria, Alluviums, (Atalar & Kilic, 2006). Tuzla, the study area in this thesis, is a region located in the east of Northern Cyprus.

This research consist of a comprehensive soil data management, correlations and modeling soil-structure interaction. The study is divided in to four phases as explained in the following sections.

1.1 Geologic Information of the Region

The geological properties of the region are simulated by Rockware based on soil properties of 43 boreholes. This software is specialized in obtaining soil stratification, estimating geological structure of an area, and defining ground water table levels as well as the topography of surfaces.

In the first phase of this study, the sub soil stratification of Tuzla region was obtained based on the borehole characteristics and their coordinates. The approximate soil profile for each parcel in Tuzla area was obtained together with the ground water table profile for the whole area.

1.2 Correlations Based on SPT Data by NovoSPT

NovoSPT is applied in order to correlate the soil properties by using standard penetration test blow count value. This software includes 270 various correlations which are

extracted in different years. In the performed SPT tests energy level, borehole diameter, sampling method and overburden corrections are based on 60%, 65-115 mm, standard sampler and Canadian Foundation Engineering Manual formula, respectively.

In this section soil data of 43 boreholes are gathered and correlations with some engineering properties are studied based on the following criteria:

1- The degree of popularity of the formulae,
2- The year of publication of the formulae,
3- Based on the prevailing soil types in the region.
4- The degree of closeness of the extracted data to the available laboratory data reported by the Department of Geology and Mining, and data from previous research in the subject area (Erhan, 2009).

After comparing the extracted bearing capacity results from NovoSPT, and the N values of each borehole with the other boreholes, borehole 24 was selected as the worst location in the region for studying soil-structure interaction.

1.3 Finite Element Models by PLAXIS

PLAXIS is a software created based on finite element method. This powerful program is applicable to calculate the physical characteristics of the soil such as settlement.

In this study the mat foundations of dimensions 10, 14, 18, 22 and 26 m were selected under pressures ranging from 10 kPa to the level of failure. Finite element model chosen in PLAXIS is the axis-symmetric model, since the shape of mat foundations are assumed square in shape. The finite element mesh consist of triangular element of 15 nodes. Settlements under different conditions are investigated, based on the above assumptions.

1.4 Curve and Surface Fitting by Matlab

Matlab is strong multi-purpose software with various applicable toolboxes provided for different fields of science. Two useful tool boxes of this huge program are utilized which are for curve and surface fitting. To do this part of research, the extracted data from PLAXIS are imported into these tool boxes and the data are modeled both in two and three dimensions. The numerical model obtained models the settlement behavior of the Specific location chosen.

Chapter 2

LOCATION AND SOIL DISTRIBUTION OF STUDY AREA

2.1 Introduction

Cyprus is the third largest island in the Mediterranean Sea, with a surface area of 9251 km^2. The general geographical status of Cyprus is shown in Figures 2.1 and the Google earth map is given in Figure 2.2.

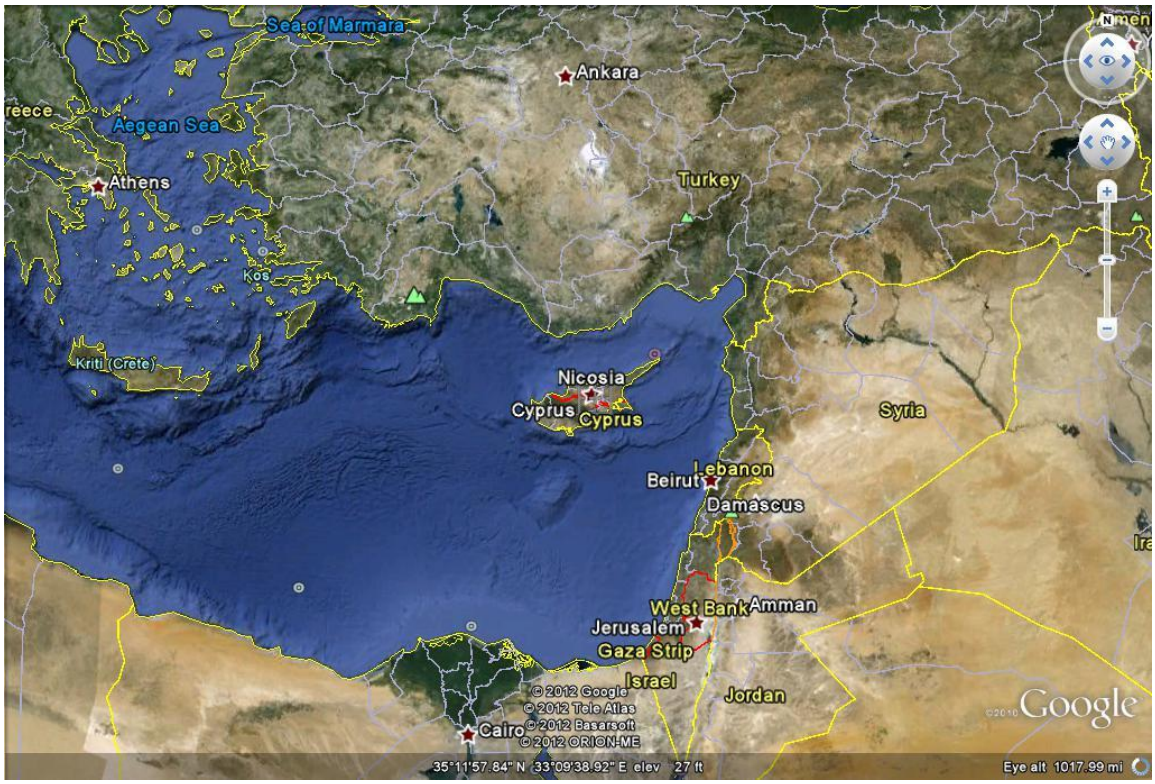

Figure 2.1. The general geographic status of Cyprus (Google earth images of Cyprus, 35 11 57.84" N 33 09 38.92" E, 27 ft)

Figure 2.2. Island of Cyprus (Google earth images of Cyprus, 35 06 53.80" N 33 29 57.93" E, 327 ft)

In general, based on the geological evolution and emplacement, Cyprus consists of six geological zones which are shown in Figure 2.3.

These zones are:

a) Troodos Zone or the Troodos Ophiolite

Troodos ophilite was formed in the upper cretaceous geologic time by the subduction of the African plate beneath the Eurasian plate.

Troodos Ophiolite is comprised of plutonic, intrusive and volcanic rocks, and covers Troodos range in the southern central part of the island (Atalar & Kilic, 2006).

b) North Cyprus (Kyrenia) Zone

Kyrenia zone may be divided into two subzones. The first subzone is composed of autochthonous sedimentary rocks of Upper Cretaceous to Middle Miocene. The Kythrea group is within this zone The second subzone is composed of allochthonous

massive and recrystallized lime stones, dolomites and marbles of Permian-Carboniferous to Lower Cretaceous age which have been thrust southward to their present position in the Miocene (Atalar & Kilic, 2006).

c) Mamonia Zone or Mamonia Complex

"The allochthonous Mamonia Zone or Mamonia Complex comprises of igneous-volcanic, sedimentary and metamorphic rocks of Middle Triassic to Upper Cretaceous age. During the Maastrichtian the movement to Cyprus took place. It only appears near Paphos in the south west part of South Cyprus (Atalar & Kilic, 2006).

d) South Cyprus Zone

"In the south of Cyprus, sedimentary rocks ranging in age from Upper Cretaceous to Miocene, are extensively exposed in an area extending between the south of the Troodos Ophiolite and the south coast from Larnaka in the east to Paphos in the west and less extensively in the north of Troodos Ophiolite. This zone is composed of mostly chalks, clays, marls and gypsum. Bentonitic Clays, Lefkara, Pakhna and Kalavasos formations are within this zone (Atalar & Kilic, 2006).

e) Mesaoria Zone

"The Mesaoria Zone is located between the Kyrenia and Troodos ranges and consists of rocks of deep and shallow marine environment of marl, sandy marl, calcarenites and terraces belonging to Pliocene and Pleistocene ages. They outcrop at the Mesaoria plane, southern slopes of the Kyrenia range and are spreading towards the Troodos mountains. Nicosia and Athalassa formations are within this zone.", (Atalar & Kilic, 2006).

f) Alluviums

The alluviums Holocene to recent in age containing gravel, sand, silt, and clay are widespread in the Mesaoria plain, especially at Nicosia and Famagusta and at the east and west coasts as well as the stream beds all over the island (Atalar & Kilic, 2006).

The most part soils of Cyprus are composed of alluvium and clays. The characteristics of this soil are low bearing capacity and low to extremely high swelling potential, (Atalar & Kilic, 2006). Tuzla, the study area, is a region located in the east of northern Cyprus. The prevailing soils in the region are alluvial deposits underlain by soft rocks. The alluvial soils have been usually conveyed by river flow and accumulated in the region (Papadopoulos et al., 2010).

In order to evaluate the soil properties of Tuzla, various laboratory and field investigations were carried out. Field investigations included standard penetration tests (SPT).

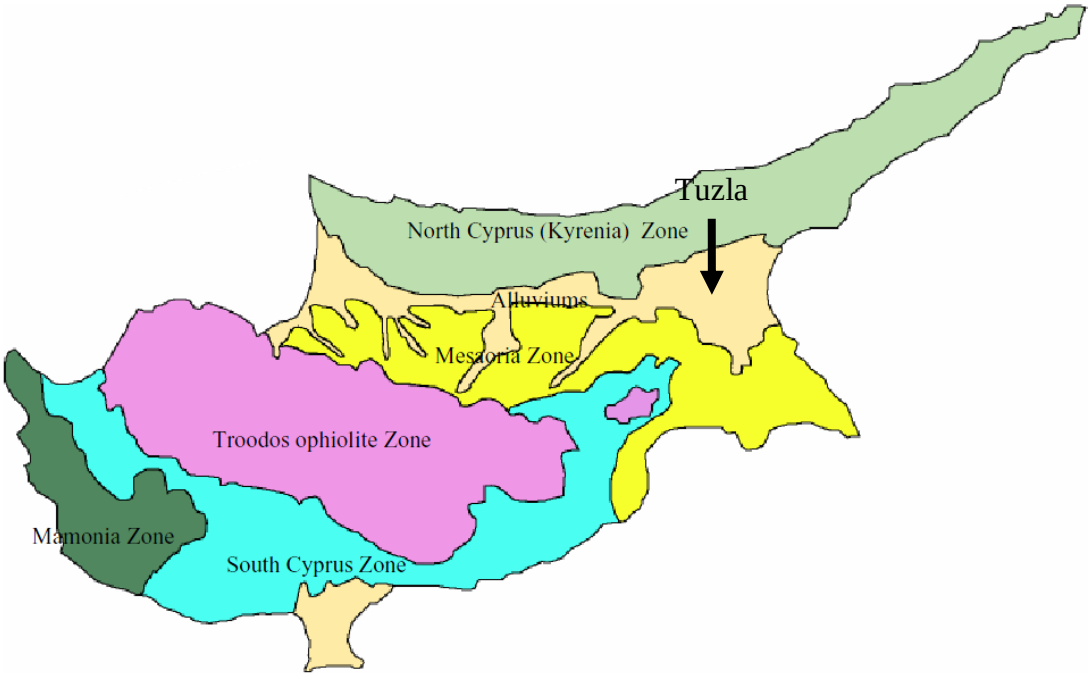

Figure 2.3. Geological zones of Cyprus (Atalar & Kilic, 2006).

2.2 Boreholes Locations in Tuzla Region

A total of 43 boreholes were drilled in the region; disturbed and undisturbed samples were recovered. The borehole locations in WGS84 (World Geodetic System dating from 1984 and last revised in 2004) coordinate system are shown in Figure 2.4 and the

coordinates of these locations are presented in Table 2.1. The depths of boreholes vary between 10 to 25 m.

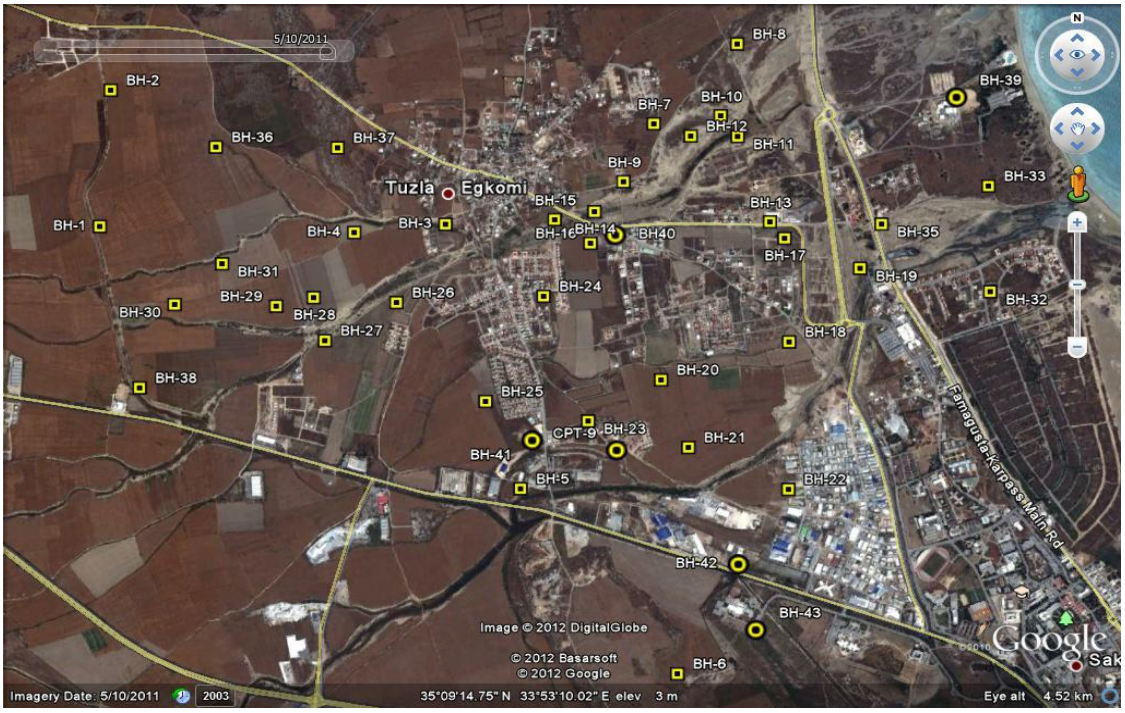

Figure 2.4. Borehole locations in the area of study (Google earth image of Tuzla, 35 0914.75" N 33 53 10.02", 3m)

In this system earth surface is divided into plots, also called parcels. In the current study the soil profile of the area have been characterized for each parcel. There are a few boreholes in each parcel as depicted in Figure 2.5 and the list of the boreholes are given in Table 2.2.

Figure 2.5 is created based on the fact that the original information published by the Department of Geology and Mining is in ED50 (European Datum 1950) coordinate system. In order to interchange this coordinate system to WGS84, one can use the formulae bellow (Gövsa, 2011):

WGS84=ED50-178.64 for x direction,

WGS84= ED50-27.56 for y direction.

Table 2.1. Coordinates of borehole locations in WGS84 coordinate system (Erhan 2009; Necdet et al. 2007)

Site location	Borehole	Coordinates		Borehole	Coordinate	
		N	E		N	E
Tuzla	BH-1	3891121.36	578544.44	BH-23	3890176.36	580827.44
	BH-2	3891798.36	578588.44	BH-24	3890793.36	580614.44
	BH-3	3891146.36	580154.44	BH-25	3890269.36	580348.44
	BH-4	3891101.36	579730.44	BH-26	3890756.36	579929.44
	BH-5	3889837.36	580515.44	BH-27	3890564.36	579597.44
	BH-6	3888927.36	581253.44	BH-28	3890777.36	579543.44
	BH-7	3891654.36	581120.44	BH-29	3890733.36	579369.44
	BH-8	3892054.36	581505.44	BH-30	3890737.36	578896.44
	BH-9	3891365.36	580981.44	BH-31	3890941.36	579115.44
	BH-10	3891697.36	581431.44	BH-32	3890835.36	582695.44
	BH-11	3891595.36	581511.44	BH-33	3891359.36	582682.44
	BH-12	3891595.36	581292.44	BH-34	3891355.36	582699.44
	BH-13	3891163.08	582189.22	BH-35	3891166.36	582186.44
	BH-14	3891215.36	580847.44	BH-36	3891520.36	579081.44
	BH-15	3891174.36	580662.44	BH-37	3891520.36	579649.44
	BH-16	3891058.36	580830.44	BH-38	3890322.36	578737.44
	BH-17	3891091.36	581734.44	BH-39	3891800.62	582533.15
	BH-18	3890577.36	581760.44	BH-40	3891102.32	580947.856
	BH-19	3890945.36	582087.44	BH-41	3890079.88	580569.613
	BH-20	3890383.36	581165.44	BH-42	3889473.53	581535.481
	BH-21	3890049.36	581295.44	BH-43	3889149.12	581619.577
	BH-22	3889845.36	581763.44			

Moreover, to draw the points in Google Earth and interchange the coordinates WGS84 to longitude and latitude system the software PHOTOMOD GeoCalculator is applied. Based on the given data in this software, Cyprus is located in UTM (Universal Transverse Mercator Geographic) zone 36N.

Table 2.2. The boreholes existing in each parcel (Necdet et al., 2007; Erhan, 2009)

No	Parcel No.	Borehole No.
1	XXIV 41 E2	BH-2
2	XXIV 42 E2	BH-8,BH-10
3	XXIV 43 W2	BH-34,BH-39
4	XXIV 51 W1	BH-33,BH35,BH-19
5	XXIV 50 E1	BH-7,BH-12,BH-11,BH-9,BH-14,BH-40,BH-13,BH-17
6	XXIV 50 W1	BH-16,BH-15,BH-3,BH-37,BH-4
7	XXIV 49 E1	BH-1,BH-36,BH-31
8	XXIV 49 E2	BH-38,BH-30,BH-29,BH-28,BH-27
9	XXIV 50 W2	BH-26,BH-24,BH-25,BH-23
10	XXIV 50 E2	BH-20,BH-18
11	XXIV 51 W2	BH-32
12	XXIV 53 W1	BH-41,BH-5
13	XXIV 58 E1	BH-21,BH-22,BH-42
14	XXIV 58 E2	BH-6,BH-43

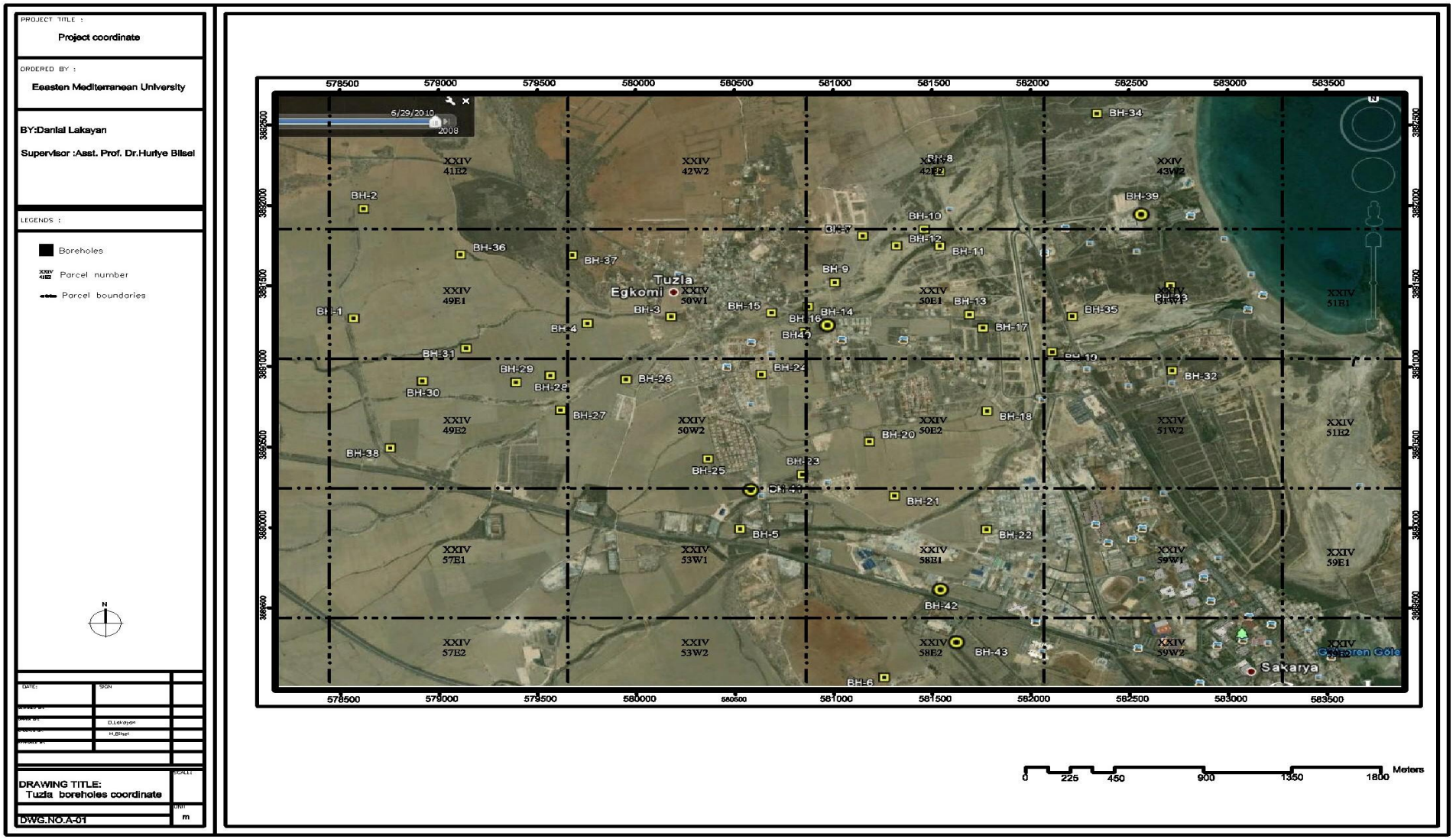

Figure 2.5. The boreholes existing in each parcel (Necdet et al. 2007; Erhan 2009)

2.2 Borelogs Information

In this investigation the borelog information used was obtained from the Department of Geology and Mining and is shown in Appendix A. The borelogs included information on soil types, depth of ground water level and the SPT depths and numbers as well as average water content at each depth.

2.3 Topography

The topography of the region is important in the design of structures. In the present study the maps estimated by Rockwork are based on borehole data. As can be seen in Figure 2.6 and 2.7, the study area is approximately flat and 0 to 12 m above sea level. The highest point of the region is located in the northwest and the lowest is placed in the eastern region close to the sea.

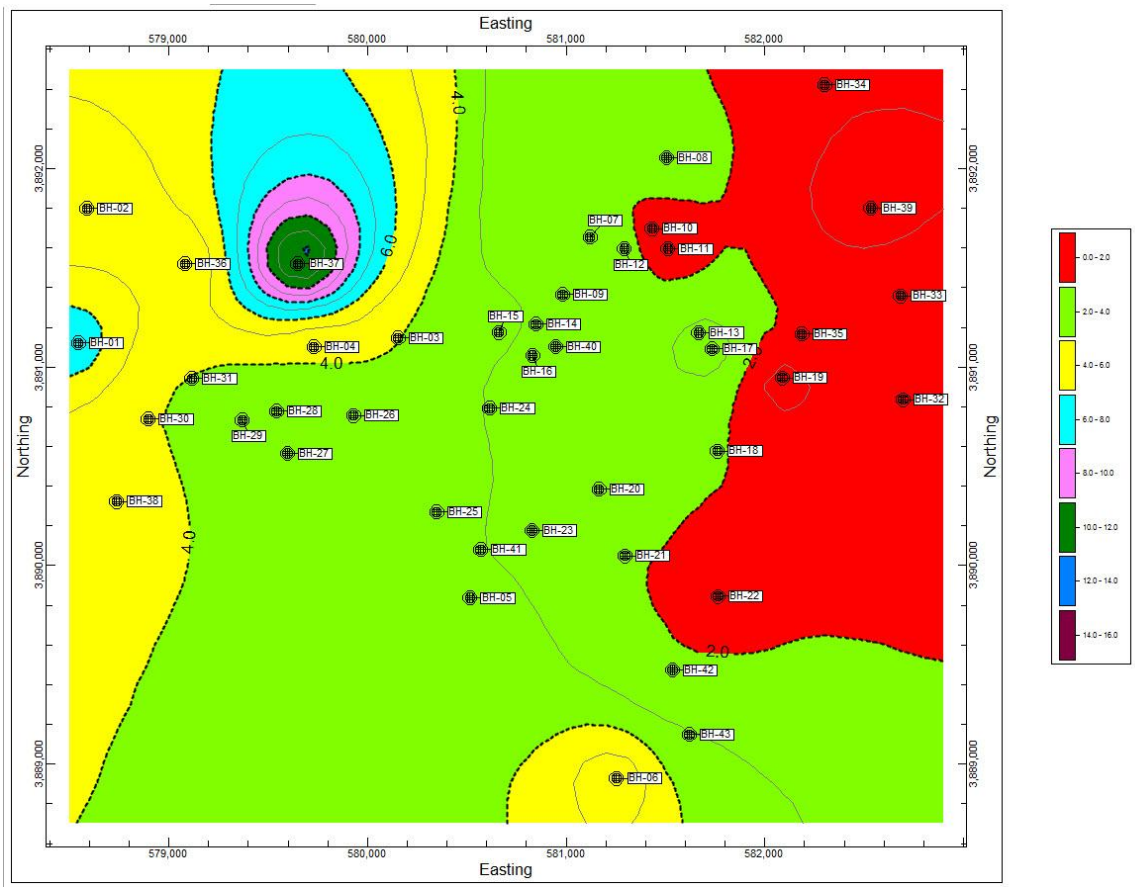

Figure 2.6. Topography map of study area (2D)

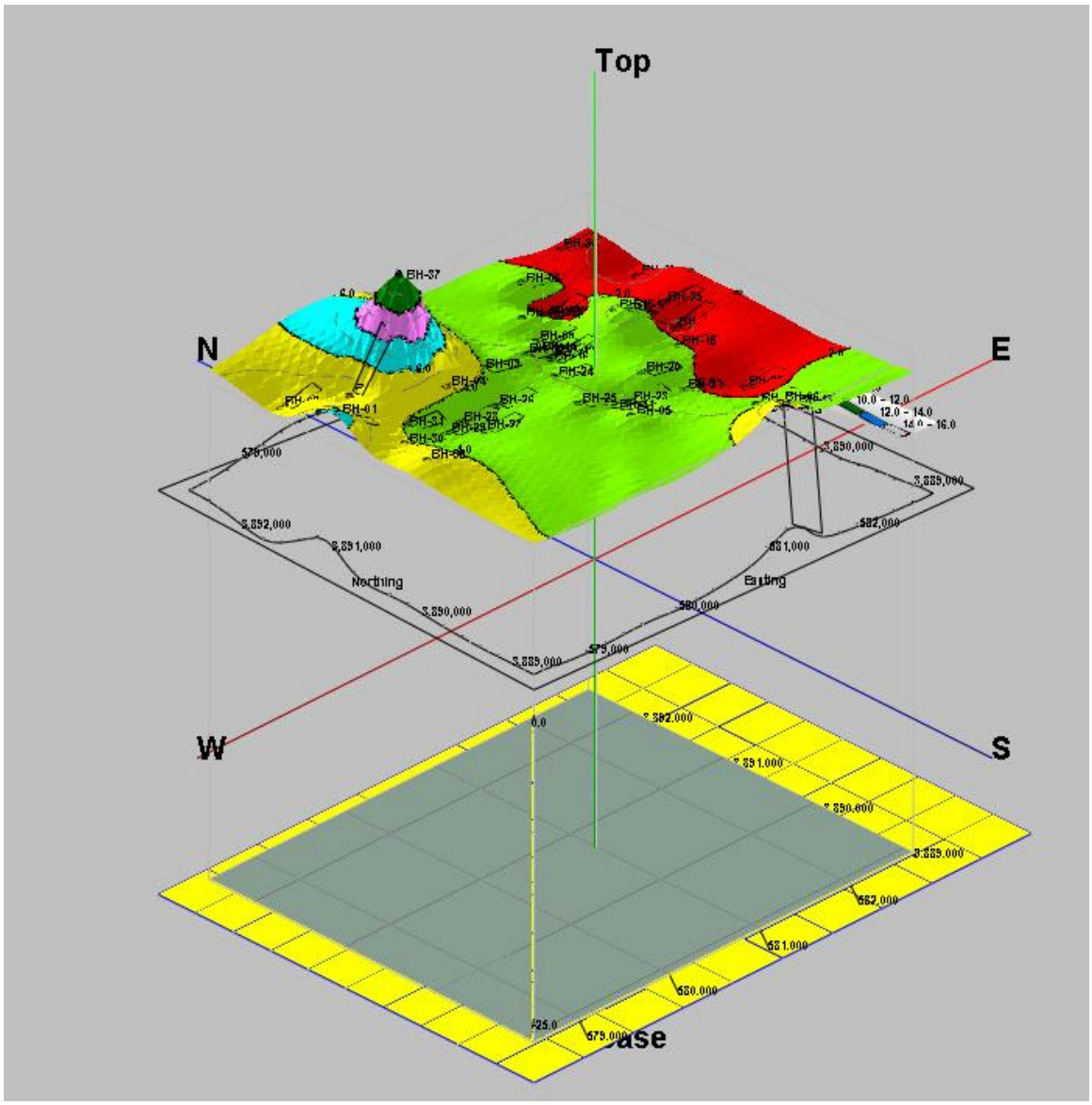

Figure 2.7. Topography map of study area (3D)

2.4 Variation of Water Table Depth

One of the important characteristics in the study of soil behavior and structural design is water table level. It can affect the SPT blow count, and hence the bearing capacity which can be calculated using one of the formulae suggested in literature (Bowles 1996; Das 2011; Budhu 2008). The position of water level can also influence the settlement which has direct relationship with the bearing capacity.

Figure 2.8 indicates that the shape of aquifer and the ground surface are the same. The only difference between them is the elevations.

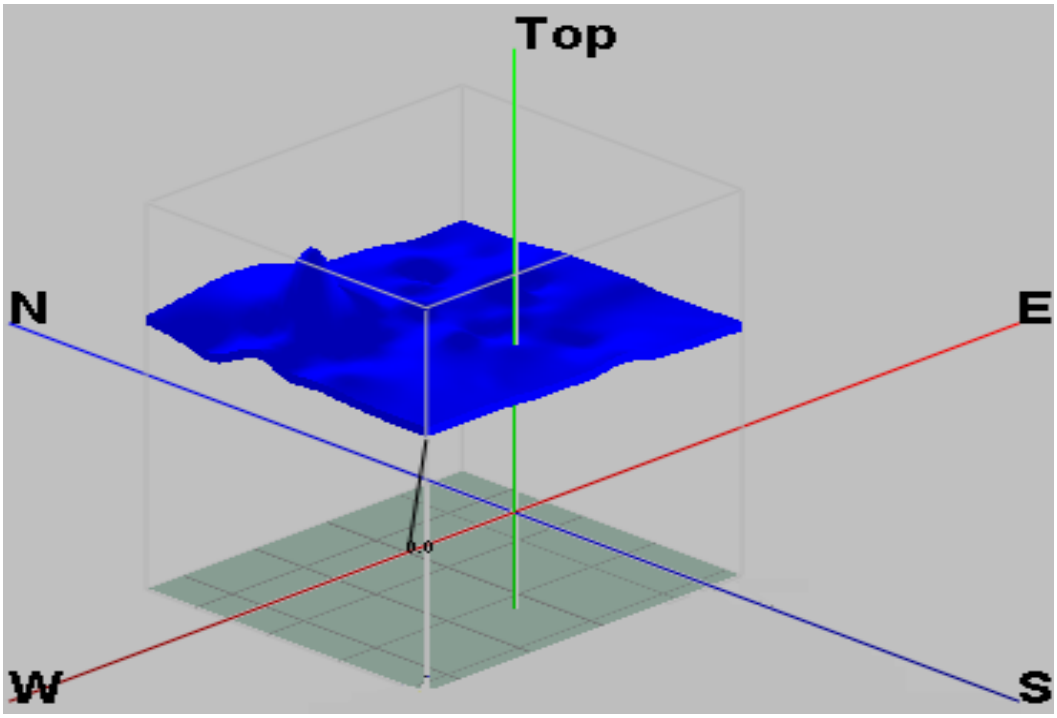

Figure 2.8.Aquifer model of study area

As can be seen in Figure 2.9, water table depth decreases in the region closer to the sea, varying from -0.84 to 10 m elevation above sea level.

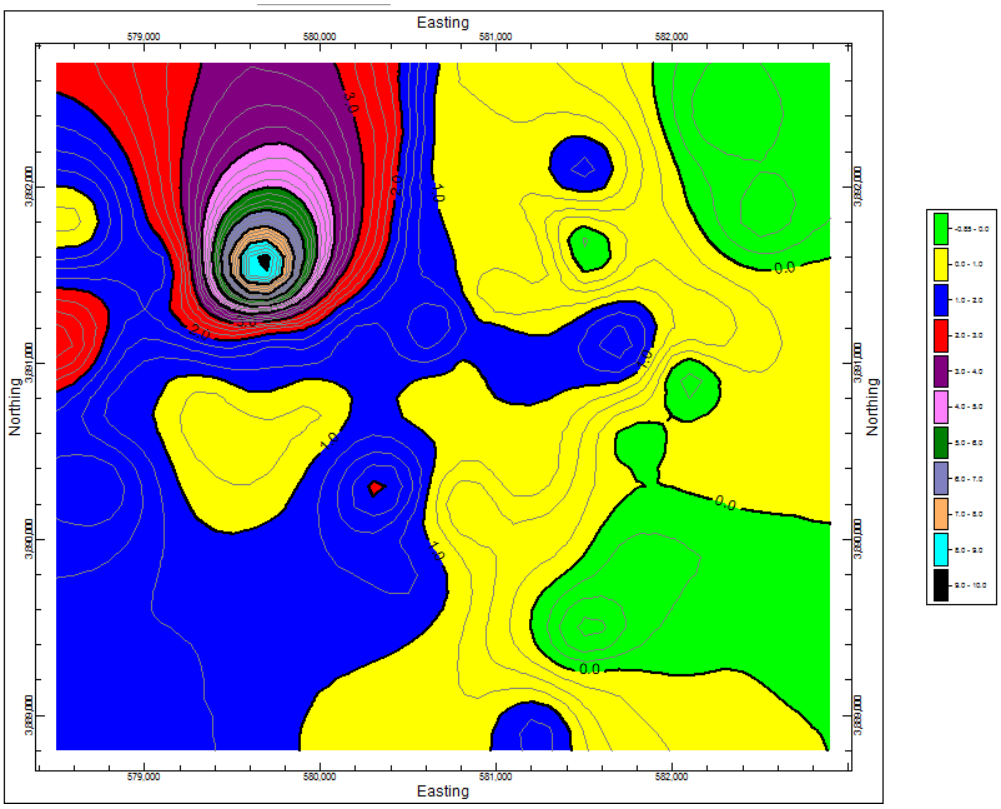

Figure 2.9.Water table level variation of study area (2D)

Figure 2.10 shows that the water table level varies proportionally with the ground surface elevation.

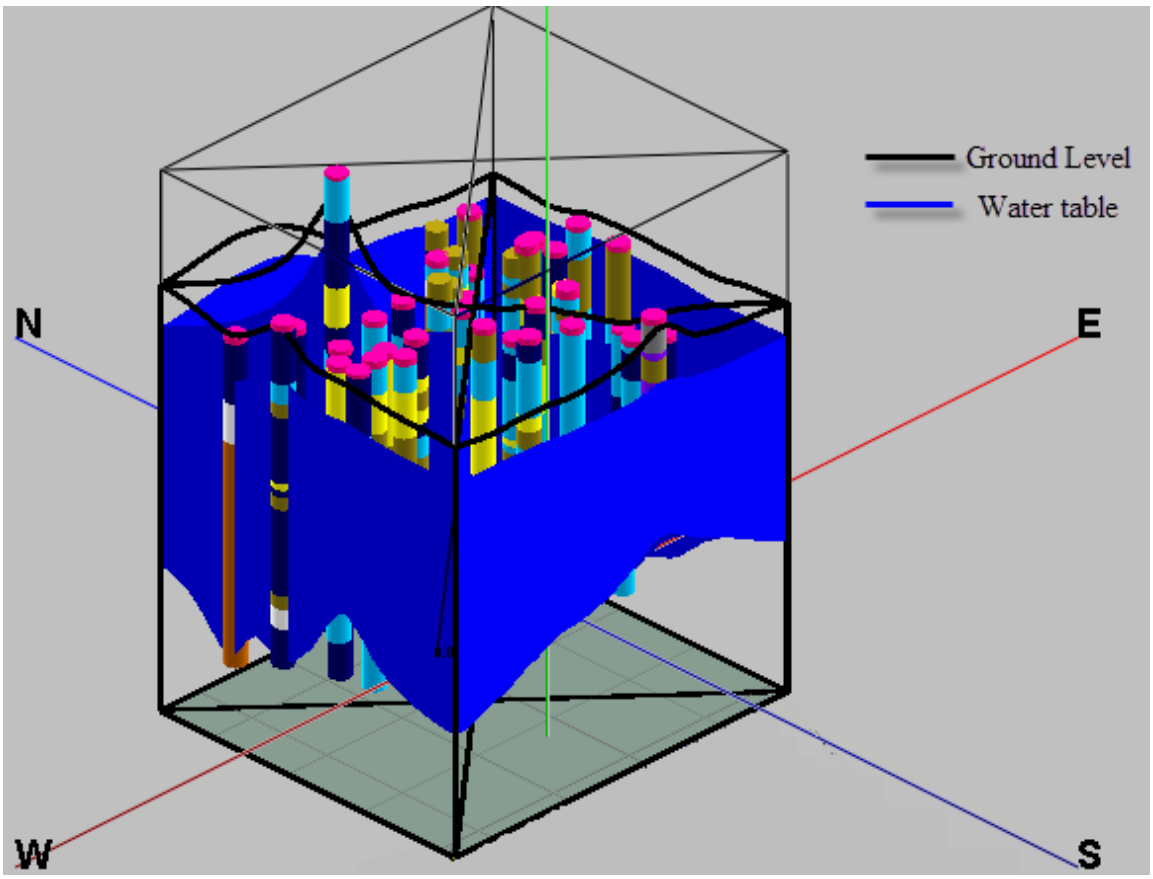

Figure 2.10. Comparison between water level and ground level

2.5 Soil Distribution

From the engineering viewpoint, characterization of soils and area lithology are important, since all civil engineering designs are dependent on the behavior of soil materials. This significance is because most structures and their materials are directly related to soils. Therefore, the accurate study of soils can basically affect the quality of the design, safety and the cost of the projects.

In Tuzla area, soil stratification varies from one parcel to another. A general view of the area is illustrated in Figure 2.11which shows the heterogeneity of the subsoils.

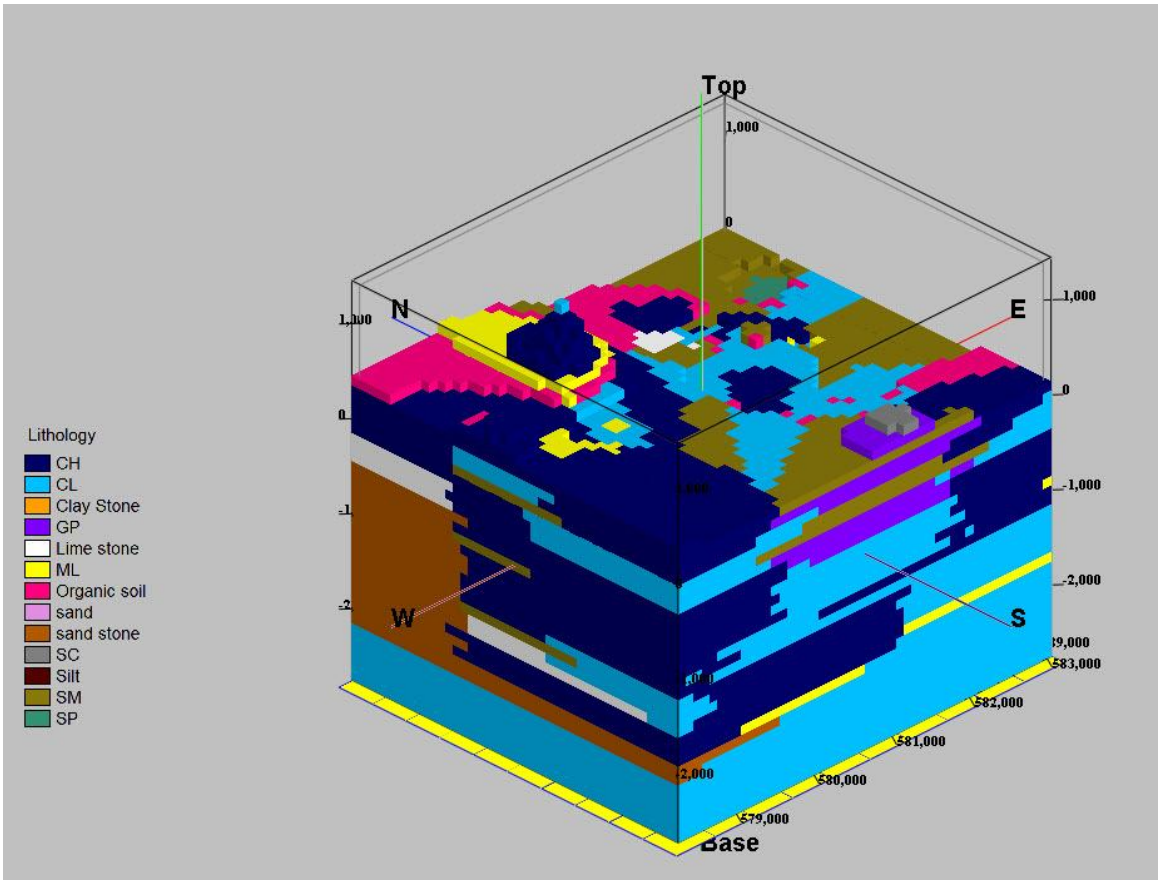

Figure 2.11.Lithology model of Tuzla

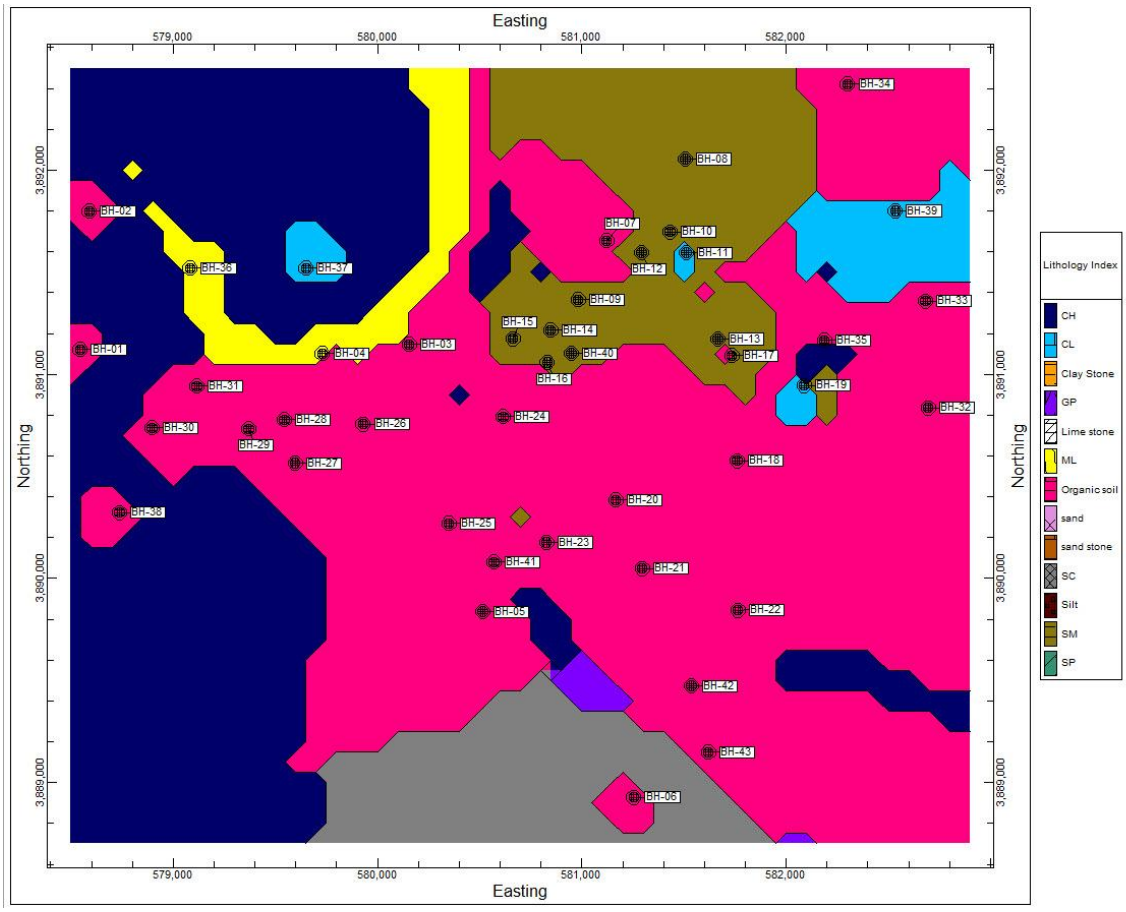

Figure 2.12.The composition of the surface soils (2D)

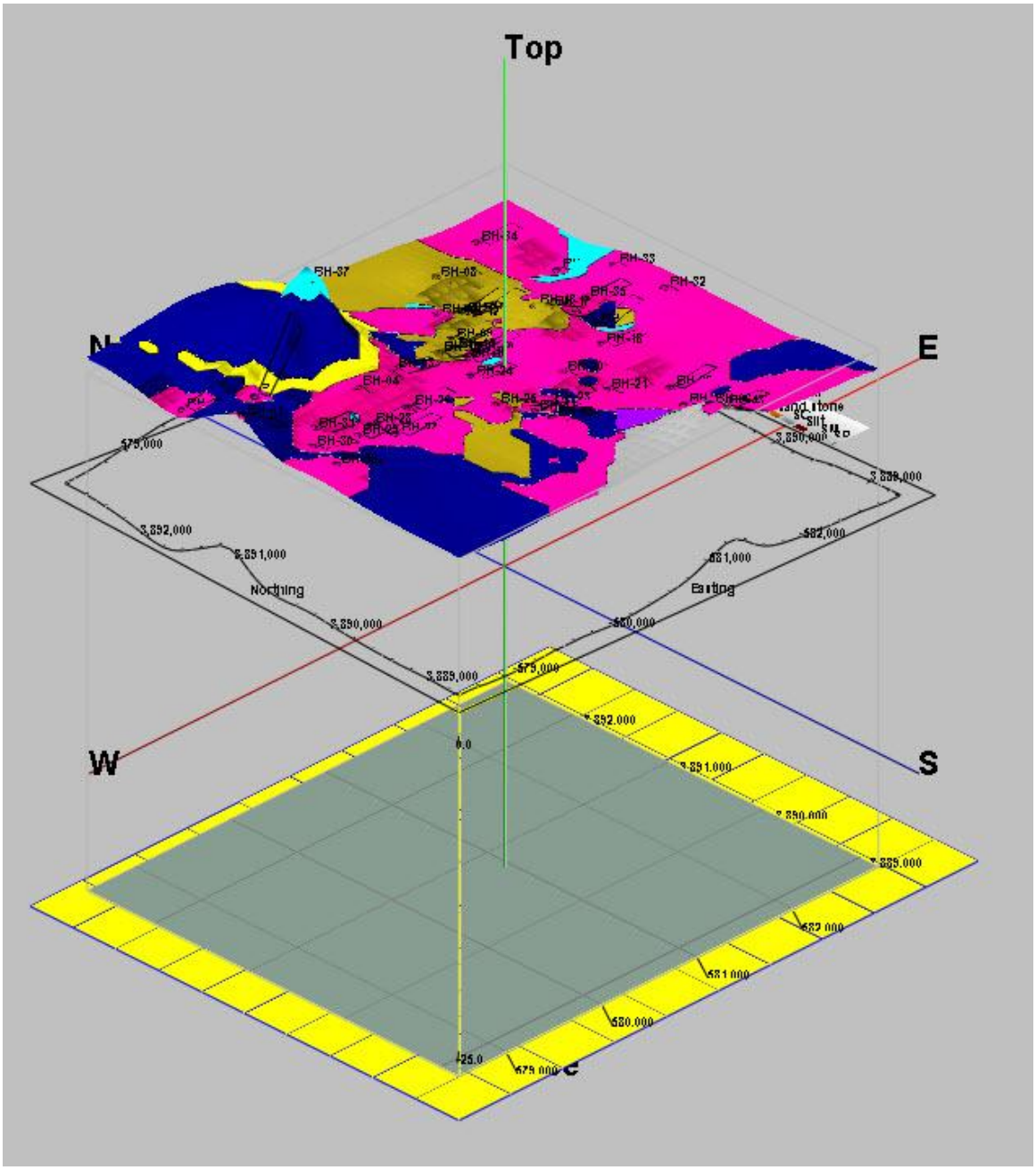

Figure 2.13.The composition surface soils (3D)

Figures 2.12 and 2.13 show that the surface soils are mainly fine soils and sands, deposited as alluvial soils in the delta of the River Pedia. It is also noted that some parts of the surface area are covered by organic soils which are very poor soils for civil engineering applications.

2.6 Soil Profiles

In this study soil profiles are obtained based on existing field data. The profiles for each parcel are given in the Appendix C and Figure 2.14 shows the soil profile between BH-23 and BH-24 for parcel number of XXIV 50 W2. There are very large differences in the soil types within short distances, which may cause differential settlement problems.

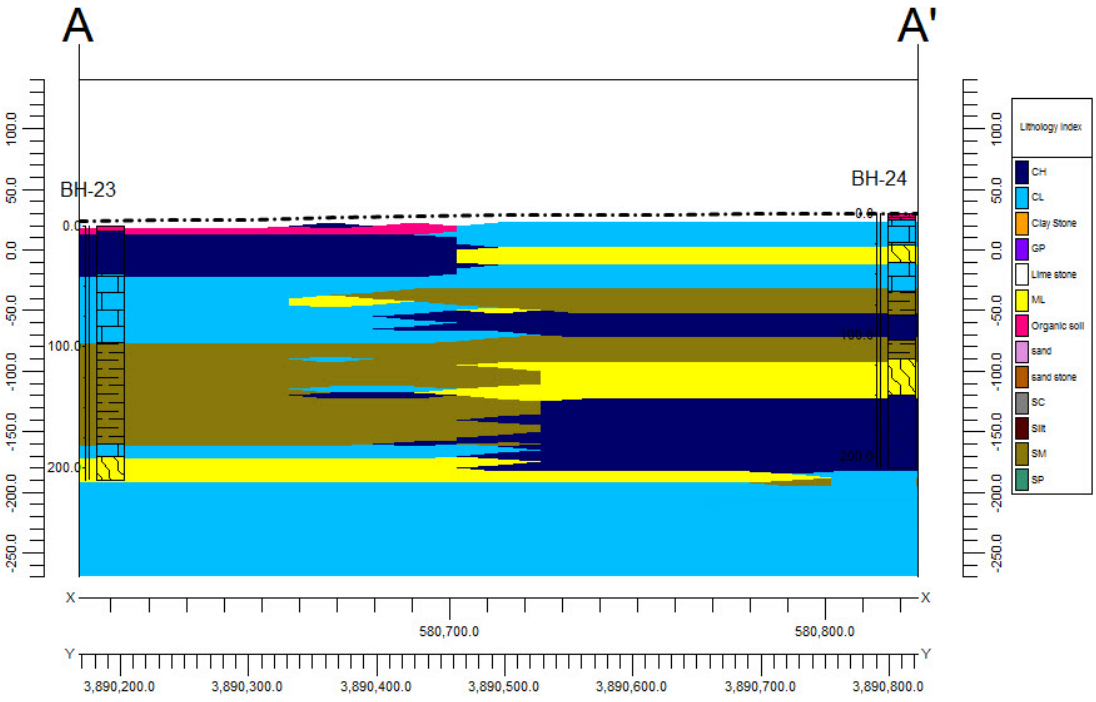

Figure 2.14. The profile of XXIV 50 W2 parcel between boreholes 23 and 24.

Chapter 3

LITERATURE REVIEW

3.1Introduction

Soil characterization and behavior are the most important parameters in the design of foundations. Therefore the site investigation and characterization are essential using one of the various methods appropriate for a specific project.

The Standard penetration test (SPT) is one of the most frequently used in situ methods for defining subsurface materials, the data of which can be used for modeling the soil behavior by finite element method (FEM) in a numerical study. This research is based on the SPT data provided by the Department of Geology and Mining, Nicosia.

3.2 Standard Penetration Test

SPT was first used by an American company in 1902, which was later modified and improved in 1927. Then Peck et al. (1953) introduced a correlation table related to number of blows, consistency for silt and clay, and relative density for sand, as shown in Table 3.1. Although nowadays it is covered by ASTM D1586 and many other various standards, such as IRTP (International Reference Test Procedure), it was not standardized till 1958 in USA. It is worth stressing that later Karol (1960) approximated the value of cohesion and friction angle corresponding to the type of soil and the number of blows, however, at that time over burden correction was not defined as it is presented in Table 3.2 (Bowles, 1996; Coduto, 2001; Budhu, 2008; Rogers, 2006).

Table 3.1. Relative density and consistency correlations based on SPT-N (Peck et al., 1953)

Relative Density Sands and Gravels	Blows (N SPT)	Consistency Silts and Clays	Strength (kPa)	Blows (N SPT)
Very loose	0–4	Very soft	0–25	0–2
Loose	4-10	Soft	25–50	2-4
Medium	10-30	Firm	50–100	4-8
Dense	30-50	Stiff	100-200	8-16
		Very Stiff	200-400	16-32
Very dense	over50			
		Hard	Over 400	Over 32

In this test a standard 5 cm outside diameter thick walled sampler is driven into ground by using a 63.5 kg hammer which is able to fall through 76 cm. The SPT N-value is calculated as the number of blows needed in order to reach a penetration of 45 cm. This value will be counted after a primary seating drive of 15 cm. The process of counting has three stages. In the first stage the number of blows is counted to a penetration depth of 15 cm, next is counted until 30 cm penetration is achieved and finally to 45 cm. At the end the SPT N-value is computed as the summation of the two latter mentioned values (Robertson., 2006).

Table 3.2. Correlations of cohesion and friction angle based on SPT-N (Karol, 1960)

Soil Type	SPT Blow Counts	Undisturbed Soil	
		Cohesion (kPa)	Friction angle (º)
Cohesive soils			
Very Soft	<2	12	0
Soft	2-4	12-24	0
Firm	4-8	24-48	0
Stiff	8-15	48-96	0
Very Stiff	15-30	96-192	0
Hard	>30	192	0
Cohesion less soils			
Loose	<10	0	28
Medium	10-30	0	28-30
Dense	>30	0	32
Intermediate soils			
Loose	<10	5	8
Medium	10-30	5-48	8-12
Dense	>30	48	12

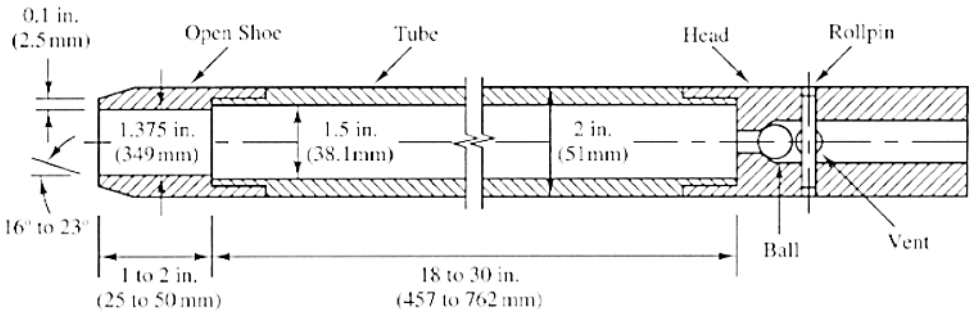

Figure 3.1. SPT thick walled sampler (Coduto, 2001)

The ASTM split-barrel sampler is illustrated in Figure 3.1. The most commonly used hammers are shown in Figure 3.2. Although none of them are 100 percent efficient, the statistics show that they have been used frequently and more than other available types. For instance US hammer (Figure 3.2. b) is used approximately 60 percent and the other two types around 20 percent. Hammer (Figure 3.2. c) is applied mostly outside of the US (Bowles, 1996; Robertson., 2006; Coduto, 2001).

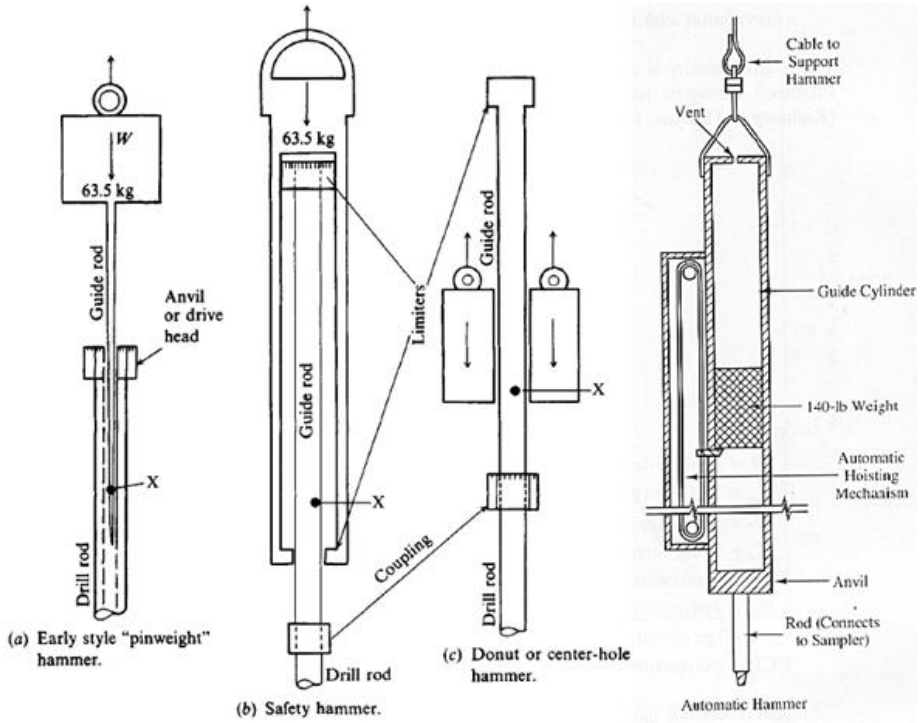

Figure 3.2. Types of hammers for SPT test, (Coduto, 2001)

3.2.1 N Value Corrections

The SPT N number is standardized by applying correction factor to account for the effect of energy delivered, overburden stress, and ground conditions. The most applicable method is the standardized SPT corrections method, which includes different factors given in the following sections (Robertson, 2006).

3.2.1.1 Overburden Pressure Factor C_N

The over burden pressure or vertical stress is weight of upper layer of soil per unit area. Therefore the effect of this overburden must be included in the SPT N value. This factor is very important because it can change penetration resistance. Gibbs and Holtz (1957), Peck and Bazaraa (1967), Peck, Hanson and Thornburn (1974), seed et al. (1975), Tokimatsu and Yoshimi (1983), Liao and Whitman (1986), Skempton (1986), Samson et al. (1986) and Canadian Foundation Engineering manual (2006) have explained overburden pressure correction for different types of soils. Figure 3.3 shows the overburden pressure factor curves from various sources.

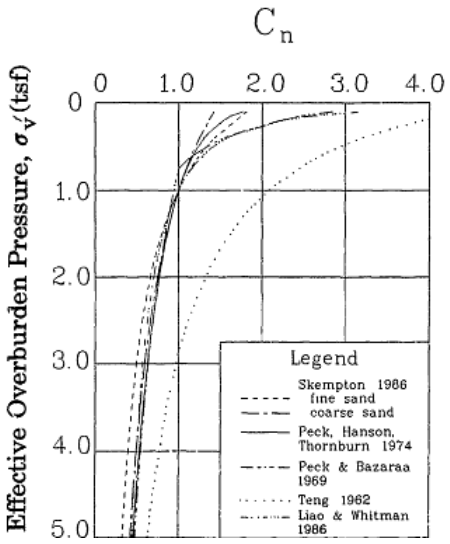

Figure 3.3. Overburden pressure factor curve (Knowles, 1991)

Table 3.3 consists of a summary of the formulae related to the discussion above.

Table 3.3. Empirical formulae of overburden correction factor (Das 2011; Budhu 2008; Takimatsu & Yoshimi 1983; Atkinson 2003; Canadian Geotechnical Society 2006)

Reference	Equation for Depth Factor C_N	Comment	Unit of б′
Gibbs and Holtz (1957)	$\frac{\text{Corrected N value}}{\text{Measured N value}}$	See Figure 3.4	-----
Peck and Bazaraa (1967)	$\frac{4}{1+4\left(\frac{б'}{p_a}\right)}$	$\frac{б'}{p_a} \leq 0.75$	kPa& ksf
	$\frac{4}{3.25+\left(\frac{б'}{p_a}\right)}$	$\frac{б'}{p_a} > 0.75$	kPa& ksf
Peck, Hanson and Thornburn (1974)	$0.77\log_{10}\left(\frac{1916}{б'}\right)$	$C_N \leq 2$	>24kPa
	$0.77\log_{10}\left(\frac{40}{б'}\right)$	$C_N \leq 2$	>0.5ksf
Seed et al.(1975)	$1-1.25\log_{10}\left(\frac{б'}{p_a}\right)$	-----	kPa& ksf
Tokimatsu and Yoshimi (1983)	$\frac{1.7}{б'+0.7}$	-----	kgf/cm^2
Liao and Whitman (1986)	$\left(\frac{95.8}{б'}\right)^{\frac{1}{2}}$	$C_N \leq 2$	kPa
	$\left(\frac{2000}{б'}\right)^{\frac{1}{2}}$	$C_N \leq 2$	psf

Table3.3. (Continued)

Reference	Equation for Depth Factor C_N	Comment	Unit of б′
Skempton (1986)	$\frac{2}{1+\frac{б'}{p_a}}$	For normally consolidated fine sand	psf
	$\frac{2}{1+\frac{б'}{p_a}}$	For normally consolidated coarse sand	psf
	$\frac{2}{1+\frac{б'}{p_a}}$	For over consolidated sand	psf
Canadian Foundation Engineering manual (2006)	$0.77\log_{10}\left(\frac{1920}{б'}\right)$ See Figure 3.5	$б' \leq 0.25\ tsf$ $(24\ kPa)$	kPa & ksf
		$\partial' > 0.25tsf$ $(24kPa)$	kPa

$$\text{Correction factor} = \frac{\text{corrected N value}}{\text{measured N value}}$$

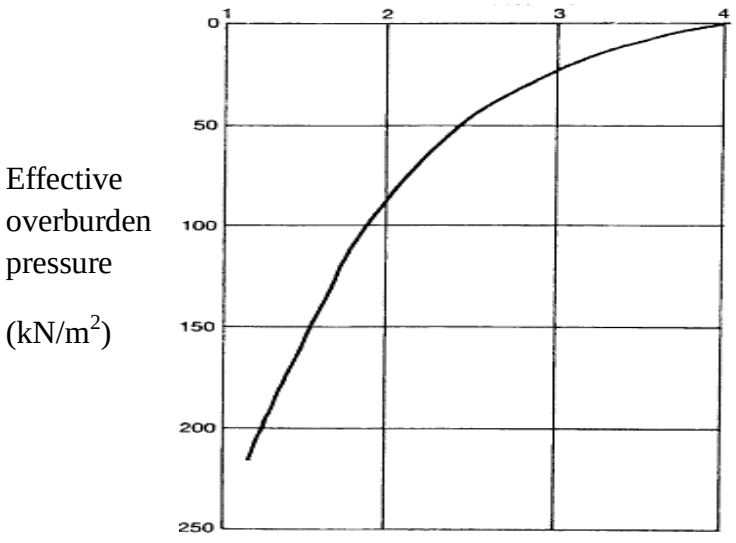

Figure 3.4. Gibbs and Holtz (1957) overburden correction factor (Atkinson, 2003)

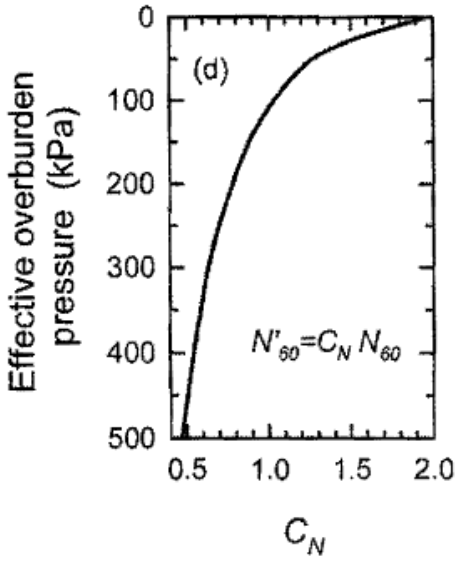

Figure 3.5. Depth factor chart for ϭ′>24 kPa (Canadian Geotechnical Society, 2006)

3.2.1.2 Energy Ratio Factor C_E

In recent researches the amount of calculated hammer energy efficiency has been indicated by E_r (%), the output energy given to the rod in the SPT ranging from 30 % to 90% and can be defined as

$$E_r\,(\%) = \frac{\text{actual energy to the sampler}}{\text{input energy}} \times 100 \qquad (3.1)$$

Theoretical input energy= W× h ≈ 0.474kN-m (4200 in-lb), (3.2)

Where,

W=Weight of the hammer ≈ 0.632kN (140 lb)

H=height of drop≈ 0.76 mm (30 in)

In fact this energy varies corresponding to the different types of hammer, anvil, and operator characteristics (Das, 2011).

Schmertmann and Palacios (1979), proved that the SPT blow count is approximately inversely proportional to the given hammer efficiency energy. Kovacs et al. (1984), Seed et al. (1984) and Robertson et al. (1983) observed that for most SPT based empirical correlations energy level of 60 % give satisfying results. Furthermore, Seed et al. (1984)

determined that for liquefaction analyses the SPT N values must be corrected to an energy level of 60 %. Therefore energy ratio factor is the proportion of E_r over 60. It is worthwhile to note that because of various methods used by different geologists and geotechnical engineers all over the world, different values of C_E have been calculated. Table 3.4 contains these values for some different countries, (Canadian Geotechnical Society, 2006).

Table 3.4. C_E factors used in different countries (Canadian Geotechnical Society, 2006)

Country	Hammer	Release	E_r(%)	E_r/60
North and South America	Donut	2 turns of rope	45	0.75
	Safety	2 turns of rope	55	0.92
	Automatic	-----	55 to 83	0.92 to 1.38
Japan	Donut	2 turns of rope	65	1.08
	Donut	Auto-Trigger	78	1.3
China	Donut	2 turns of rope	50	0.83
	Automatic	Trip	60	1.0
U.K.	Safety	2 turns of rope	50	0.83
	Automatic	Trip	60	1.0
Italy	Donut	Trip	65	1.08

3.2.1.3 Borehole Diameter Factor C_B

Up to now, geotechnical engineers have performed SPT test with various diameters. For instance in Japan the test is usually made in 66 mm or 86 mm boreholes but never larger than15 mm. Nixon (1982) however could do the test in 200 mm borehole. It is worth

noting that some countries usually use size 65-115 mm diameter for this test. Therefore, the borehole diameters usually are classified to the sizes 65-115mm, 150 mm, and 200 mm.

Although it is possible to neglect the role of testing in rather large boreholes in cohesive soils, there are some evidences found in sands which result for lower N values in larger boreholes. Table 3.5 suggests the borehole diameter factor C_B with minimum correction factors (Skempton, 1986).

Table 3.5. Borehole diameter correction factor (Rogers, 2006)

Borehole diameter (mm)	Correction factor
65-115	1.0
150	1.05
200	1.15

3.2.1.4 Rod Length Factor C_R

Rod length is another factor which influences the SPT. Morgano and Liang (1992) extracted some tables and curves to prove this effect as shown in Table 3.6 and Figure 3.6, and presented rod length correction factors in Table 3.7 for this aim.

Table 3.6.Maximum energy transferred by various rod lengths (Morgano & Liang, 1992)

Rod length ft(m)	Ultimate Resistance, kips-(kN)																	
	0.5(2.23)			1.0(4.45)			2.5(11.1)			4.0(17.8)			7.0(31.2)			13.0(57.9)		
	EMX[1]	EMX	e_t[2]	EMX	EMX	e_t	EMX	EMX	e_t	EMX	EMX	e_t	EMX	EMX	e_t	EMX	EMX	e_t
	kip.ft	kJ[3]	%	kip.ft	kJ	%	kip.ft	kJ	%	kip.ft	kJ	%	kip.ft	kJ	%	kip.ft	kJ	%
10 (3.05)	0.23	0.31	82	0.24	0.33	86	0.25	0.34	89	0.25	0.34	89	0.25	0.34	89	0.25	0.34	89
20 (6.10)	0.24	0.33	86	0.24	0.33	86	0.25	0.34	89	0.25	0.34	89	0.25	0.34	89	0.25	0.34	89
50 (15.24)	0.26	0.35	93	0.26	0.35	93	0.26	0.35	93	0.26	0.35	93	0.26	0.35	93	0.26	0.35	93
100 (30.49)	0.26	0.35	93	0.26	0.35	93	0.26	0.35	93	0.26	0.35	93	0.26	0.35	93	0.26	0.35	93

[1] Emx-Energy transferred to rod.
[2] et= Emx/Ei where Ei is the actual kinetic energy (Ei=0.5 mv2=0.8 wih) of the ram.
[3] 1kip.ft=1.356kJ

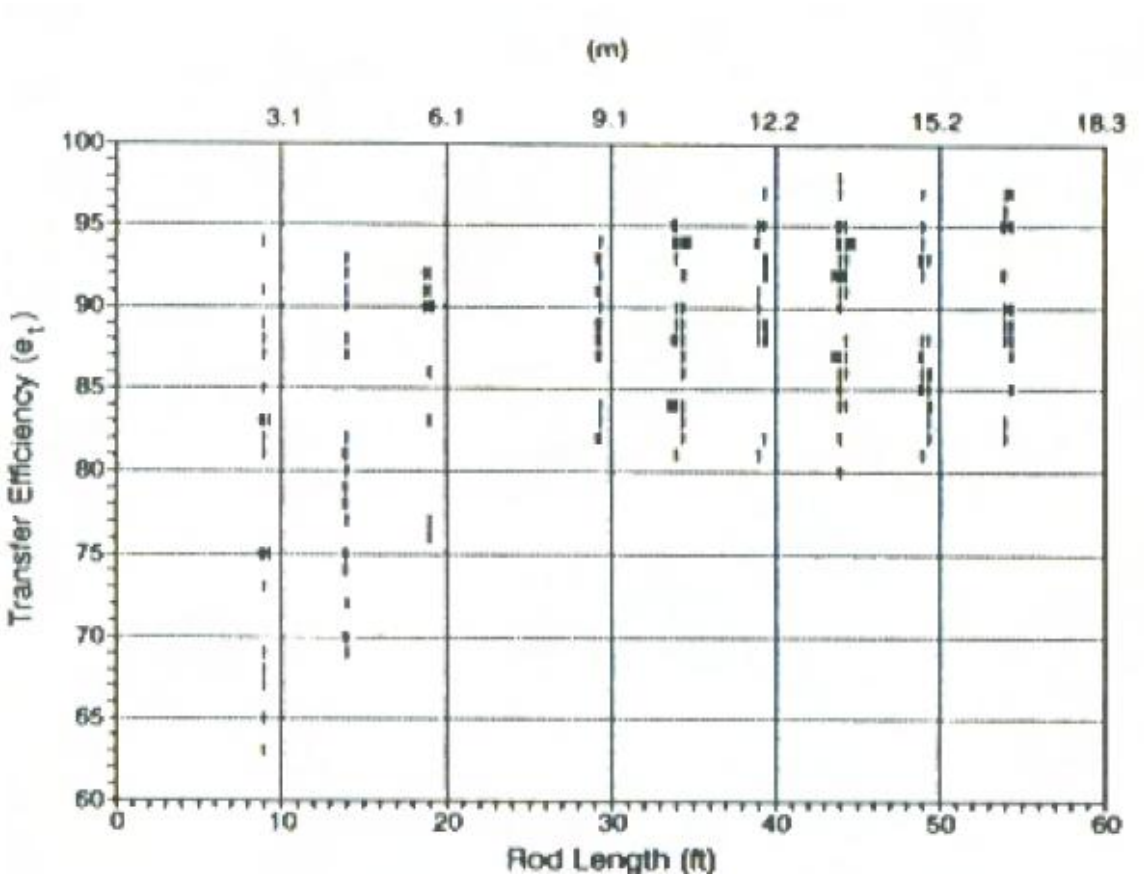

(a)

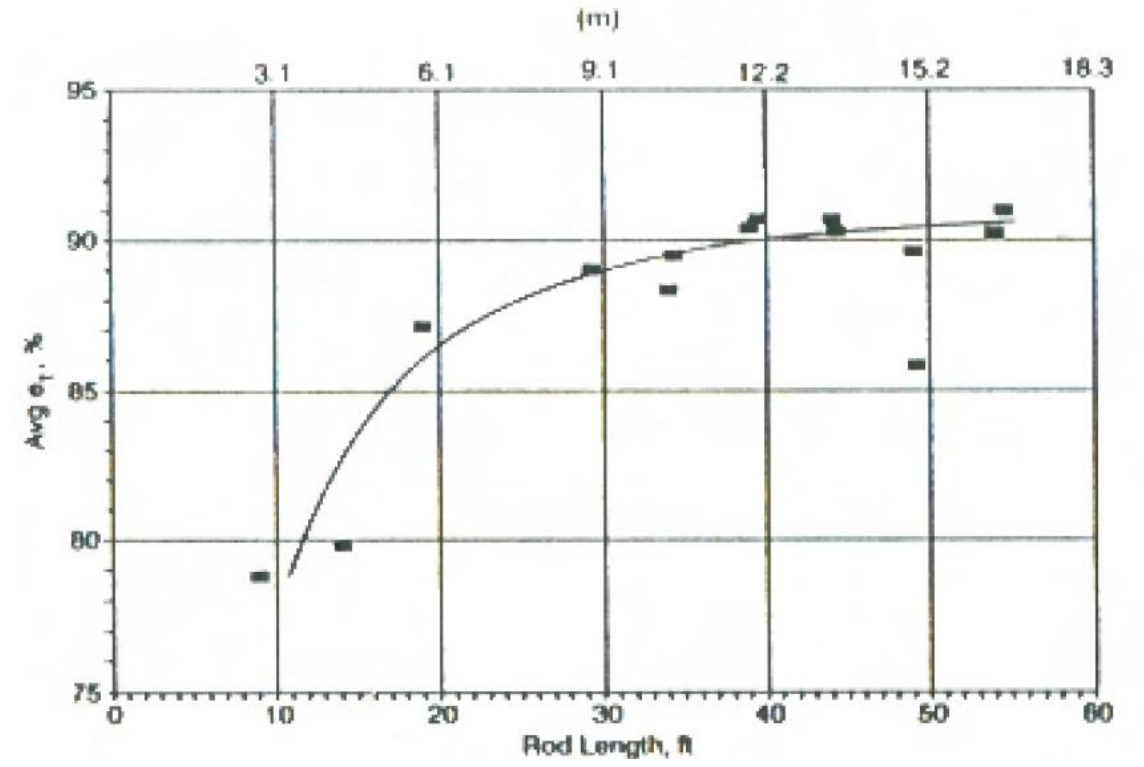

(b)

Figure 3.6. (a) Transfer efficiency for various rod lengths (b) Average transfer efficiency for various rod lengths, (Morgano & Liang, 1992).

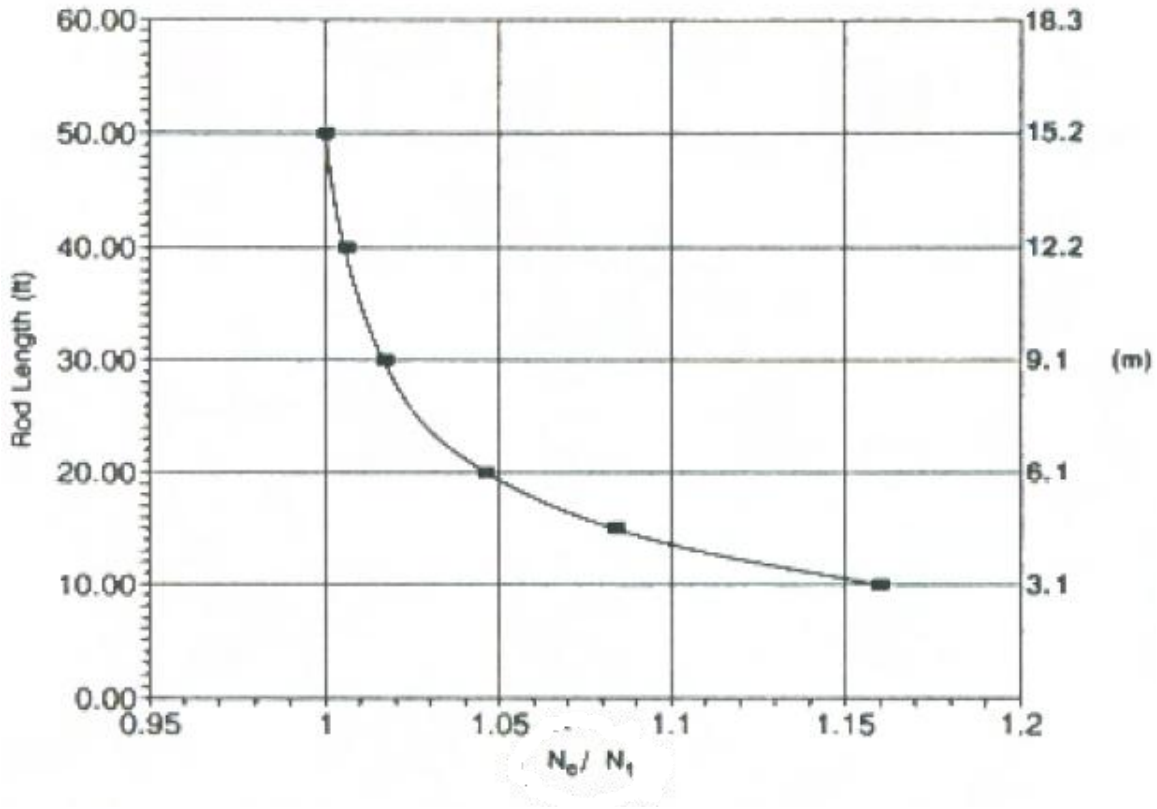

Figure 3.7. Correction factor for various rod lengths (Morgano & Liang, 1992)

Table 3.7. Currently used rod length correction factors (Rogers, 2006)

Rod length (m)	Correction factor
3-4	0.75
4-6	0.85
6-10	0.95
10-30	1.0
>30	<1.0

3.2.1.5 Sampling Method Factor C_s

Generally there exist two sampling methods for SPT which depend on advancement of the sampler. Therefore, in order to standardize SPT-N value, correction factors are suggested by Rogers (2006) as can be depicted in Table 3.8.

Table 3.8. Sampling method correction (Rogers, 2006).

Sampling method	Correction
Standard sampler	1.0
Sampler without liner	1.1-1.13

3.2.2 Young's Modulus of Elasticity Correlations

The modulus of elasticity which is known also as Young's modulus of soil is a parameter of soil elasticity and it is most frequently used in the approximation of settlement from static loads. This parameter can be computed by using empirical correlations, or laboratory insitu test methods on undisturbed samples.

There are some equations for correlation between Young's Modulus and N value. For instance AASHTO (1996), Bowles (1996) ,Bowles and Denver(1982), D'Appolonia et al. (1970), Ghahramani and Behpoor (1989) for saturated clays, Kulhawy and Mayne (1990), Mezenbach (1961), Papadopoulos (1992), Schultz and Muhs (1967), Skempton (1986), Stroud (1988) and Tan et al. (1991) could extract some empirical or theoretical formulae for this mission (Afkhami, 2009).

Mezenbach (1961) defined a correlation between Young's Modulus and N-value as given in Equation 3.3.

$$E_S = C_1 + C_2 N \ (kg/cm^2) \quad (3.3)$$

Later Bowels (1988) proposed a new formula based on particle size, given in Equation 3.4.

$$E_S = C_1 (N + C_2) \ (kg/cm^2) \quad (3.4)$$

Where, C_1 and C_2 in both formulae are dependent on particle size, water table and the of N value.

Papadopoulos (1992) obtained the Equation 3.5(Som & Das, 2006).

$$E_S = 75+8N \quad (kg/cm^2) \tag{3.5}$$

3.2.3 Friction Angle Correlations

One of the important engineering characteristics of soils is friction angle φ. Victor de Mello (1971) extracted an empirical relationship among the blow count, friction angle and effective stress, as illustrated in Figure 3.8.

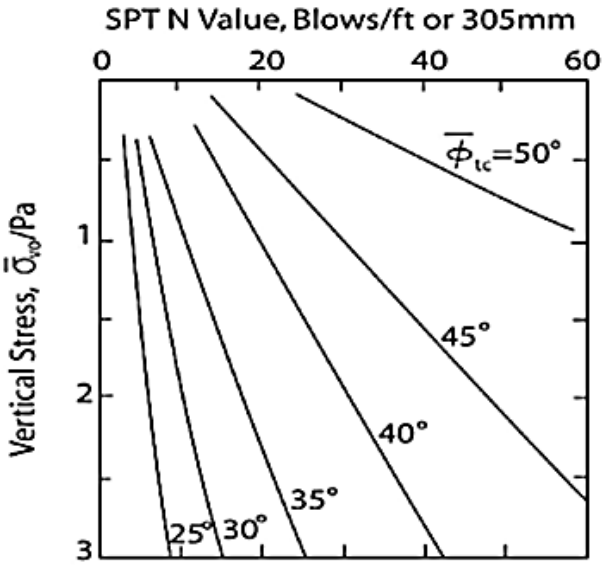

Figure 3.8. De Mello's empirical calculation to approximate friction angle in sand (Robertson, 2006)

It is worth stressing that these correlations are revised by many researchers and still they are being improved.

As it can be seen from the Table 3.9 and Figure 3.9, Peck et al. (1974) provided some relationships between friction angle and SPT-N value (Kulhawy & Mayne, 1990). Also

Equation 3.6 is offered by Wolff (1989) that is attributed to Peck et al. (1974) (Das, 2011).

$$\varphi = 27.1 + 0.3N_{60} - 0.00054[N_{60}]^{2} \quad (3.6)$$

Later, Schmertmann (1975) suggested a new formula which analyses the SPT data as given in Equation 3.7 (Kulhawy & Mayne, 1990).

$$\varphi = \tan^{-1}[N/(12.2+20.3(\sigma'/P_a))]^{0.34} \quad (3.7)$$

The other formulae which are remarkable in this section are given by Hatanaka and Uchida (1996) in Equations 3.8-3.9 (Robertson 2006; Ruwan 2008).

$$\varphi = (15.4\ (N_1)_{60})^{0.5} + 20^{o}, \quad (3.8)$$

$$\varphi = 3.5\ (N)^{1/2} + 22.3^{o} \quad (3.9)$$

Rajapakse (2008) revised Equation 3.9 based on Bowels (2004) relationships and particle size of soil. He could compute three relationships and change the second part of equation to 20 for fine sand, 21 for medium sand, and 22 for coarse sand (Ruwan, 2008).

Table 3.9. Correlation between N_{60} value and friction angle by Peck et al. (1974) (Jackson et al, 2008)

SPT below count (305 mm)	Consistency	Friction angle(degrees)	
		Peck,Hanson and Thornburn (1974)	Meyerhof (1976)
0 -4	Very Loose	<28	<30
4 - 10	Loose	28 - 30	30 - 35
10 - 30	Medium	30 -36	35 - 40
30 -50	Dense	36 - 41	40 - 45
>50	Very Dense	>41	>45

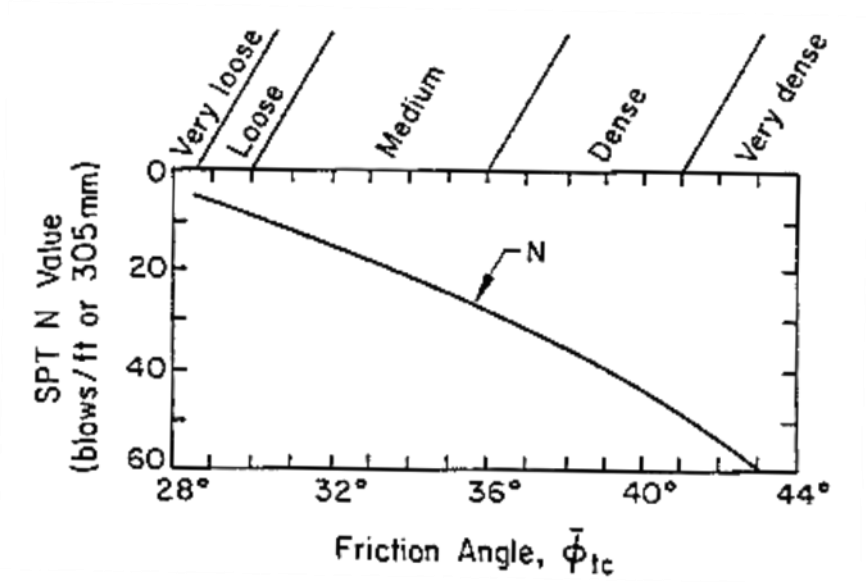

Figure 3.9. Peck et al. (1974) relationship between N and Φ (Kulhawy & Mayne, 1990)

3.2.4 Undrained Shear Strength Correlations

Undrained shear strength is another characteristic which is vital for recognizing soil properties. It is usually correlated to unconfined compressive strength (q_u) as given in Equation 3.10 (Hara et al., 1974).

$$S_u=0.5q_u \tag{3.10}$$

Terzaghi & Peck (1967) suggested a relationship for fine grained soils and to determine q_u from SPT blow count. Later other researchers considered other approaches to determine S_u, such as from plasticity index (PI). Sanglerat (1972) suggested a new formula to achieve this goal by studying the fine-grained soils and silicate. Another researcher who demonstrated the effect of PI on S_u is Stroud (1974). He considered the results of unconsolidated undrained test (UU). He concluded that the undrained shear strength depends on plasticity index and N value. So when PI increases, S_u decreases. Therefore he divided the relationships to three categories which are shown in Table 3.10, (Stroud, 1974). However Sowers (1979) concluded a relationship vice versa. It is worthy to note that Schmertmann (1975) mentioned that side friction influences standard penetration test resistance by more than 70%. Moreover Ladd et al. (1977) reported that there is a little difference between these values in cohesive soils, (Robertson., 2006).

Finally Décourt (1990), Nixon (1982), Ajayi and Balogum (1988), Sivrikaya & Toğrol (2009) and Hettiarachchi & Brown (2009) updated formulae by previous experiences and new experimental data. All these relationships are given in detail in Figure 3.10 and Table 3.10.

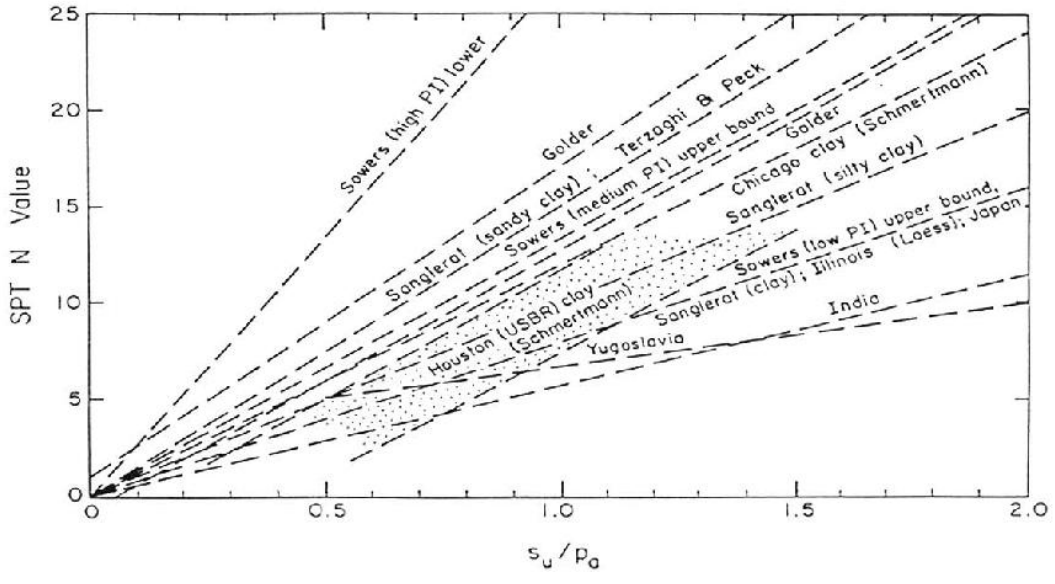

Figure 3.10. Relationships between S_u and SPT blow count (Robertson, 2006).

Table 3.10. Relationships between S_u and SPT blow count

Researchers	Soil Description	Undrained Shear Strength (kPa)
Sanglerat (1972)	Clay Silty clay	12.5N 10N
Terzaghi & Peck (1967)	Fine-grained soil	6.25N
Hara et al. (1974)	Fine-grained soil	$29N^{0.72}$
Sowers (1979)	Highly plastic soil	12.5N
	Medium plastic clay	7.5N
	Low plastic soil	3.75N
Nixon (1982)	Clay	12N
Sivrikaya & Toğrol (2002)	Highly plastic soil	$4.85N_{field}$ $6.82N_{60}$
	Low plastic soil	$3.35N_{field}$ $4.93N_{60}$
	Fine-grained soil	$4.32N_{field}$ $6.18N_{60}$
Stroud (1974)	PI<20	(6-7)N
	20<PI<30	(4-5)N
	PI>30	4.2N
Décourt (1990)	Clay	12.5N $15N_{60}$
Ajayi &Balogun (1988)	Fine-grained soil	1.39N+74.2
Hettiarachchi & Brown (2009)	Fine-grained soil	$4.1N_{60}$
Sirvikaya (2009)	UU Test	$3.33N - 0.75w_n + 0.20LL + 1.67PI$
	UU Test	$4.43N_{60} - 1.29w_n + 1.06LL + 1.02PI$
	UCS Test	$2.41N - 0.82w_n + 0.14LL + 1.44PI$
	UCS Test	$3.24N_{60} - 0.53w_n - 0.43LL + 2.14PI$

3.2.5 Shear Wave Velocity Correlations

Shear wave velocity, V_s is one of the factors for determining dynamic response of soil. The first studies about V_s are obtained from laboratory test results hence some common relations were generated. There are different methods for determining correlations of V_s, such as cross-hole, seismic CPT, spectral analysis of surface waves (SASW), and suspension logging. By using these methods measurement of V_s in various depths has been possible.

As can be seen in Table 3.11, various correlations are suggested for different soil types. Investigating on 192 samples, Imai and Yoshimura (1975) found an empirical equation for seismic velocities and indicator data which were obtained from soil parameters. Sykora and Stokoe (1983) stated that uncorrected SPT-N might be for finding V_s, geological age and soil type instead of alone. Then they suggested a strong relationship which is the comparison of dynamic shear resistance and standard penetration resistance (Sykora & Koester, 1988). Iysian (1996) extracted a new correlation for all soils by investigating on data which were obtained from eastern part of Turkey. He could not find any correlation for gravels. Jafari et al. (2002) examined the statistical correlation based on earlier studies. They achieved a new statistical relation between N value and shear wave velocity. Hasancebi and Ulusay (2006) revised the statistical correlations by a survey of 97 samples which were extracted from north western part of Turkey. They have defined new empirical relationships for sand, clay and all soil types regardless of their constituents. Finally, Ulugergerli and Uyanık (2007) presented an empirical correlation by studying on 327 samples which were chosen from different regions of Turkey and obtained seismic velocities and relative density curve for these data. They found different values between upper and lower bounds in lieu of a single curve.

3.2.6 Shear Modulus Correlations

Shear modulus, G, is an important parameter in studying soil dynamic response. Shear wave velocity can be estimated from G_{max}, and also soil density, ρ, using Equation 3.11.

$$G_{max} = \rho V s^2 \tag{3.11}$$

G_{max} is often used together with modulus reduction (G/Gmax-γ) and damping (D-γ) curves to solve dynamic problems when shear strains drive the soil beyond its elastic range. Modulus reduction curves describe the reduction of secant modulus with increase in cyclic shear strain, γ_c. Damping curves describe the hysteretic energy dissipated by the soil with increase in γ_c. These curves can be obtained through laboratory cyclic loading tests, but are typically assumed for a given soil type. The curves obtained by Seed and Idriss (1970) for sand and by Vucetic and Dobry (1991) for clay are shown in Figures 3.11-3.12.

Ground motion is another subject which can be examined by shear modulus based on comparison of the reference shear wave velocity and obtained V_s. For instance Choi and Stewart (2005) obtained attenuation relations by applying the average of shear wave velocity which is known as V_{s30}.

Table 3.11. Correlations between shear wave velocity and SPT blow count

Researchers	Soil Type	Shear Wave Velocity Correlation
Imai and Yoshimura(1970)	All soils	76N0.33
Shibata(1970)	sand	$31.7N^{0.54}$
Ohba and Toriuma(1970)	All soils	$84N^{0.31}$
Ohta et al (1972)	Sand	$87.2N^{0.36}$
Fujiwara(1972)	All soils	$92.1N^{0.337}$
Ohsaki and Iwasaki(1973)	All soils	$81.4N^{0.39}$
Imai etal(1975)	All soils	$89.9N^{0.341}$
Imai(1977)	All soils	$91N^{0.337}$
	Sand	$80.6N^{0.331}$
	Clay	$80.2N^{0.292}$
Ohta and Goto(1978)	All soils	$85.35N^{0.343}$
Seed and Idrees(1981)	All soils	$61.4N^{0.5}$
Imai and Tonouchi(1982)	All soil	$96.9N^{0.314}$
Sykora and Stokoe(1983)	Sand	$100.5N^{0.29}$
Jinan(1987)	All siols	$116.1(N+0.3185)^{0.202}$
Okamoto et al(1989)	Sand	$125N^{0.3}$
Lee(1990)	Sand	$57.4N^{0.49}$
	Silt	$105.64N^{0.32}$
	Clay	$114.43N^{0.31}$
Athanasopoulos(1995)	All soils	$10.6N^{0.36}$
	Clay	$76.55N^{0.445}$
Sisman(1995)	All soils	$32.8N^{0.51}$
Iyisan(1996)	All soils	$51.5N^{0.516}$
Kanai(1966)	All soils	$19N^{0.6}$
Jafari et al(1997)	All soils	$22N^{0.85}$
Pitilakis et al.(1999)	Sand	$145(N_{60})^{0.173}$
	Clay	$132(N_{60})^{0.271}$
Kiku et al(2001)	All soils	$68.3N^{0.292}$
Jeferi et al(2002)	Silt	$22N^{0.77}$
	Clay	$27N^{0.73}$
Hasancebi and Ulusay(2006)	All soil	$90N^{0.309}$
	Sand	$90.82N^{0.319}$
	Clay	$97.89N^{0.269}$
Hasancebi and Ulusay(2007)	All soils	23.39Ln(N)+405.61
	All soils	$52.9\ e^{-0.011N}$
Dimken(2009)	All soils	$58N^{0.39}$
	Sand	$73N^{0.33}$
	Silt	$60N^{0.36}$
	Clay	$44N^{0.43}$

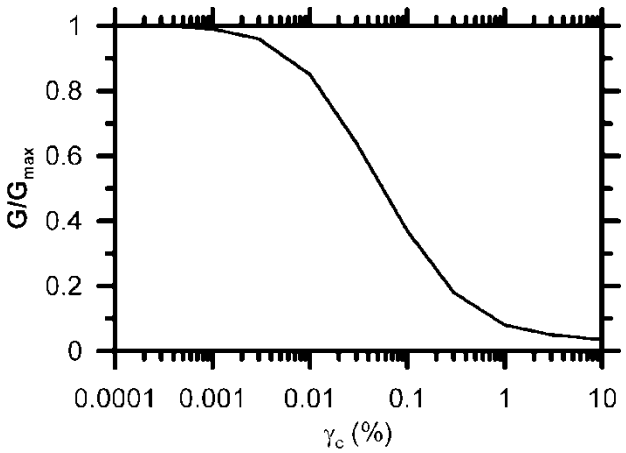

Figure 3.10.Modulus-reduction curves for sand (Seed & Idriss, 1970)

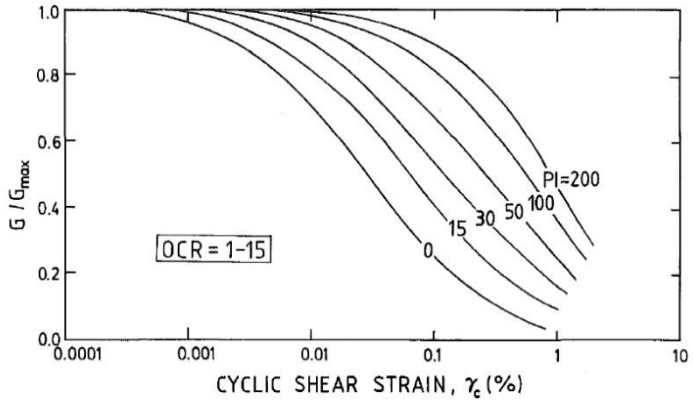

Figure 3.11.Modulus-reduction curves for clay (Vucetic & Dobry, 1991)

Imai and Yoshimura (1970) offered the first formula corresponding to soil unit weight which is shown in Table 3.11. They stressed that the relationship is valid when there is no large difference between studied soil and existing soil. Parallel to their work, Ohaba and Toriumi (1970) suggested a new equation as the result of their observations in Osaka. They varied the obtained Rayleigh wave velocities and also assumed that unit weight is equal to 16.67 kN/m^3 as well as Imai and Yoshimura (1970). Ohta et al. (1972) could extract a new correlation through a survey of 100 sampled data which were obtained from 15 regions. Findings based on the study of diluvial sandy and cohesive soil, and alluvial sandy and cohesive soil, showed that G in cohesive soils is a little larger than sandy soils with similar N value but it may not occur. Ohsaki and Iwasaki (1973) established new numerical relationships revised on another correlation which was extracted earlier. They considered sand and cohesive soil like that Ohaba and Toriumi (1970) although they believed that the correlation should be different for each soil type. Hera et al. (1974)

presented another relationship based on collected data from 25 regions. They classified data based on soil formation similar to the previous works, and extracted correlations between G and N values in cohesive soil. Imai and Tonouchi (1982) studied 400 samples which were chosen from different regions of Japan and consequently introduced empirical correlations for S-wave and P wave distinctly. Kramer (1996) modified the correlation which was established by Imai and Tonouchi (1982). Other researchers have listed and introduced different correlations based on previously published data .The most available correlations are listed in Table 3.12.

Table 3.12.Different correlations between shear modulus and SPT blow count.

Researchers	Soil Type	Shear Modulus Correlation(MPa)
Imai and Yoshimura(1970)	Mixed soil	$1000N^{0.78}$
Ohba and Toriuma(1970)	Alluvial sand,clay	$1220N^{0.62}$
Ohata et al(1972)	Tertiary soil, diluvial sandy and cohesivesoil	$1390N^{0.72}$
Ohsaki and Iwasaki(1973)	All soils	$1218N^{078}$
	Sandy soil	$650N^{0.94}$
	Intermediate soil	$1182N^{0.76}$
	Cohesive soil	$1400N^{0.71}$
	All soils	$1200N^{0.8}$
Hera et al(1974)	Alluvial,diluvialandtertiarydeposit	$158N^{0.668}$
Imai and Tonouchi(1982)	Alluvial clay	$176N^{0.607}$
	Alluvial sand	$125N^{0.611}$
	Diluvial clay	$251N^{0.555}$
	Diluvial sand	$177N^{0.631}$
	All soil	$144N^{0.68}$
Seed et al(1983)	No data about this	65N
Anbazhagan and Sitharam(2010)	Silty sand with less percentage of clay	$24.28N^{0.55}$
Kramer(1996)	Sandy soil	$325(N_{60})^{0.68}$

3.3 Mat Foundations

Foundation is defined as a connector joining the structure to the soil and which transfers the loads from the buildings to the soil. Mat foundation can be considered as one of the important types of shallow foundations which are used to control the differential settlements in weak soils.

Various methods are established to compute bearing capacity and settlement of mat foundations. One of the common methods is the manual computation using analytical approaches. Nowadays with the advent of geotechnical software, both analytical and finite element approaches can be done more efficiently.

3.3.1 Review of Bearing Capacity

Bearing capacity (q) is a vital engineering parameter for designing structures, and is defined as the amount of soil resistance against an applied load. The proposed structure can be designed by allowable bearing capacity (q_{all}) which is the outcome of dividing the ultimate bearing capacity (q_{ult}) by a factor of safety (FS). In geotechnical engineering problems it is common to consider this factor as 3. There are various analytical approaches for determining bearing capacity which are explained as follows.

Karl Terzaghi (1943) was one of the pioneers who offered plenary theory about q_{ult}. He defined shallow foundation as the foundation with the least dimension, B to be less than or equal to the depth at which it is placed. Later another scientist, Meyerhof (1951), suggested a new theory related to bearing capacity which was applicable for different foundations. Then Hansen (1970) offered relationship for this factor. He highlighted that this equation is special for continuous foundations. Vesic (1975) revised this formula and investigated the value of bearing capacity factors neglecting the effect of slope. There are some other researchers such as Hu (1964) and Balla (1962) who offered relationships which are not as applicable as previously mentioned ones. Later a general relationship for ultimate bearing capacity for a case without slope, inclined foundation base or load inclination, is defined as in Equation 3.12 (Das, 2009).

$$q_{ult} = cN_cF_{cs}F_{cd} + qN_qF_{qs}F_{qd} + 0.5\,\gamma\, BN_\gamma F_{\gamma s}F_{\gamma d} \qquad (3.12)$$

Where,

N_c,N_q,N_γ = Bearing capacity factors, (given in Table 3.14).

F_{cs}, F_{qs}, $F_{\gamma s}$ = Shape factors.

F_{cd}, F_{qd}, $F_{\gamma d}$ = Depth factors.

The commonly used formulae for the shape and depth factors are given in Equations 3.13-3.30.

1) Meyerhof (1963) shape factors

For φ=0;

$$F_{cs}=1+0.2\left(\frac{B}{L}\right) \quad (3.13)$$

$$F_{qs}=F_{\gamma s}=1 \quad (3.14)$$

For φ greater than or equal to 10;

$$F_{cs}=1+0.2\left(\frac{B}{L}\right)\tan^2\left(45+\left(\frac{\varphi}{2}\right)\right) \quad (3.15)$$

$$F_{qs}=F_{\gamma s}=1+0.1\left(\frac{B}{L}\right)\tan^2\left(45+\left(\frac{\varphi}{2}\right)\right) \quad (3.16)$$

2) Meyerhof (1963) depth factors:

For φ=0

$$F_{cd}=1+0.2\left(\frac{Df}{B}\right) \quad (3.17)$$

$$F_{qd}=F_{\gamma d}=1 \quad (3.18)$$

For φ greater than or equal to 10

$$F_{cd}=1+0.2\left(\frac{Df}{B}\right)\tan\left(45+\left(\frac{\varphi}{2}\right)\right) \quad (3.19)$$

$$F_{qd}=F_{\gamma d}=1+0.1\left(\frac{Df}{B}\right)\tan\left(45+\left(\frac{\varphi}{2}\right)\right) \quad (3.20)$$

3) De Beer (1970) shape factors :

$$Fcs=1+0.2\left(\frac{Nq}{Nc}\right)\left(\frac{B}{L}\right) \quad (3.21)$$

$$qs=1+\left(\frac{B}{L}\right)\tan\varphi \quad (3.22)$$

$$F\gamma s=1-0.4\left(\frac{B}{L}\right) \quad (3.23)$$

4) Hansen (1970) depth factors:

For $\left(\frac{Df}{B}\right)$ equal or less than 1:

$$F_{cd}=1+0.4\left(\frac{Df}{B}\right) \text{ for } \varphi=0 \quad (3.24)$$

$$F_{cd}=F_{qd}-\frac{1-Fqd}{Nqtan\varphi} \quad (3.25)$$

$$F_{qd}=1+tan\varphi(1-\sin\varphi)^2\left(\frac{Df}{B}\right) \quad (3.26)$$

$$F_{\gamma d}=1 \quad (3.27)$$

For $\left(\frac{Df}{B}\right)$ greater than 1:

$$F_{cd}= 1+0.4 \tan^{-1}\left(\frac{Df}{B}\right) \quad (3.28)$$

$$F_{qd}=1+2\tan\varphi(1- \sin\varphi)^2 \tan^{-1}\left(\frac{Df}{B}\right) \quad (3.29)$$

$$F_{\gamma d}=1 \quad (3.30)$$

Table 3.13. Bearing capacity factors (Das, 2009).

φ	N_c	N_q	N_γ	φ	N_c	N_q	N_γ
0	5.14	1	0	26	22.25	11.85	8
1	5.38	1.09	0.002	27	23.94	13.2	9.46
2	5.63	1.2	0.01	28	25.8	14.72	11.19
3	5.9	1.31	0.02	29	27.86	16.44	13.24
4	6.19	1.43	0.04	30	30.14	18.4	15.67
5	6.49	1.57	0.07	31	32.67	20.63	18.56
6	6.81	1.72	0.11	32	35.49	23.18	22.02
7	7.16	1.88	0.15	33	38.64	26.09	26.17
8	7.53	2.06	0.21	34	42.16	29.44	31.15
9	7.92	2.25	0.28	35	46.12	33.3	37.15
10	8.35	2.47	0.37	36	50.59	37.75	44.43
11	8.8	2.71	0.47	37	55.63	42.92	53.27
12	9.28	2.97	0.6	38	61.35	48.93	64.07
13	9.81	3.26	0.74	39	67.87	55.96	77.33
14	10.37	3.59	0.92	40	75.31	64.2	93.69
15	10.98	3.94	1.13	41	83.86	73.9	113.99
16	11.63	4.34	1.38	42	93.71	85.38	139.32
17	12.34	4.77	1.66	43	105.11	99.02	171.14
18	13.1	5.26	2	44	118.37	115.31	211.41
19	13.93	5.8	2.4	45	133.88	134.88	262.74
20	14.83	6.4	2.87	46	152.1	158.51	328.73
21	15.82	7.07	3.42	47	173.64	187.21	414.32
22	16.88	7.82	4.07	48	199.26	222.31	526.44
23	18.05	8.66	4.82	49	229.93	265.51	674.91
24	19.32	9.6	5.72	50	266.89	319.07	873.84
25	20.72	10.66	6.77				

3.3.2 Review of Settlement

Settlement is another factor which should be considered before design of structures. This parameter is divided into immediate and time dependent settlement. In this study the settlement calculations based on SPT results will be considered only.

Terzaghi and Peck (1948) explained settlement based on plate load test result initially. They considered the effects of water table and depth of footing. They suggested two correction factors to account for their effect. They also introduced another relationship between bearing capacity and N value. Meyerhof (1956) suggested a new formula for settlement by studying eight structures and assuming that allowable bearing pressure is more than 50%. Peck and Bazaraa (1969) revised Terzaghi & Peck's (1948) equation based on the settlement variations. They used corrected N value for computing the relationships. Burland and Burbidge (1985) predicted a new relationship between settlement and N_{60}. They classified their suggested formula based on soil type and the effective stress of layers.

3.3.3 A Brief Explanation of Finite Element Method

Finite element method (FEM) is an accurate and economic way to study the soil structure interaction. In this method progressive mathematical procedures are applied by considering a mesh including similar geometrical shapes which are called elements. Then, critical elements are investigated in order to see the effect of soil subjected to structural loads (Srilakshmi & Rekha, 2011). In the old methods in order to interpret the behavior of a mat foundation, which will be investigated in this study, two vital simplifying hypotheses where considered. The first is an infinitely rigid mat and the second one-dimensional bending (ACI, 1988). Assuming these two assumptions for some types of mats, such as stiff mats under the uniformly distributed load may not lead to considerable mistakes. In case that the first assumption is made, bearing capacity can be specified by static modeling, while high pressure accumulations close to utilized forces

and the regions with low pressure far from the forces are neglected. Applying the second assumption allows to estimate in one dimension only instead of two.

To tackle these restrictions, finite element method is evolved which has solved the problems mentioned above easily by the aid of basic computer codes (Edward, 1995).

PLAXIS is one of the available powerful software which enables the geotechnical engineers to utilize FEM in the shortest time. The application of this software, besides some important expressions related to FEM are explained in detail in the following chapters.

Chapter 4

ENGINEERING PARAMETERS RETRIEVED FROM NOVOSPT

4.1Introduction

NovoSPT is advanced software which supports nearly 270 different correlations. This software is able to perform some corrections by choosing corresponding formulae according to the suggested methods, based on soil type and also by using recommendation section of software as shown in Figure 4.1.

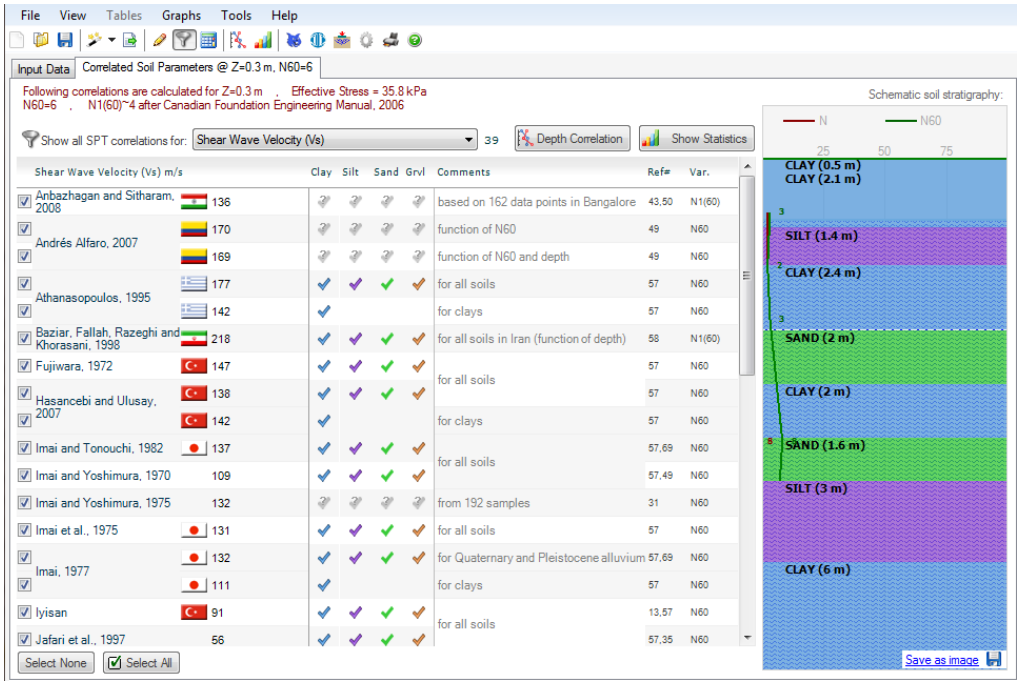

Figure 4.1. Recomendation tools of the software

Soil properties and SPT records are the main data required for computing correlations as depicted in Figure 4.2. This program is able to recognize these data which are indeed the outcome of other software such as Microsoft Excel by selecting “import tools” option.

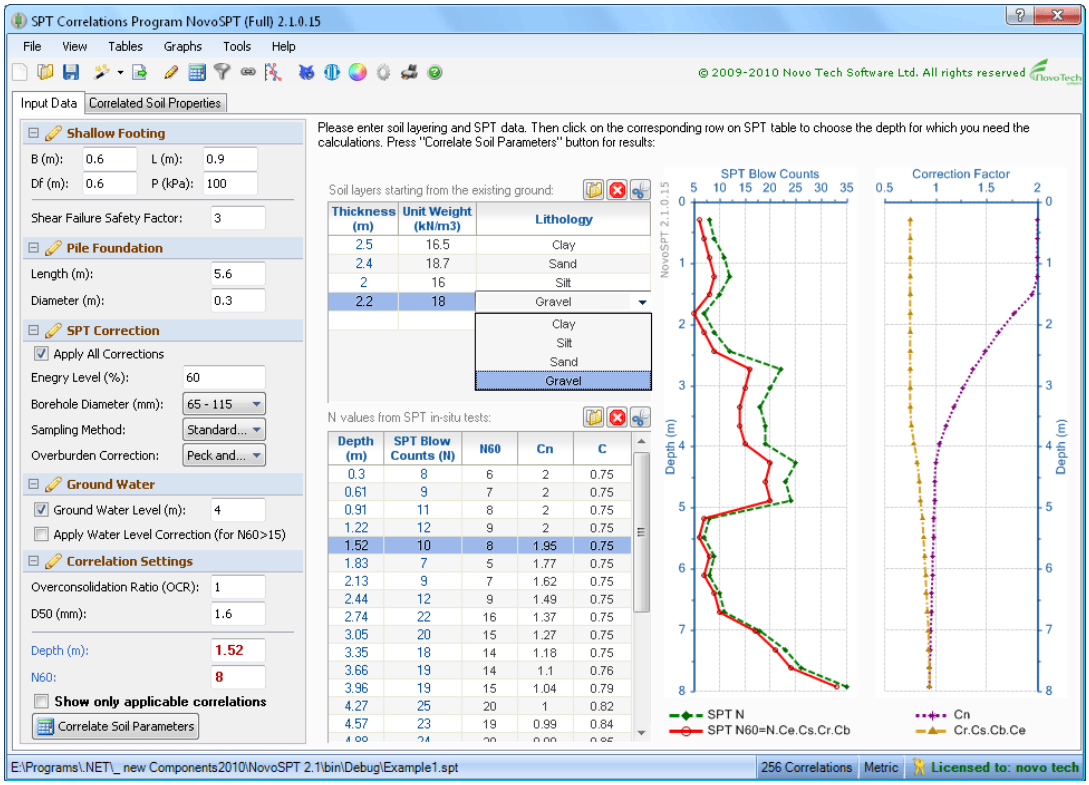

Figure 4.2. Input Soil Properties and SPT document

NovoSPT calculates N value corrections in home pages according to initial input data. The corrections shown by C_e, C_b, C_s, C_r and C_n are the energy level, borehole diameter, sampling method, rod-length and overburden corrections respectively. Finally the program gives the correlation and soil layer identification in "correlated soil parameter" tab sheet based on initial soil properties and corrected N values as shown in Figure 4.1.

Initial properties of 43 boreholes which are used in this research are based on in situ data reported by the Department of Geology and Mining, and graduate theses on Geotechnical Engineering of Eastern Mediterranean University as shown in Appendix A.

Project: BH-24 Job No.: Client: Emu Borehole:BH24

Consistency		Clay	Silt	Sand	Grvl	Comments	Ref#	Var.
AASHTO, 1988	Soft	*				for fine-grained soils	55	N60
Terzaghi and Peck, 1948	Soft	*				for fine-grained soils	3	N60

List of 33 correlations for ::Young's Modulus (Es)::

Young's Modulus (Es) MPa		Clay	Silt	Sand	Grvl	Comments	Ref#	Var.
Ghahramani and Behpoor, 1989	0.5	*				Saturated clays, N60<25	7	N60
Papadopoulos, 1992	9.9	~	~	~	~		25	N60
Skempton, 1986	8.6	~	~	~	~			N60
Stroud, 1988	~ 1.5 to 6	~	~	~	~	Weak rocks	47	N60

List of 32 correlations for ::Friction Angle::

Friction Angle deg		Clay	Silt	Sand	Grvl	Comments	Ref#	Var.
Ayuthaya	28.8	~	~	~	~		24	N60
Ayuthaya	29.3	~	~	~	~		24	N1(60)
Chonburi	28	~	~	~	~		24	N60
Chonburi	30.3	~	~	~	~		24	N1(60)
Hatanaka and Uchida, 1996	29.3	~	~	~	~		2	N1(60)
Hatanaka and Uchida, 1996	28.9	~	~	~	~		30,51	N1(60)
Hatanaka and Uchida, 1996	25.9	~	~	~	~		25	N1(60)
JRA, 1990	-	~	~	~	~	for N60>5 , Fi<=45	4	N60
Kampengsen	29.3	~	~	~	~		24	N60
Kampengsen	32.9	~	~	~	~		24	N1(60)
Kulhawy and Mayne, 1990	27.9	~	~	~	~		30	N60
Meyerhof, 1959	32	~	~	~	~	Dr from Yoshida, 1988		N60
Ohsaki et al., 1959 and Kishida, 1967	22.7	~	~	~	~		4	N60
Peck et al., 1953	27.9	~	~	~	~		4	N60
Peck, Hanson and Thornburn, 1974	27.5	~	~	~	~	is not recommended for shallow depths (less than 1 to 2 metres)	12,51	N1(60)
Schmertmann, 1975	27.9	~	~	~	~		51	N60
Shioi and Fukui, 1954	21.2	~	~	~	~	in general	1	N70
Shioi and Fukui, 1954	21.8	~	~	~	~	for roads and bridges	1	N70
Shioi and Fukui, 1954	27.9	~	~	~	~	for buildings	1	N70
Wolff, 1989	28.3	~	~	~	~	an approximation based on Peck et al., 1974	30	N1(60)
Wolff, 1989	28	~	~	~	~	an approximation based on Peck et al., 1974	63	N60

List of 22 correlations for ::Undrained Shear Strength (Su) of Clay/Silt::

Undrained Shear Strength (Su) of Clay/Silt kPa		Clay	Silt	Sand	Grvl	Comments	Ref#	Var.
Alayi and Baloqun, 1988	78	*					39	N60
Bowles, 1988	8	*					54	N60
Decourt, 1989	32	*				from triaxial UU tests	47	N60
Ghahramani and Behpoor, 1989	22	*				based on over 100 data in Iran, N60<25	7	N60
Hara et al., 1974	64	*					30,51	N60
Hatef and Keshavarz, 2004	54	*				based on 482 SPT and unconfined compression tests in Shiraz city (Iran)	39	N60
Hettiarachchi and Brown, 2009	12	*				based on several SPT test in US	63	N60
Japanese Road Association	28	*				valid for N60<5	9	N60
Kulhawy and Mayne, 1990	18	*					30	N60
Meyerhof, 1956	60	*					8	N60
Peck et al., 1974	24	*						N1(60)
Reese, Touma and O'Neill, 1976	21	*					8	N60
Sowers, 1979	~ 14 to 30	*				Lean clays (CL)		N60
Sowers, 1979	~ 30 to 52	*				Fat clays (CH)		N60
Stroud and Butler, 1975	-	*				valid for N60>5	8	N60
Stroud, 1974	14	*				Insensitive overconsolidated clays	47	N60
Stroud, 1989	14	*				PI=15%	55	N60
Stroud, 1989	16	*				PI=50%	55	N60
Stroud, 1989	15	~	~	~	~	In-sensitive weak rock with N60<200		N60
Tavares, 1988	24	*				for clays in Brazil	39	N60
Terzaghi and Peck, 1967	39	*					8	N60

List of 63 correlations for ::Shear Wave Velocity (Vs)::

Shear Wave Velocity (Vs) m/s		Clay	Silt	Sand	Grvl	Comments	Ref#	Var.
Anbazhagan and Sitharam, 2008	136	~	~	~	~	based on 162 data points in Bangalore	43,50	N1(60)

NovoSPT v 2.32.2012.114 Licensed to: Eastern Mediterranean University , All correlations for N60=2 at depth 2 m; Corrected SPT N1(60)~4 after Canadian Foundation Engineering Manual, 2006

Figure 4.3. NovoSPT output for Borehole 24 at 2 m depth.

4.2 Output Data

As it can be seen from Figure 4.3, after importing data manually, NovoSPT extracts a report for each depth which shows the type of the correlations and magnitude of correlated values. It is worth stressing that these data should be recorded by performer accurately.

4.3 Correlations Based on Different Methods

There are 270 correlations in NovoSPT. This is a large range of selection. Therefore the data are filtered through several phases which are explained in the following sections.

Figure 4.4 illustrates Young's Modulus correlation which ranges over 0 to 10 MPa, with an average of 9.63 MPa. Thus data are chosen which are located close to this mean value. As a result, Bowels (1996), Bowels and Denver (1982), Mezenbach (1961), Papadopulus (1992), Schultze and Muhs (1967) and Skempton (1986) correlations satisfy this criterion regardless of soil type.

In the next phase, regarding the fact that the correlations which are mentioned above are not suitable for this region which is comprised of different types of soils, those data are eliminated which do not cover all soil types. Consequently, the two formulae Papadopulus (1992) and Skempton (1986) are chosen as shown in Table 4.1 .

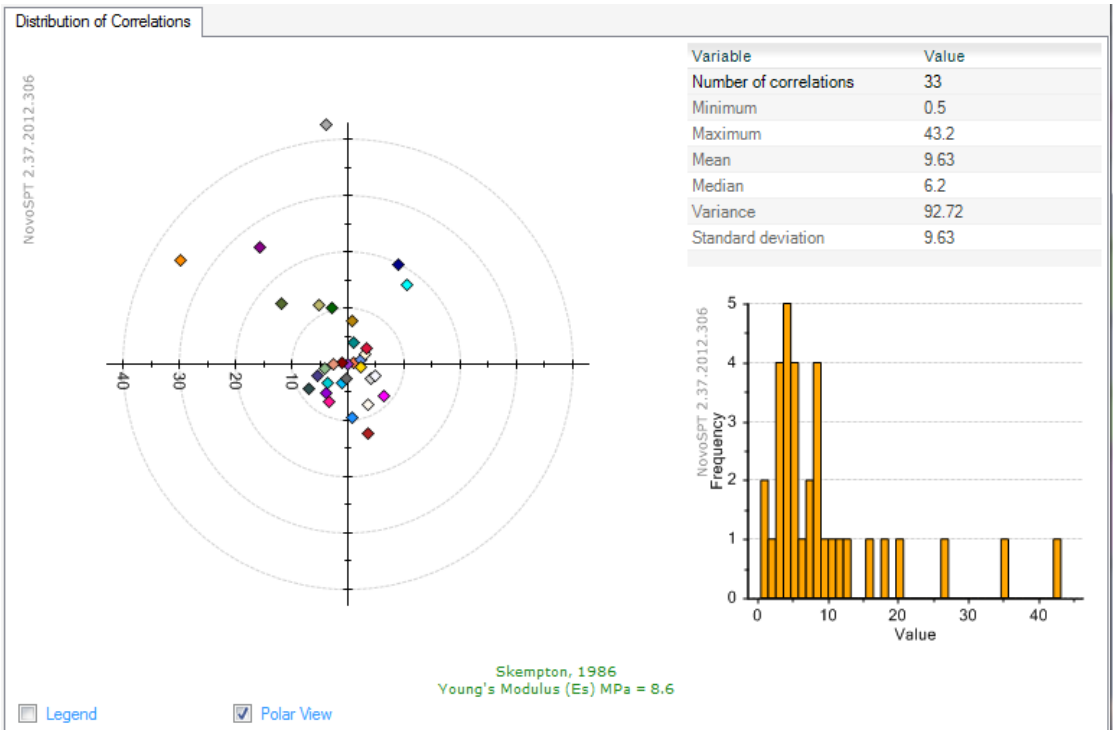

Figure 4.4.Comparison of Young's modulus of elasticity correlations

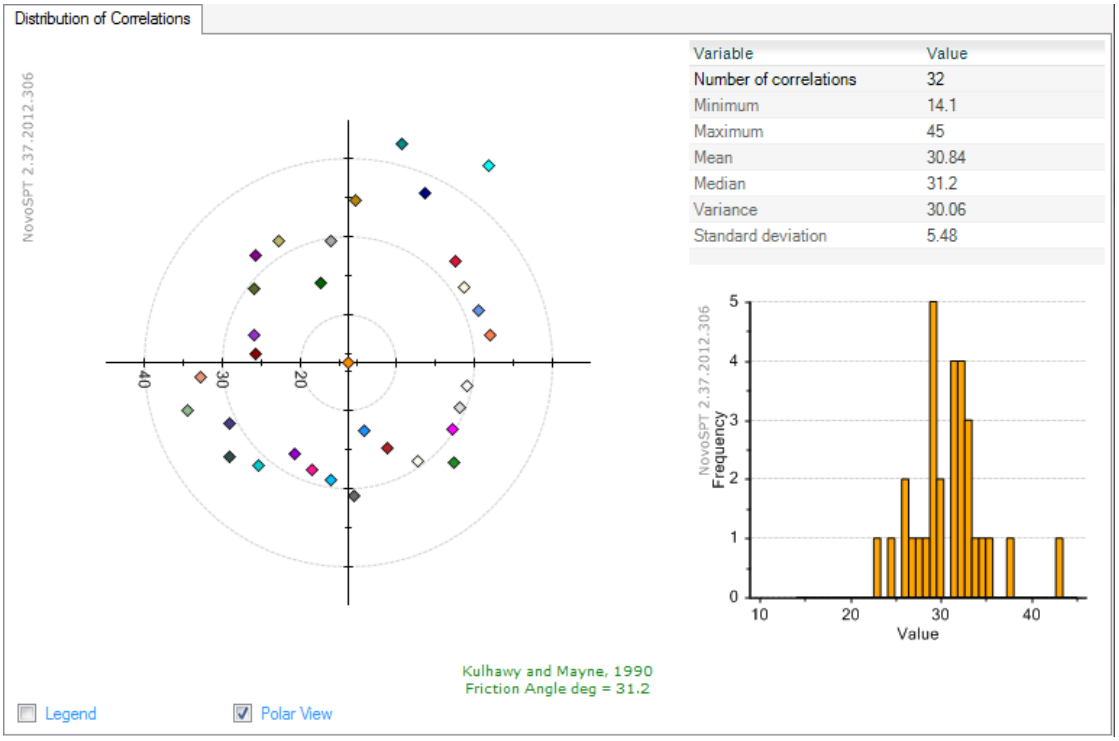

Figure 4.5. Comparison of friction angle correlations

Table 4.1.Correlation results for borehole 24 which are extracted from NovoSPT

Depth1	Depth2	Soil type	SPT Blow Count Depth	N Value	N_{60} Value	$N_{1(60)}$ Value	Young's Modulus; E_s (MPa)		Friction Angle (º)		Undrained Shear Strength ; S_u of Clay/Silt (kPa)		Shear Wave Velocity; Vs (m/s)		Shear Modulus G_{max} (kPa)
							Papadopoulos (1992)	Skempton (1986)	Hatanaka and Uchida (1996)	Kulhawy and Mayne, (1990)	Bowles (1988)	Hettiarachchi and Brown (2009)	Seed and Idriss (1981)	Tomio Inazaki (2006)	Seed et al. (1986)
0	0.5	OL													
0.5	2.6	CL	2	3	2	3	9.9	8.6	---	---	8	12	106	146	34
2.6	4	ML					10.7	9.8	---	---	10	16	123	161	49
4	6.4	CL	4	2	2	2	9.1	7.3	---	---	5	8	87	127	36
			6	3	3	3	9.9	8.6	---	---	8	12	106	146	46
6.4	8.4	SM					13.9	14.8	29.3	31.2	---	---	174	204	70
8.4	10.4	CH					14.7	14.8	---	---	22	37	184	213	70
10.4	12	SM	10.5	8	8	8	13.9	14.8	29.3	31.2	---	---	174	204	76
12	15	ML	12	7	7	6	13.1	13.6	---	---	18	29	162	195	75
15	21	CH					13.9	14.8	---	---	20	33	74	204	84
21	30	CL					16.3	18.6	---	---	28	45	204	228	92

Figure 4.5 shows the friction angle correlations. Note that most of the correlations are placed on points with a distance of nearly 30 degrees around the origin. Also the average of these correlations is 30.84 degrees. Dunham (1954), Hatanaka and Uchida (1996), Kulhawy and Mayne (1990), Moh et al. (1989), Peck et al. (1974), Schertmann (1975), Shioi and Fukui (1959), Terzaghi (1996), Peck et al. (1953) and Wolff (1989) are applicable to all soil types. Two formulae, Hatanaka and Uchida (1996) and Kulhawy and Mayne (1990) are selected based upon two factors: their popularity, and the range of their application in geotechnical engineering. These correlations are available in Table 4.1. Finally, according to Figure 4.6, comparing the friction angles of the estimated data and the exprimental data from the Department of Geology and Mining, it can be concluded that the difference between the average of these two data groups is low. Therfore the results of this study matches with the experimental data.

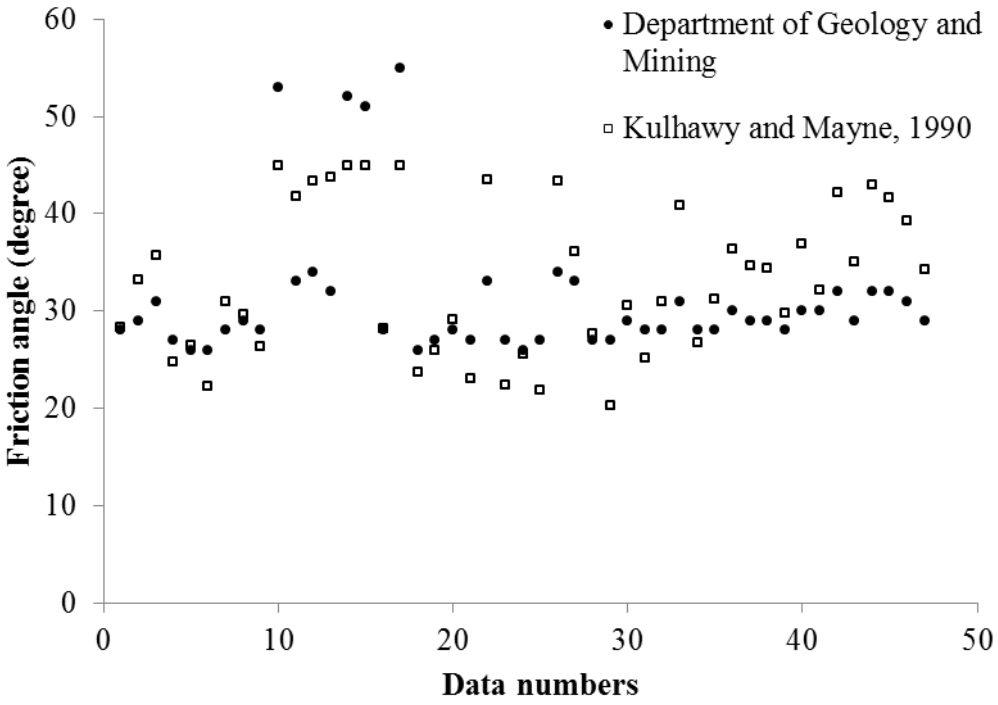

Figure 4.6. Comparison of friction angles of the estimated data and the experimental data of Department of Geology and Mining.

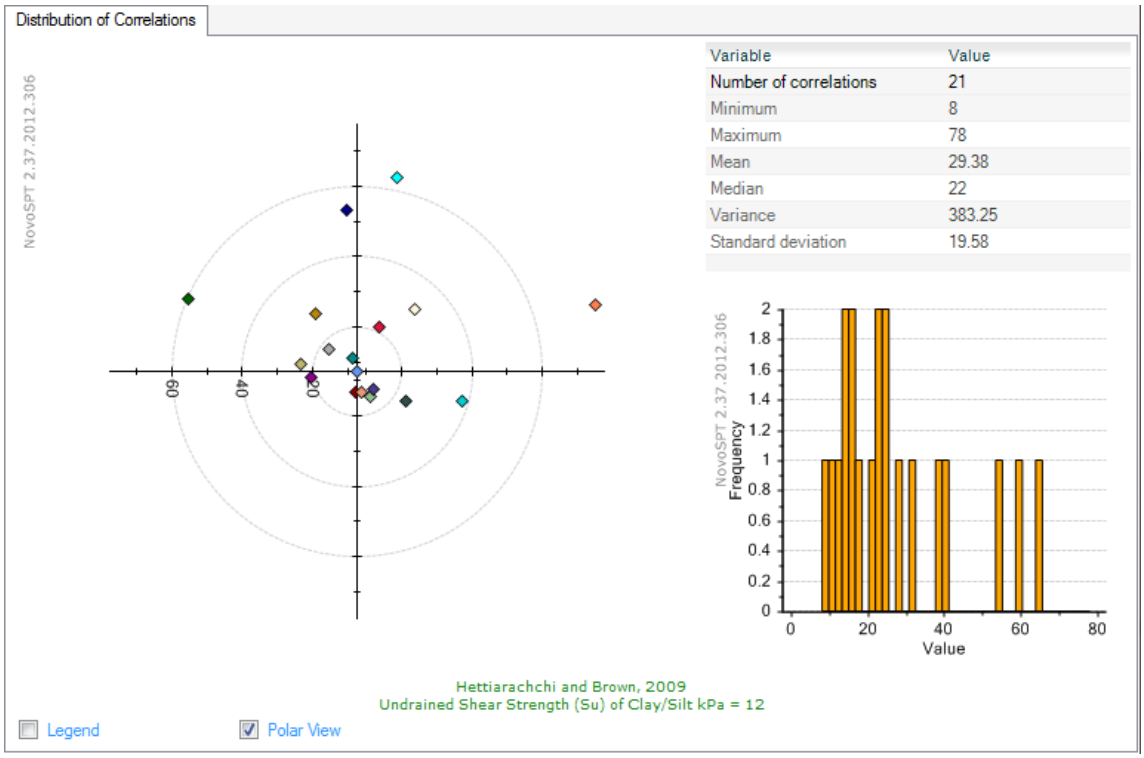

Figure 4.7. Comparison of undrained shear strength correlations

Another parameter which is correlated by NovoSPT is undrained shear strength, S_u. As it is illustrated in Figure 4.7, most of the correlation data are located inside a circle with radius 20 kPa. It should be noted that inside this circle approximately most of the points accumulate around 10 kPa. Therefore based on this observation, the two formulae, Bowels (1988) and Hettiarachchi and Brown (2009) are selected. The results of these correlations are accessible in Table 4.1. Similar to previous section, as it is shown in Figure 4.8, comparing the estimated data related to undrained shear strength and the experimental data available from Department of Geology and Mining, it can be observed that the average of their difference is low. Therefore, it is concluded once again that the results of our research match with the experimental data.

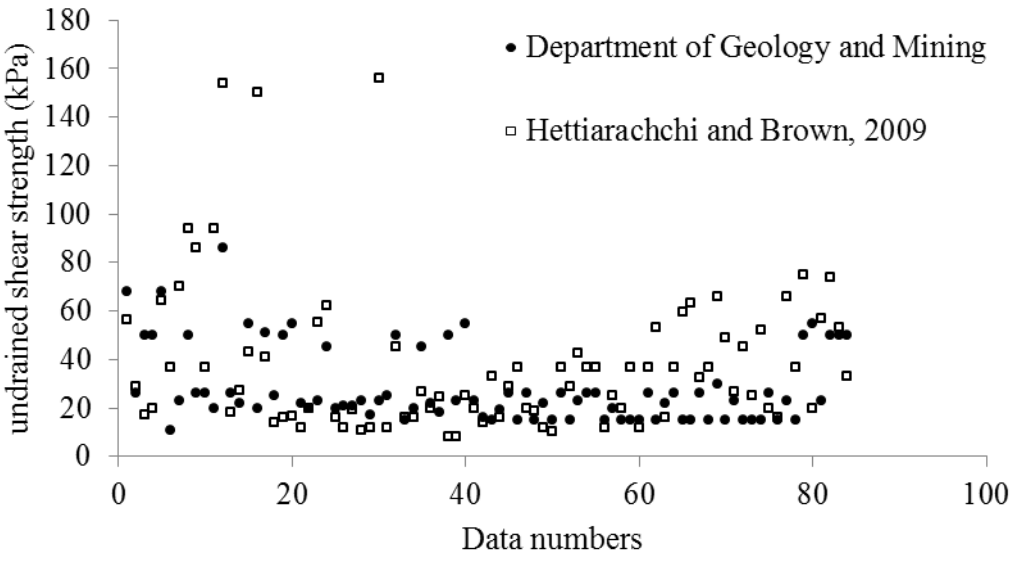

Figure 4.8. Comparison of undrained shear strength of estimated data and the data from the Department of Geology and Mining

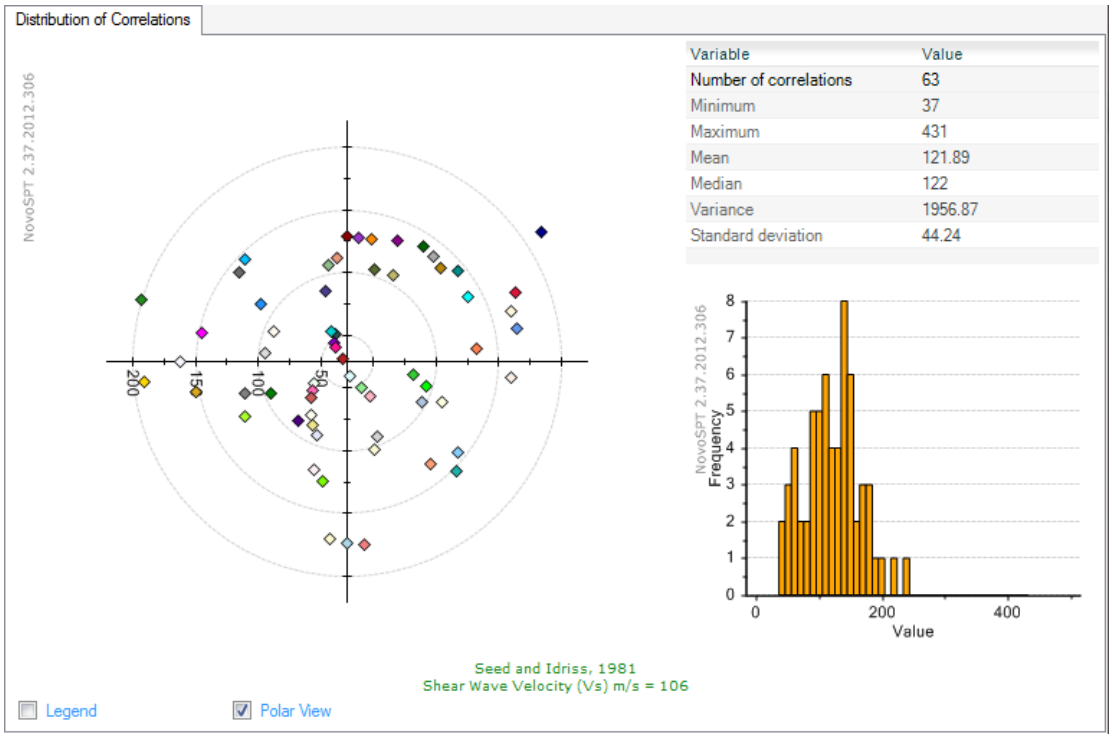

Figure 4.9. Comparison of shear wave velocity correlations

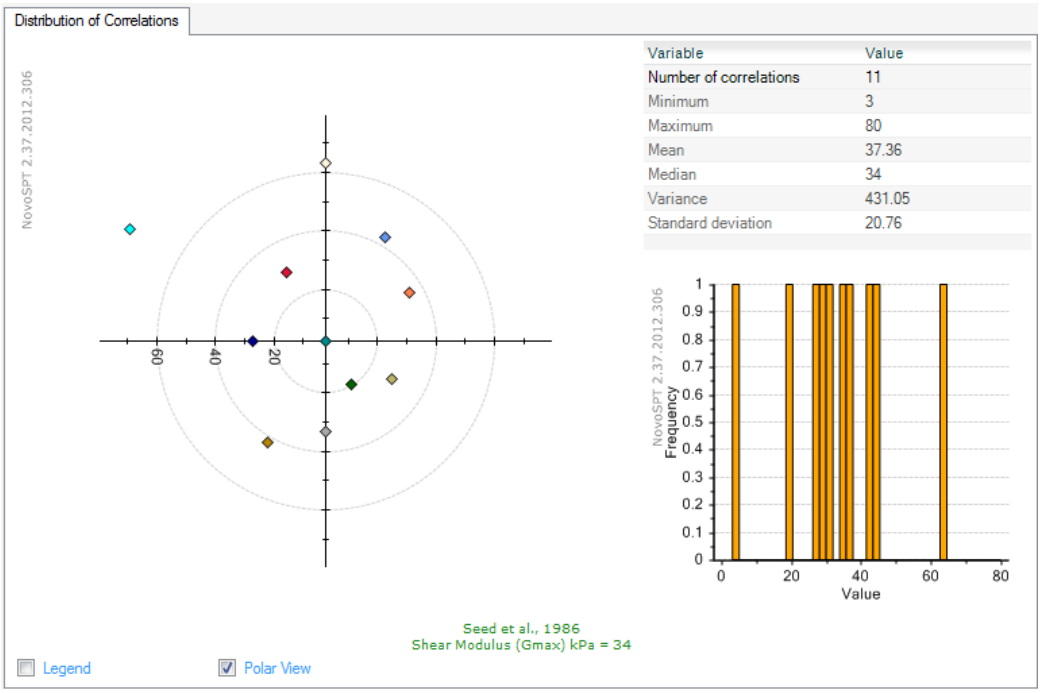

Figure 4.10. Comparison of shear modulus correlations

Shear wave velocity, V_s is another correlation which can be extracted from NovoSPT. It can be noticed in Figure 4.9 that the accumulation of most of the points is in the range of 100 to 150 kPa. As a result, two formulae, Seed and Idriss (1981) and Tomio Inazaki (2006) are offered for all soil types. There are, however no experimental data of shear wave velocity available for Tuzla area. The results of these formulae are summarized in Table 4.1.

Finally the last correlation, obtained from NovoSPT in this research is shear modulus (G). Note that for this case according to Figure 4.10 correlation points are concentrated between 20 and 40 kPa. Considering the average of these values which is 37.36 kPa, Seed et al. (1986) is chosen which is both near the average value and also suggested for all soil types. The results of this correlation are given in Table 4.1.

To sum up the discussions related to the last phase, those correlations are chosen which give results in agreement with the existing laboratory and in situ data available for the area. Also, because of huge amount of data the correlations of only borehole 24, which is

the worst one, are presented here and the correlations for all the other locations are included in the Appendix C. Moreover, in order to estimate the data which are not calculable such as void ratio, dry and saturated unit weights, Equations 4.1-4.3 (Das, 2011) Equations 4-4 and 4-5 (Das, 2008), and to approximate permeability Table 4.2 are applied.

Table 4.2. Rang of coefficient of permeability for various soil types (Das, 2011)

Type of soil	Hydraulic conductivity, *k* (cm/sec)
Medium to coarse gravel	Clays 10^{-1} or less
Coarse to fine sand	10^{-1} to 10^{-3}
Fine sand, silty sand	10^{-3} to 10^{-5}
Silt, clayey silt, silty clay	10^{-4} to 10^{-6}
Clays	10^{-7} or less

$$\gamma = \frac{(1+w)G_s\gamma_w}{1+e} \quad (4.1)$$

$$\gamma_d = \frac{G_s\gamma_w}{1+e} = \frac{\gamma}{1+w} \quad (4.2)$$

$$\gamma_s = \frac{(G_s+e)\gamma_w}{1+e} \quad (4.3)$$

$$\nu \approx 0.25 + 0.00225(\mathrm{PI}) \quad \text{For Clays} \quad (4.4)$$

$$\nu = 0.1 + 0.3\left(\frac{\phi'_t - 25^\circ}{45^\circ - 25^\circ}\right) \quad \text{For Sand} \quad (4.5)$$

4.4 Bearing Capacity Correlations

The correlations related to this parameter which are available in NovoSPT are Burland and Burbidge (1985), Terzaghi (1943), Bowles and Meyerhof (1976), and Parry (1977). A sample of the correlation results related to borehole 24 are shown in Table 4.4.

Meyerhof, (1976) correlation for bearing capacity based upon N value and is based on 25 mm tolerable limit of settlement is given in Equation 4.6 and Equation 4.7.

$$q_{all} = N_{60}.K_d/F_1 \quad \text{for} \quad B \leq F_4 \qquad (4.6)$$

$$q_{all} = N_{60}.K_d.(B+F_3)/(B.F_2) \quad \text{for} \quad B > F_4 \qquad (4.7)$$

where,

$K_d = 1+D/(3B) \leq 1.33$

$F_1 = 0.05$, $F_2 = 0.08$, $F_3 = 0.30$, $F_4 = 1.20$ (SI units)

Parry, (1977) correlation is for bearing capacity based upon N value and for granular soils with 25mm tolerable settlement.

$$q_{all} = 30\ N_{60} \quad \text{for} \quad D_f \leq B \qquad (4.8)$$

Burland and Burbidge, (1985) is defined for bearing capacity based upon N value obtained from 200 samples and for granular soils with 25mm tolerable settlement.

$$q_{all} = 2540.N_{60}^{1.4}/(10^{t}.B^{0.75}) \qquad (4.9)$$

where t stands for time and B indicates width of foundation.

Terzaghi (1943) Formula:

$$q_{ult} = (q\ N_q) + (\ 0.5\ \gamma B N_\gamma) \qquad (4.10)$$

where

q = is the overburden stress at foundation level (D_f),

$N_q = e[\pi.\tan(\phi)]\ [\tan(\pi/4+\phi/2)]^2$ (Bowles,1996)

$N_\gamma = 1.5(N_q-1)\ \tan(\phi)$ (Brinch & Hansen, 1970)

ϕ = friction angle correlated from the equation proposed by Hatanaka and Uchida, (1996) based on SPT at foundation level.

Table 4.3. The output of approximating BH- 24 data by NovoSPT

Depth1	Depth2	Soil type	Void Ratio	Dry Unit Weight	Saturated Unit Weight	Young's Modulus	Friction Angle	Undrained Shear Strength of Clay/Silt	Shear Wave Velocity	Shear Modulus	Dilatancy Angle	Poisson Ratio	Permeability
			e	γ_{dry}	γ_{sat}	E_s (MPa)	φ (º)	S_u (kPa)	V_s (m/s)	G_{max} (kPa)	Ψ (º)	ν	k (cm/s)
0	0.5	OL											
0.5	2.6	CL	0.69	16.1	20.1	8.6	---	12	106	34	0	0.301	10 -7
2.6	4	ML	0.84	14.4	19	9.8	---	16	123	49	0	0.256	10 -4
4	6.4	CL	0.81	14.1	18.6	7.95	---	10	96.5	41	0	0.286	10 -7
6.4	8.4	SM	0.6 6	15.7	19.6	14.8	31.2	---	174	70	1.2	0.193	10 -3
8.4	10.4	CH	1	13.6	18.6	14.8	---	37	184	70	0	0.324	10 -7
10.4	12	SM	1	13	18	14.8	31.2	---	174	76	1.2	0.193	10 -3
12	15	ML	0.86	14.3	18.9	13.6	---	29	162	75	0	0.256	10 -4
15	21	CH	0.91	14.3	19	14.8	---	33	74	84	0	0.335	10 -7
21	30	CL	0.65	16.5	20.4	18.6	---	45	204	92	0	0.387	10-7

Table 4.4. Bearing capacity correlation by NovoSPT

D_f (m)	B (m)	Burland and Burbidge, (1985) (for 25mm settlement)	Terzaghi (1943)	Bowles & Meyerhof, (1976) (for 25mm settlement)	Parry, (1977) (for 25mm settlement)
0.5	10	46.76	479.43	91.63	195
	14	40.67	657.26	90.44	232.5
	18	33.68	835.09	89.78	252
	22	28.97	1012.92	89.37	252
	26	25.56	1190.75	89.08	252
1	10	46.76	535.55	93.13	195
	14	40.67	713.38	91.5	232.5
	18	33.68	891.21	90.61	252
	22	28.97	1069.04	90.04	252
	26	25.56	1246.86	89.64	252
1.5	10	46.76	591.66	94.63	195
	14	40.67	769.49	92.57	252
	18	33.68	947.32	91.43	252
	22	28.97	1125.15	90.71	252
	26	25.56	1302.98	90.21	252
2	10	52.34	647.78	96.13	195
	14	40.67	825.61	93.63	252
	18	33.68	1003.44	92.25	252
	22	28.97	1181.27	91.38	252
	26	25.56	1359.09	90.78	252

Chapter 5

FINITE ELEMENT MODELING BY PLAXIS 2D

5.1Introduction

Geotechnical engineers are frequently required to solve complex soil-interaction problems. PLAXIS is becoming an increasingly popular tool for solving such problems. While PLAXIS is a powerful tool for handling complex geotechnical problems, users need to be properly trained to develop the necessary skills for running and obtaining meaningful results using the program.

In 1970, since there was a need for a tool to run the finite element method and constitutive models for geotechnical design, a group of the Technical University of Delft under the supervision of Professor Pieter A. Vermeer started a research related to this matter. Immediate cause for this research was the question from the Dutch Ministry of Public Works to find a solution to predict the possible movement of the famous Dutch Oosterschelde-Dam which protects an important part of the Netherlands against flooding.

This resulted in a software code that enabled elastic-plastic calculations for plane strain problems based on high-order elements. Later, the code was enriched and could deal with axi-symmetric problems too. It was in that time that the name PLAXIS, short for "Plasticity Axi-Symmetry" was used for the first time.

In 1986 a new phase of the research was started with the purpose to make the use of the Finite Element Method applicable to practicing geotechnical engineers. This ended in use of the codes at the universities for various projects. Later in 1993, it was started to use PLAXIS code outside the university (Kuory et al., 2002).

Nowadays, there are various types of codes of this software available for the users, such as PLAXIS 2D, Plax Flow, PLAXIS 3D, 3DFoundation, 3DTunnel.

5.2 Finite Elements and Nodes

There are different definitions for element and nodes in PLAXIS software which are aided to solve geotechnical problems. Therefore, these definitions are given in the following sections, from PLAXIS V8 Manual, (Kuory et al., 2002). The information given refers to mats since this is the foundation type used in this study.

5.2.1 Soil Element

As it is mentioned before, in finite elements method progressive mathematical procedures are applied by considering the mat foundation as a mesh including similar geometrical shapes which are called elements. There are two types of elements in this software which are both triangular; 15 nodes element with 12 stress points and 6 nodes element with 3 stress points, as illustrated in Figure 5.1.

The model chosen in this study is axisymmetric, since the shape of mat foundations are considered to be square. The element type chosen is 15-nodes with 12 sear points.

5.3 Input Program

Soil properties for each layer, type of modeling for each material and geometry are variable factors which are defined manually as input to the program. These data are included as initial soil parameters, coordinates of layers and various modeling which are defined in PLAXIS. The models of the software are explained in the following sections.

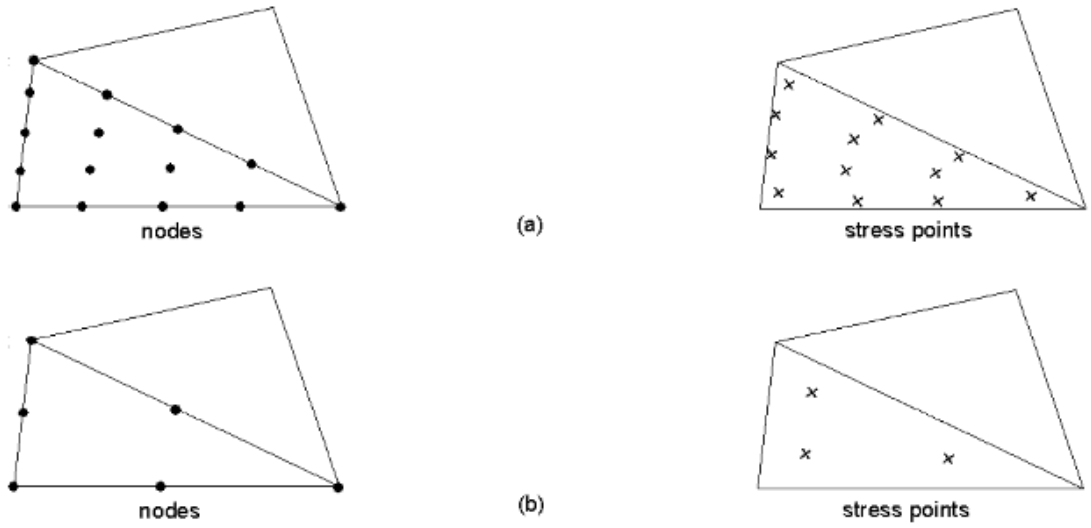

Figure 5.1. Element types in PLAXIS (Kuory et al., 2002).

5.3.1 Modeling of Soil Behavior

PLAXIS V8 can be used to study the soil behavior in various models including Linear, Mohr-Coulomb, jointed rock, hardening, soft soil and soft soil creep model. Mohr-Coulomb model is chosen in this study.

5.3.1.1 Linear Elastic Model (LE)

This model shows that Hooke's law of "isotropic linear elasticity" consists of Young's modulus and Poisson's ratio factors. It is a very initial model for simulating stiff material.

5.3.1.2 Hardening Soil Model (HS)

As it is mentioned in PLAXIS V8 manual this is an elastoplastic type of hyperbolic model, formulated in the framework of friction hardening plasticity. It is a hardening model that does not account for softening due to soil dilatancy and de-bonding effects. This model satisfied all soil types and is investigated invariable compaction when soil under of initial force.

5.3.1.3 Jointed Rock Model

This anisotropic elastic –plastic model is used to simulate the behavior of rock layers including stratification and particular fault directions. Plasticity can only happen in a

maximum of three shear directions. The intact rock is assumed to behave fully elastic with constant stiffness properties.

5.3.1.4 Soft Soil Model (SS)

This model is of the type of Cam-Clay used for normally-consolidated Clay-type soils and its best performance is when primary compression is considered.

5.3.1.5 Soft Soil Creep Model (SSC)

This model is used when the soil creep is considered. In fact, high degree of creep phenomenon occurs when we have soft soil such as normally consolidated clay, silt and peat are to be modeled (Kuory et al., 2002).

5.3.1.5 Mohr Coulomb Model (MC)

Mohr Coulomb model is another model which is widely used to investigate on primary soil behavior. This model needs five factors to approximate deformations which are experimentally determined. These factors are the common parameters in geotechnical engineering: Young's modulus, E, Poisson's ratio, ν, Friction angle, φ, cohesion, c, and dilatancy angle, ψ which are explained in previous sections (Kuory et al., 2002).

5.3.2 Types of Soil Behavior

Generally, PLAXIS simulates the effect of the load, which is the stress-strain relationship, as the main output of these simulations. Therefore, study on pore water is also vital, as it affects the stress-strain behavior of soils. For this aim, PLAXIS suggests three models which are introduced as follows.

5.3.2.1 Drained Behavior

This case is used when excess pore water pressure information is not important for simulating soil behavior. Thus it is applied on drained soil or coarse sand under low load.

5.3.2.2 Undrained Behavior

This model is used for a full development of excess pore water pressure, which occurs when a soil has low permeability as in clays or under a high rate of loading'. This parameter is a good choice for calculation of consolidation or secondary settlement.

5.3.2.3 Non-Porous Behavior

This case is used when initial and excess pore pressure information is not important for simulating soil behavior. Thus it is only applied for drained soil or coarse sand under low load (Kuory et al., 2002).

5.3.3 Model Generation

As it is seen in the discussions above soil properties has been applied for modeling the mat foundation. Data for different layers of soil were estimated earlier by Rockware software (see Appendix B) and correlated by NovoSPT. The simulated model of these data by PLAXIS V8 2D is depicted in Figure 5.2.

5.3.3.1 Mesh Generation

PLAXIS offers five types of mesh density which are, very coarse, coarse, medium, fine and very fine mesh. These meshes are generated spontaneously when selected the related button, but may be different shape in each cluster. In this study very fine mesh was selected as shown in Figure 5.2.

5.3.3.3 Initial Conditions

Initial conditions should be defined, after creating geometry model and generate mesh. PLAXIS specifies these by two ways: one way is defining initial water pressure and another way is generation of effective stress. In this study depth of water table is probed by information obtained from Department of Geology and Mining, and data from projects consulted by the Building Sciences Research Centre and the graduate theses on Geotechnical Engineering of the Eastern Mediterranean University.

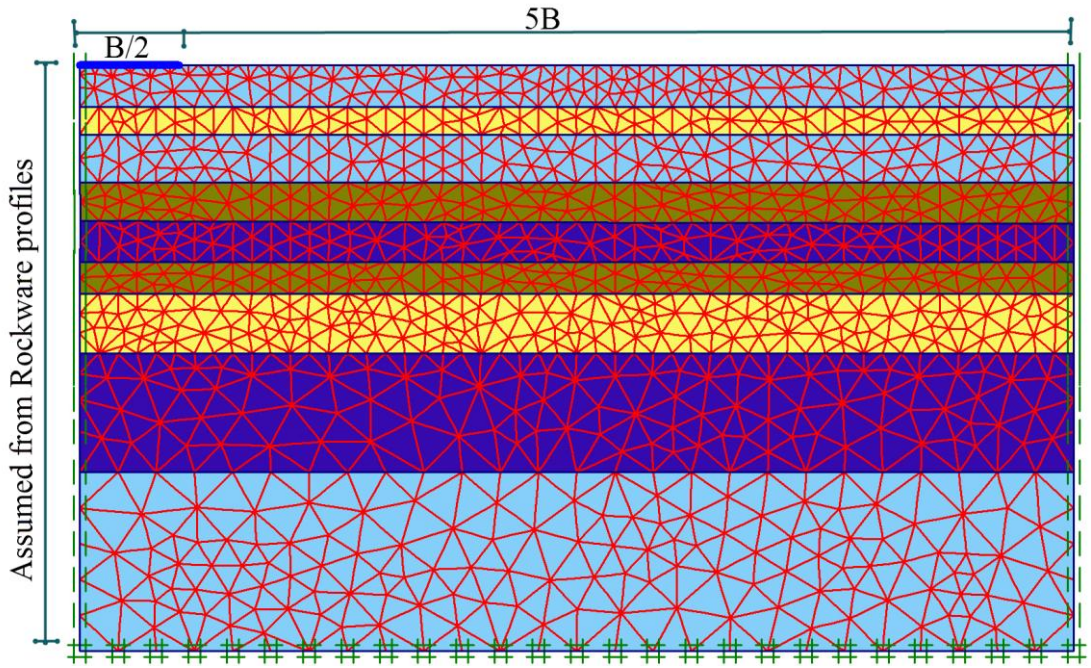

Figure 5.2. Mesh and geometry for finite element model

5.4 Calculation

After extraction of mesh and geometry, and also applying the initial conditions the calculation steps start. Program has offered three calculation types: plastic calculation, consolidation analysis and phi-c reduction (safety analysis). These steps are explained as follows.

a) Plastic calculation: used when plastic analysis is considered. Therefore it is not needed to analyze of excess pore pressures - time relationship in this type. This fact does not hold for creep model which is reflected in the software.

b) Consolidation analysis: This choice is selected when soil volume changes are considered. Therefore the software analyzes excess pore pressures - time relationship precisely. In the case when all excess pore pressures dissipate, it is required to choose the "minimum pore pressure" option.

In the current study "all excess pore pressure" is not reduced. Therefore "minimum pore pressure" is not applied. This shows that the consolidation settlement of the area is not finished during the time under assumption. "minimum

excess pore pressure" value is different for each soil but usually it is assume to be 1.

c) Phi-c reduction (safety analysis): This type is used when safety factor is determined. To achieve this aim "phi-c reduction" is defined after the steps. Hence it is not used for the first step. Also in order to perform "phi-c reduction" shear parameters should be decreased (Kuory et al., 2002).

5.5.1 Loading Types for Calculation Steps

After defining calculation type, the loading is selected. Load types are explained as follows.

a) "Staged construction": This kind of loading is the most significant type in the category of loading. In "staged construction" type PLAXIS allows to adjust the dimensional properties, load formation, water pressure distribution and reassigning of the material.

b) Total multipliers: This is utilized to determine the conclusive values of exterior loads. Finally as the last step of these proses, the exact conclusive value of external load should be used.

c) "Incremental multiplier": is chosen when the incremental value of exterior load should be used, (Kuory et al., 2002).

5.5.2 Calculation Steps

In this study, there are 6 calculation phases: the first phase is to calculate elastic settlement by "plastic analysis" method choosing the "stage construction" type. In the other phases, the calculation of the consolidation settlement is carried out as "Consolidation analysis" by "staged construction" load type. These phases are shown in Figure 5.3.

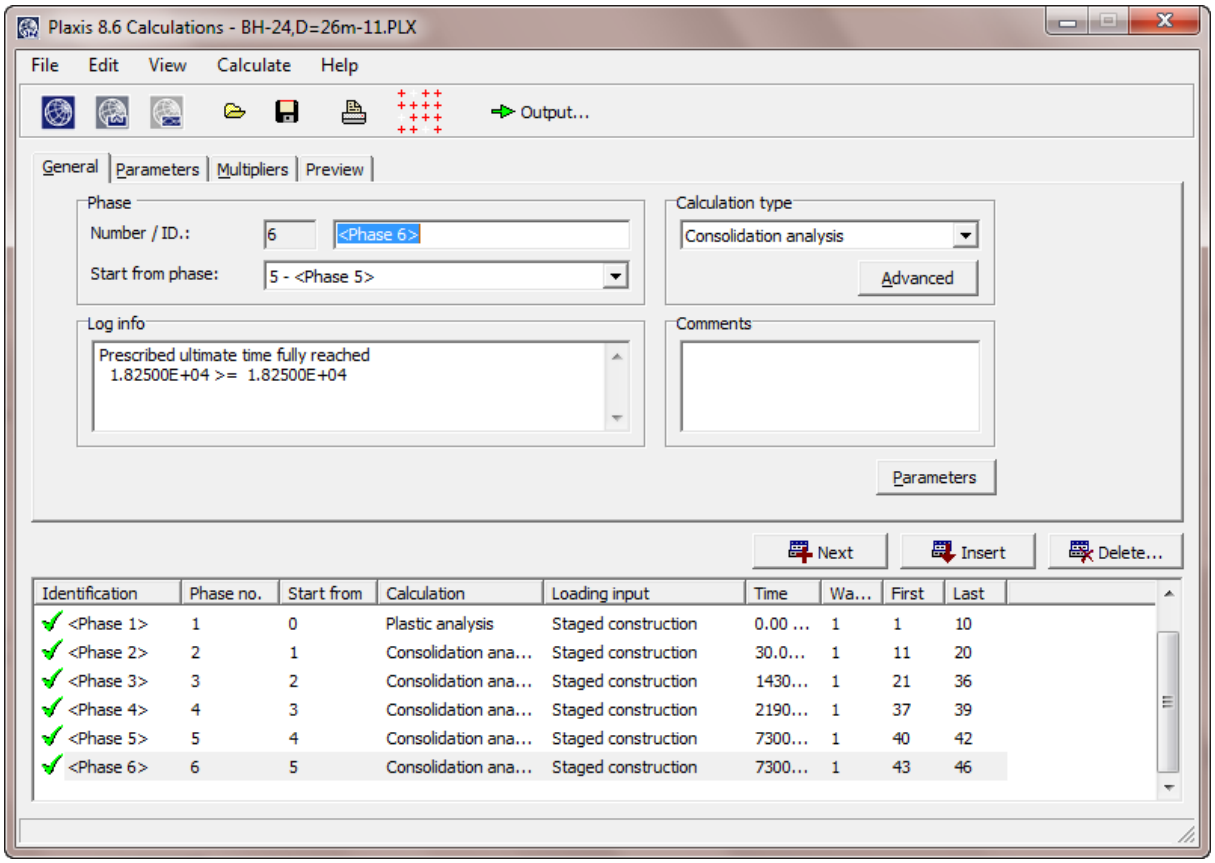

Figure 5.3. Calculation phases of this study.

5.6 Output

After calculation, some data can be extracted by PLAXIS software such as stresses, pore pressures and displacements for soils as a result of finite element analysis.

5.7 Curves

In the “calculation” tab there are some options to give results of the finite element model. This tool enables us to do comparison of finite element results obtained at different points. To achieve this, the points should be selected before performing calculation steps (Kuory et al., 2002).

Chapter 6

RESULTS AND DISCUSSIONS OF FINITE ELEMENT MODELLING

6.1 Introduction

In this chapter a database on the characteristics of soil which are categorized by NovoSPT and are analyzed and interpreted by a finite element method program (PLAXIS) have been discussed. The relationships obtained are plotted and a discussion including the comparison among them is done. Finally, a model describing the behavior of the soil is created using the curve fitting method of Matlab software.

Assessing he extracted bearing capacity data by NovoSPT and comparing the SPT-N values from each borehole, the location of borehole 24 is selected as the area with the weakest soil properties. Mat foundations of dimensions 10, 14, 18, 22 and 26 meters were selected and subjected to pressures ranging from 10 kPa to the stress level at which soil fails. The finite element mesh at failure is illustrated in Figure 6.1. The analysis of data are presented in Appendix D.

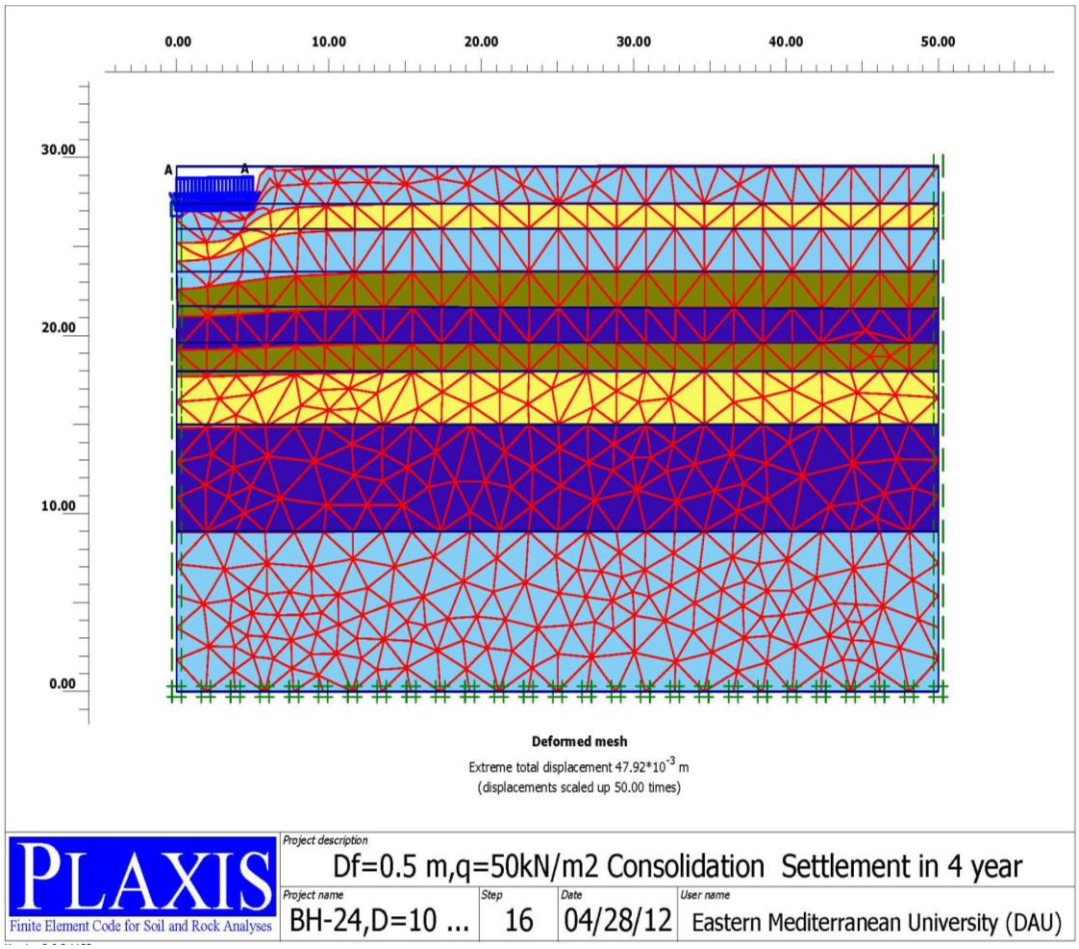

Figure 6.1.Deformation mesh.

6.2 Total Settlement Analysis

The results of the analysis of the settlement of 133 models at depths of 0.5, 1.0, 1.5 and 2.0 meters, are shown in the Figures 6.2 - 6.6 and given in Appendix D. The amount of settlement increases with the load per unit area. But with the increase of depth of the foundation, the magnitude of elastic settlement decreases, while consolidation settlement increases. This behavior can be explained as deeper the foundation depth closer will be the loaded area to the consolidating layer below the water table.

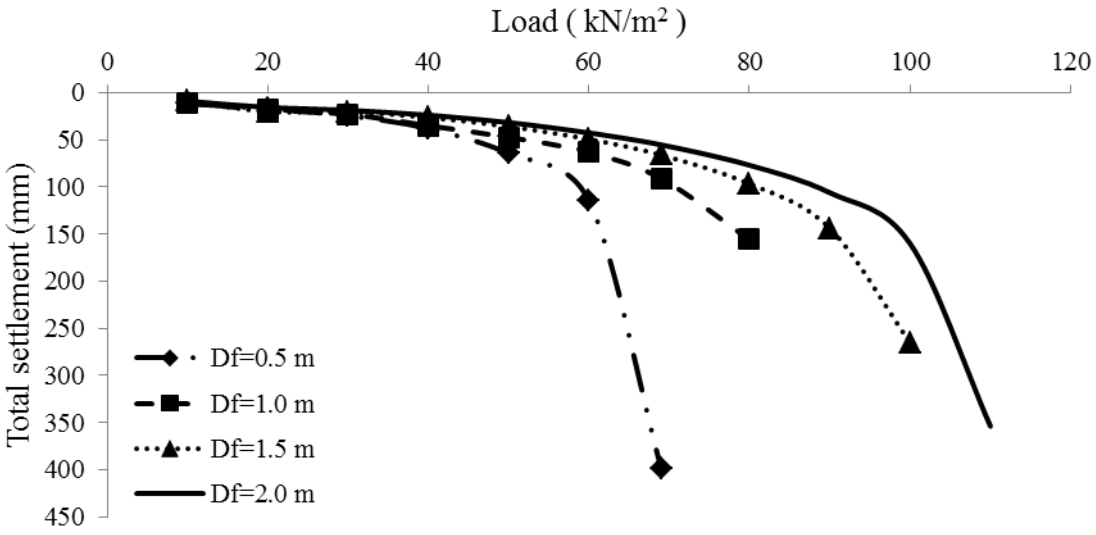

Figure 6.2. Total settlement in 50 years for 10 m footing width.

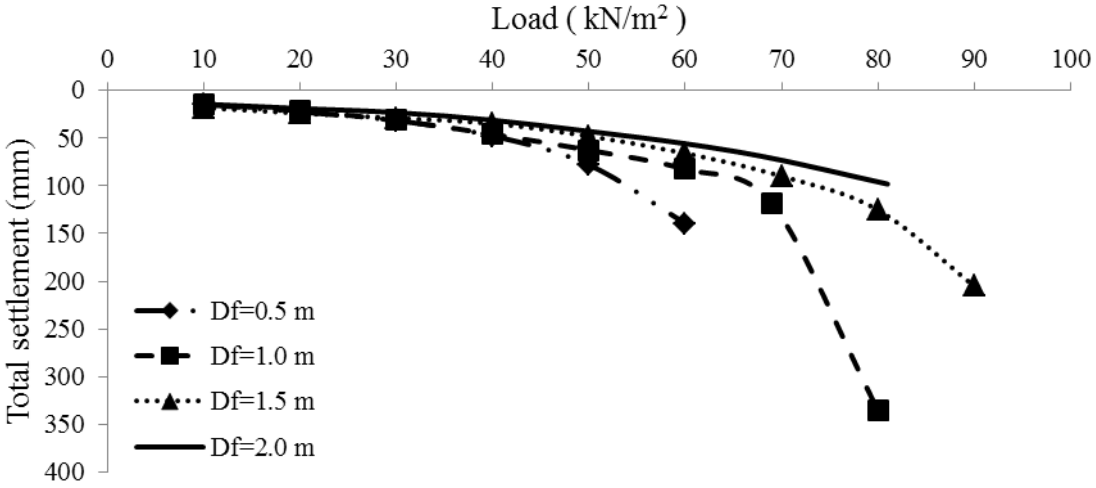

Figure 6.3.Total settlement in 50 years for 14 m footing width

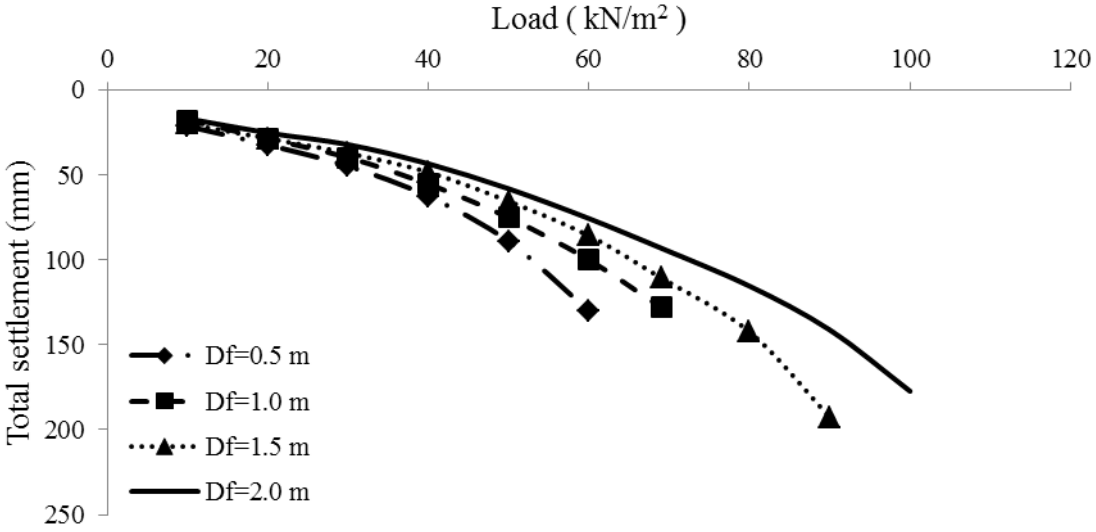

Figure 6.4.Total settlement in 50 years for 18 m footing width

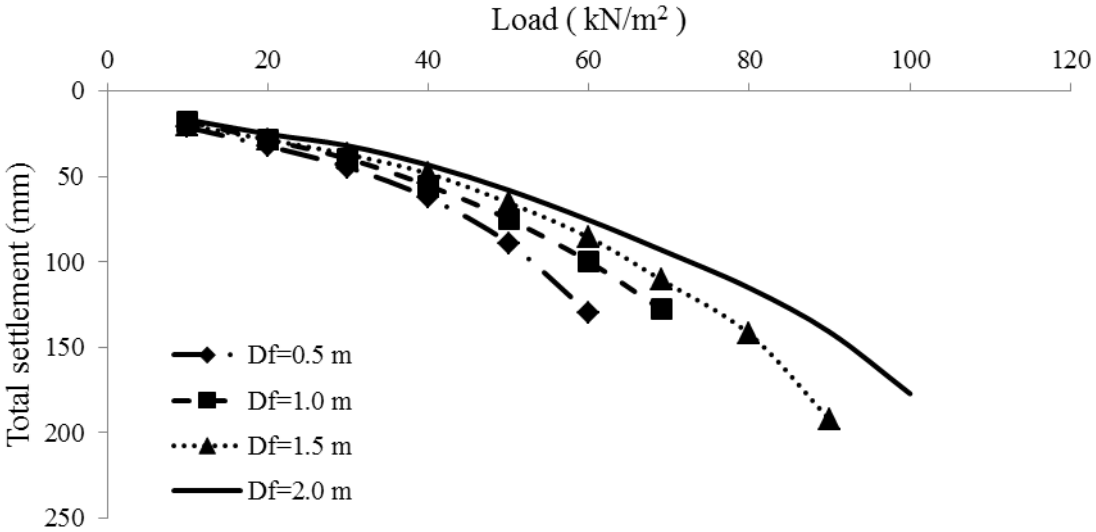

Figure 6.5.Total settlement in 50 years for 22 m footing width

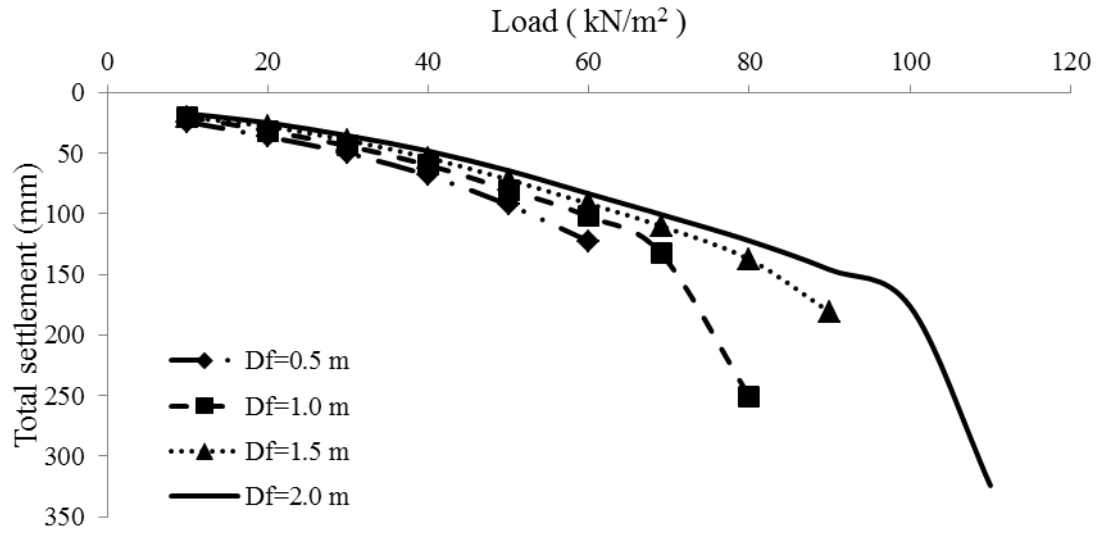

Figure 6.6.Total settlement in 50 years for 26 m footing width

6.3 Consolidation Settlement Analysis

Investigating the consolidation charts up to 50 years, one can conclude that the consolidation slows down yet progresses further in time. This is because mostly fine grained soils prevail in the region with a low coefficient of permeability. The analysis is stopped at 50 years due to the assumption that if the allowable life time of a building is considered as 10 years, it can be increased by renewing the building to a lifespan of 50 years. The consolidation analysis results are presented in Figure 6.7 and Appendix D.

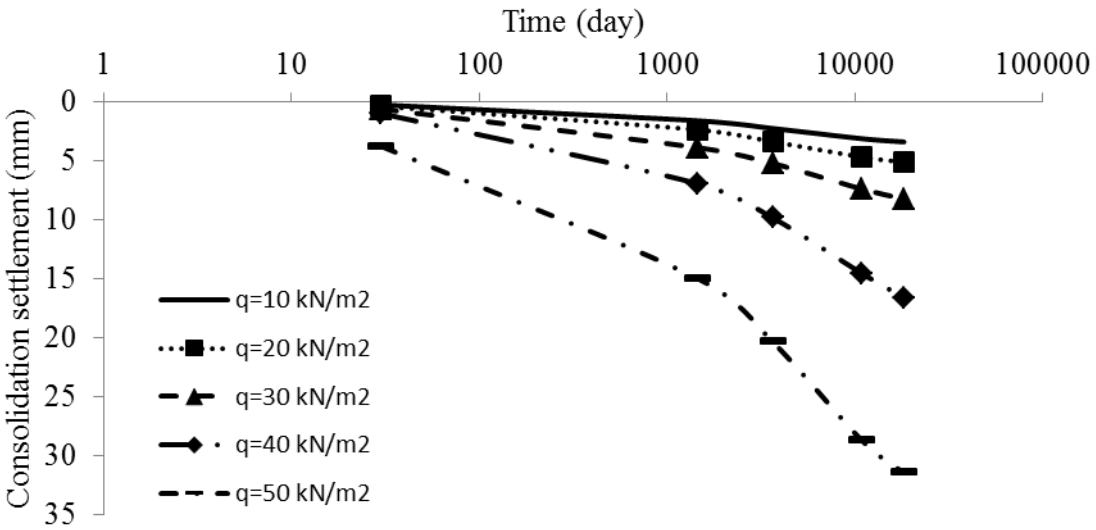

Figure 6.7.Consolidation settlement curves for 10 m footing width at 0.5 m depth.

6.4 Bearing Capacity Analysis

If the allowable total settlement is assumed to be 50 mm, based on Table 6.1 (Das, 2011), the magnitude of bearing capacity of the region corresponding to the depth and foundation dimension can range between 30 and 65 kPa. For a factor of safety of 3, the allowable bearing capacity varies between 10 and 20 kPa.

In the last part of this chapter, the extracted bearing capacity by NovoSPT (4 correlations), by general bearing capacity equation which is explained in Chapter 3 and also by PLAXIS are compared. The results are presented in Figure 6.8 as well as in Table 6.2. As it is clear from the figure there is a significant difference between the results of finite element analysis by PLAXIS and general bearing capacity equation.

Table 6.1. Recommendations of European Committee for Standardization on Differential Settlement Parameters, (Das B. , 2011)

Item	Parameter	Magnitude	Comments
Limiting values for serviceability (European Committee for Standardization, I 994a)	S_T	25 mm	Isolated shallow foundation
		50 mm	Raft foundation
	ΔS_T	5 mm	Frames with rigid cladding
		10mm	Frames with flexible cladding
		20mm	Open frames
	β	1/ 500	---
Maximum acceptable foundation movement (European Committee for Standardization, I 994b)	S_T	50	Isolated shallow foundation
	ΔS_T	20	Isolated shallow foundation
	β	≈1/ 500	---

ST: Tolerable settlement, ΔST: Tolerable differential settlement, β: Angular distortion

Moreover, Figure 6.8 depicts that while the Bowels and Meyerhof (1976) correlation has a small difference with general bearing capacity equation, Burland and Burbidge (1985) shows a noticed difference from the results found by PLAXIS. As a result, the most reliable correlation to calculate bearing capacity from SPT-N value can be concluded from this study to be Burland and Burbidge (1985) correlation. It should be noted that comparing the bearing capacity results, Perry (1977) and Terzaghi (1943) correlations have given significantly higher estimates than the other correlations.

Table 6.2.Comparison of bearing capacity values from different methods .

D_f (m)	B (m)	Burland and Burbidge (1985), for 25mm settlement	Terzaghi (1943)	Bowles/Meyerhof, (1976),for 25mm settlement	Parry (1977),for 25mm settlement	General BC Equation based on Meyerhof's formulae	General BC Equation based on de Beer and Hansen's formulae	Based on elastic settlement charts (for 25 mm settlement)	Based on total settlement charts in 50 years
0.5	10	46.76	479.43	91.63	195	83.51	83.90	43.19	44.58
	14	40.67	657.26	90.44	232.5	83.29	83.48	43.26	40.71
	18	33.68	835.09	89.78	252	83.18	83.25	29.30	35.62
	22	28.97	1012.92	89.37	252	83.10	83.10	25.02	32.92
	26	25.56	1190.75	89.08	252	83.05	83.00	22.39	30.04
1	10	46.76	535.55	93.13	195	92.30	93.43	56.25	54.45
	14	40.67	713.38	91.5	232.5	91.87	92.59	43.94	42.35
	18	33.68	891.21	90.61	252	91.64	92.12	36.85	38.59
	22	28.97	1069.04	90.04	252	91.49	91.82	32.60	36.57
	26	25.56	1246.86	89.64	252	91.39	91.61	30.64	30.04
1.5	10	46.76	591.66	94.63	195	101.09	102.95	65.18	60.40
	14	40.67	769.49	92.57	252	100.45	101.69	52.26	51.07
	18	33.68	947.32	91.43	252	100.10	100.99	44.14	54.69
	22	28.97	1125.15	90.71	252	99.88	100.54	40.05	40.94
	26	25.56	1302.98	90.21	252	99.72	100.23	38.01	37.47
2	10	52.34	647.78	96.13	195	109.88	112.47	72.63	65.33
	14	40.67	825.61	93.63	252	109.03	110.79	59.27	55.42
	18	33.68	1003.44	92.25	252	108.56	109.85	41.53	49.85
	22	28.97	1181.27	91.38	252	108.26	109.26	47.48	44.51
	26	25.56	1359.09	90.78	252	108.05	108.85	45.56	41.23

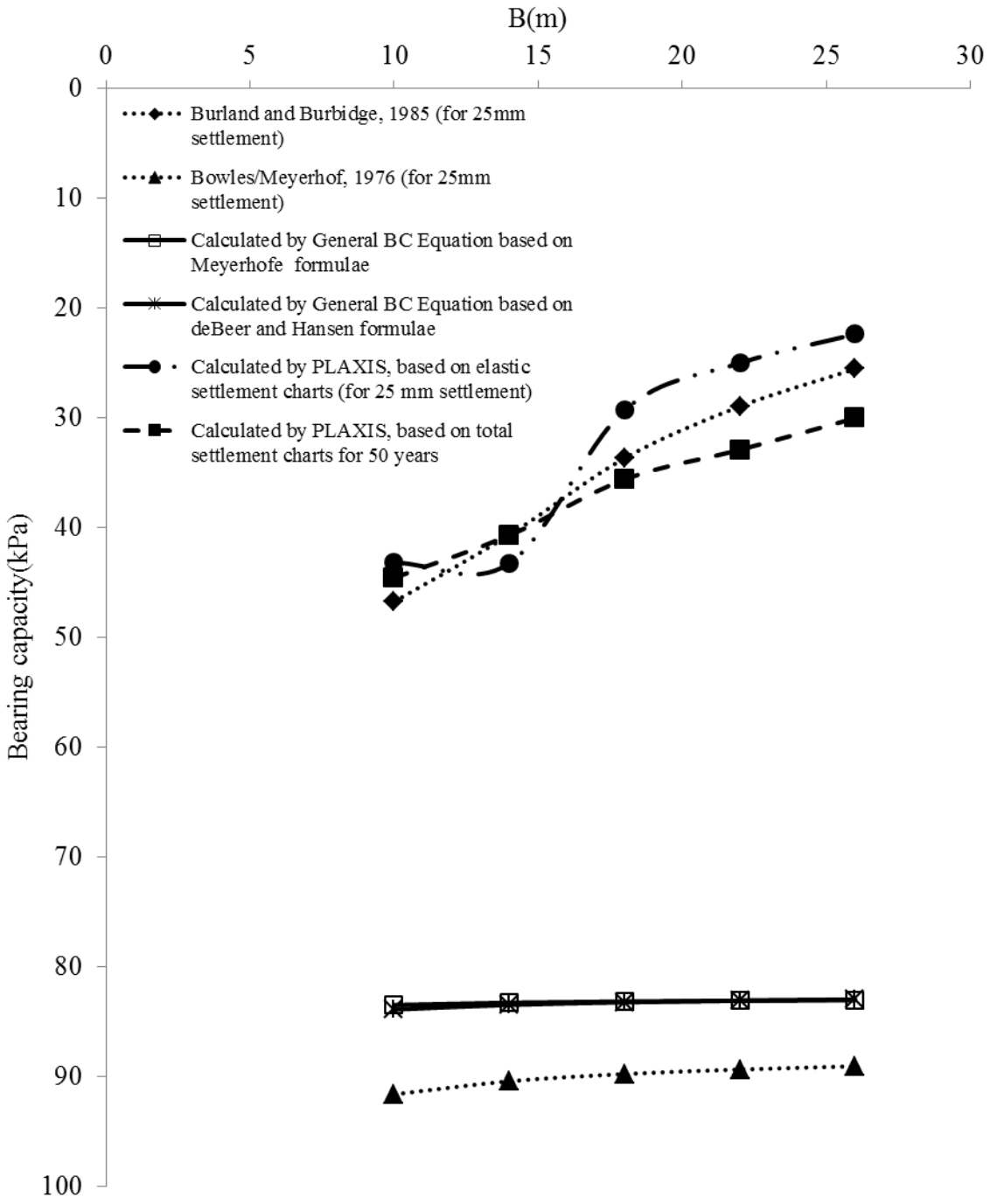

Figure 6.8. Comparison of bearing capacity values from different methods .

As can be observed in Figure 6.8, the bearing capacity approaches without settlement control overestimate the bearing capacity. However, Meyerhof (1976) approach limiting settlement to 25 mm also gives similar results. Whereas finite element method gives much smaller values and Burland and Burbidge (1985) is the only method discussed herein, which is in good agreement with these results.

Figure 6.9 shows the comparison of bearing capacity for different foundation depths. As it can be seen from this figure, bearing capacity increases with depth. To justify this fact it should be noted that soil consolidates under higher loads at deeper foundation depths, hence becomes denser. Therefore, it is natural to expect an increase for bearing capacity as well.

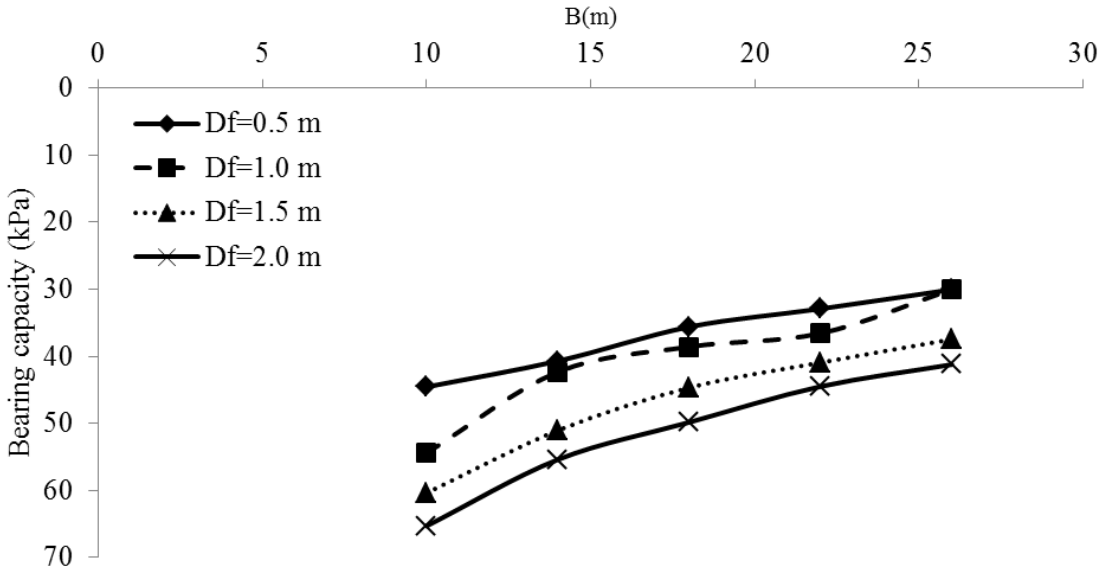

Figure 6.9. Comparison of bearing capacity values at different foundation depths .

6.5 The Effect of Water Table Level on Settlement

Water table level is one of the important factors which affect settlement. The increase or decrease of the water table level can occur either as a consequence of natural events such as raining/draught or as a result of mankind activities like pumping water used for personal or industrial purposes.

In this study, the measured water level is equal to 2.30 m. The variation of water level is considered to be ±0.5. Therefore, according to Figure 6.10 it is clear that settlement increases regardless of the variation of water level. The reason can be justified by considering the fact that while water level drops the effective stresses increase which leads to an increase in settlement. On the other hand when the water level rises, the fine grained soils become submerged and therefore able to consolidate. Hence the settlements increase. This can be considered as a hazard for foundations mainly due to possibility of

large differential settlements, which may cause detrimental damage to the structures.

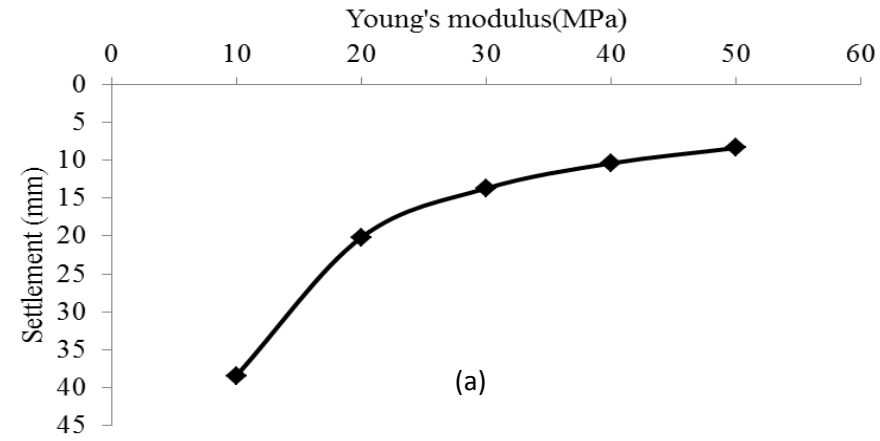

(a)

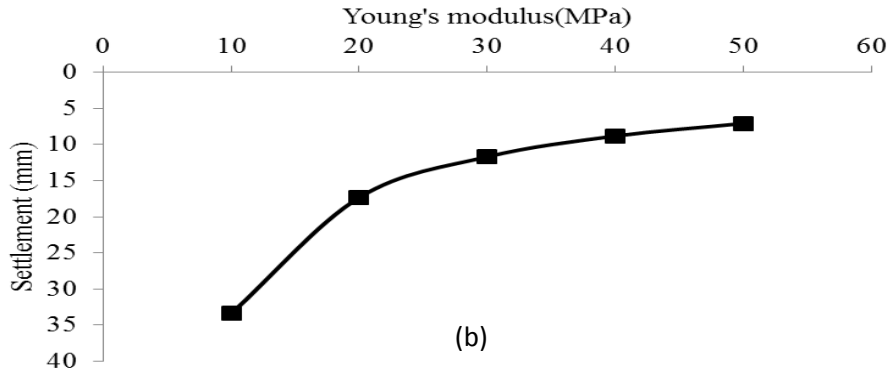

(b)

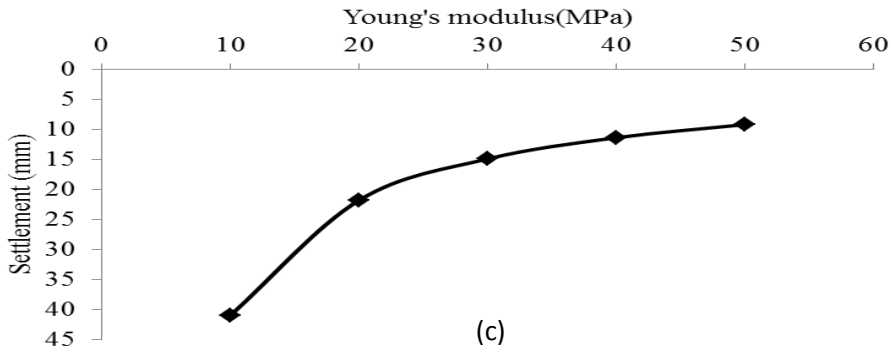

(c)

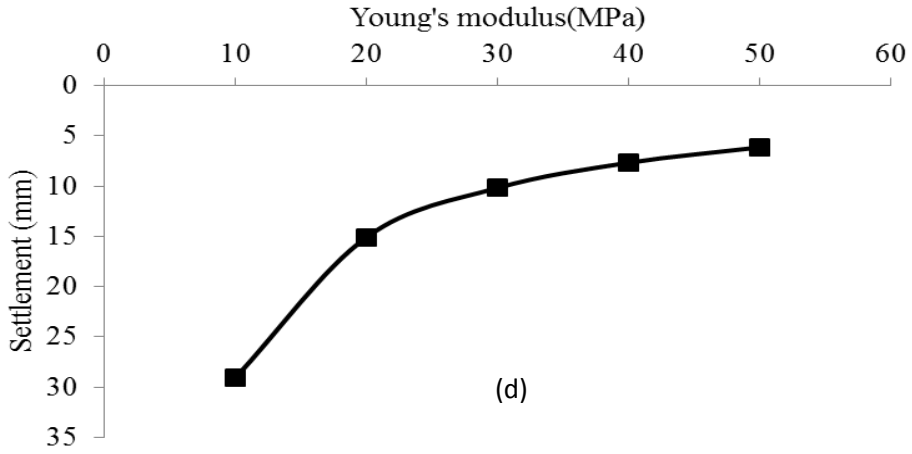

(d)

Figure 6.10. Foundation settlements with respect to water table level at foundation depths of (a) 0.5 m, (b) 1.0 m, (c) 1.5 m and (d) 2.0 m.

6.6 The Effect of Variations of Modulus of Elasticity

Modulus of elasticity is one of the parameters, the variation of which can have a great impact on settlement. There are many ways to modify the modulus of elasticity, such as by soil mix and jet grout methods. In mix method the soil is mixed with another soil type with higher modulus of elasticity. Thus increasing the stiffness of the soils on which structures are to be built. In jet grout method, a grout is injected into soil by a special instrument as shown in Figure 6.11. It should be noted that in some cases both methods can be applied together.

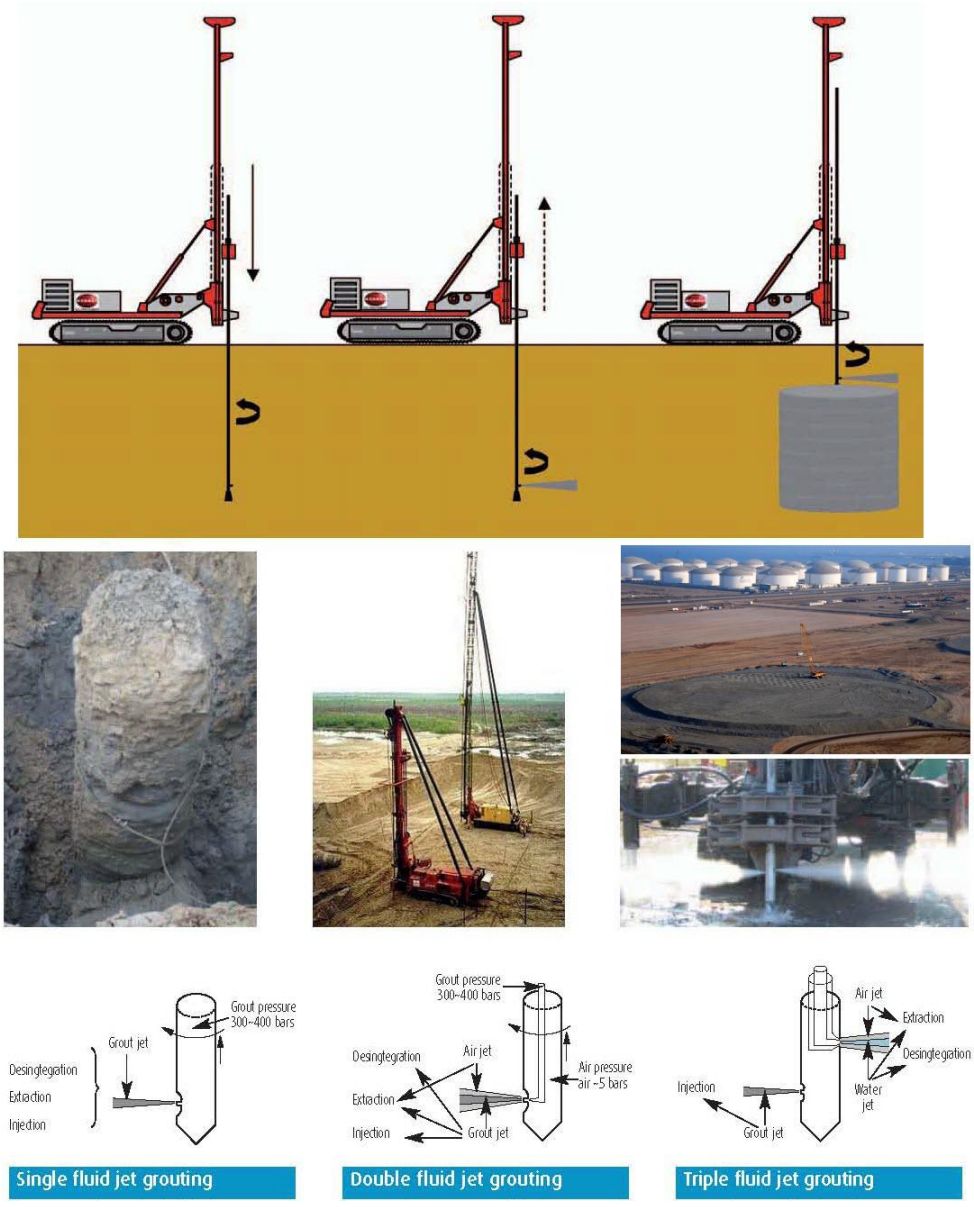

Figure 6.11.Jet grouting method (Menard Co., 2011)

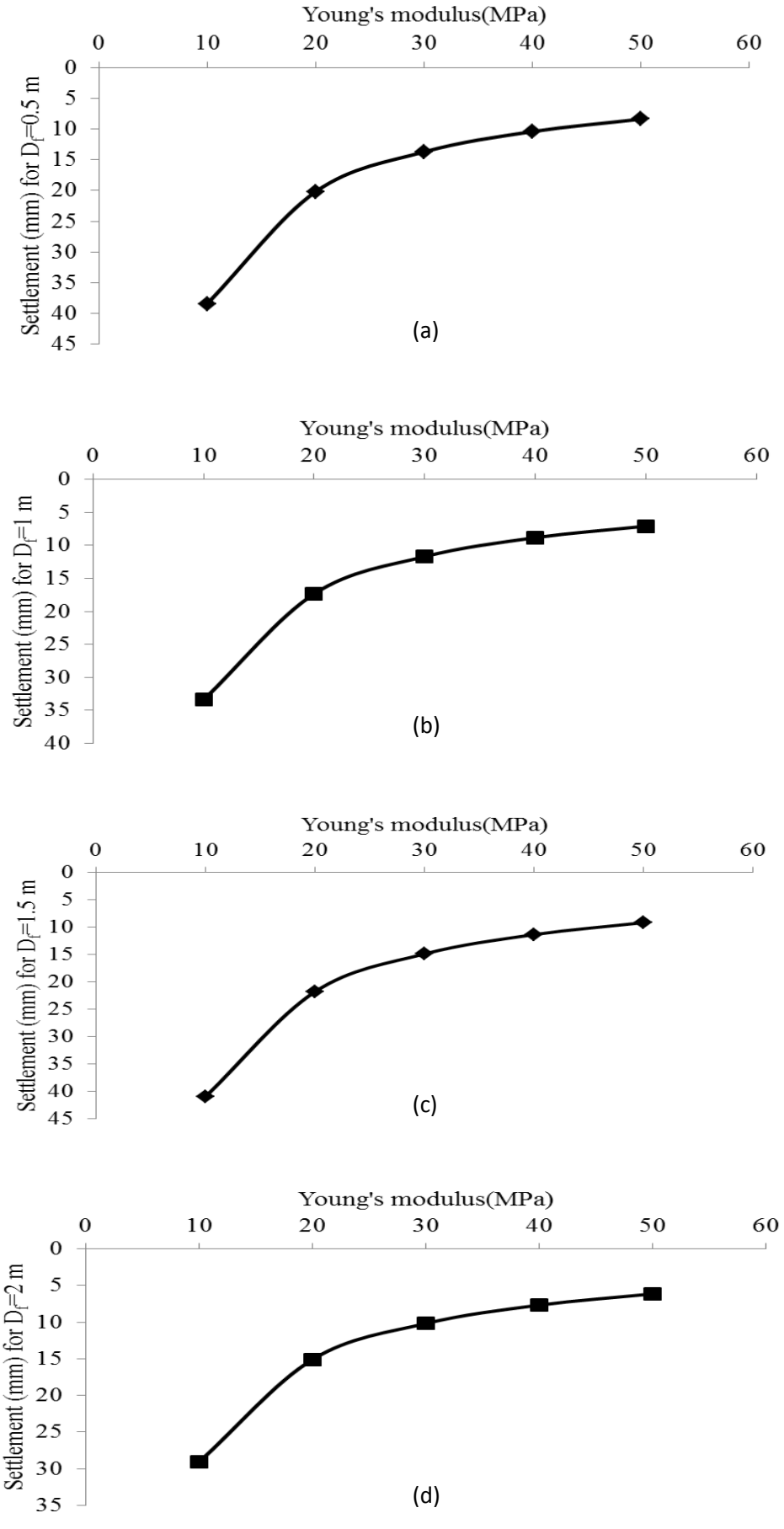

Figure 6.12. The relationship of settlement with modulus of elasticity at foundation depths of (a) 0.5 m, (b) 1.0 m, (c) 1.5 m and (d) 2.0 m.

As it is observed in Figure 6.12, the settlement of the soils in the region decreases with the increase of modulus of elasticity.

6.7 Mathematical Model of Settlement of Tuzla Soils based on SPT-N

Matlab is a multipurpose powerful tool which enables research in various fields to perform time consuming calculations in a percent of a second. This useful software also possesses various tool boxes. Curve fitting is one of the most frequently used tool box of Matlab. This tool box is special for fitting numerical data which ranges over an independent interval.

There are various categories of different types of functions available in curve fitting tool box which enable us to fit the data to a curve passing nearly the same positions on the plane of considered data, and also take the corresponding mathematical function. Therefore, there are two possibilities in Matlab in order to study the behavior of data: that are discussing the fitted curve which is known as graphical method as well as analyzing the mathematical known formula which is called theoretical method. In order to fit some data the first step is to choose a function which can be either selected from the available category in tool box or defined by the user in "Custom Equations" option, provided that the data matches with the initial conditions of the function. The available functions in this software are classified as "Exponential", "Fourier", "Gaussian", "Polynomial", "Power", "Rational", "sum of sine functions", and "Weibull". One can find a brief explanation of these categories in Table 6.3.

Table 6.3. The available functions in Matlab for curve fitting (Mathwork, 2011).

Function Name	Type	Comment
Exponential	$ae^{(bx)}$	a,b are constant
Fourier	$a_0 + a_1\cos(wx) + b_1\sin(wx)$	a_0 ,a_1,w and b_1 are constant
Gaussian	$a_1e(-((x-b_1)/c_1)^2)$	a_1,$b_1$andc_1 are constant
Polynomial	$P_nx_n + P_{n-1}x_{n-1}+\ldots+P_1x+P_0$	$P_n\ldots P_0$ are constant
Power	ax^b	a,b are constant
Rational	P(x) /Q(x)	P(x) and Q(x)are polynomials and $Q(x) \neq 0$
Weibull	$abx^{(b-1)}e^{(-axb)}$	a,b are constant

In this research we fit the extracted data related to borehole 24 by PLAXIS by applying the mentioned tool box. It should be mentioned that this borehole is a representative one, chosen out of 43 existing boreholes.

6.7.1 Choosing the Best Fitted Function

It is not only possible to study one data class in curve fitting tool box, but also to compare different data categories with at least one common characteristic. Besides one can fit a set of data with various functions simultaneously and select the best curve among them as well as its corresponding formula.

Matlab provides two ways in order to compare the fitted data and find the best formulae. The first way is to use some statistical indexes available in “Goodness of fit” section. This section consists of “The sum of squares due to error (SSE)”, “R-Square”, “Degrees of freedom adjusted R-Square”, “Root Mean Squared Error (RMSE)” which are explained in Table 6.4.

The second way in order to determine the goodness of data fitting is to analyze a type of graph which is available in “Residuals” option from the view menu. In this method for

each fitted curve a graph including some straight lines which join the successive points together is sketched separately. Then comparing these straight lines which are called residues, the most similar graph to a straight line indicates the best fitting. To achieve the best curve, we applied various kinds of the mentioned functions above to the chosen data. Comparing both the goodness of fit and residuals of the outcomes, one can determine that the best function in order to justify the behavior of our data is exponential function. Figure 6.13 and Table 6.5 confirm this fact. According to Table 6.5, since the values of indexes for the exponential function are the nearest values to the expected numbers for a good fitting, one can conclude that the exponential model is the best indicator of the behavior of the data under study.

Besides the theoretical model, also one can observe this behavior by comparing different fitted curves applied to the data. To distinguish the best curve among the sketched graphs, the residual graphs can be studied as well as the graphs themselves. To do this, comparing the corresponding residuals the best curve is the curve whose residuals is the most similar to a straight line.

Table 6.4. Goodness of fit indexes (Mathwork, 2011)

Name	Description	Formula
SSE	Total deviation of the response values from the fitted curve to the response values.	$\sum_{i=1}^{n} w_i(y_i - \hat{y}_i)^2$
SSR	Squares of the regression.	$\sum_{i=1}^{n} w_i(\hat{y}_i - \bar{y}_i)^2$,
SST	Total sum of squares.	$\sum_{i=1}^{n} w_i(y_i - \bar{y}_i)^2$,
R-Square	Square of the correlation between the response values and the predicted response values.	$\frac{SSR}{SST} = 1 - \frac{SSE}{SST}$
Adjusted R-Square	Applies the R-square error according to the residual degrees of freedom.	-------
RMSE	Fit standard as well as the standard error of the regression.	$RMSE = s = \sqrt{MSE}$
MSE	square error or the residual mean square	$\frac{SSE}{v}$
v	Residual degrees of freedom is defined as the number of response values n minus the number of fitted coefficients m estimated from the response values.	$V = n - m$

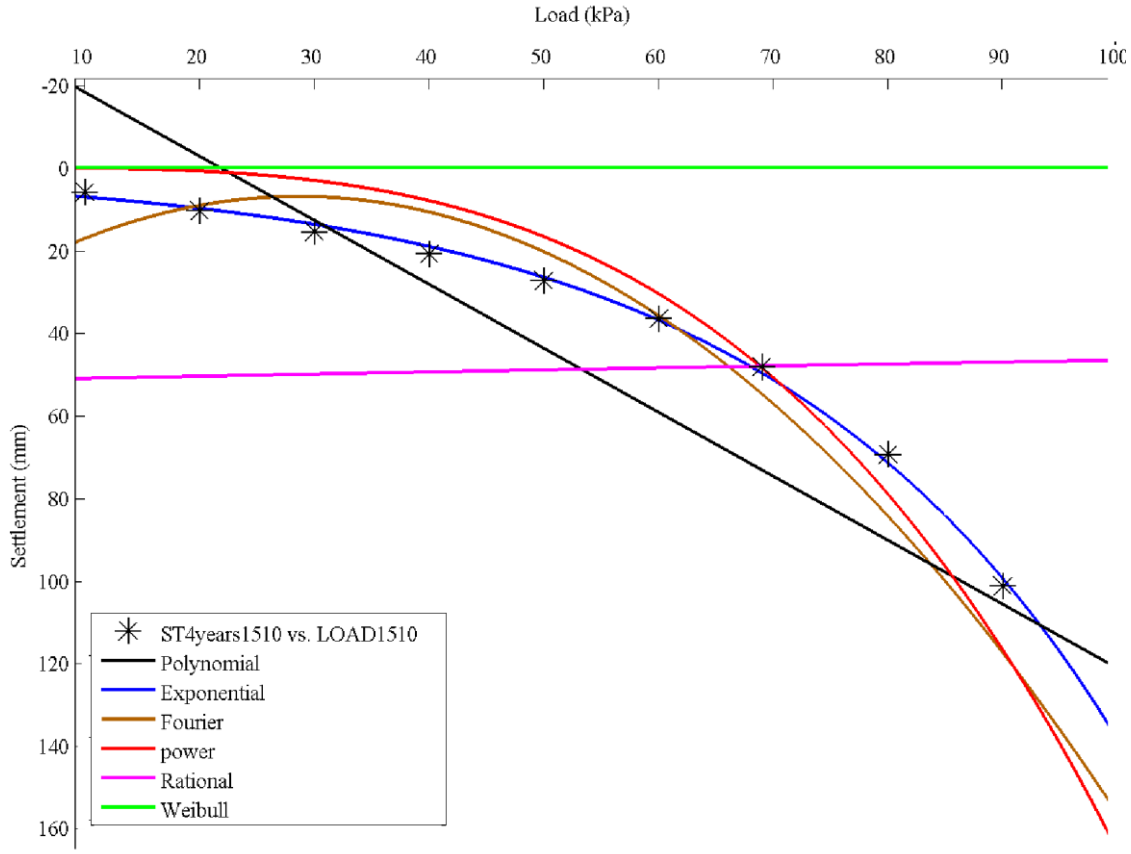

(a)

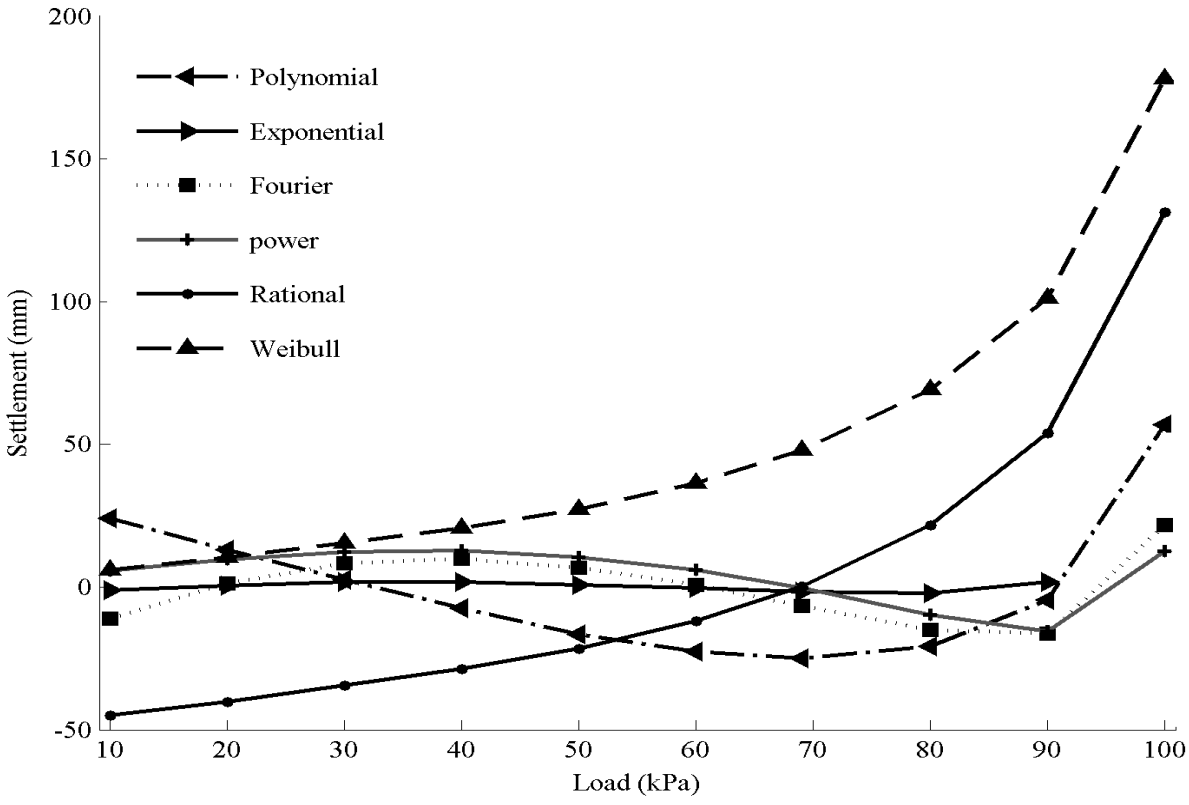

(b)

Figure 6.13.Choosing best fit by comparing different graph types through residuals: (a) Fitting data, (b) Residual Curves.

Table 6.5. Goodness of fit indexes for different types of curves

Model	SSE	R-square	Adjusted R-square	RMSE
Exponential	18.41	0.9976	0.9973	1.622
Fourier	1350	0.9473	0.9209	15
Polynomial	5917	0.769	0.7401	27.2
Power	1087	0.9576	0.9522	11.66
Rational	2.692e+004	-0.05137	-0.1828	58.01
Weibull	5.192e+004	-1.027	-1.281	80.56

According to the Figure 6.13 the exponential function possesses the most straight residual.

6.7.2 Interpreting the Selected Model

Regarding the discussion above we offer the exponential model below for the observed data:

$$S_T(q) = ae^{bq} \qquad (6.1)$$

Where Table 6.2 is bearing capacity, $S_t(q)$ is total settlement and a, b are real numbers.

In order to calculate bearing capacity, q, as it is mentioned before in Table 6.2, we use the average ratio of general bearing capacity over the extracted bearing capacity by PLAXIS; that is 2.25. Consequently q here is obtained by dividing calculated bearing capacity by general equation with 2.25. Also to define the error of the suggested function, we consider an error coefficient, c, which is obtained from comparing the solutions of the found equation with the available settlements. It is worth stressing that c ranges

depending on q. As the result of these assumptions the main equation can be written as below:

$$S_T(q) = c.\,a e^{\frac{bq}{2.25}} \quad (6.2)$$

since "a" and "b" are dependent on both Df and B, the variations of these coefficients over ranging Df and B is studied. A summary of this observation is enclosed in Table 6.6. To achieve this aim also we model Df, B, and "a" in one phase and Df, B, and "b" in another phase separately and three dimensionally. Observing the obtained results leads to the fact that Df and B satisfy the general formula of a plane in 3- dimensional space which is shown in Figure 6.14 and can be defined as below,

$$f(D_f, B) = P00 + P10.D_f + P01.B \quad (6.3)$$

Where P00, P10, P01 are real numbers, which are available in details in Table 6.7. Also according to the sketched graphs in Figures 6.15 to 6.20, these coefficients are obtained from polynomials with degree four with the general formula below:

$$P_x(t) = P_a t^4 + P_b t^3 + P_c t^2 + P_d t + P_e \quad (6.4)$$

where, Pa, Pb, Pc, Pd, and Pe are coefficients of the mentioned polynomials which are represented in Tables 6.8- 6.9. Therefore Equation 6.5 can be obtained according to Equations 6.2-6.4, which is dependent on time, width and depth of foundation depicted as below.

$$S_T(q, D_f, B, t) = c.\left[(P00_a(t) + P10_a(t).D_f + P1_a(t).B)\, e^{\frac{P00_b(t)+P10_b(t).D_f + P1_c(t).B\, q}{2.25}}\right] \quad (6.5)$$

It should be noted that by establishing this new result, the best fit of the exponential function which is mentioned at the first of this section and is beyond of the scope of this research, can be related to time parameter indirectly which requires much more study on the whole database including 43 boreholes.

Table 6.6. The calculated coefficients “a” and “b” with respect to depth and width of foundation.

D_f	B	30 days		4 years		10 years		30 years		50 years	
		a	b	a	b	a	b	a	b	a	b
0.5	10	3.02	0.05229	3.43	0.05462	3.79	0.05446	4.10	0.0556	4.96	0.05209
1	10	2.93	0.04152	4.15	0.04079	4.71	0.04062	5.80	0.03984	6.22	0.03988
1.5	10	3.20	0.03458	5.09	0.03303	5.72	0.03314	6.23	0.03393	6.51	0.03415
2	10	2.74	0.03322	4.69	0.03167	5.94	0.02978	5.56	0.03265	5.80	0.03287
0.5	14	5.15	0.04521	5.99	0.04664	6.22	0.04785	6.49	0.04981	6.77	0.05012
1	14	2.67	0.0482	3.61	0.04797	3.11	0.05233	2.03	0.06154	1.57	0.06653
1.5	14	4.02	0.03574	5.76	0.0356	6.38	0.03587	7.24	0.03608	7.85	0.03576
2	14	4.48	0.03006	7.51	0.02836	8.44	0.0282	9.85	0.02782	10.78	0.02732
0.5	18	8.13	0.03807	9.52	0.03952	10.11	0.04016	11.10	0.0337	11.38	0.04136
1	18	7.91	0.03157	10.27	0.0322	11.06	0.03284	12.10	0.411	13.20	0.03327
1.5	18	6.77	0.02988	10.24	0.02877	11.37	0.02889	13.07	0.02872	14.34	0.02816
2	18	6.44	0.02656	10.19	0.02565	11.41	0.02557	13.05	0.02547	13.98	0.02528
0.5	22	11.61	0.03021	13.14	0.03276	13.90	0.03357	14.76	0.035	15.13	0.03576
1	22	8.67	0.03102	10.59	0.03268	11.30	0.03346	11.92	0.03497	11.69	0.03639
1.5	22	8.72	0.02647	10.21	0.03208	12.13	0.03027	14.79	0.02833	16.55	0.02721
2	22	8.18	0.02407	12.53	0.02388	14.20	0.02369	16.61	0.02331	17.90	0.02307
0.5	26	14.19	0.02614	16.70	0.02789	17.91	0.02846	19.03	0.03005	19.67	0.03067
1	26	18.09	0.029	16.57	0.02469	16.74	0.02635	17.98	0.02781	18.09	0.029
1.5	26	10.26	0.024	14.51	0.0244	16.09	0.02469	18.36	0.02485	19.68	0.02467
2	26	9.14	0.02276	14.43	0.02234	16.58	0.02212	19.44	0.02184	20.92	0.02163

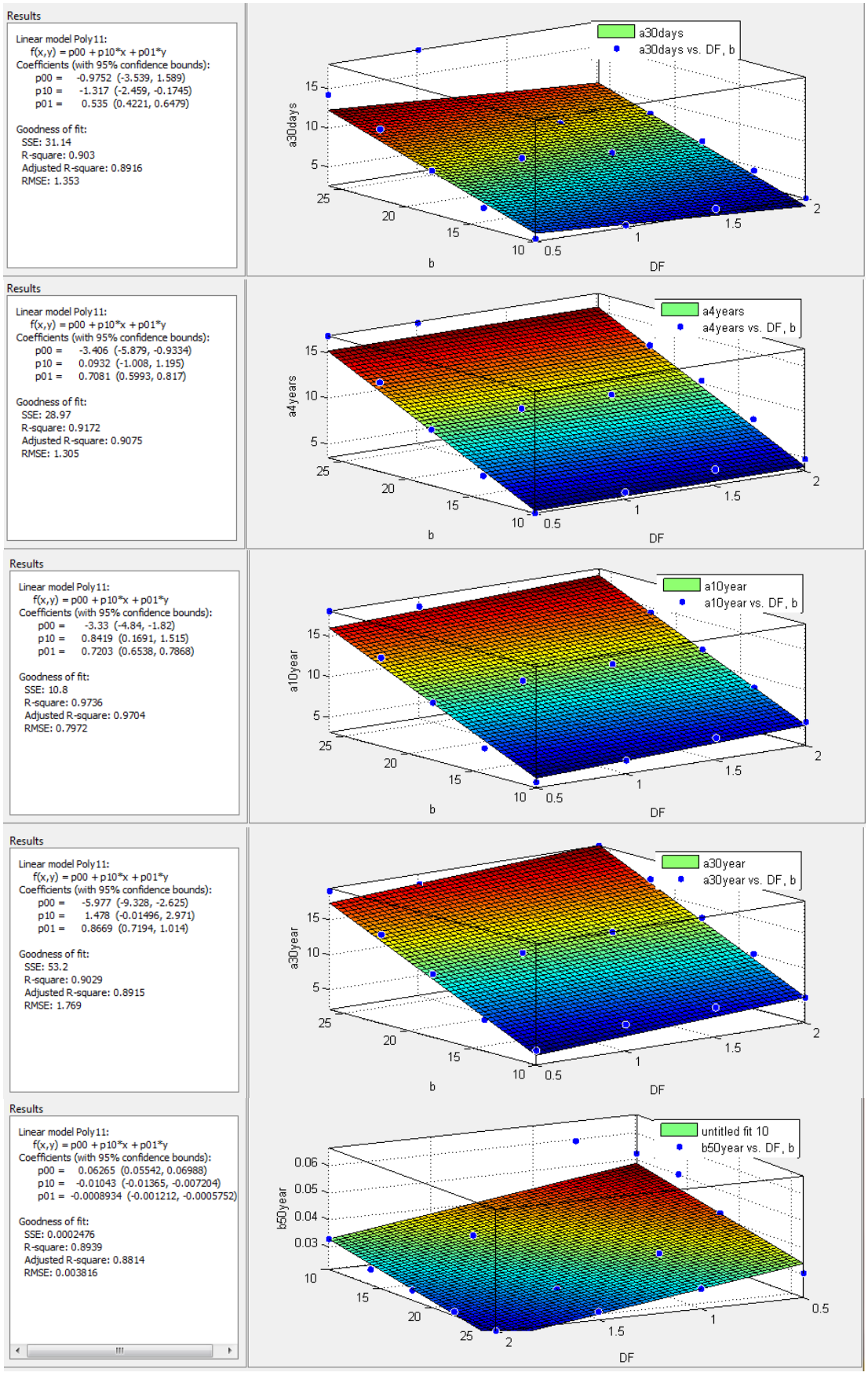

Figure 6.14. Defining coefficients “a” and “b” by sketching 3D planes to scale

Table 6.7. The calculated coefficients P00, P10, P1 for both a and b based on time.

Time	a			b		
	P00	P10	P1	P00	P10	P1
30	-0.9752	-1.317	0.535	0.03243	-4.10E-03	-0.00537
1460	-3.41	0.09	0.71	6.28E-02	-9.32E-03	-9.92E-04
3650	-3.33	0.8419	0.7203	0.06408	-1.03E-02	-0.00098
10950	-5.977	1.478	0.8669	0.05905	-0.0257	-0.00105
18250	-6.484	1.943	0.9002	0.06265	-0.01043	-0.00089

Table 6.8. The coefficients for parameter "a".

$P_x(t)$	P_a	P_b	P_c	P_d	P_e
P00	2.829E-015	-9.337E-011	9.011E-007	-0.002851	-0.8905
P10	-1.803E-016	6.026E-012	-5.971E-008	0.0001988	0.5291
P1	-6.707E-016	2.452E-011	-2.89E-007	0.001363	-1.358

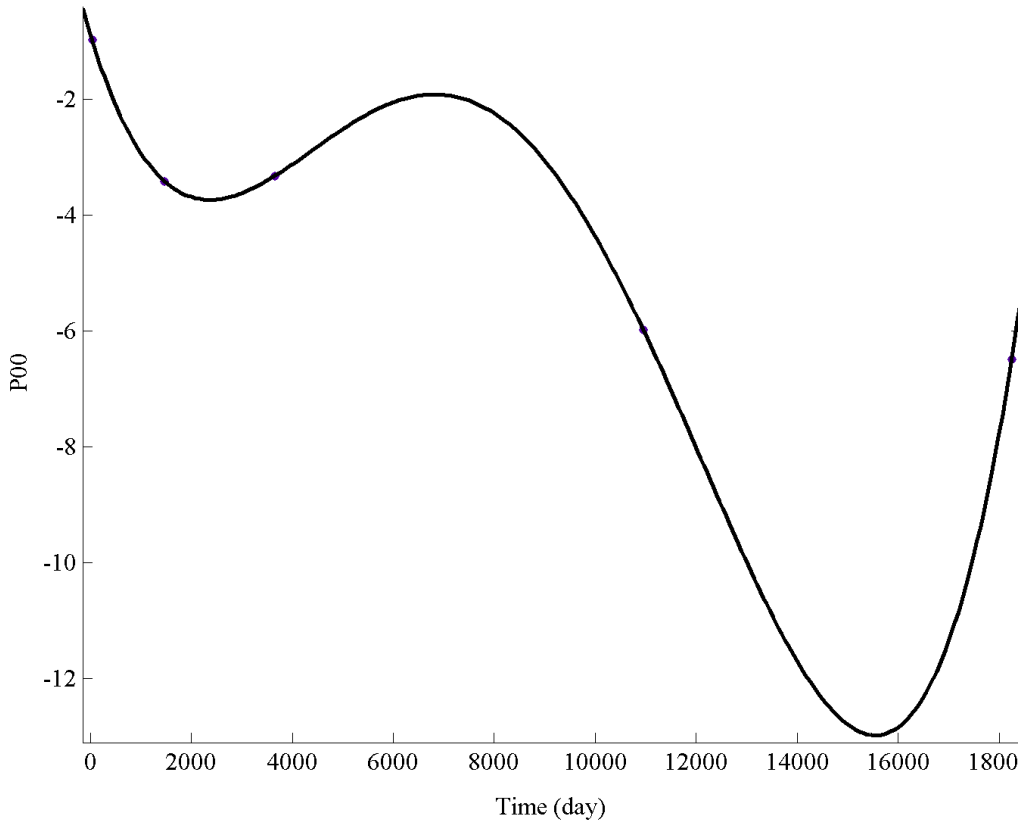

Figure 6.15. The curve fitting of the coefficients of P00 for parameter "a"

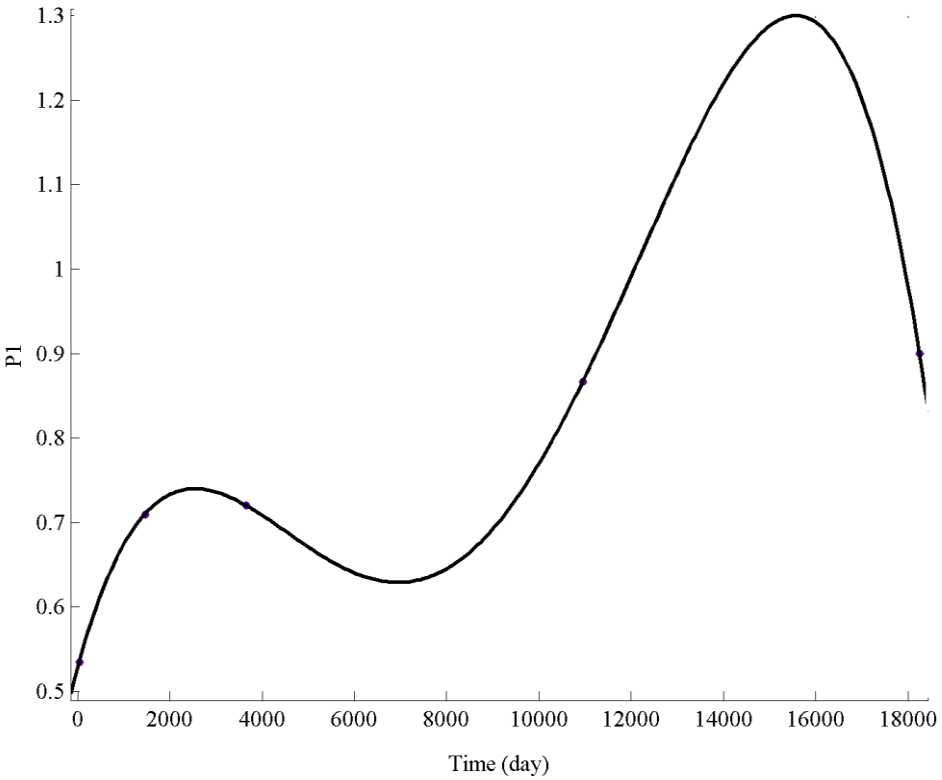

Figure 6.16. The curve fitting of the coefficients of P1 for parameter “a”

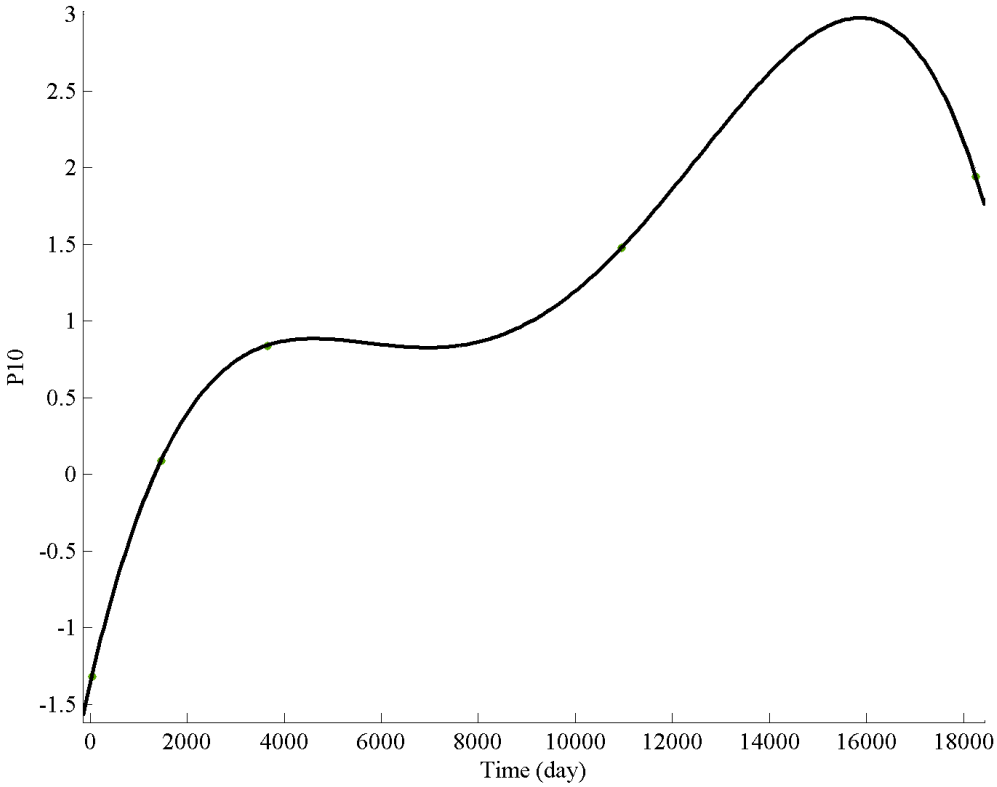

Figure 6.17. The curve fitting of the coefficients of P10 for parameter “a”

Table 6.9. Coefficients for parameter “b”.

$P_x(t)$	P_a	P_b	P_c	P_d	P_e
P00	-2.73E-017	9.494E-013	-1.001E-008	3.418E-005	0.03141
P10	-4.212E-018	1.447E-013	-1.498E-009	4.989E-006	-0.005513
P1	6.84E-018	-2.071E-013	1.806E-009	-5.913E-006	-0.003924

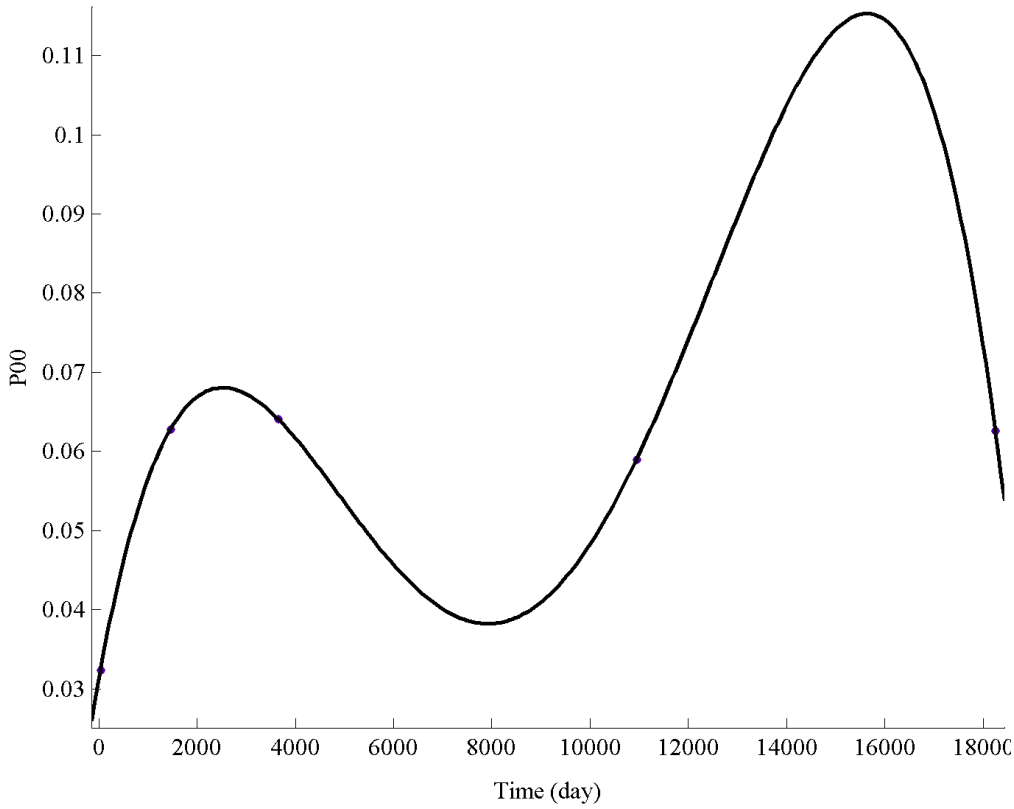

Figure 6.18. The curve fitting of the coefficients of P00 for parameter “b”

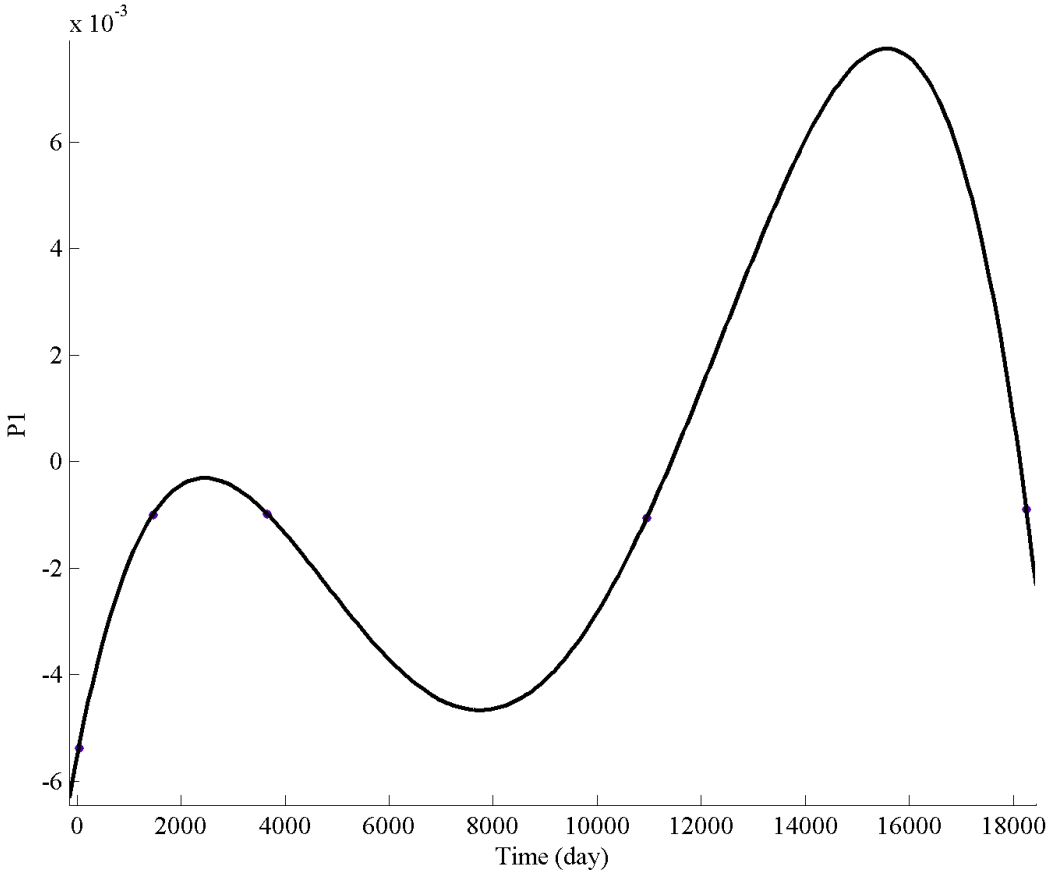

Figure 6.19. The curve fitting of the coefficients of P1for parameter "b"

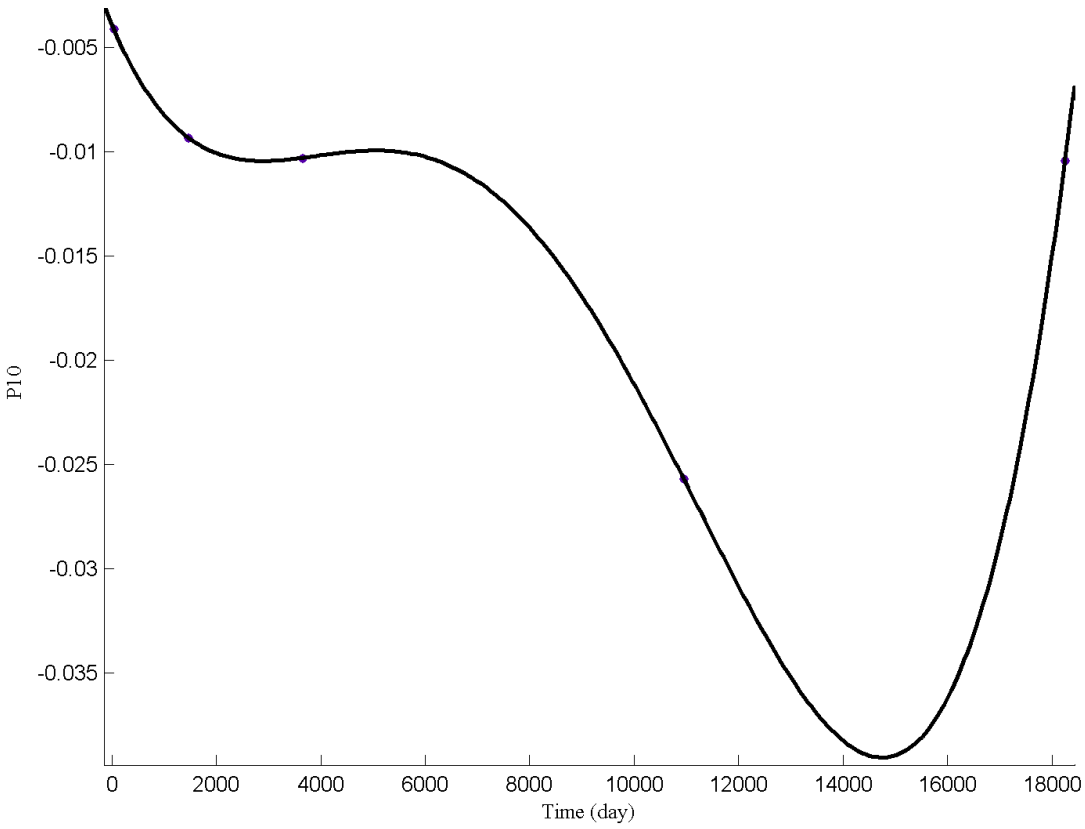

Figure 6.20. The curve fitting of the coefficients of P10 for parameter "b"

Chapter 7

CONCLUSIONS

As the outcome of the performed operations by Rockware, NovoSPT,and PLAXIS the following results are concluded:

1. From the geological point of view, the region has a very heterogeneous stratification. Thus to understand the soil-structure behavior thoroughly, it is believed that further investigations are required.

2. If allowable total settlement is assumed to be 50 mm, based on Table 6.1 (Das, 2011), the magnitude of bearing capacity of the region with respect to depth and foundation dimensions can range between 30 and 65 kPa, which reduces to an allowable bearing capacity range of 10-20 kPa with a factor of safety of 3.

3. Water table depth is a factor which should be considered in the foundation design. While this parameter varies in the region under the study, settlement increases. Since the soil of the region is fine, with the rise of water level the thickness of consolidating stratum increases, hence the settlement under the foundation increases, and with the drop of water level, effective stresses increase which leads to an increase in settlement. In both ways, it can cause a considerable hazard for the design because of the advent of differential settlement phenomenon.

4. Another important concern which has impact on design of foundation is the softening of the soil in the region. In this survey, corresponding to the factor of safety the

magnitude of load imposed to the soil before the soil collapses can vary between 20 to 40 kPa. It should be noted that softening should be considered in case that the settlement is needed to be controlled by various factors such as piles.

5. The consolidation does not stop at the end of 50 years. Since consolidation settlement is influenced by the foundation depth, the magnitude of total settlement should be investigated with respect to the depth of the building.

6. One of the methods of controlling the settlement is the improvement of modulus of elasticity of the soils, which can be performed by different methods, such as mixing soil and jet grout injection. Based on the possibility of increasing modulus, settlement of the soils of the region is investigated to be decreasing using the finite element approach.

7. By comparing the bearing capacity values obtained using different methods, a considerable difference between manual calculations and finite element analysis by software is observed. The best correlation in order to estimate bearing capacity via SPT-N value for Tuzla soil is Burland and Burbidge (1985) correlation. Also the closest correlation to general bearing capacity equation is Bowels and Meyerhof (1976) correlation. Moreover, it is recommended to compute the bearing capacity of this region by considering the consolidation settlements.

8. Observing the fitted settlement curves, it can be concluded that generally all the obtained settlement curves satisfy an exponential relation which is dependent on width and depth of foundation. Also each of the coefficients of this relation separately meets the surface passing these two parameters. It should be noted that the coefficients of the obtained formulae of the mentioned surfaces are dependent on time as well. Consequently a polynomial with degree four is interpolated for these coefficients together with time.

9. Finally based on the findings above, an exponential relation for the total settlement is derived as a function of bearing capacity, depth and width of mat foundations and time . It is worthwhile to note that in order to improve the proposed formula, the next step in future is to make it shorter and define a justifiable error coefficient for predicting soil behavior accurately for the whole region. To achieve this aim modeling the settlement at each borehole location and comparing the results are required.

REFERENCES

ACI. (1988). Suggested Analysis and Design Procedures for Combined Footings and Mats. ACI 336.2R-88, 9.

Afkhami, A. (2009). NovoSPT User Manual. North Vancouver: Novo Tech Software.

Ajayi, L., & Balogum, L. (1988). Penetration Testing in Tropical Lateritic. Penetration Testing, ISOPT-1, 315-328.

Anbazhagan, P., & Sitharam, T. (2010). Relationship between Low Strain Shear Modulus and Standard Penetration Test 'N' Values. ASTM Geotechnical Testing Journal, Vol 33(2),150–64.

Atalar, C., & Kilic, R. (2006). Geotechnical Properties of Cyprus Clays. The Geological Society of London, No.419.

Athanasopoulos, G. A. (1995). Empirical Correlations Vs-NSPT for Coils of Greece: A Comparative Study of Reliability. Proc. 7th Int. Conf. on Soil Dynamics and Earthquake Engineering (Chania, Crete) ed. A. S. Cakmak (Southampton: Computational Mechanics), 19-36.

Atkinson, M. (2003). Structural Foundations Manual. NewYork: Spon Press.

Balla, A. (1962). Bearing Capacity of Foundations. Soil Mech. Found. Div., ASCE.

Bowles, J. E. (1996). Foundation Analysis and Desigen. Singapore: McGraw-Hill Companies, Inc.

Budhu, M. (2008). Foundations and Earth Retaining Structures. New York: John Wiley & Sons, Inc.

Canadian Geotechnical Society. (2006). Canadian Foundation Engineering Manual. British Columbia: Canadian Geotechnical Society.

Choi, Y., & Stewart, J. (2005). Nonlinear SPT Amplification as Function of 30 m Shear Wave Velocity. Earthquake Spectra, Vol 21 (1), 1-30.

Coduto, D. P. (2001). Foundation Design. New Jersy: Prentice Hall.

Das, B. (2011). Principeles of Foundation Engineering. Stamford: Global Engineering.

Das, B. M. (2008). Advanced soil mechanics. New york: Taylor and Franncis.

DeBeer, E. E. (1970). Experimental Determination of the Shape Factors of Sand. Geotechnique, Vol 20, 307.

Décourt, L. (1990). The standard penetration test. Oslo: Norwegian Geotechnical Institute Publication.

Dikmen, U. (2009). Statistical Correlations of Shear Wave Velocity and Penetration Resistance for Soils. Journal of Geophysics and Engineering, Vol 6, 61-72.

Edward, J. U. (1995). Design and Performance of Mat Foundations:State–of-the-Art Review. American Concrete Institute, SP-152, 96-97.

Erhan, G. (2009). Assessment of Liquefaction/Cyclic Failure Potential of Tuzla Soils. MSc Thesis, Eastern Mediterranean University (North Cyprus).

Fujiwara, T. (1972). Estimation of Ground Movements in Actual Destructive Earthquakes. Proc. 4th European Symp. Earthquake Engineering, London, 125–32.

Google earth image of Tuzla. (35 0914.75" N 33 53 10.02", 3m).

Google earth images of Cyprus. (35 06 53.80" N 33 29 57.93" E, 327 ft). Accessed 11/5/2012.

Google earth images of Cyprus. (35 11 57.84" N 33 09 38.92" E, 27 ft.). Accessed 11/5/2012.

Gövsa, Y. (2011). Tuzla Coordinate system. (D. Lakyan, & H. Bilsel, Interviewers)

Hansen, J. B. (1970). A Revised and Extended Formula for Bearing Capacity. Copenhagen: Danish Geotechnical Institute.

Hara et al. (1974). Shear Modulus and Shear Strength of Cohesive Soils. Soils and Foundation, Vol. 14 (3),1-12.

Hasancebi, N., & Ulusay, R. (2006). Empirical correlations between shear wave velocity and penetration resistance for ground shaking assessments. Bull. Eng. Geol. Environ., Vol. 66, 203-213.

Hettiarachchi, H., & Brown, T. (2009). Use of SPT Blow Counts to Estimate Shear Strength Properties of Soils: Energy Balance Approach. J. Geotech. Geoenviron. Eng., Vol. 135(6), 830–834.

Hu, G. G. (1964). Variable-Factors Theory of Bearing Capacity. Journal of Soil Mechanics & Foundations Div, Vol. 90, 85-95.

Imai, T. (1977). P-and S-Wave Velocities of the Ground in Japan. Proc.9th Int. Conf. on Soil Mechanics and Foundation Engineering, Vol. 2, 127–32.

Imai, T., & Tonouchi, K. (1982). Correlation of N-Value with S-wave Velocity and Shear Modulus. Proc. 2nd European Symp. Of Penetration Testing, Amsterdam, 57–72.

Imai, T., & Yoshimura, Y. (1970). Elastic Wave Velocity and Soil Properties in Soft Soil. , Tsuchito-Kiso 1970, Vol. 18, 17-22.

Imai, T., & Yoshimura, Y. (1975). The Relation of Mechanical Properties of Soils to P and S-Wave Velocities for Ground in Japan. Technical Note, OYO Corporation.

Iyisan, R. (1996). Correlations between Shear Wave Velocity and In-Situ Penetration Test Results. Tech. J. Chamber Civil Eng. Turkey, (in Turkish)., Vol. 7, 1187–99.

Jackson et al. (2008). MDT Geotechnical Engineering Manual. Montana: Engineering Consulting Firm of Roy Jorgensen Associate, Inc.

Jafari, M. K., Asghari, A., & Rahmani, I. (1997). Empirical Correlation between Shear Wave Velocity (Vs) and SPT-N Value for South of Tehran Soils. Proc. 4th Int. Conf. on Civil Engineering, Tehran, Iran (in Persian).

Jafari., M. K., Shafiee, A., & Ramzkhah, A. (2002). Dynamic Properties of the Fine Grained Soils in South of Tehran. J. Seismol. Earthq. Eng., Vol. 4, 25–35.

Jinan, Z. (1987). Correlation between Seismic Wave Velocity and the Number of Blow of SPT and Depth. Chin. J. Geotech. Eng., ASCE, Vol. 13, 92–100.

Kanai, K. (1966). Conf. on Cone Penetrometer the Ministry of Public Works and Settlement, Ankara, Turkey.

Karol, R. H. (1960). Soils and Soil Engineering Prentice Hall,Englewood Cliffs, NJ, 194 p. Prentice Hall,Englewood Cliffs, NJ.

Kiku et al. (2001). In-Situ Penetration Tests and Soil Profiling in Adapazari, Turkey. Proc. ICSMGE/TC4 Satellite Conf. on Lessons Learned from Recent Strong Earthquakes, 259–65.

Knowles, V. R. (1991). Settlement of Shallow Footings on Sand. Washington D.C.: Department of the Army.

Kramer, S. (1996). Geotechnical Earthquake Engineering. Delhi (India): Pearson Education Ptd. Ltd.

Kulhawy, F., & Mayne, P. (1990). Manual on Estimating Soil Properties for Foundation Design. NewYork: Electric Power Research Institute.

Kuory et al. (2002). Plaxis V8 2D Manual. Delft: A. A. Balkema.

Lee, S. H. (1990). Regression Models of Shear Wave Velocities. J. Chin. Inst. Eng., Vol. 13, 519–32.

M.Das, B. (2009). Shallow Foundations Bearing Capacity and Settlement. New York: Taylor and Francis.

M.F.Atkinson. (2003). Structural Foundations Manual. NewYork: Spon Press.

Mathwork. (2011). Curve fitting toolbox.

Menard Co. (2011, 8 25). Menard. Retrieved 07/6/2012, from http://www.menard-web.com

Meyerhof, G. (1963). Some Recent Research on the Bearing Capacity of Foundations. Canadian Geotech. J, Vol. 1 (1), 16-26.

Meyerhof, G. G. (1951). The ultimate bearing capacity of foundations. . Geotechnique, Vol2-301.

Morgano, C. M., & Liang, R. (1992). Energy Transfer in SPT - Rod length effect. Proceedings of the 4rd International Conference on the Application of Stress-Wave Theory to Piles (s. 121-127). Barends: The Hague.

N. N. Som, S. C. (2006). Theory and Practice of Foundation Design. New Dehli: PHI Learning Pvt. Ltd.

Necdet et al. (2007). Tuzla ve Civarinin Jeolojik-Jeoteknik Araştirma Projesi. Lefkosa: Department of Geology and Mining.

Nixon, I. (1982). Standard Penetration Test: State of the Art Report. Amsterdam: Proceedings of the 2nd European Symposium on Penetration Testing.

Ohba, S., & Toriuma, I. (1970). Dynamic Response Characteristics of Osaka Plain. Proc. Ann. Meeting AIJ.

Ohba, S., & Toriumi, I. (1970). Research on vibration characteristics of soilde positsin Osaka, part2,on velocities of wave propagation and predominant periods of soil deposits. Technical meeting of Architectural Institute of Japan.

Ohsaki, Y., & Iwasaki, R. (1973). On Dynamic Shear Moduli and Poisson's Ratio of Soil Deposits. Soil Foundation, Vol. 13, 61–73.

Ohta et al. (1972). Elastic Moduli of Soil Deposits Estimated by N-Values. Proceedings of the 7th annual conference (pp. 265-8). The Japanese Society of Soil Mechanic sand Foundation Engineering.

Ohta, T., Hara, A., Niwa, M., & Sakano, T. (1972). Elastic Shear Moduli as Estimated from N-Value. Proc. 7th Ann. Convention of Japan Society of Soil Mechanics and Foundation Engineering, 265–8.

Ohta, Y., & Goto, N. (1978). Empirical Shear Wave Velocity Equations in Terms of Characteristic Soil Indexes. Earthq. Eng. Struct. Dyn. , Vol. 6, 167–87.

Okamoto et al. (1989). Comparison of surface versus subsurface wave source for P–S logging in sand layer. Proc. 44th Ann. Conf. JSCE, Vol 3, 996–7.

Papadopoulos et al. (2010). Design by pile load testing of drilled shafts in Cyprus alluvial.

PECK et al. (1953). Foundation Engineering. New York: John Wiley & Sons.

Pitilakis et al. (1999). Geotechnical and geophysical description of Euro-Seistests, using field and laboratory tests, and moderate strong ground motions. J. Earthq. Eng., Vol. 3, 381–409.

Robertson., P. K. (2006, January). Guide to In-Situ Testing. Signal Hill: Gregg Drilling & Testing, Inc.

Rogers, J. D. (2006, May). Subsurface Exploration Using the Standard Penetration. Environmental & Engineering Geoscience, Vol. XII, No. 2, s. 161–179.

Ruwan, R. (2008). Geotechnical Engineering Calculations and Rules of Thumb. Burligton: Elsevier Inc.

Sanglerat, G. (1972). The Penetration and Soil exploration; Interpretation of Penetration Diagrams — Theory and Practice. Amsterdam: Elsevier Publishing Co.

Seed et al. (1983). Evaluation of Liquefaction Potential Using Field Performance Data. Journal of Geotechnical Engineering.

Seed, H. B., & Idriss, I. M. (1970). Soil Moduli and Damping Factors for Dynamic Response Analyses. Berkeley, California: Earthquake Engineering Research Center, University of California.

Seed, H. B., & Idriss, I. M. (1981). Evaluation of Liquefaction Potential Sand Deposits Based on Observation of Performance in Previous Earthquakes. ASCE National Convention (MO), 81–544.

Shibata, T. (1970). Analysis of Liquefaction of Saturated Sand During Cyclic Loading. Disaster Prevention Res. Inst. Bull., Vol. 13, 563–70.

Sirvikaya, O. (2009). Comparison of artificial neural networks models with correlative works on undrained shear strength. Eurasian Soil Science, Vol. 42 (13), 1487–1496.

Sisman, H. (1995). The relation between seismic wave velocities and SPT, pressuremeter tests. MSc Thesis, Ankara University (in Turkish).

Skempton, A. W. (1986). Standard Penetration Test Procedures and the Effects in Sands of Overburden Pressure, Relative Density, Particle size, Ageing and Over Consolidation. Gotechnique, Vol. 36, No. 3, 425-447.

Solsten, E. (1991). Cyprus: A country study. Retrieved 10/20/2011, from Country Studies: http://countrystudies.us/cyprus/

Som, N. N., & Das, S. C. (2006). Theory and Practice of Foundation Design. New Dehli: PHI Learning Pvt. Ltd.

Sowers, G. F. (1979). Introductory Soil Mechanics and Foundations. New York: Macmillan.

Srilakshmi, G., & Rekha, B. (2011). Analysis of Mat Foundation using Finite Element Method. International Journal of Earth Sciences and Engineering, Vol. 4 (6), 113-5.

Stroud, M. A. (1974). The Standard Penetration Test in Insensitive Clays and Soft. Proceedings of the 1st European Symposium on Penetration Testing, Stockholm, Vol. 2(2), 367-375.

Sykora, D. E., & Stokoe, K. H. (1983). Correlations of in-situ measurements in sands of shear wave velocity. Soil Dyn. Earthq. Eng., Vol. 20, 125–36.

Sykora, D. W., & Koester, P. J. (1988). Correlations between dynamic shear resistance and standard penetration resistance in soils. Earthq. Eng. Soil Dyn., Vol. 2, 389–404.

Takimatsu, K., & Yoshimi, Y. (1983). Empirical Correlation of Soil Liquefaction Based on SPT N-Value and Fines Content. Soils and Foundations,Vol. 23, No. 4.

Terzaghi, K. (1943). Theoretical Soil Mechanics. New York: John Wiley.

Terzaghi, K., & Peck, R. (1967). Soil Mechanics in Engineering Practice. NewYork: John.

Ulugergerli, U. E., & Uyanik, O. (2007). Statistical Correlations between Seismic Wave Velocities and SPT Blow Counts and the Relative Density of Soils. Journal of Testing and Evaluation, Vol. 35, 1–5.

Vesic, A. (1975). Bearing Capcity of Shallow Foundation. H. F. Winterkorn and H. Y. Fang içinde, Foundation Engineering Handbook. New York: Van Nostrand Reinhold Co.

Vucetic, M., & Dobry, R. (1991). Effect of Soil Plasticity on Cyclic Response. ASCE Journal of Geotechnical Engineering, Vol. 117, No. 1, 89-107.

APPENDICES

Appendix A: Geotechnical properties of boreholes

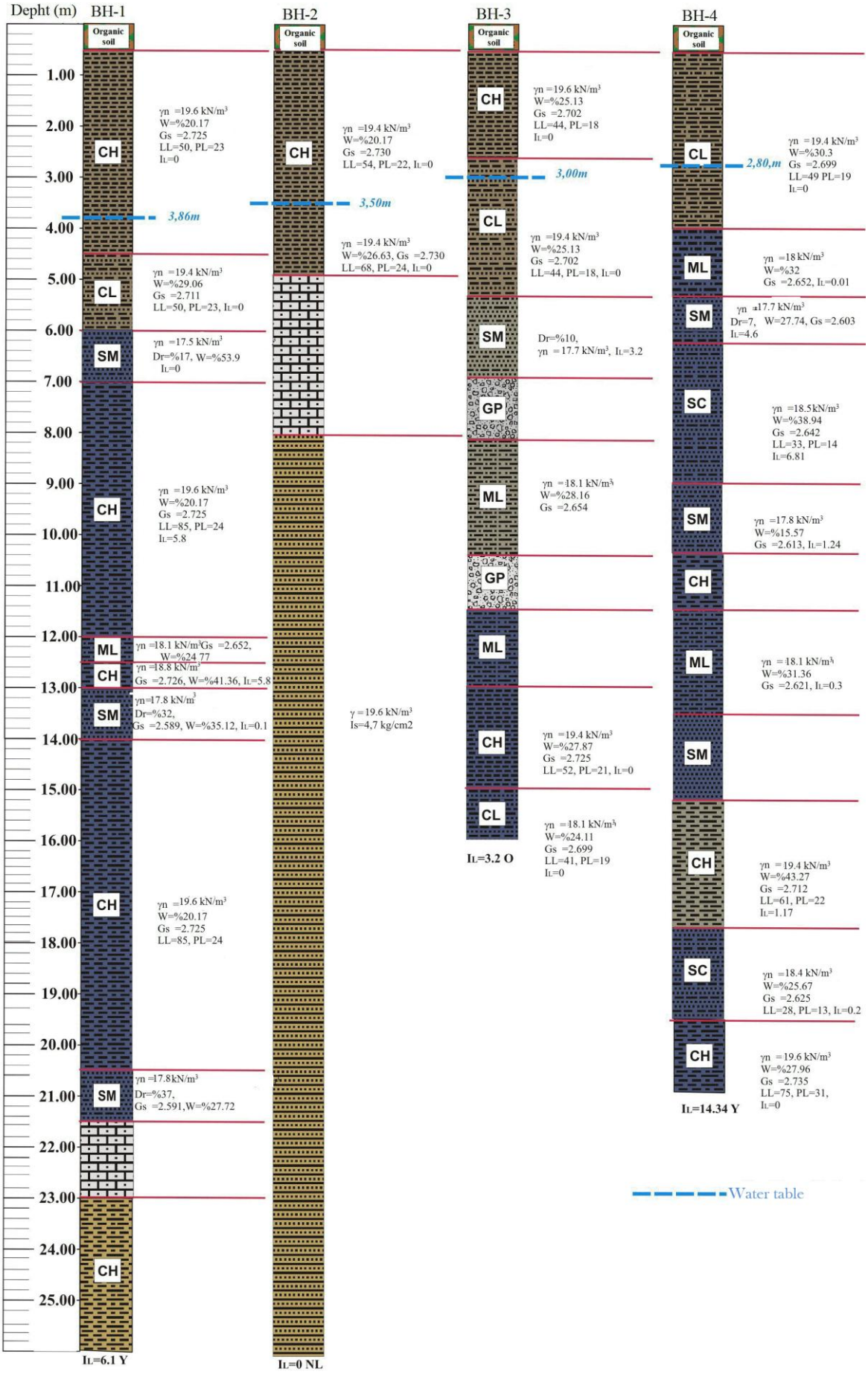

Figure 8.1. Geotechnical properties of borehole 1 until 4, (Necdet et al., 2007).

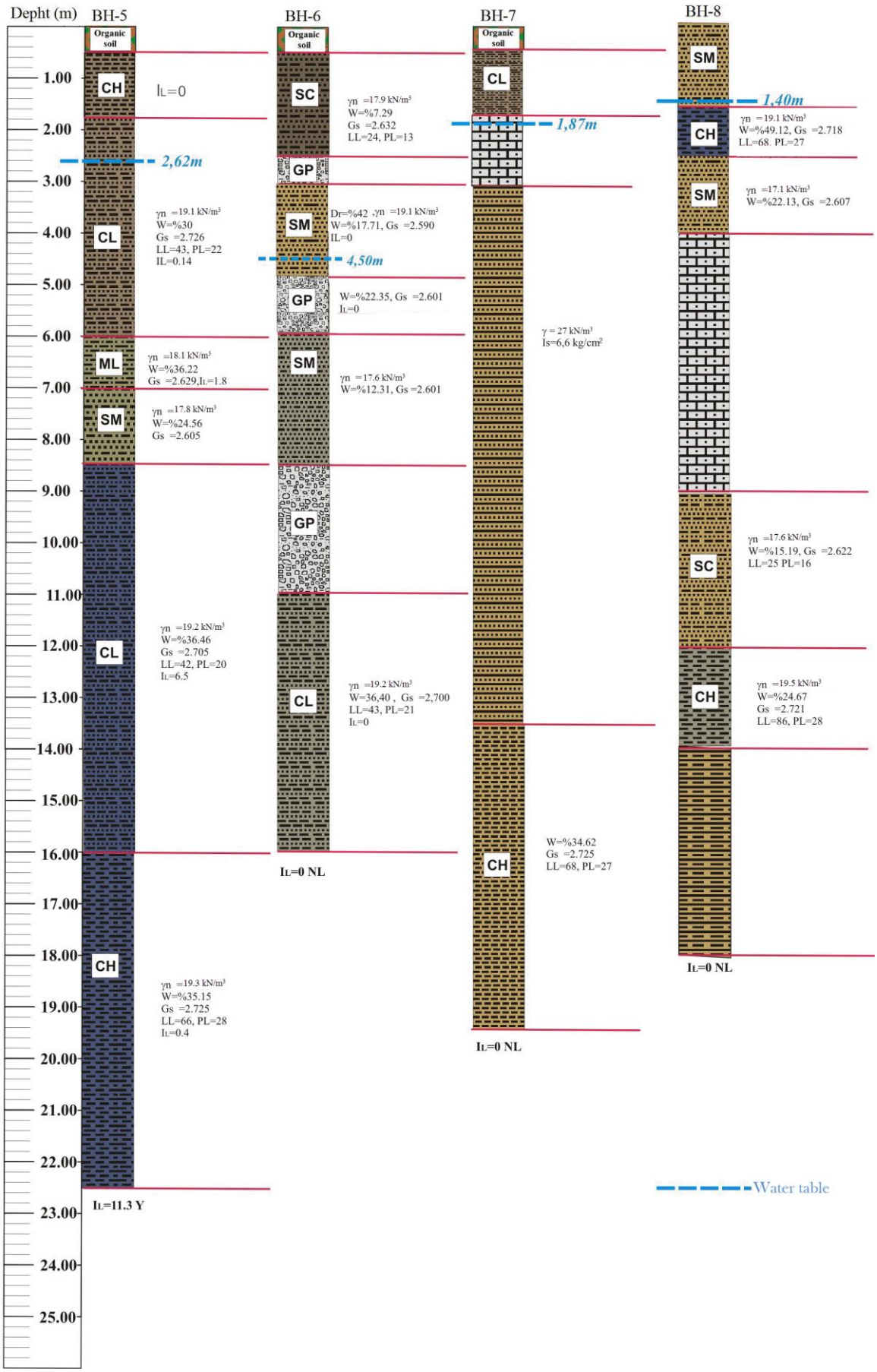

Figure 8.2. Geotechnical properties of borehole 5 until 8, (Necdet et al., 2007).

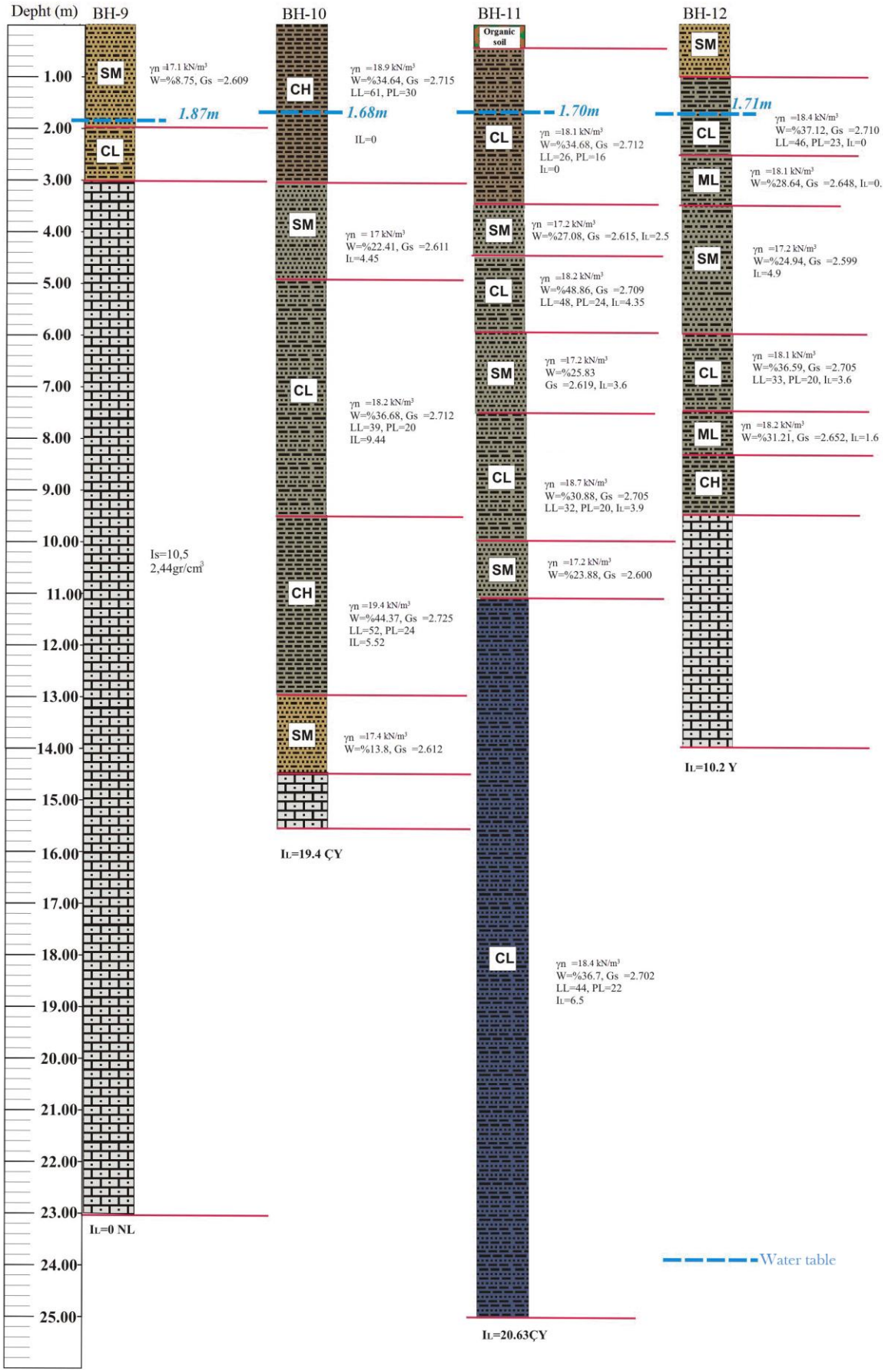

Figure 8.3. Geotechnical properties of borehole 9 until 12, (Necdet et al., 2007).

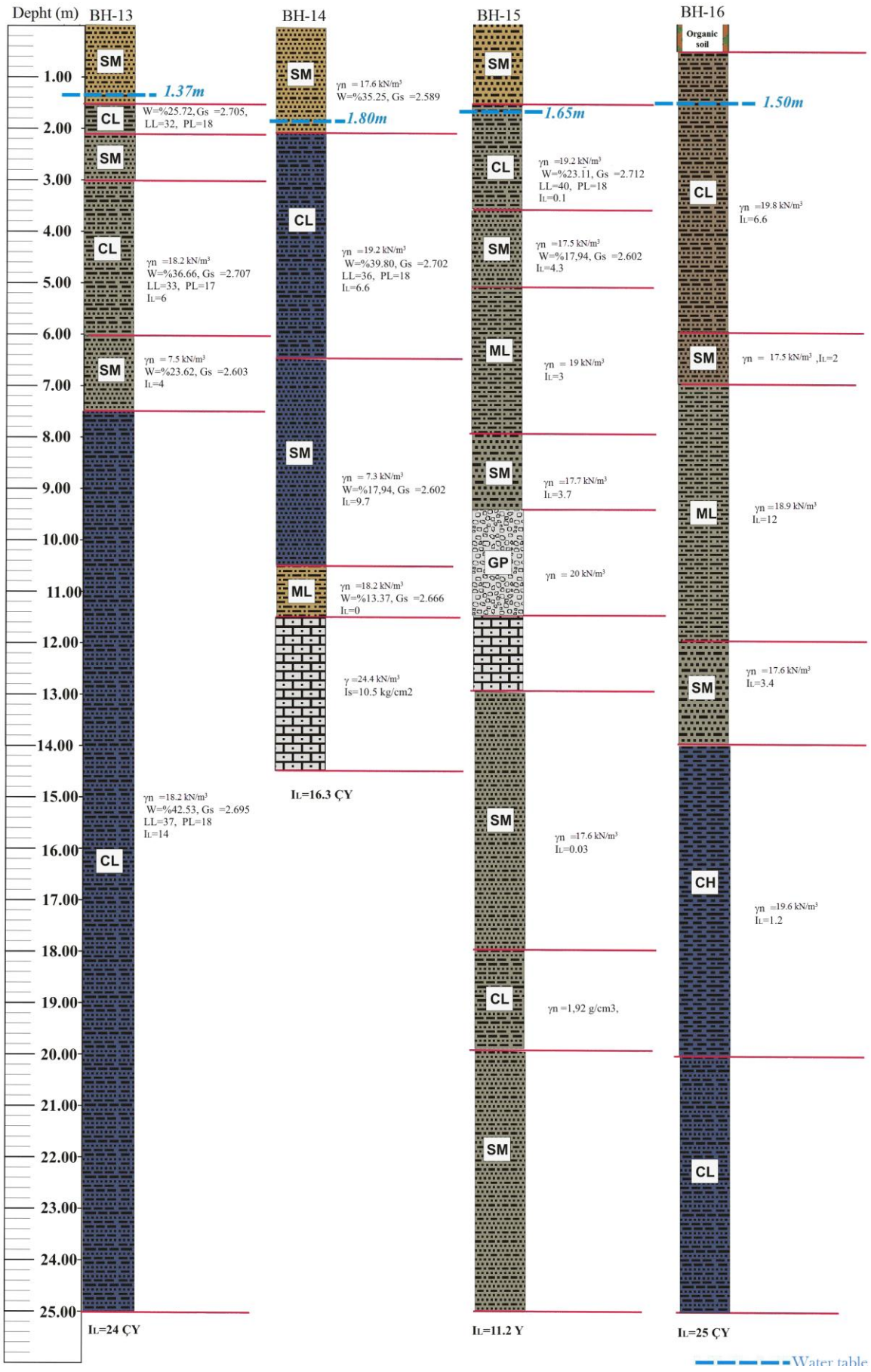

Figure 8.4. Geotechnical properties of borehole 13until 16, (Necdet et al., 2007).

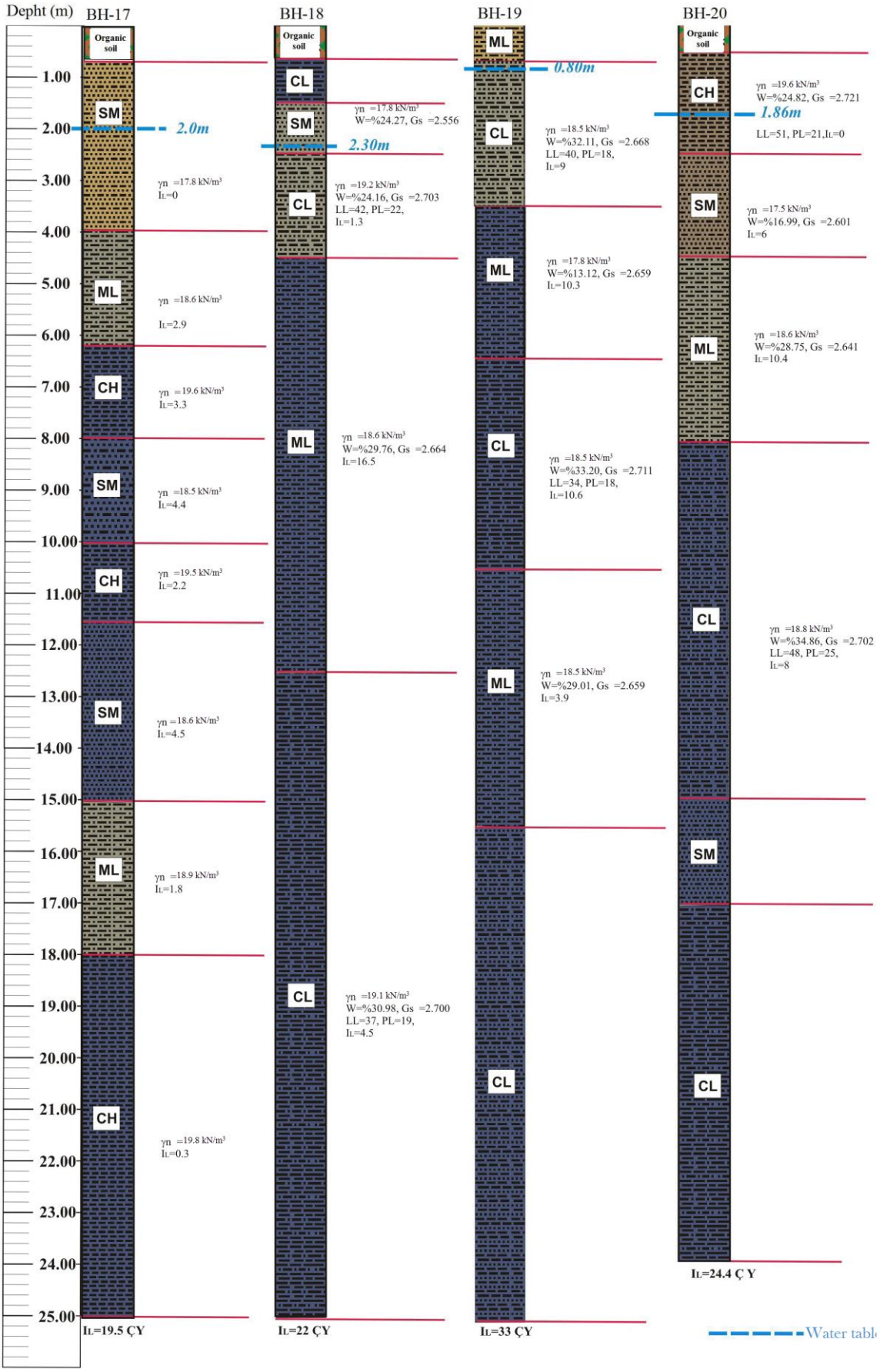

Figure 8.5. Geotechnical properties of borehole 17 until 20, (Necdet et al., 2007).

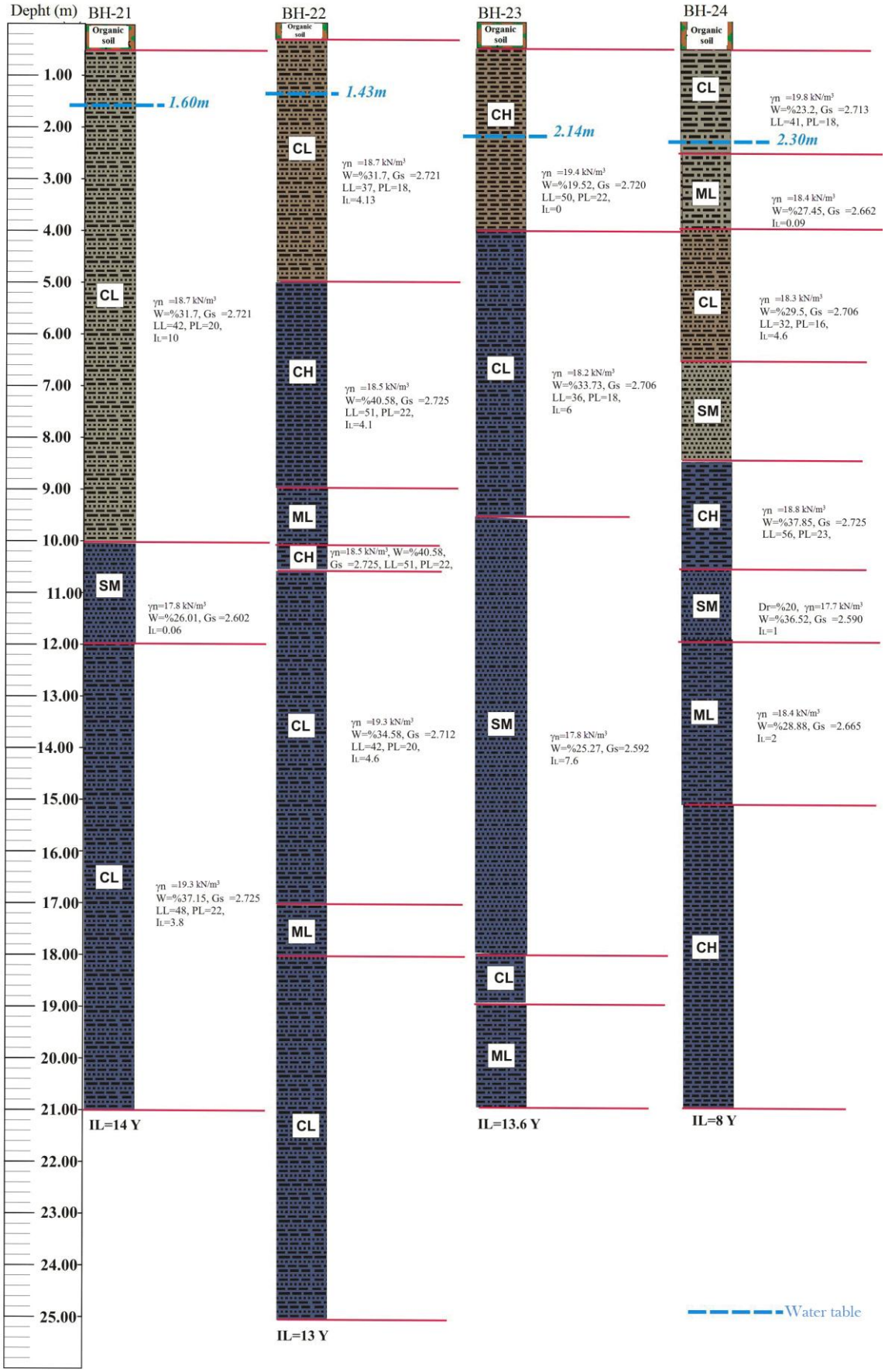

Figure 8.6.Geotechnical properties of borehole 21 until 24, (Necdet et al., 2007).

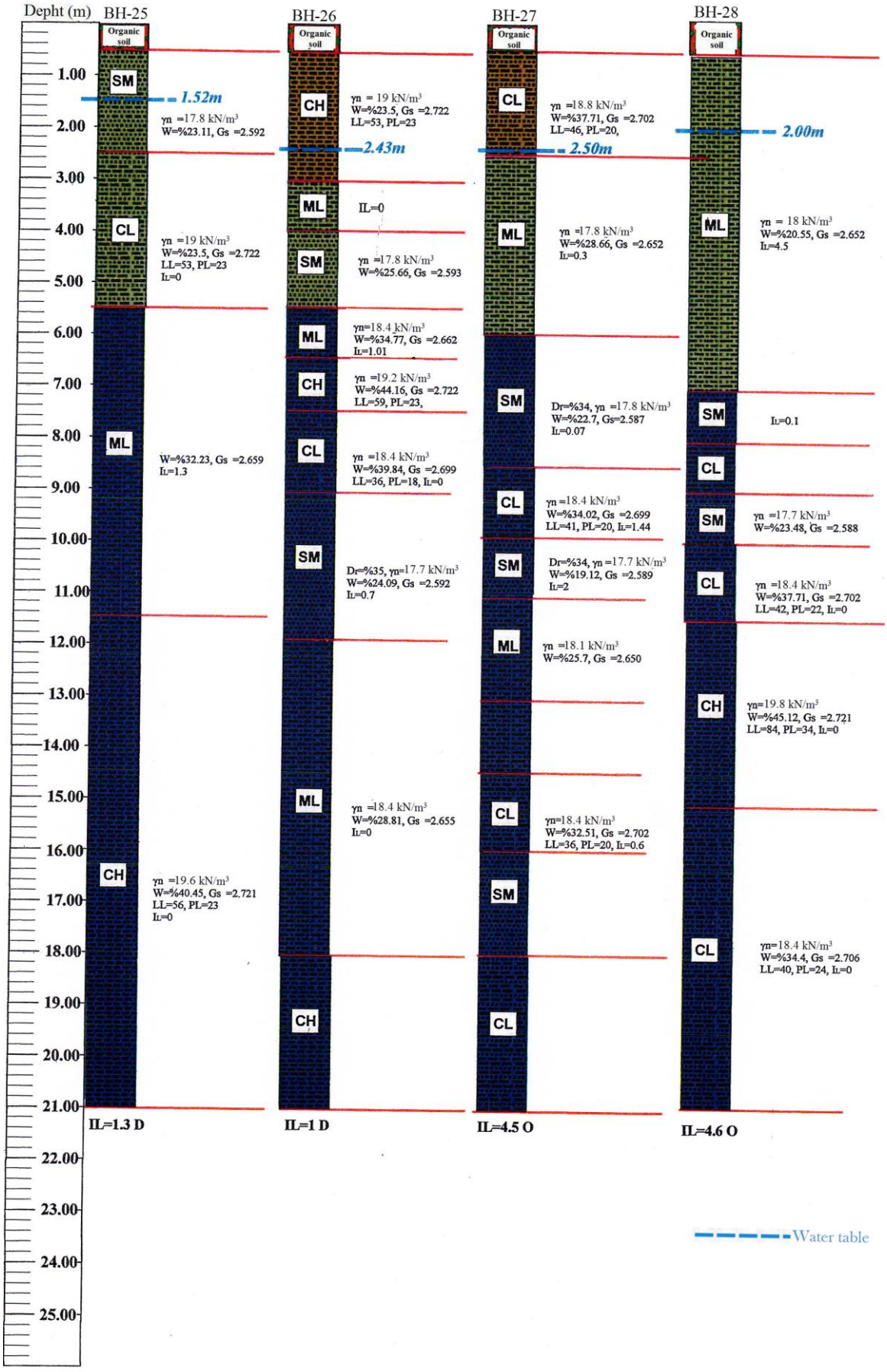

Figure 8.7.Geotechnical properties of borehole 25until 28, (Necdet et al., 2007).

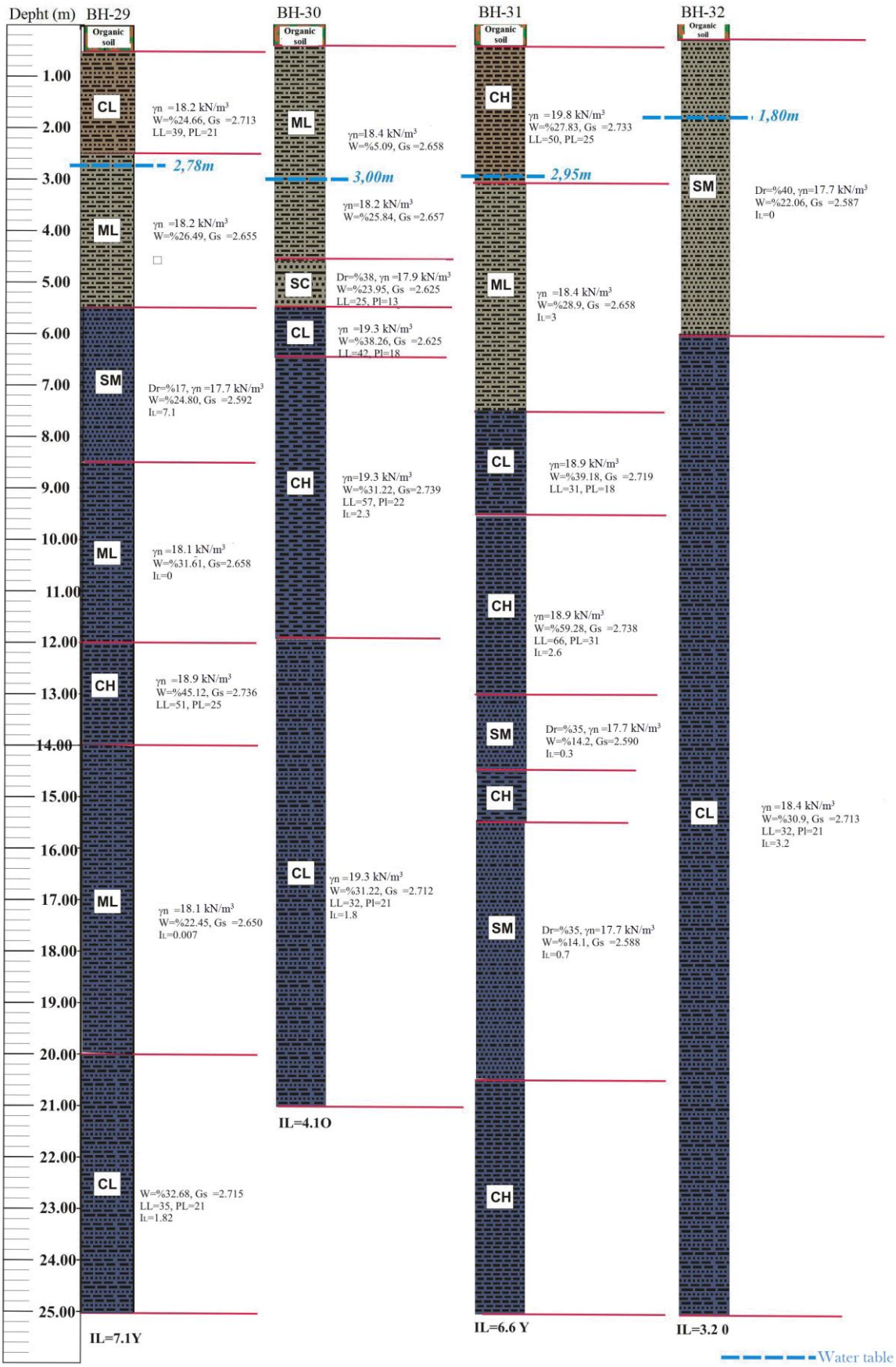

Figure 8.8.Geotechnical properties of borehole 29until 32, (Necdet et al., 2007).

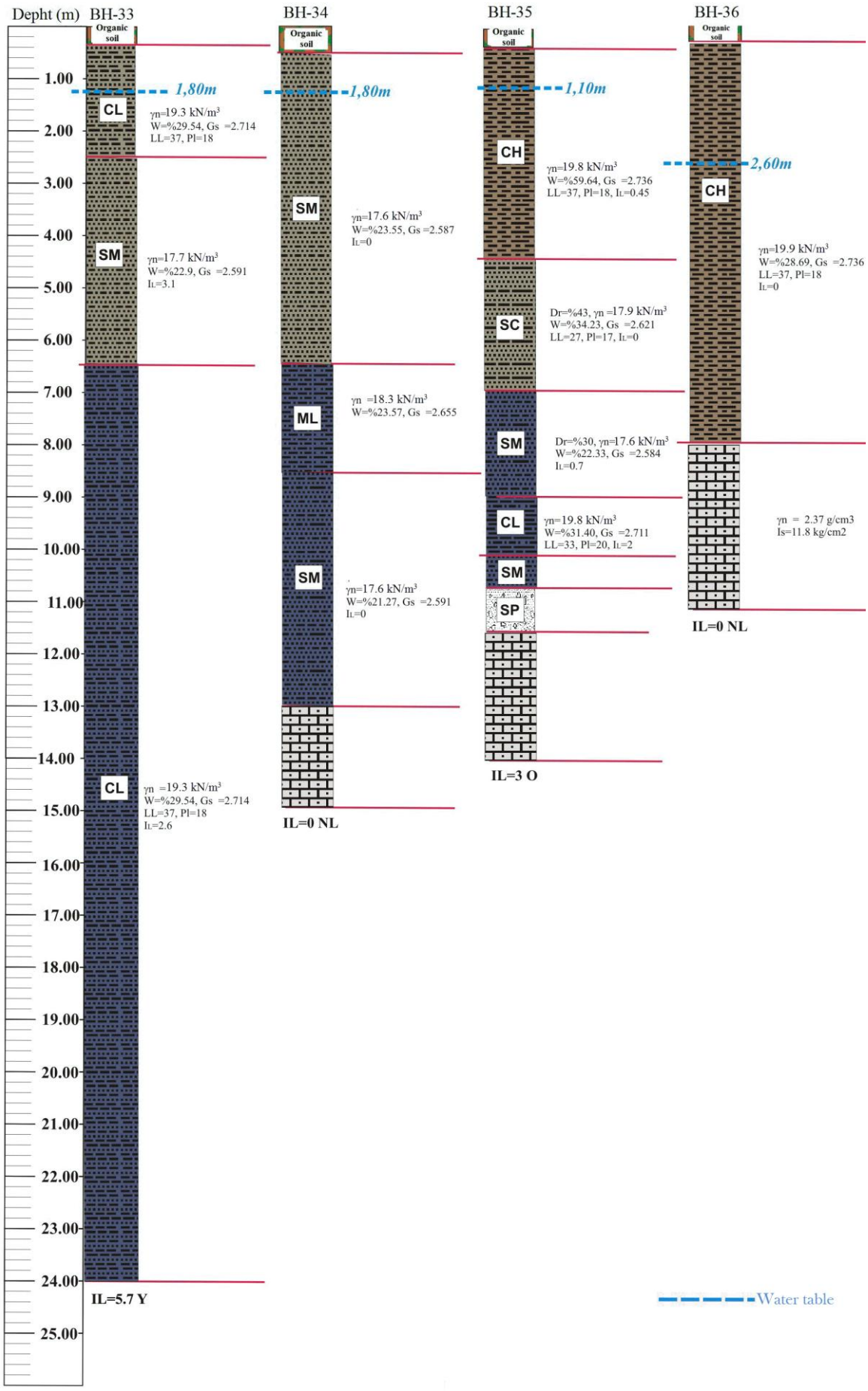

Figure 8.9.Geotechnical properties of borehole 32until 36, (Necdet et al., 2007).

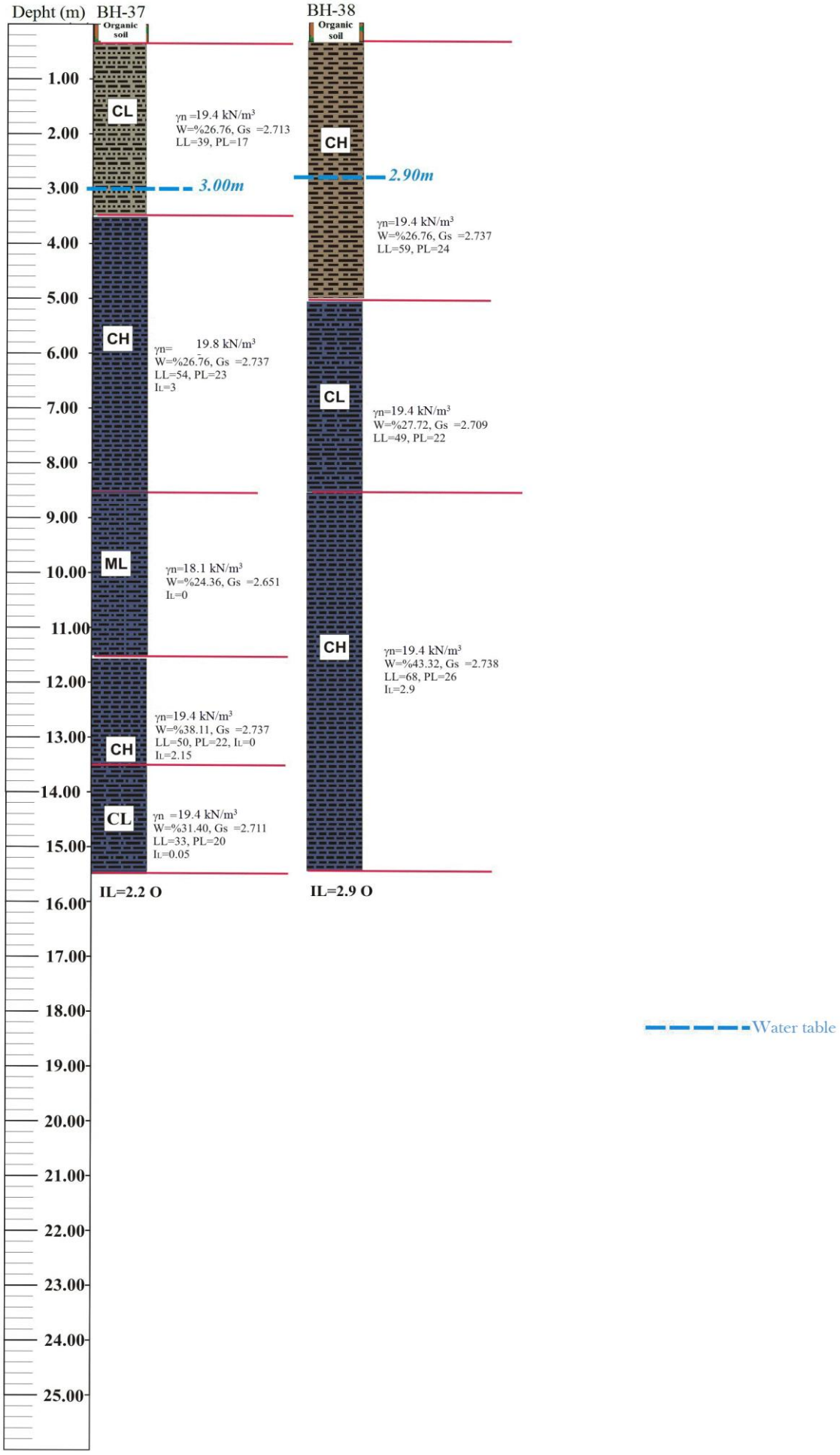

Figure 8.10.Geotechnical properties of borehole 37and 38, (Necdet et al., 2007).

Appendix B: Soil Profiles

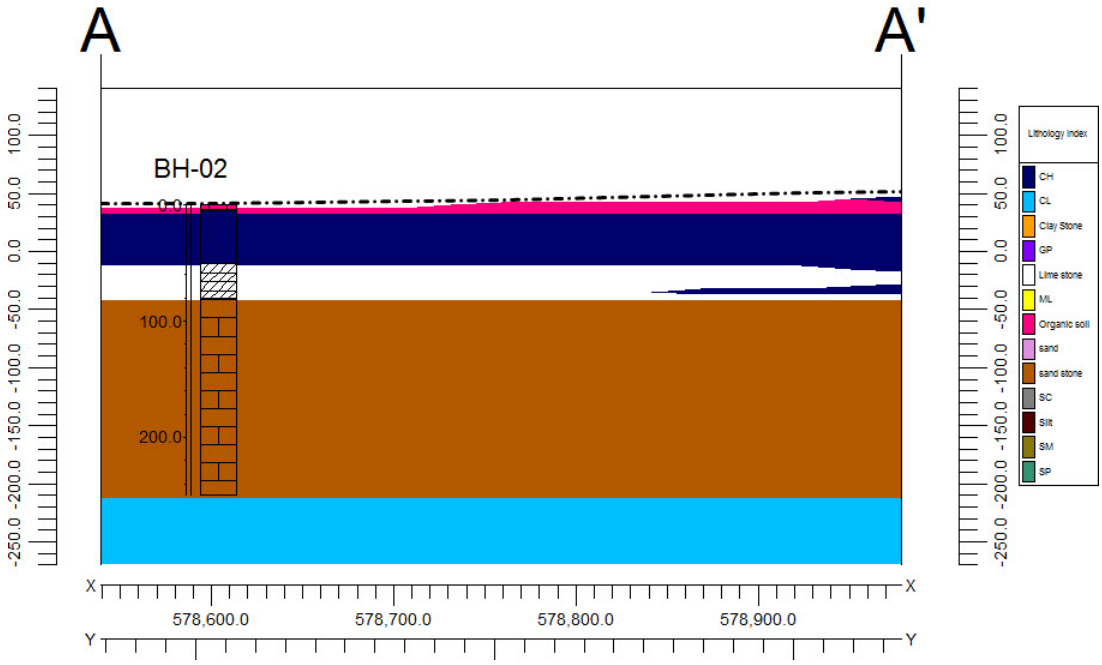

Figure 9.1. The profile of XXIV 41 E2 parcel borehole 2.

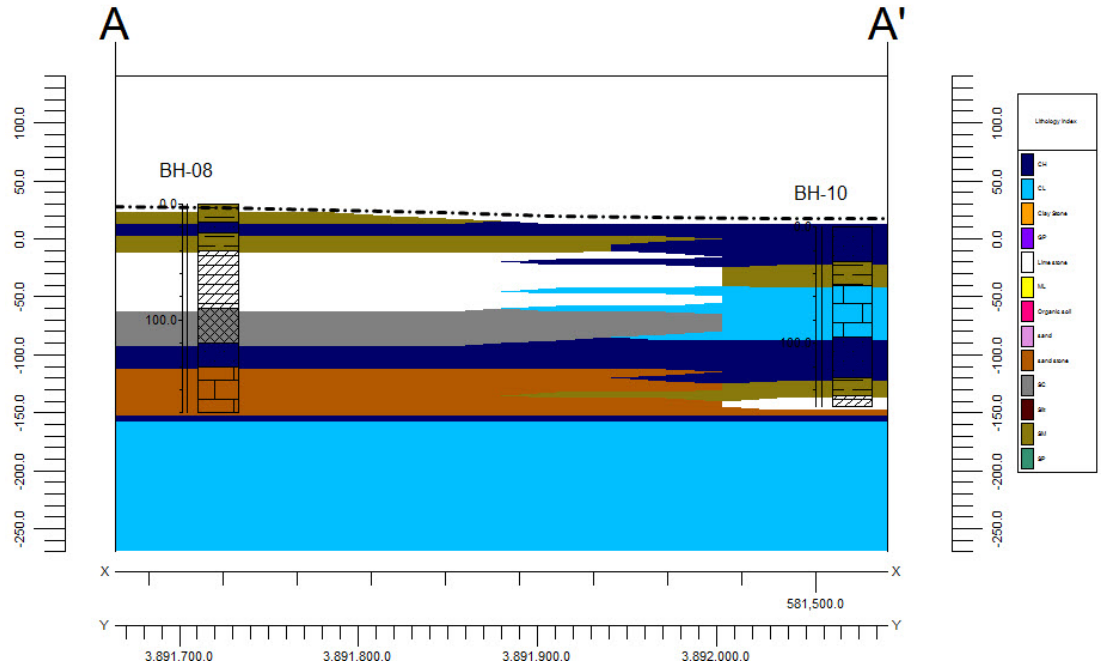

Figure 9.2. The profile of XXIV 42 E2 parcel between borehole 8 and 10.

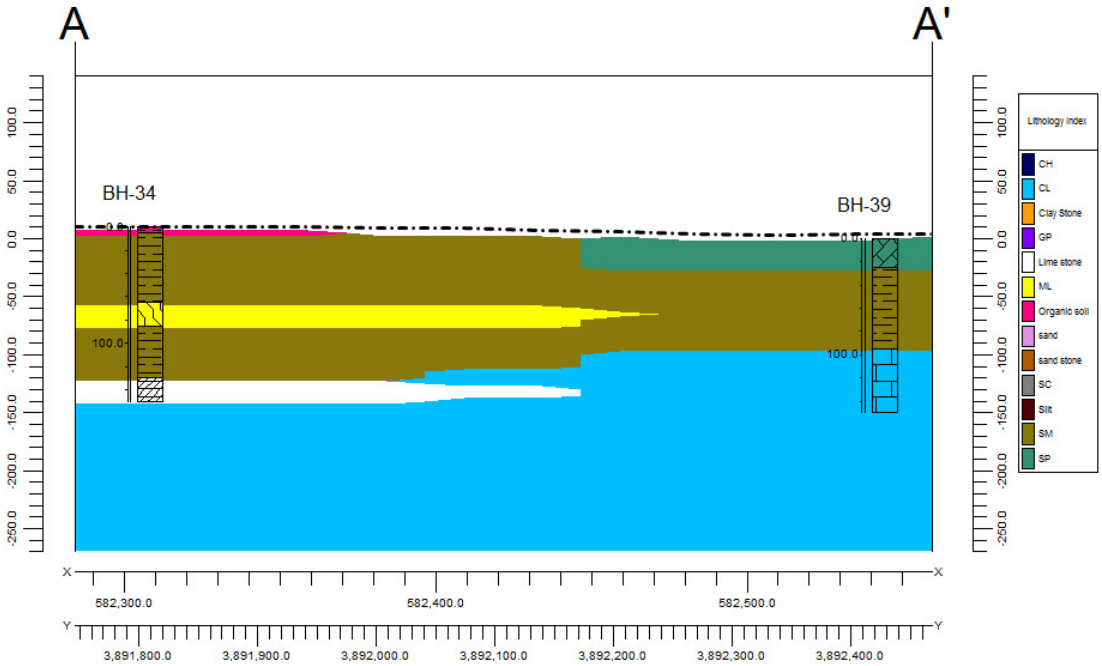

Figure 9.3. The profile of XXIV 43 W2 parcel between borehole 34 and 39.

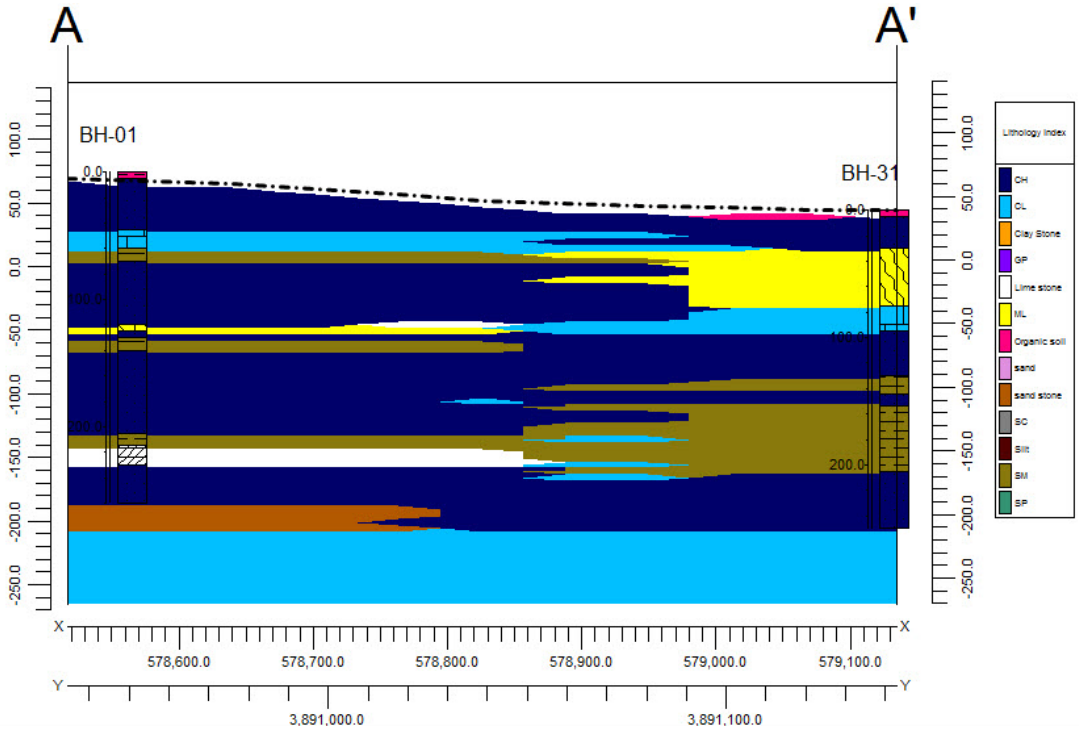

Figure 9.4. The profile of XXIV 49 E1 parcel between borehole 1 and 31.

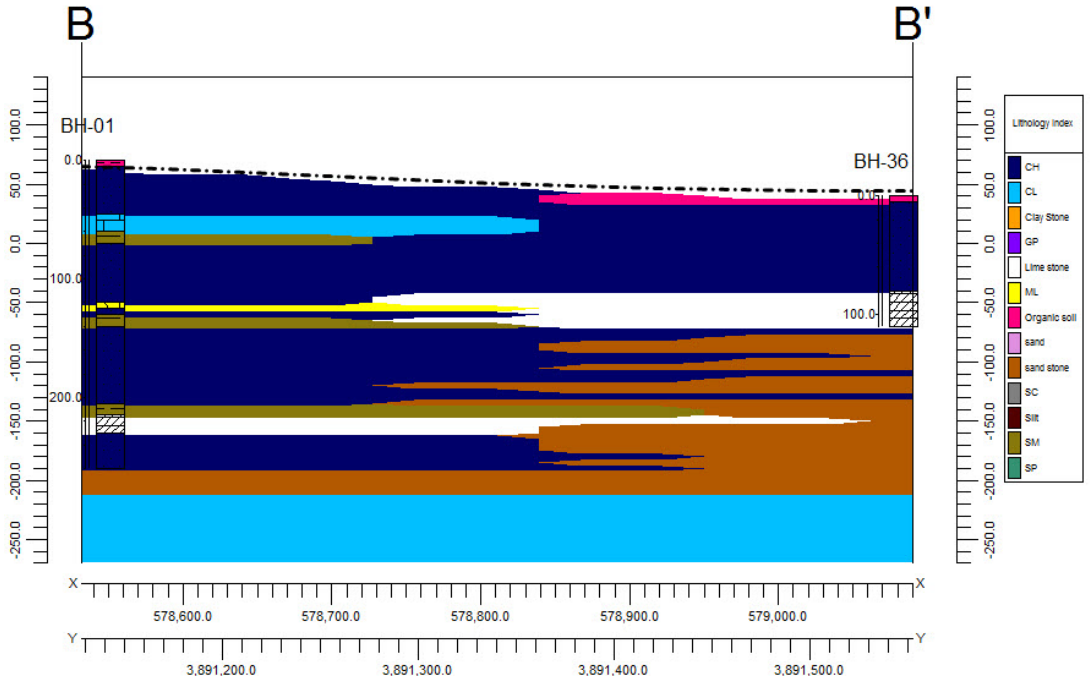

Figure 9.5. The profile of XXIV 49 E1 parcel between borehole 1 and 36.

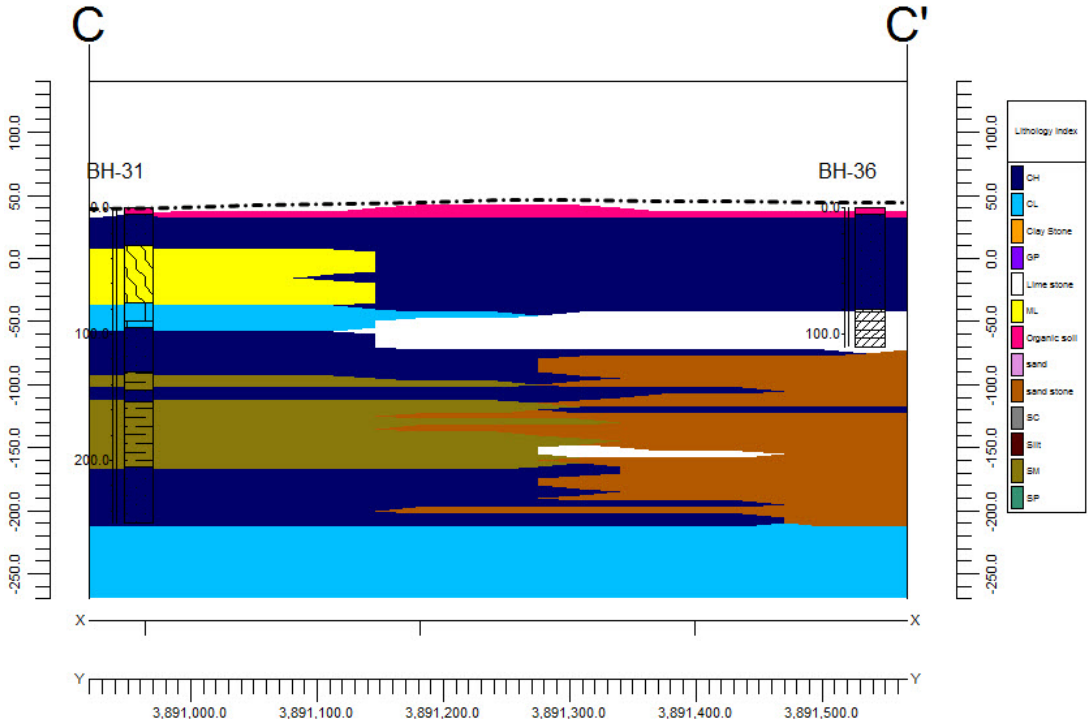

Figure 9.6. The profile of XXIV 49 E1 parcel between borehole 31 and 36.

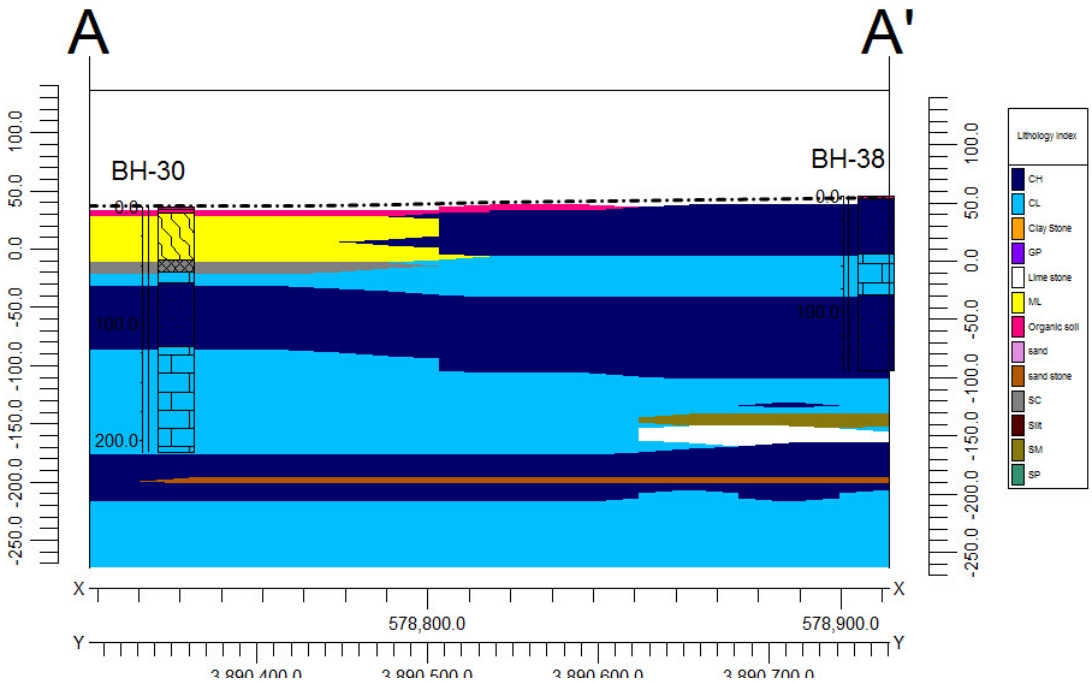

Figure 9.7. The profile of XXIV 49 E2 parcel between borehole 30 and 38.

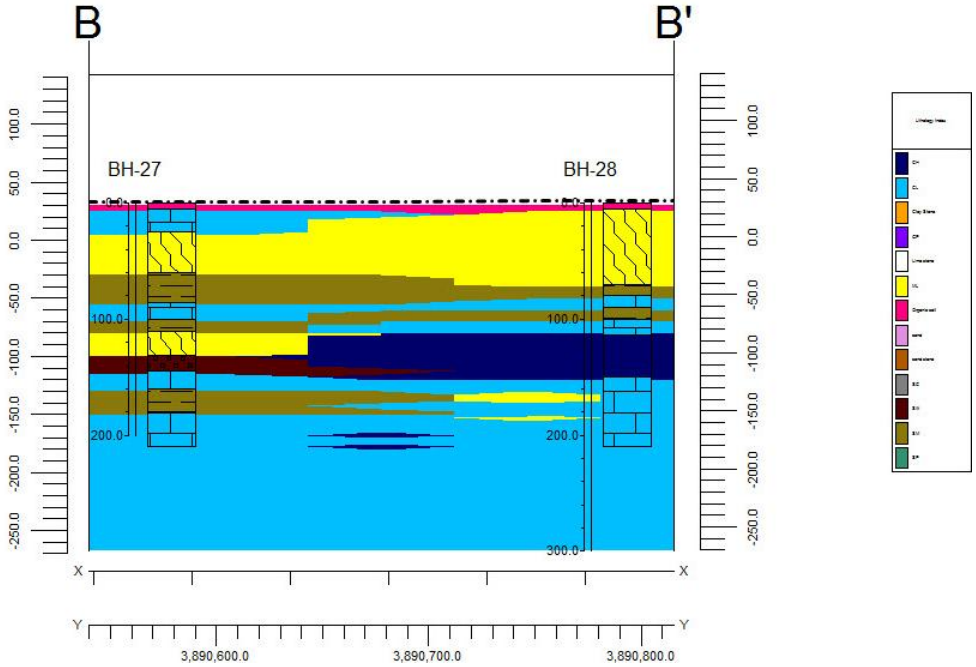

Figure 9.8. The profile of XXIV 49 E2 parcel between borehole 27 and 28.

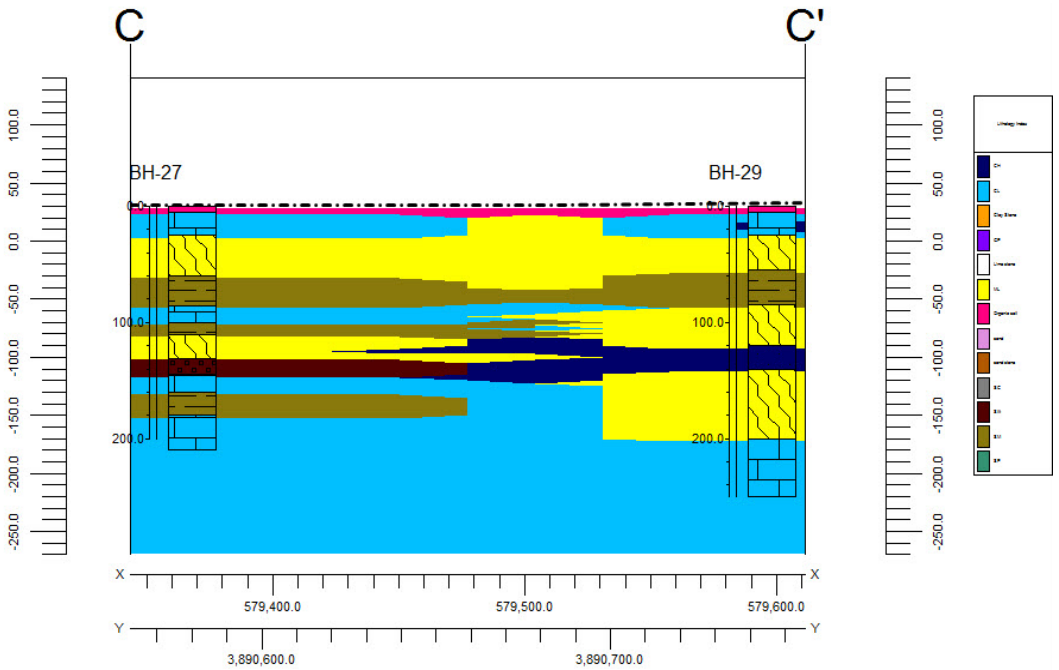

Figure 9.9. The profile of XXIV 49 E2 parcel between borehole 27 and 29.

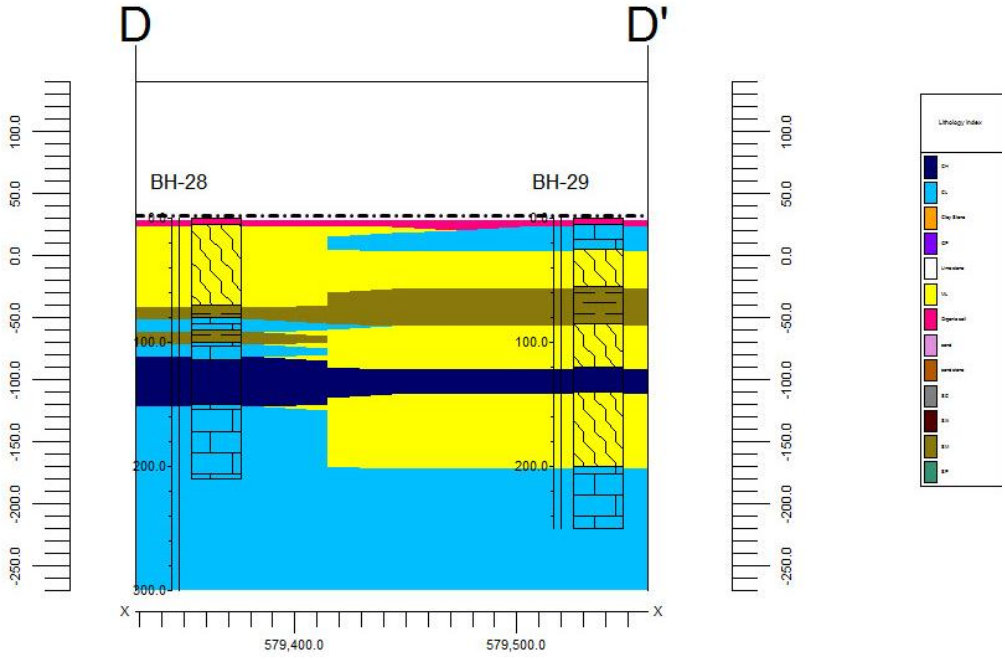

Figure 9.10. The profile of XXIV 49 E2 parcel between borehole 28 and 29.

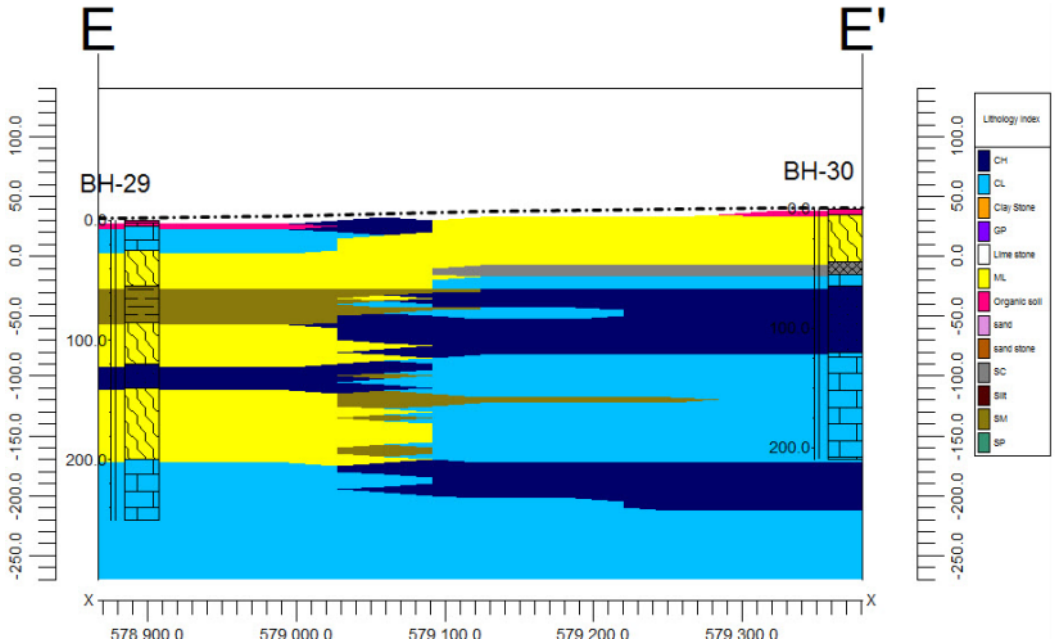

Figure 9.11. The profile of XXIV 49 E2 parcel between borehole 29 and 30.

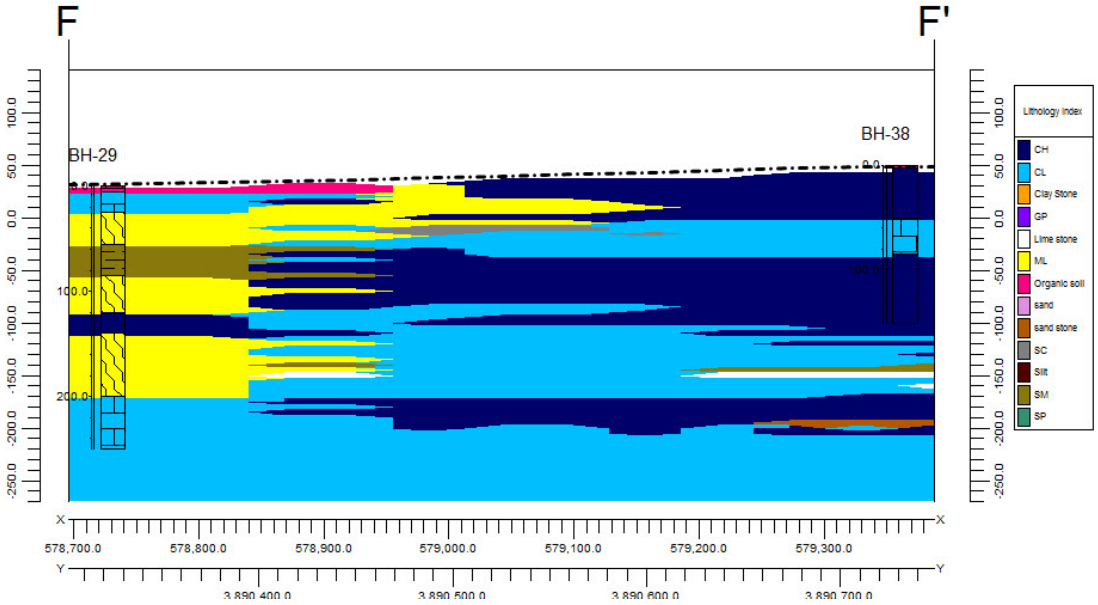

Figure 9.12. The profile of XXIV 49 E2 parcel between borehole 29 and 38.

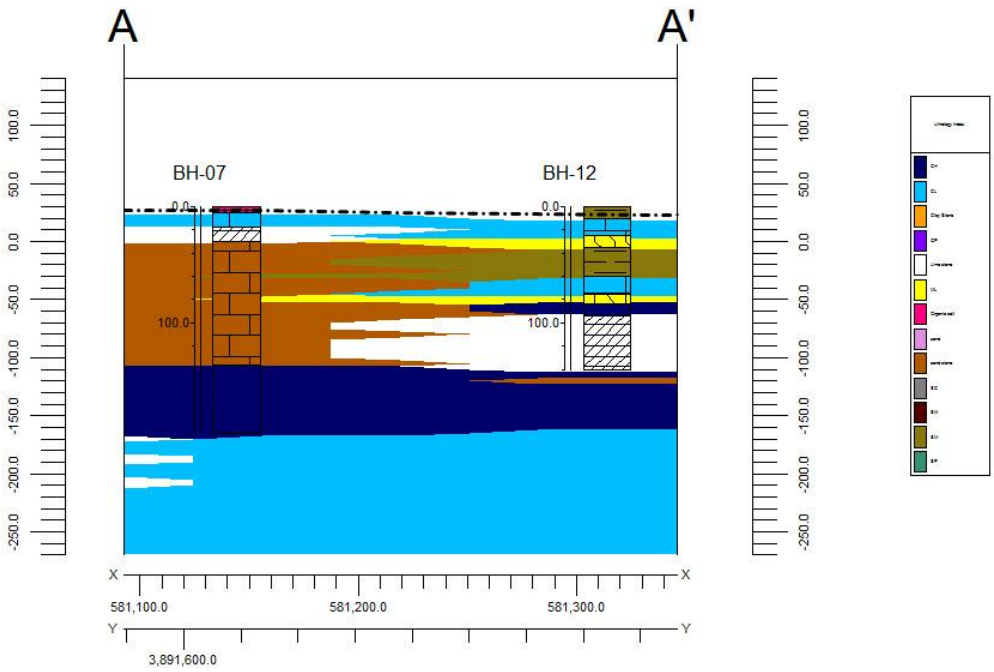

Figure 9.13. The profile of XXIV 50 E1 parcel between borehole 7 and 12.

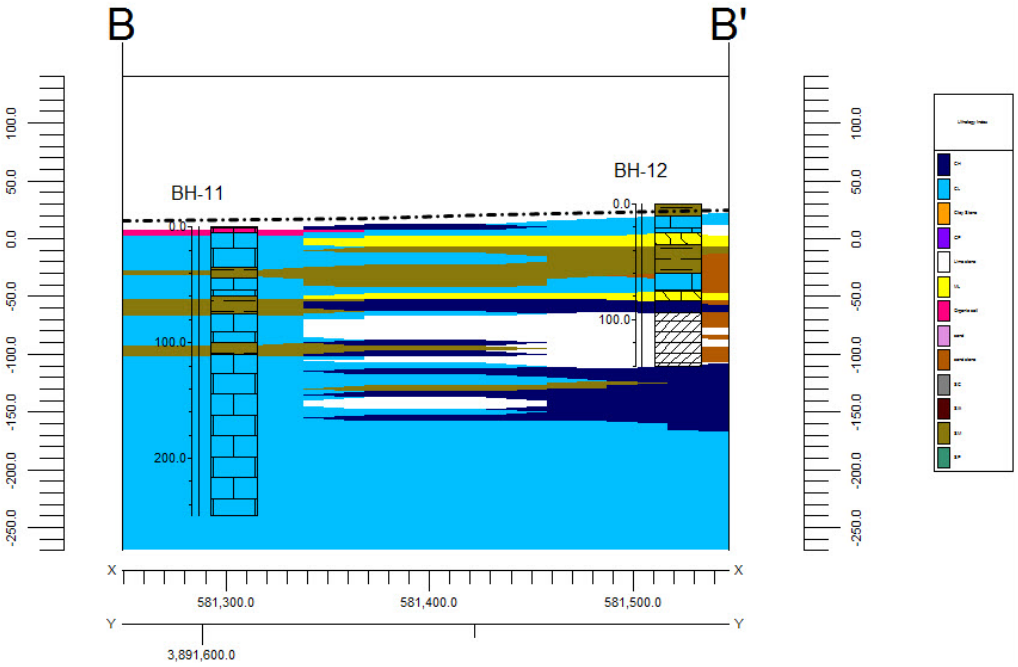

Figure 9.14. The profile of XXIV 50 E1 parcel between borehole 11 and 12.

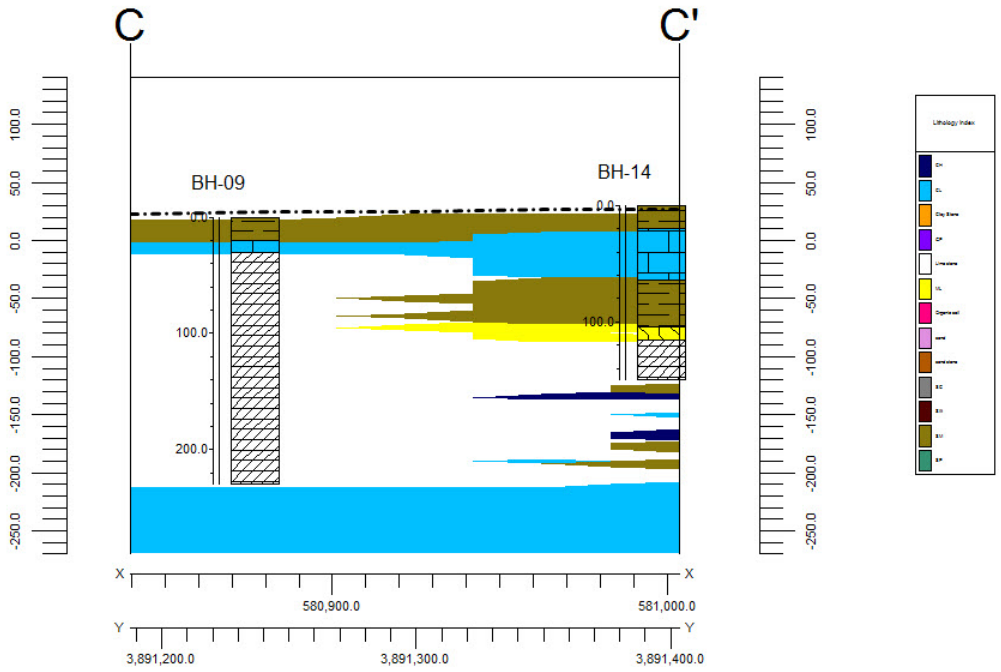

Figure 9.15. The profile of XXIV 50 E1 parcel between borehole 9 and 14.

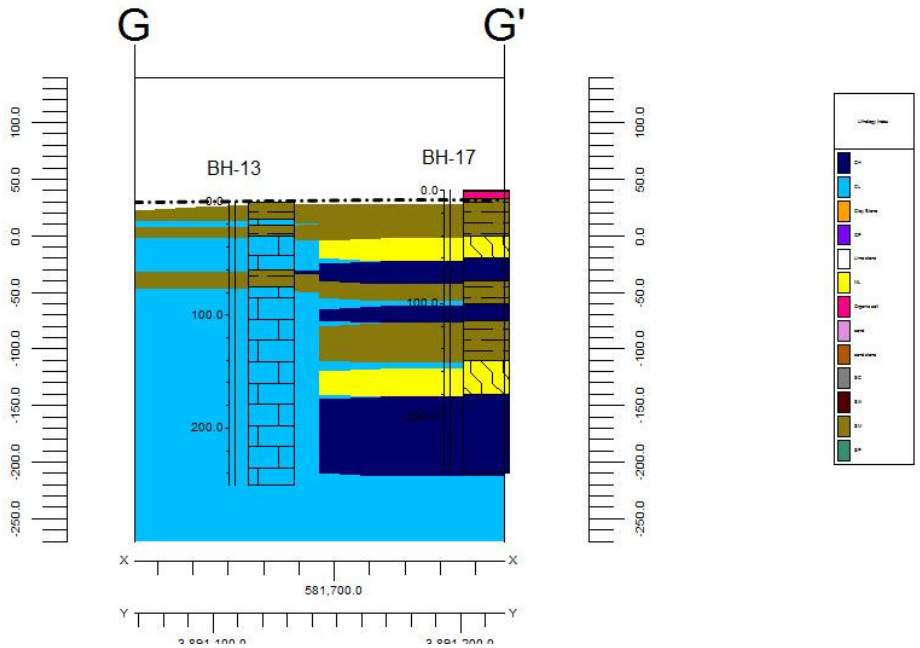

Figure 9.16. The profile of XXIV 50 E1 parcel between borehole 13 and 17.

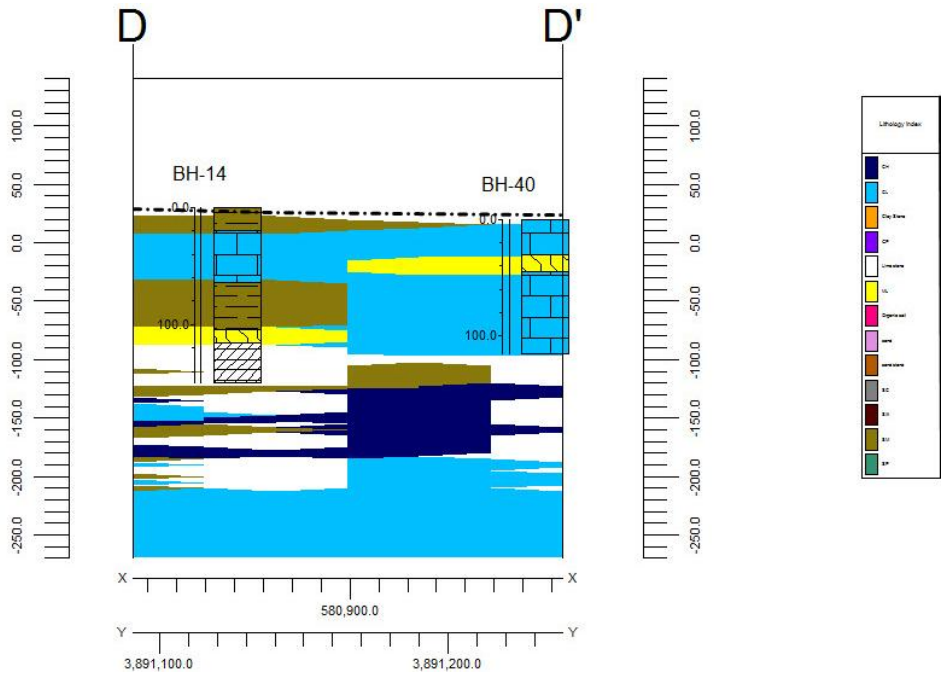

Figure 9.17. The profile of XXIV 50 E1 parcel between borehole 14 and 40.

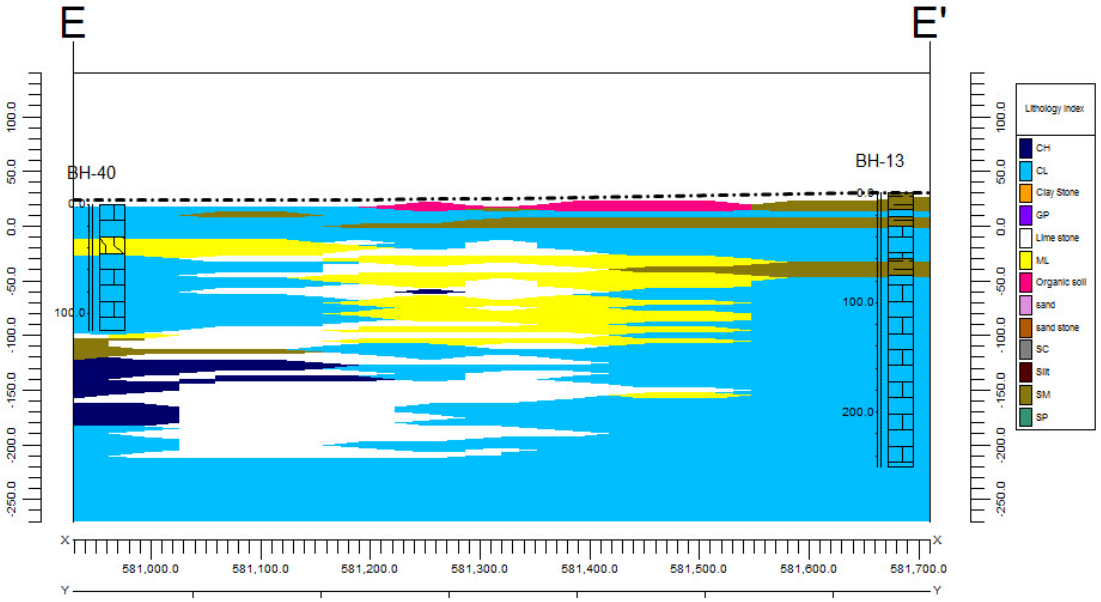

Figure 9.18. The profile of XXIV 50 E1 parcel between borehole 40 and 13.

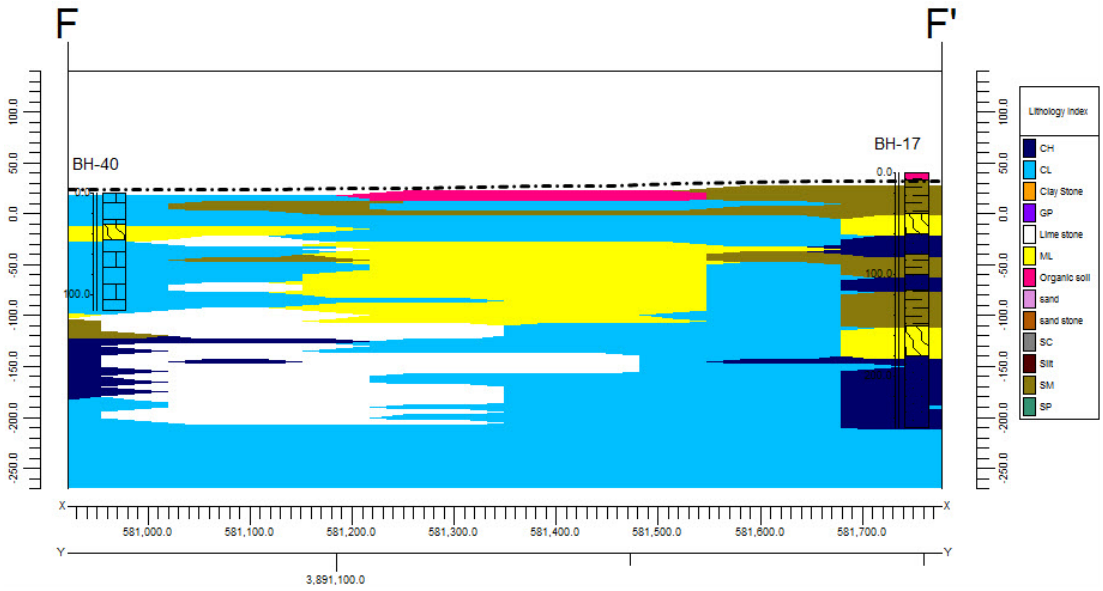

Figure 9.19. The profile of XXIV 50 E1 parcel between borehole 40 and 17.

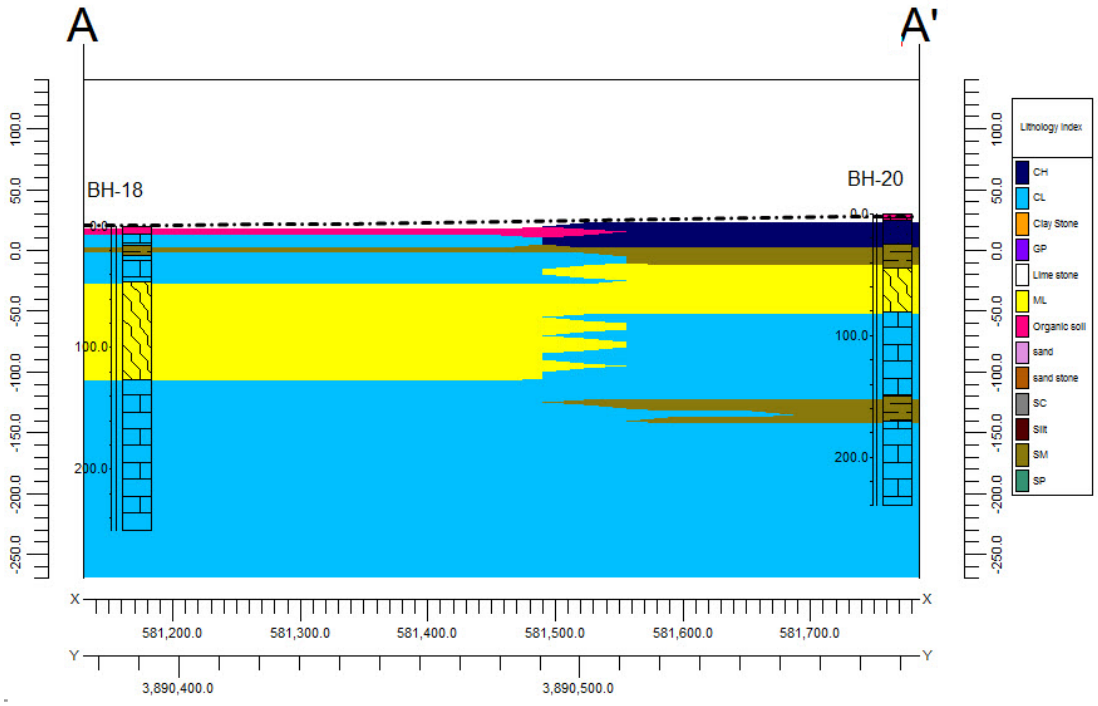

Figure 9.20. The profile of XXIV 50 E2 parcel between borehole 18 and 20.

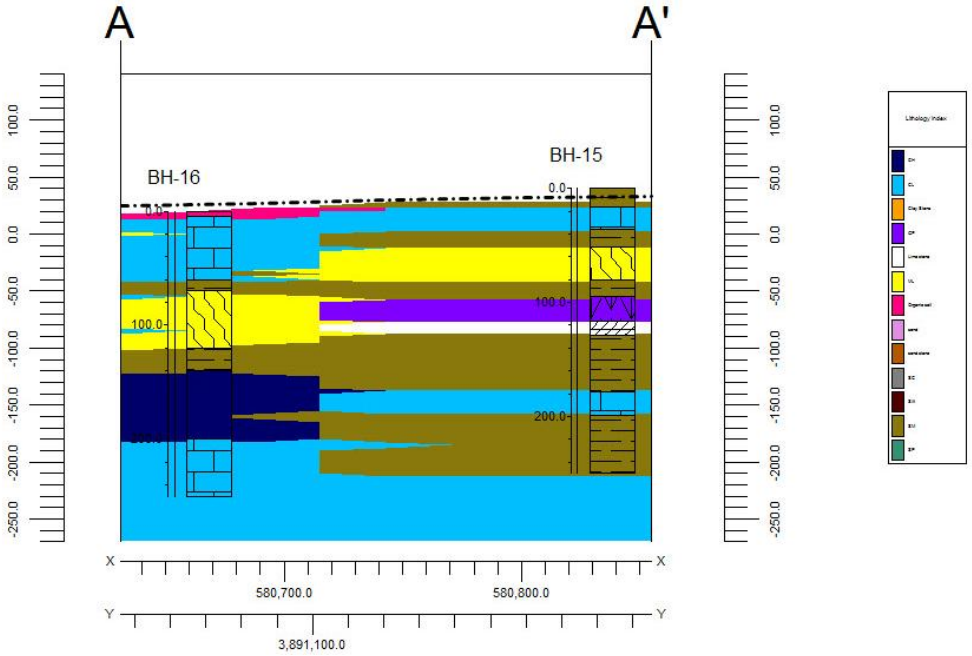

Figure 9.21. The profile of XXIV 50 W1 parcel between borehole 16 and 15.

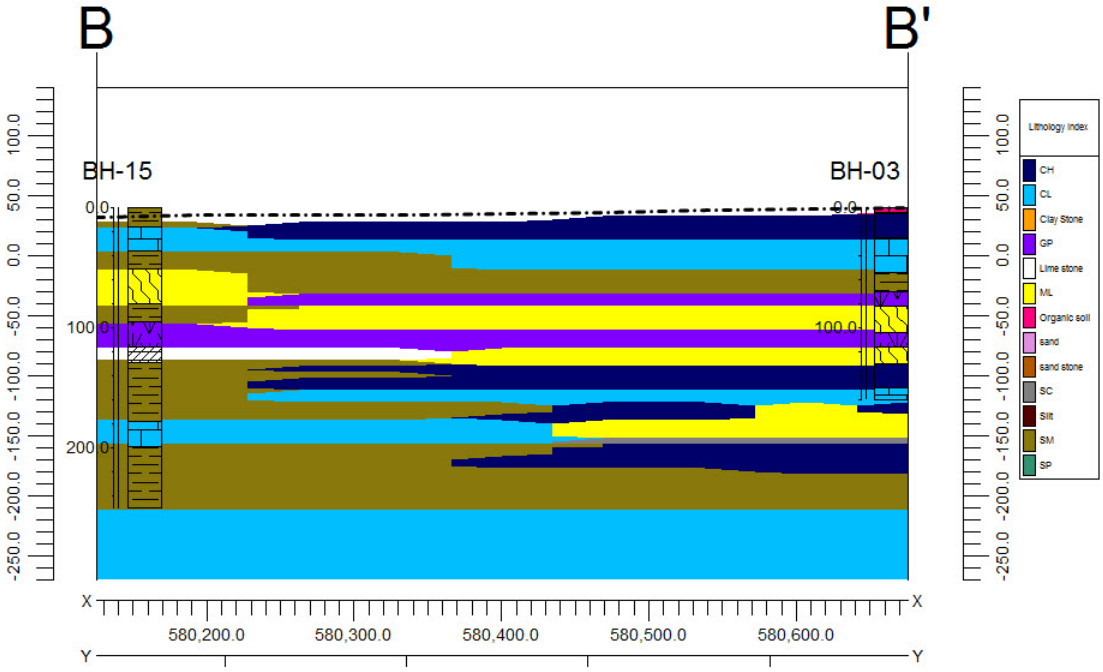

Figure 9.22. The profile of XXIV 50 W1 parcel between borehole 15 and 3.

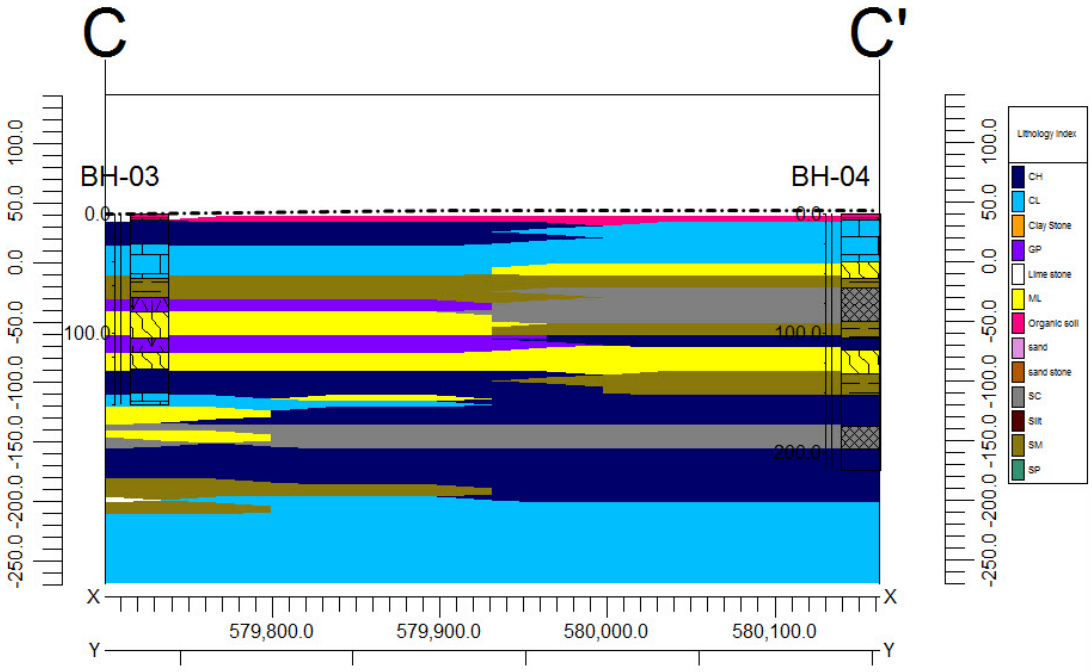

Figure 9.23. The profile of XXIV 50 W1 parcel between borehole 3 and 4.

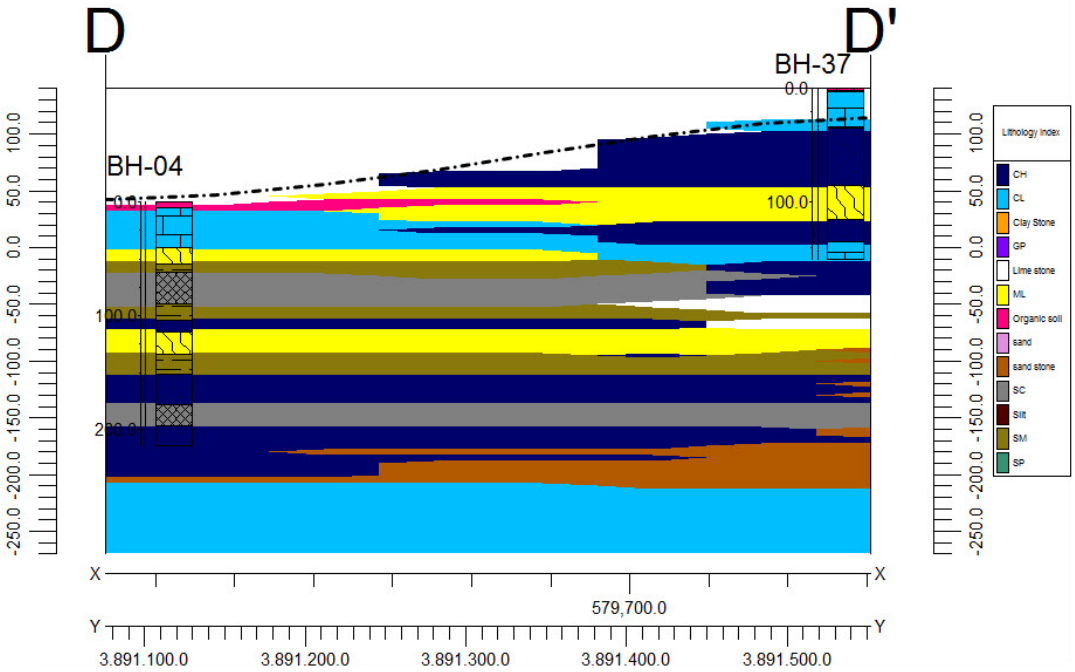

Figure 9.24. The profile of XXIV 50 W1 parcel between borehole 4 and 37.

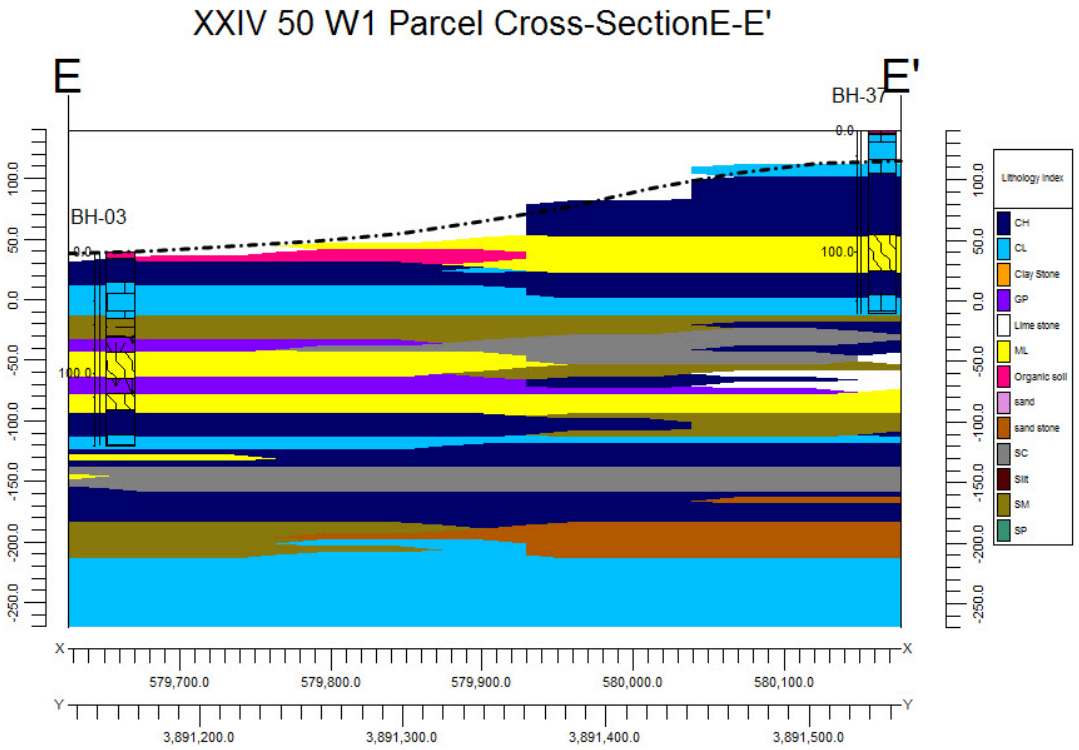

Figure 9.25. The profile of XXIV 50 W1 parcel between borehole 3and 37.

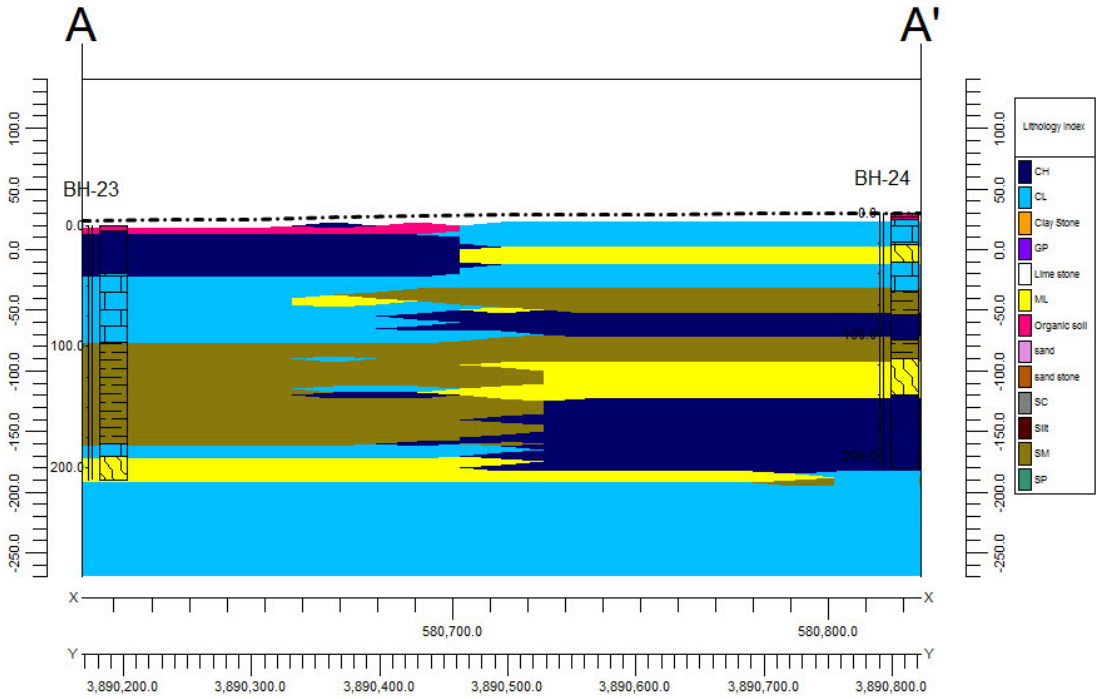

Figure 9.26. The profile of XXIV 50 W2 parcel between borehole 23 and 24.

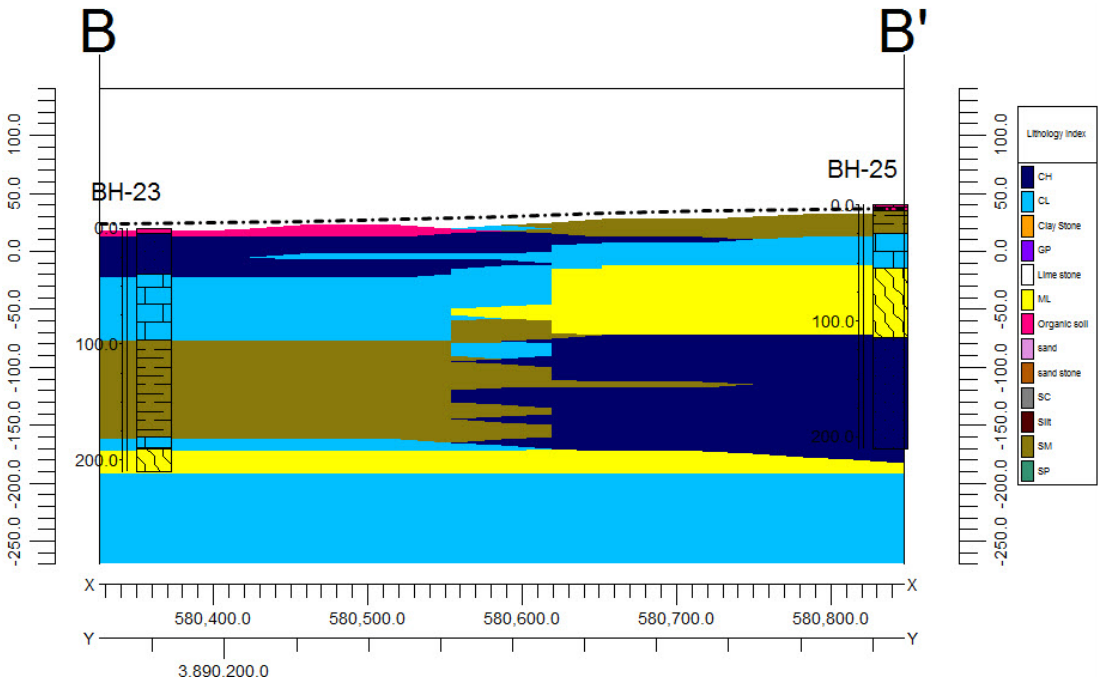

Figure 9.27. The profile of XXIV 50 W2 parcel between borehole 23 and 25.

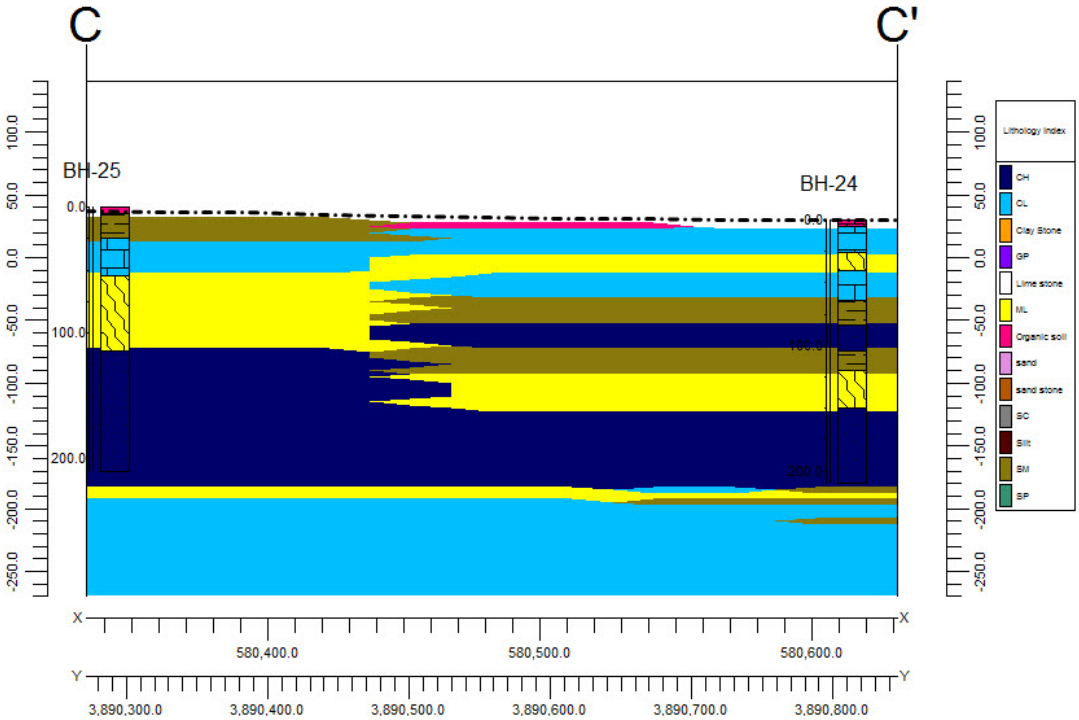

Figure 9.28. The profile of XXIV 50 W2 parcel between borehole 25 and 24.

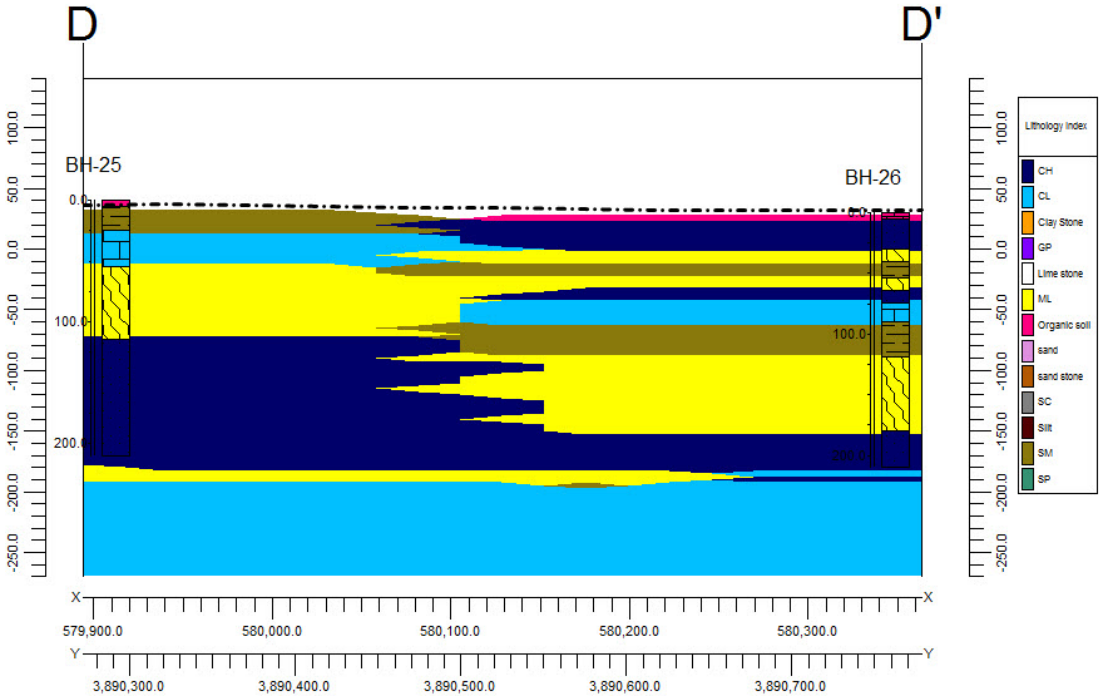

Figure 9.29. The profile of XXIV 50 W2 parcel between borehole 25 and 26.

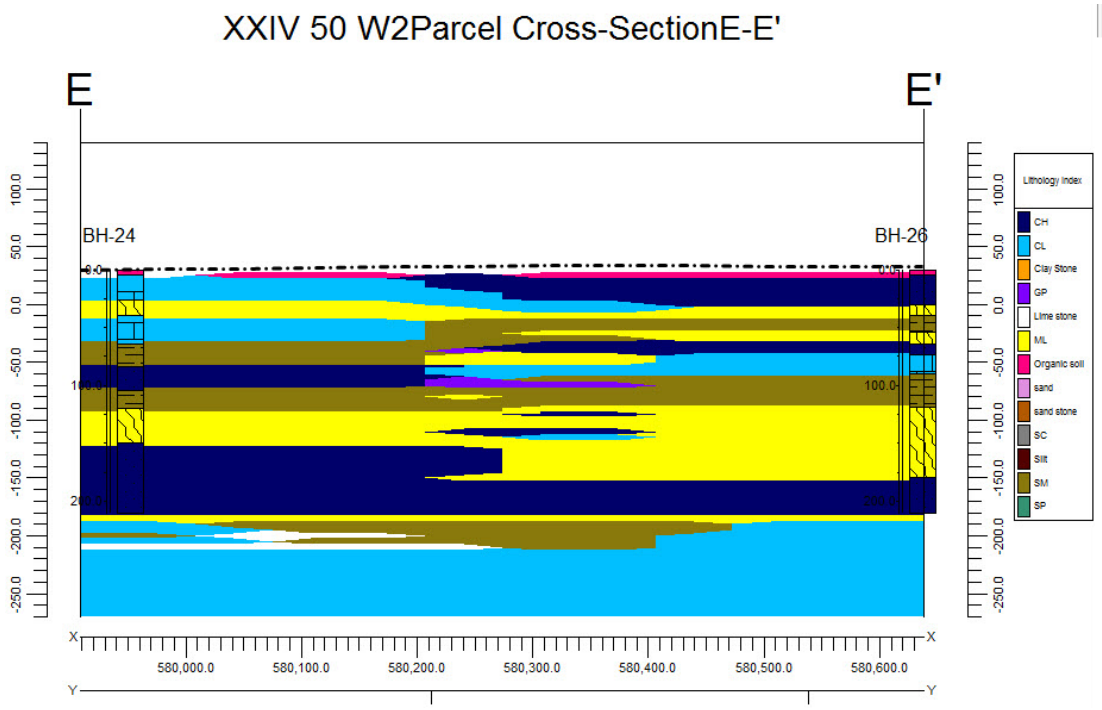

Figure 9.30. The profile of XXIV 50 W2 parcel between borehole 24 and 26.

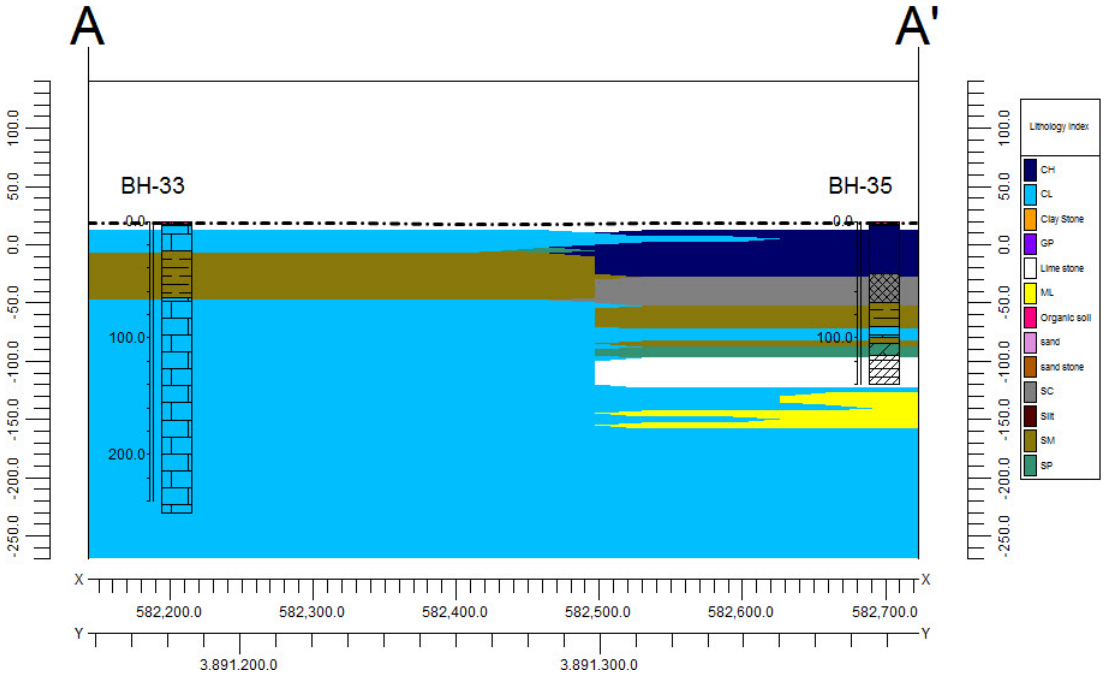

Figure 9.31. The profile of XXIV 51 W1 parcel between borehole 33 and 35.

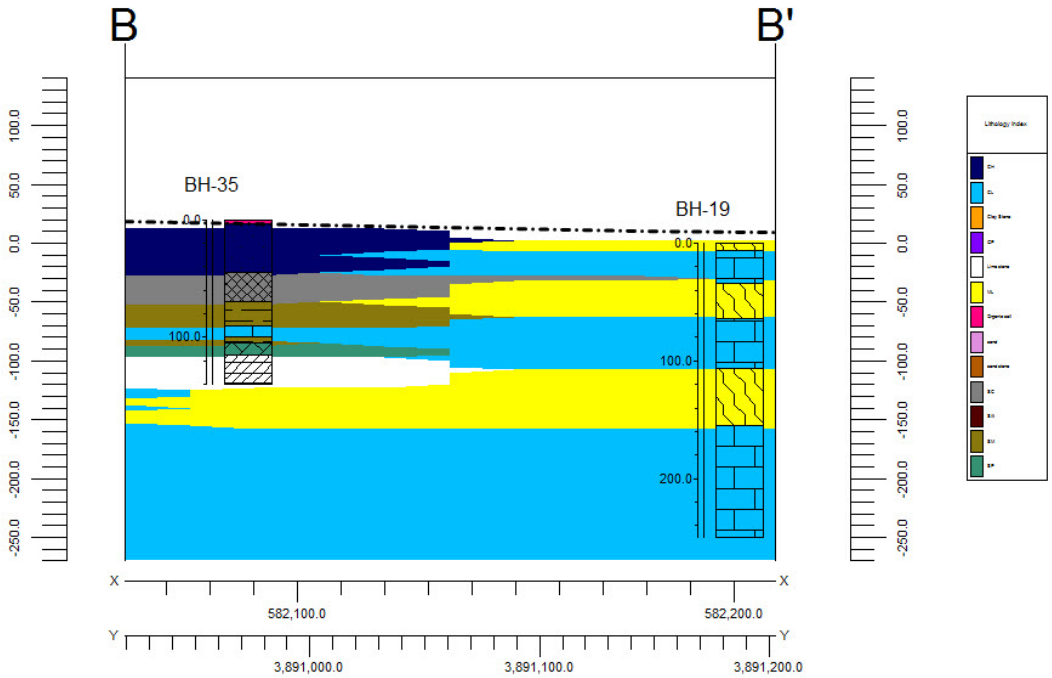

Figure 9.32. The profile of XXIV 51 W1 parcel between borehole 35 and 19.

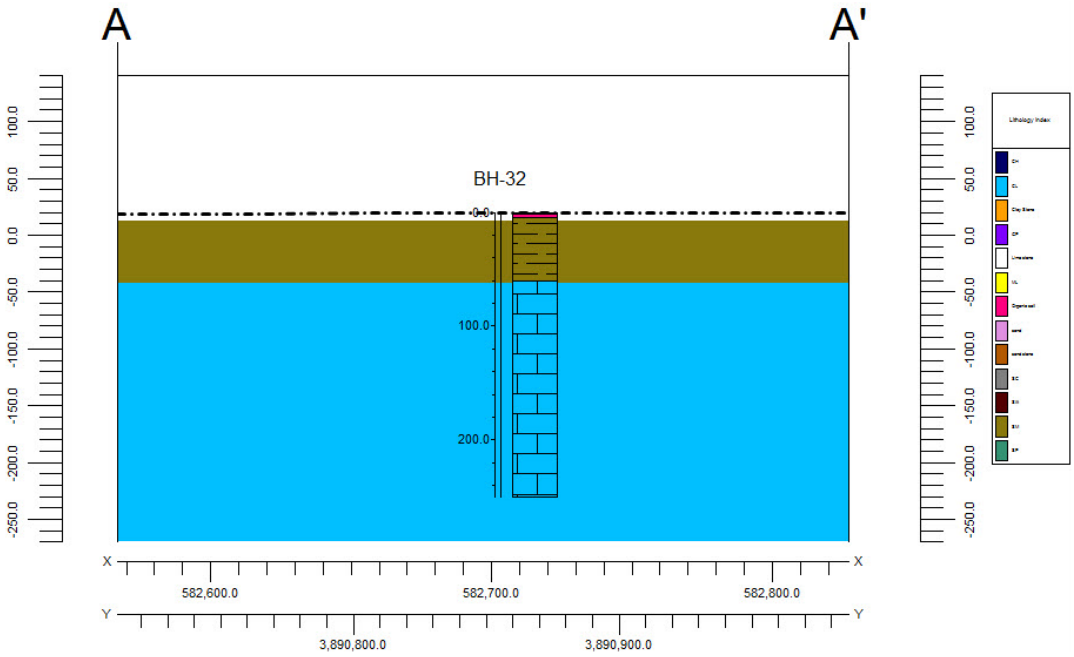

Figure 9.33. The profile of XXIV 51 W2 parcel borehole 32.

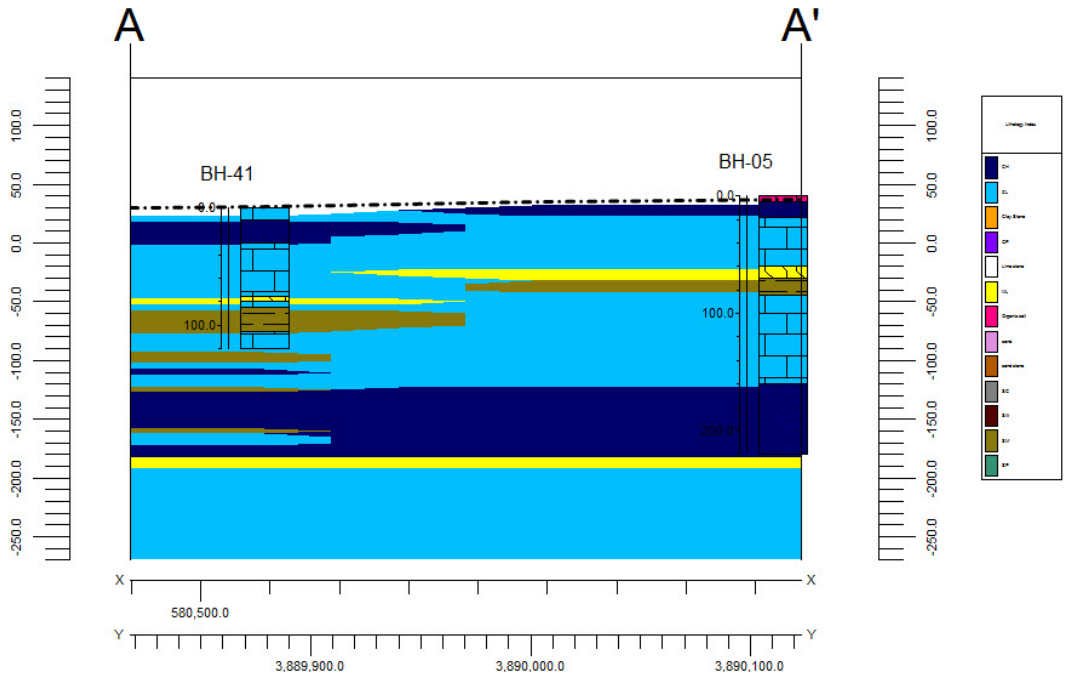

Figure 9.34. The profile of XXIV 53 W1 parcel between borehole 41 and 5.

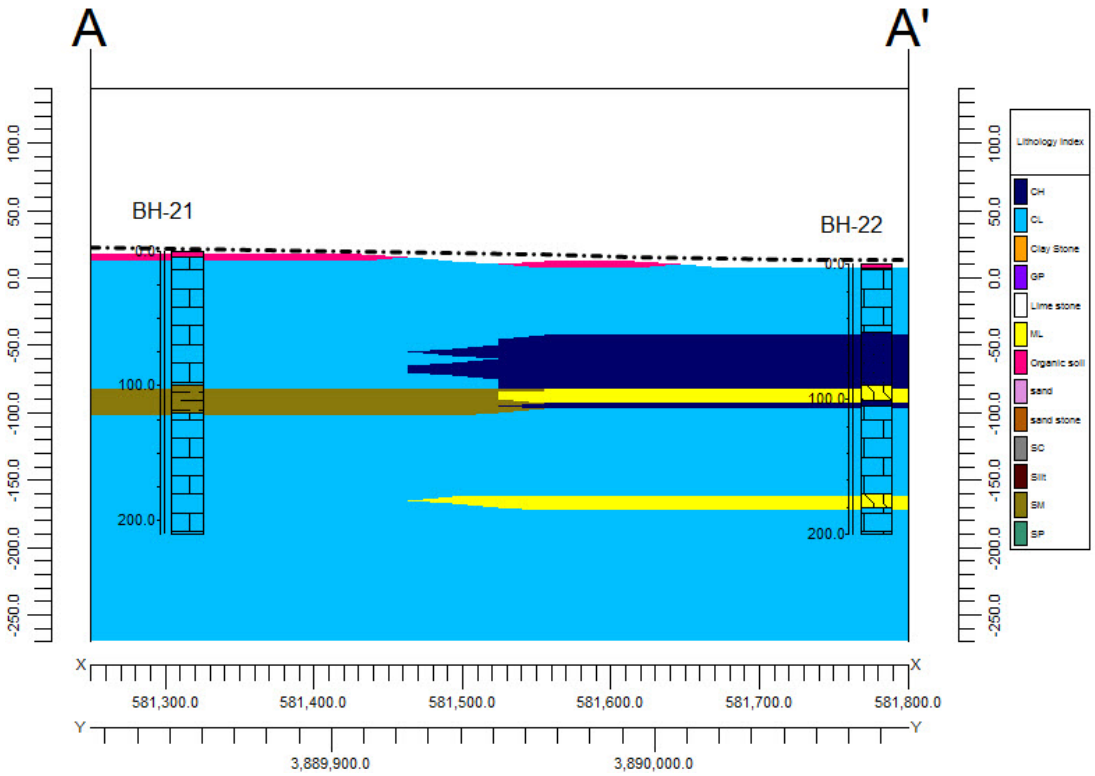

Figure 9.35. The profile of XXIV 58 E1 parcel between borehole 21 and 22.

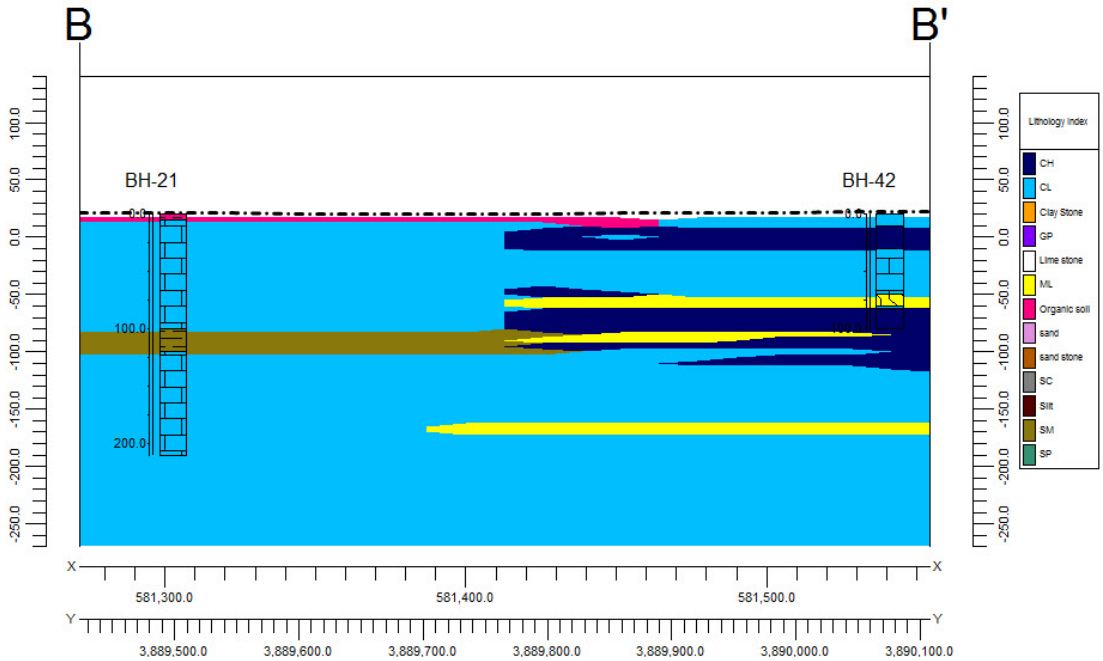

Figure 9.36. The profile of XXIV 58 E1 parcel between borehole 21 and 42.

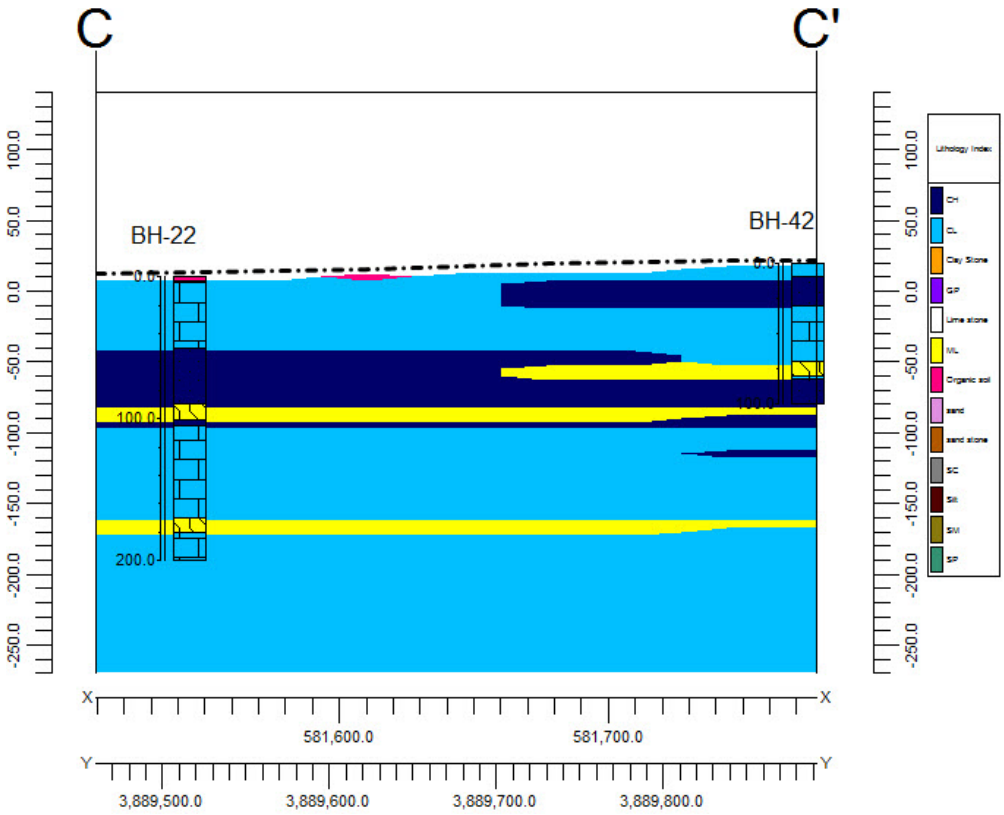

Figure 9.37. The profile of XXIV 58 E1 parcel between borehole 22 and 42.

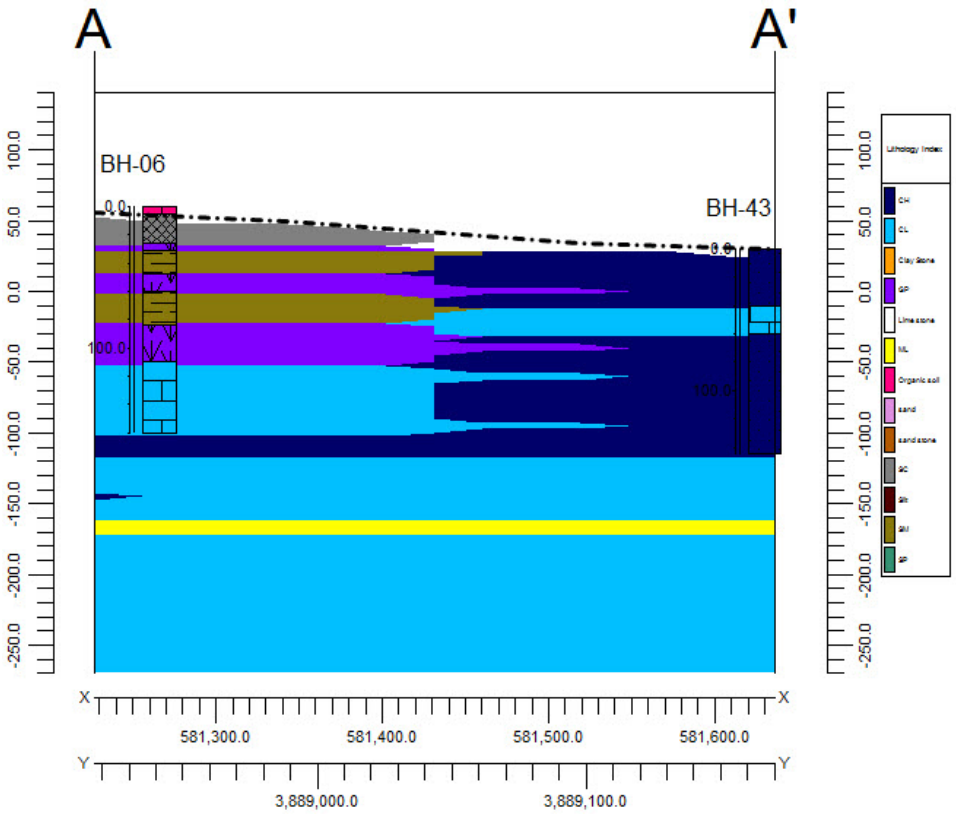

Figure 9.38. The profile of XXIV 58 E2 parcel between borehole 6 and 43.

Appendix C: Soil Properties

Table 10.1. The output of approximating Borehole 1 data by NovoSPT.

Depth1	Depth2	Soil type	Void Ratio	Unit Weight	Dry Unit Weight	Saturated Unit Weight	Young's Modulus	Friction Angle	Undrained Shear Strength of Clay/Silt	Shear Wave Velocity	Shear Modulus	Dilatancy Angle	Poisson Ratio	Permeability
			e	γ	γ_{dry}	γ_{Sat}	E_s (MPa)	φ (°)	S_u (kPa)	V_s (m/s)	G_{max} (kPa)	Ψ (°)	ν	k (cm/s)
0	0.5	OS												
0.5	4.5	CH	0.67	19.6	16.3	20.3	22	---	56.5	227.5	59	0	0.31075	10^{-7}
4.5	6	CL	0.8	19.4	15	19.5	13.6	---	29	162	63	0	0.286	10^{-7}
6	7	SM	1.28	17.5	11.4	17	11	28.3	---	137	60	0	0.1495	10^{-3}
7	12	CH	0.67	19.6	16.3	20.3	10.2	---	17.33	127.67	62.67	0	0.36925	10^{-7}
12	12.5	ML	0.83	18.1	14.5	19	8.6	---	12	106	50	0	0.25675	10^{-4}
12.5	13	CH	1.04	18.8	13.3	18.4	11	---	20	137	73	0	0.304	10^{-7}
13	14	SM	0.96	17.8	13.2	18.1	21	33.2	---	221	103	3.2	0.223	10^{-3}
14	20.5	CH	0.74	18.8	15.6	19.9	11	---	20	137	65	0	0.3355	10^{-7}
20.5	21.5	SM	0.86	17.8	13.9	18.6	32.9	35.7	---	291	144	5.7	0.2605	10^{-3}
21.5	23	LS[4]	0.07	24	23.3	24	76.7	44.7	---	466	198	14.7	0.3955	0
13	26	CH	0.95	19.6	14	18.8	11	---	20	137	65	0	0.32425	10^{-7}

[4] Lime Stone

Table 10.2. The output of approximating Borehole 2 data by NovoSPT.

Depth1	Depth2	Soil type	Void Ratio	Dry Unit Weight	Saturated Unit Weight	Young's Modulus	Friction Angle	Undrained Shear Strength of Clay/Silt	Shear Wave Velocity	Shear Modulus	Dilatancy Angle	Poisson Ratio	Permeability
			e	γ_{dry}	γ_{Sat}	E_s (MPa)	φ (º)	S_u (kPa)	V_s (m/s)	(G_{max}) kPa	Ψ (º)	ν	(k) m/day
0	0.5	OS											
0.5	5	CH	0.72	15.9	20.1	24.45	---	64.5	237.5	66.5	0	0.3355	10^{-7}
5	8	LS	0.07	23.3	24	51.7	45	---	376	119	15	0.4	0
8	25	SS[5]	0.26	19.8	21.9	51.7	43.8	---	376	142.50	13.8	0.382	0

[5] Sand Stone

Table 10.3. The output of approximating Borehole 3 data by NovoSPT.

Depth1	Depth2	Soil type	Void Ratio	Dry Unit Weight	Saturated Unit Weight	Young's Modulus	Friction Angle	Undrained Shear Strength of Clay/Silt	Shear Wave Velocity	Shear Modulus	Dilatancy Angle	Poisson Ratio	Permeability
			e	γ_{dry}	γ_{Sat}	E_s (MPa)	φ (º)	S_u (kPa)	V_s (m/s)	G_{max} (kPa)	Ψ (º)	ν	k (cm/s)
0	0.5	OS											
0.5	2.5	CH	0.73	15.7	19.9	16	---	37	184	55	0	0.3085	10^{-7}
2.5	5.4	CL	0.74	15.5	19.8	26	---	70	253	79	0	0.3085	10^{-7}
5.4	7	SM	1.25	11.5	17.1	8.6	24.8	---	106	48	0	0.097	10^{-3}
7	8.2	GP	0.59	16.3	20.1	40.4	43.4	---	328	114	13.4	0.376	1
8.2	10.4	ML	0.88	14.1	18.8	37.9	---	109	316	117	0	0.25675	10^{-4}
10.4	11.6	GP	0.59	16.3	20.1	40.4	43.4	---	328	114	13.4	0.376	1
11.6	13	ML	0.88	14.1	18.8	18.6	---	45	204	75	0	0.25675	10^{-4}
13	15	CH	0.8	15.2	19.6	33.6	---	94	294	124	0	0.31975	10^{-7}
15	16	CL	0.85	14.6	19.2	31	---	86	281	124	0	0.2995	10^{-3}

Table 10.4. The output of approximating Borehole 4 data by NovoSPT.

Depth1	Depth2	Soil type	Void Ratio	Dry Unit Weight	Saturated Unit Weight	Young's Modulus	Friction Angle	Undrained Shear Strength of Clay/Silt	Shear Wave Velocity	Shear Modulus	Dilatancy Angle	Poisson Ratio	Permeability
			e	γ_{dry}	γ_{Sat}	E_s (MPa)	φ (º)	S_u (kPa)	V_s (m/s)	G_{max} (kPa)	Ψ (º)	ν	k (cm/s)
0	0.5	OS											
0.5	4	CL	0.81	14.9	19.4	16	---	37	184	55	0	0.3175	10^{-7}
4	5.4	ML	0.94	13.6	18.5	12.3	---	25	150	54	0	0.25675	10^{-4}
5.4	6.2	SM	0.88	13.9	18.5	8.6	26.5	---	106	41	0	0.1225	10^{-3}
6.2	9	SC	0.98	13.3	18.3	7.3	22.3	---	87	40	0	0.0595	10^{-3}
9	10.4	SM	0.7	15.4	19.5	13.6	31	---	162	68	1	0.19	10^{-3}
10.4	11.4	CH	1	13.5	18.5	11	---	20	137	60	0	0.33775	10^{-7}
11.4	13.6	ML	0.9	13.8	18.5	18.6	---	45	204	75	0	0.25675	10^{-4}
13.6	15.2	SM	0.88	13.9	18.5	13.6	31	---	162	68	1	0.19	10^{-3}
15.2	17.8	CH	1	13.5	18.5	33.6	---	94	294	124	0	0.33775	10^{-7}
17.8	19.7	SC	0.79	14.6	19.1	13.6	29.6	---	162	75	0	0.169	10^{-3}
19.7	21.5	CH	0.79	15.3	19.7	51.7	---	154	376	144	0	0.349	10^{-7}

Table 10.5. The output of approximating Borehole 5 data by NovoSPT.

Depth1	Depth2	Soil type	Void Ratio	Dry Unit Weight	saturated Unit Weight	Young's Modulus	Friction Angle	Undrained Shear Strength of Clay/Silt	Shear Wave Velocity	Shear Modulus	Dilatancy Angle	Poisson Ratio	Permeability
			e	γ_{dry}	γ_{Sat}	E_s (MPa)	φ (º)	S_u (kPa)	V_s (m/s)	G_{max} (kPa)	Ψ (º)	ν	k (cm/s)
0	0.5	OS											
0.5	1.8	CH	0.67	16.3	20.3	18.6	---	45	204	106	0	0.31075	10^{-7}
1.8	6	CL	0.86	14.7	19.3	10.4	---	18	130	46	0	0.29725	10^{-4}
6	7	ML	0.98	13.3	18.2	8.6	---	12	106	47	0	0.25675	10^{-3}
7	8.4	SM	0.64	15.8	19.8	9.8	26.4	---	123	56	0	0.121	10^{-3}
8.4	16	CL	0.92	14.1	18.9	13.13	---	27	153	74	0	0.2995	10^{-7}
16	23	CH	0.91	14.3	19	17.95	---	43	199	107	0	0.3355	10^{-7}

Table 10.6. The output of approximating Borehole 6 data by NovoSPT.

Depth1	Depth2	Soil type	Void Ratio	Dry Unit Weight	Saturated Unit Weight	Young's Modulus	Friction Angle	Undrained Shear Strength of Clay/Silt	Shear Wave Velocity	Shear Modulus	Dilatancy Angle	Poisson Ratio	Permeability
			e	γ_{dry}	γ_{Sat}	E_s (MPa)	φ (º)	S_u (kPa)	V_s (m/s)	(G_{max}) kPa	Ψ (º)	ν	k (cm/s)
0	0.5	OS											
0.5	2.6	SC	0.58	16.7	20.3	49.8	45	---	368	85	15	0.4	10^{-3}
2.6	3.1	GP	0.59	16.3	20.1	40.4	43.4	---	328	114	13.4	0.376	1
3.1	4.8	SM	0.78	14.5	18.9	28.6	41.8	---	268	84	11.8	0.352	10^{-3}
4.8	6	GP	0.59	16.3	20.1	40.4	43.4	---	368	85	13.4	0.376	1
6	8.4	SM	0.66	15.7	19.6	24.2	38.2	---	242	88	8.2	0.298	10^{-3}
8.4	11	GP	0.59	16.3	20.1	40.4	43.4	---	328	114	13.4	0.376	1
11	16	CL	0.92	14.1	18.9	50.4	---	150	371	139	0	0.2995	10^{-7}

Table 10.7. The output of approximating Borehole 7 data by NovoSPT.

Depth1	Depth2	Soil type	Void Ratio	Dry Unit Weight	Saturated Unit Weight	Young's Modulus	Friction Angle	Undrained Shear Strength of Clay/Silt	Shear Wave Velocity	Shear Modulus	Dilatancy Angle	Poisson Ratio	Permeability
			e	γ_{dry}	γ_{Sat}	E_s (MPa)	φ (º)	S_u (kPa)	V_s (m/s)	G_{max} (kPa)	Ψ (º)	ν	k (cm/s)
0	0.5	OS											
0.5	1.75	CL	0.81	14.9	19.4	23.6	---	62	238	53	0	0.3175	10^{-7}
1.75	3	LS	0.07	23.3	24	62.3	45	---	416	86	15	0.4	0
3	13.6	SS	0.26	19.8	21.9	76.7	45	---	466	82	15	0.4	0
13.6	19.5	CH	0.87	14.6	19.2	45.45	---	133.5	342	166	0	0.34225	10^{-7}

Table 10.8. The output of approximating Borehole 8 data by NovoSPT.

Depth1	Depth2	Soil type	Void Ratio	Dry Unit Weight	Saturated Unit Weight	Young's Modulus	Friction Angle	Undrained Shear Strength of Clay/Silt	Shear Wave Velocity	Shear Modulus	Dilatancy Angle	Poisson Ratio	Permeability
			e	γ_{dry}	γ_{Sat}	E_s (MPa)	φ (°)	S_u (kPa)	V_s (m/s)	G_{max} (kPa)	Ψ (°)	ν	k (cm/s)
0	1.6	SM	0.66	15.7	19.7	9.8	31.3	---	123	33	1.3	0.1945	10^{-3}
1.6	2.5	CH	1.12	12.8	18.1	17.3	---	41	194	47	0	0.34225	10^{-7}
2.5	4	SM	0.86	14	18.6	26.7	43.8	---	257	64	13.8	0.382	10^{-3}
4	9	LS	0.07	23.3	24	76.7	45	---	466	82	15	0.4	0
9	12	SC	0.72	15.3	19.5	63.6	45	---	421	141	15	0.4	10^{-3}
12	14	CH	0.74	15.6	19.9	76.7	---	236	466	169	0	0.3805	10^{-7}
14	18	SS	0.26	19.8	21.9	76.7	42.9	---	466	217	12.9	0.3685	0

Table 10.9. The output of approximating Borehole 9 data by NovoSPT.

Depth1	Depth2	Soil type	Void Ratio	Dry Unit Weight	Saturated Unit Weight	Young's Modulus	Friction Angle	Undrained Shear Strength of Clay/Silt	Shear Wave Velocity	Shear Modulus	Dilatancy Angle	Poisson Ratio	Permeability
			e	γ_{dry}	γ_{Sat}	E_s (MPa)	φ (º)	S_u (kPa)	V_s (m/s)	G_{max} (kPa)	Ψ (º)	ν	k (cm/s)
0	2	SM	0.66	15.7	19.7	76.7	45	---	466	82	15	0.4	10^{-3}
2	3	CL	1.02	13.4	18.5	7.3	---	8	87	32	0	0.2725	10^{-7}
3	23	LS	0.07	23.3	24	76.7	43.8	---	466	207.5	13.8	0.382	0

Table 10.10. The output of approximating Borehole 10 data by NovoSPT.

Depth1	Depth2	Soil type	Void Ratio	Dry Unit Weight	Saturated Unit Weight	Young's Modulus	Friction Angle	Undrained Shear Strength of Clay/Silt	Shear Wave Velocity	Shear Modulus	Dilatancy Angle	Poisson Ratio	Permeability
			e	γ_{dry}	γ_{Sat}	E_s (MPa)	φ (º)	S_u (kPa)	V_s (m/s)	G_{max} (kPa)	Ψ (º)	ν	k (cm/s)
0	3	CH	0.93	14	18.9	17.3	---	41	194	47	0	0.31975	10^{-7}
3	5	SM	0.88	13.9	18.6	9.2	28.15	---	114.5	40.5	0	0.14725	10^{-3}
5	9.5	CL	1.04	13.3	18.4	9.2	---	14	114.5	48.5	0	0.29275	10^{-7}
9.5	13	CH	1.03	13.4	18.5	9.8	---	16	123	59	0	0.313	10^{-7}
13	14.5	SM	0.71	15.3	19.4	61	45	---	412	146	15	0.4	10^{-3}
14.5	15.5	LS	0.07	23.3	24	76.7	44.7	---	466	198	14.7	0.3955	0

Table 10.11. The output of approximating Borehole 11 data by NovoSPT.

Depth1	Depth2	Soil type	Void Ratio	Dry Unit Weight	Saturated Unit Weight	Young's Modulus	Friction Angle	Undrained Shear Strength of Clay/Silt	Shear Wave Velocity	Shear Modulus	Dilatancy Angle	Poisson Ratio	Permeability
			e	γ_{dry}	γ_{Sat}	E_s (MPa)	φ (º)	S_u (kPa)	V_s (m/s)	G_{max} (kPa)	Ψ (º)	ν	k (cm/s)
0	0.5	OS											
0.5	3.5	CL	1.02	13.4	18.5	9.8	---	16.5	111.5	31.5	0	0.2725	10^{-7}
3.5	4.6	SM	0.93	13.5	18.4	7.3	23.7	---	87	34	0	0.0805	0
4.6	6	CL	1.22	12.2	17.7	8.6	---	12	106	43	0	0.304	10^{-3}
6	7.5	SM	0.92	13.7	18.4	8.6	26	---	106	43	0	0.115	10^{-7}
7.5	10	CL	0.89	14.3	19	11	---	20	137	57.5	0	0.277	10^{-7}
10	11	SM	0.87	13.9	18.5	9.8	29.1	---	123	43	0	0.1615	0
11	25.5	CL	1.01	13.5	18.5	14.4875	---	55.5	166.625	83.625	0	0.2995	0

Table 10.12. The output of approximating Borehole 12 data by NovoSPT.

Depth1	Depth2	Soil type	Void Ratio	Dry Unit Weight	Saturated Unit Weight	Young's Modulus	Friction Angle	Undrained Shear strength of Clay/Silt	Shear Wave Velocity	Shear Modulus	Dilatancy Angle	Poisson Ratio	Permeability
			e	γ_{dry}	γ_{Sat}	E_s (MPa)	φ (°)	S_u (kPa)	V_s (m/s)	G_{max} (kPa)	Ψ (°)	ν	k (cm/s)
0	1	SM	0.66	15.7	19.7	9.8	29.1	---	123	43	0	0.1615	10^{-3}
1	2.5	CL	1.05	13.2	18.3	23.6	---	62	238	53	0	0.30175	10^{-7}
2.5	3.5	ML	0.88	14.1	18.8	9.8	---	16	123	40	0	0.25675	10^{-4}
3.5	6	SM	0.89	13.8	18.5	9.8	29.1	---	123	43	0	0.1615	10^{-3}
6	7.5	CL	1.04	13.3	18.4	9.8	---	16	121.5	48.5	0	0.27925	10^{-7}
7.5	8.4	ML	0.91	13.9	18.6	17.3	---	41	199	61	0	0.25675	10^{-4}
8.4	9.4	CH	1.03	13.4	18.5	28.6	---	78	268	147	0	0.313	10^{-7}
9.4	14	LS	0.07	23.3	24	76.7	44.7	---	466	198	14.7	0.3955	0

Table 10.13. The output of approximating Borehole 13data by NovoSPT.

Depth1	Depth2	Soil type	Void Ratio	Dry Unit Weight	Saturated Unit Weight	Young's Modulus	Friction Angle	Undrained Shear strength of Clay/Silt	Shear Wave Velocity	Shear Modulus	Dilatancy Angle	Poisson Ratio	Permeability
			e	γ_{dry}	γ_{Sat}	E_s (MPa)	φ (º)	S_u (kPa)	V_s (m/s)	G_{max} (kPa)	Ψ (º)	ν	k (cm/s)
0	1.5	SM	0.66	15.7	19.7	9.8	30.6	---	123	36	0.6	0.184	10^{-3}
1.5	2.1	CL	0.87	14.5	19.1	9.8	---	16	123	33	0	0.2815	10^{-7}
2.1	3	SM	3.29	6.07	13.7	9.8	30.6	---	123	36	0.6	0.184	10^{-3}
3	6	CL	1.03	13.3	18.4	8.55	---	12	105	36.5	0	0.286	10^{-7}
6	7.5	SM	3.29	6.07	13.7	7.3	23	---	87	37	0	0.07	10^{-3}
7.5	25	CL	1.11	12.8	18	10.725	---	19.25	132.5	56	0	0.29275	10^{-7}

Table 10.14. The output of approximating Borehole 14data by NovoSPT.

Depth1	Depth2	Soil type	Void Ratio	Dry Unit Weight	Saturated Unit Weight	Young's Modulus	Friction Angle	Undrained Shear strength of Clay/Silt	Shear Wave Velocity	Shear Modulus	Dilatancy Angle	Poisson Ratio	Permeability
			e	γ_{dry}	γ_{Sat}	E_s (MPa)	φ (º)	(S_u) kPa	V_s (m/s)	G_{max} (kPa)	Ψ (º)	ν	k (cm/s)
0	2	SM	0.99	13	18	23.6	43.5	---	238	53	13.5	0.3775	10^{-3}
2	6.4	CL	0.97	13.7	18.7	8.17	---	10.67	99.67	39	0	0.2905	10^{-7}
6.4	10.4	SM	3.2	6.19	13.8	7.3	22.4	---	87	40	0	0.061	10^{-3}
10.4	11.6	ML	0.66	16.1	20	29.2	---	80	271	83	0	0.25675	10^{-4}
11.6	15	LS	0.07	23.3	24	76.7	44.7	---	466	198	14.7	0.3955	0

Table 10.15. The output of approximating Borehole 15data by NovoSPT.

Depth1	Depth2	Soil type	Void Ratio	Dry Unit Weight	Saturated Unit Weight	Young's Modulus	Friction Angle	Undrained Shear Strengthof Clay/Silt	Shear Wave Velocity	Shear Modulus	Dilatancy Angle	Poisson Ratio	Permeability
			e	γ_{dry}	γ_{Sat}	E_s (MPa)	φ (°)	S_u (kPa)	V_s (m/s)	G_{max} (kPa)	Ψ (°)	ν	k (cm/s)
0	1.6	SM	0.66	15.7	19.7	7.3	25.5	---	87	27	0	0.1075	10^{-3}
1.6	3.6	CL	0.74	15.6	19.8	8.55	---	12	105	37	0	0.2995	10^{-7}
3.6	5.1	SM	0.75	14.8	19.1	7.3	25.5	---	87	27	0	0.1075	10^{-3}
5.1	8	ML	0.83	14.5	19	11	---	20	137	51	0	0.25675	10^{-4}
8	9.5	SM	0.9	13.7	18.4	7.3	21.9	---	87	42	0	0.0535	10^{-3}
9.5	11.6	GP	0.59	16.3	20.1	40.4	43.4	---	328	114	13.4	0.376	1
11.6	12.9	LS	0.07	23.3	24	76.7	44.7	---	466	198	14.7	0.3955	0
12.9	17.8	SM	0.66	15.7	19.6	26.7	36.1	---	257	114	6.1	0.2665	10^{-3}
17.8	19.9	CL	0.92	14.1	18.9	52.3	---	156	378	154	0	0.2995	10^{-7}
19.9	25	SM	0.66	15.7	19.6	7.3	20.3	---	87	46	0	0.0295	10^{-3}

Table 10.16. The output of approximating Borehole 16data by NovoSPT.

Depth1	Depth2	Soil type	Void Ratio	Dry Unit Weight	Saturated Unit Weight	Young's Modulus	Friction Angle	Undrained Shear strength of Clay/Silt	Shear Wave Velocity	Shear Modulus	Dilatancy Angle	Poisson Ratio	Permeability
			e	γ_{dry}	γ_{Sat}	E_s (MPa)	φ (°)	S_u (kPa)	V_s (m/s)	G_{max} (kPa)	Ψ (°)	ν	k (cm/s)
0	0.5	OS											
0.5	6	CL	0.69	16.1	20.2	8.55	---	12	105	37	0	0.2995	10^{-7}
6	7	SM	0.86	14	18.6	9.8	27.7	---	123	50	0	0.1405	10^{-3}
7	12	ML	0.84	14.4	19	6.65	---	6	74	40	0	0.25675	10^{-4}
12	14	SM	0.66	15.7	19.6	7.3	20.3	---	87	49	0	0.0295	10^{-3}
14	20	CH	0.88	14.5	19.2	18.5	---	45	202.5	98	0	0.3355	10^{-7}
20	25	CL	1.11	12.8	18	52.3	---	156	378	154	0	0.29275	10^{-7}

Table 10.17. The output of approximating Borehole 17data by NovoSPT.

Depth1	Depth2	Soil type	Void Ratio	Dry Unit Weight	Saturated Unit Weight	Young's Modulus	Friction Angle	Undrained Shear Strengthof Clay/Silt	Shear Wave Velocity	Shear Modulus	Dilatancy Angle	Poission Ratio	Primeability
			e	γ_{dry}	γ_{Sat}	E_s (MPa)	φ (°)	S_u (kPa)	V_s (m/s)	G_{max} (kPa)	Ψ (°)	ν	k (cm/s)
0	0.7	OS											
0.7	4	SM	0.97	13.2	18.1	9.8	30.6	---	123	36	0.6	0.184	10^{-7}
4	6	ML	0.88	14.2	18.9	8.6	---	12	106	39	0	0.25675	10^{-4}
6	8	CH	0.67	16.3	20.3	7.3	---	---	87	42	0	0.38725	10^{-7}
8	10	SM	0.6	16.2	19.9	16	34.2	---	184	68	4.2	0.238	10^{-3}
10	11.5	CH	0.67	16.3	20.3	9.8	---	16	123	58	0	0.38725	10^{-7}
11.5	15	SM	0.59	16.3	20	9.8	25.2	---	123	62	0	0.103	10^{-3}
15	18	ML	0.82	14.7	19.2	11	---	20	137	72	0	0.25675	10^{-4}
18	36.5	CH	0.65	16.5	20.4	12.9	---	26.5	155.5	98.5	0	0.38725	10^{-7}

Table 10.18. The output of approximating Borehole 18data by NovoSPT.

Depth1	Depth2	Soil type	Void Ratio	Dry Unit Weight	Saturated Unit Weight	Young's Modulus	Friction Angle	Undrained Shear strength of Clay/Silt	Shear Wave Velocity	Shear Modulus	Dilatancy Angle	Poisson Ratio	Permeability
			e	γ_{dry}	γ_{Sat}	E_s (MPa)	φ (º)	S_u (kPa)	V_s (m/s)	G_{max} (kPa)	Ψ (º)	ν	k (cm/s)
0	0.7	OS											
0.7	1.6	CL	0.81	14.9	19.4	11	---	20	137	64	0	0.3175	10^{-7}
1.6	2.4	SM	0.78	14.3	18.7	11	30.9	---	137	47	0.9	0.1885	10^{-3}
2.4	4.6	CL	0.75	15.5	19.7	9.8	---	16	123	40	0	0.295	10^{-7}
4.6	12.6	ML	0.84	14.3	18.9	8.32	---	11.2	101.8	47.8	0	0.25675	10^{-7}
12.6	30	CL	0.85	14.6	19.2	12.3	---	24.67	149.67	87.67	0	0.2905	10^{-7}

Table 10.19. The output of approximating Borehole 19data by NovoSPT.

Depth1	Depth2	Soil type	Void Ratio	Dry Unit Weight	Saturated Unit Weight	Young's Modulus	Friction Angle	Undrained Shear strength of Clay/Silt	Shear Wave Velocity	Shear Modulus	Dilatancy Angle	Poisson Ratio	Permeability
			e	γ_{dry}	γ_{Sat}	E_s (MPa)	φ (°)	S_u (kPa)	V_s (m/s)	G_{max} (kPa)	Ψ (°)	ν	k (cm/s)
0	0.6	ML	0.52	17.5	20.9	7.3	---	8	87	26	0	0.25675	10^{-4}
0.6	3.4	CL	0.91	14	18.8	7.3	---	8	87	28	0	0.2995	10^{-7}
3.4	6.4	ML	0.69	15.7	19.8	7.3	---	8	87	25.5	0	0.25675	10^{-4}
6.4	10.6	CL	0.95	13.9	18.8	7.95	---	10	96.5	26.5	0	0.286	10^{-7}
10.6	15.5	ML	0.85	14.3	18.9	17.95	---	43	199	65	0	0.25675	10^{-4}
15.5	25	CL	0.65	16.5	20.4	18.6	---	45	204	92	0	0.38725	10^{-7}

Table 10.20. The output of approximating Borehole 20data by NovoSPT.

Depth1	Depth2	Soil type	Void Ratio	Dry Unit Weight	Saturated Unit Weight	Young's Modulus	Friction Angle	Undrained Shear strength of Clay/Silt	Shear Wave Velocity	Shear Modulus	Dilatancy Angle	Poisson Ratio	Permeability
			e	γ_{dry}	γ_{Sat}	E_s (MPa)	φ (º)	S_u (kPa)	V_s (m/s)	G_{max} (kPa)	Ψ (º)	ν	k (cm/s)
0	0.5	OS											
0.5	2.5	CH	0.73	15.7	19.9	12.3	---	25	150	73	0	0.3175	10^{-7}
2.5	4.4	SM	0.73	15	19.3	11	30.9	---	137	47	0.9	0.1885	10^{-3}
4.4	8.1	ML	0.83	14.4	19	12.3	---	25	150	62	0	0.25675	10^{-4}
8.1	15	CL	0.94	13.9	18.8	11	---	20	137	66	0	0.30175	10^{-7}
15	17	SM	0.97	13.2	18.1	12.3	27.2	---	150	77	0	0.133	10^{-3}
17	24	CL	0.85	14.6	19.2	12.3	---	25	150	88	0	0.30175	10^{-7}

Table 10.21. The output of approximating Borehole 21data by NovoSPT.

Depth1	Depth2	Soil type	Void Ratio	Dry Unit Weight	saturated Unit Weight	Young's Modulus	Friction Angle	Undrained Shear strength of Clay/Silt	Shear Wave Velocity	Shear Modulus	Dilatancy Angle	Poisson Ratio	Permeability
			e	γ_{dry}	γ_{Sat}	E_s (MPa)	φ (°)	S_u (kPa)	V_s (m/s)	G_{max} (kPa)	Ψ (°)	ν	k (cm/s)
0	0.5	OS											
0.5	10	CL	0.92	14.2	19	9.2	---	14	114.5	40.5	0	0.2995	10^{-7}
10	12	SM	0.84	14.1	18.7	31.7	40.9	---	285	102	10.9	0.3385	10^{-3}
12	21	CL	0.94	14.1	18.9	14.8	---	33	174	85	0	0.30175	10^{-3}

Table 10.22. The output of approximating Borehole 22data by NovoSPT.

Depth1	Depth2	Soil type	Void Ratio	Dry Unit Weight	Saturated Unit Weight	Young's Modulus	Friction Angle	Undrained Shear strength of Clay/Silt	Shear Wave Velocity	Shear Modulus	Dilatancy Angle	Poisson Ratio	Permeability
			e	γ_{dry}	γ_{Sat}	E_s (MPa)	φ (º)	S_u (kPa)	V_s (m/s)	G_{max} (kPa)	Ψ (º)	ν	k (cm/s)
0	0.3	OS											
0.3	5	CL	0.92	14.2	19	9.8	---	16	121.5	39.5	0	0.29275	10^{-7}
5	9	CH	1.07	13.2	18.3	13.6	---	29	162	61	0	0.31525	10^{-7}
9	10.1	ML	0.83	14.4	19	33.6	---	94	294	101	0	0.25675	10^{-4}
10.1	10.5	CH	1.07	13.2	18.3	13.6	---	29	162	61	0	0.31525	10^{-7}
10.5	17	CL	0.89	14.3	19.1	16	---	37	184	76	0	0.2995	10^{-7}
17	18	ML	0.83	14.4	19	12.3	---	25	150	74	0	0.25675	10^{-4}
18	20	CL	0.94	14.1	18.9	50.4	---	150	371	139	0	0.30175	10^{-7}

Table 10.23. The output of approximating Borehole 23data by NovoSPT.

Depth1	Depth2	Soil type	Void Ratio	Dry Unit Weight	Saturated Unit Weight	Young's Modulus	Friction Angle	Undrained Shear strength of Clay/Silt	Shear Wave Velocity	Shear Modulus	Dilatancy Angle	Poisson Ratio	Permeability
			e	γ_{dry}	γ_{Sat}	E_s (MPa)	φ (º)	S_u (kPa)	V_s (m/s)	G_{max} (kPa)	Ψ (º)	ν	k (cm/s)
0	0.5	OS											
0.5	4	CH	0.68	16.2	20.3	11	---	20	137	41	0	0.313	10^{-7}
4	9.6	CL	0.99	13.6	18.6	10.45	---	18.5	128	50	0	0.2905	10^{-7}
9.6	18	SM	0.82	14.2	18.7	11.7	26.8	---	142.5	71	0	0.127	10^{-3}
18	19	CL	0.94	14.1	18.9	14.8	---	33	174	85	0	0.3085	10^{-7}
19	21	ML	0.9	13.8	18.5	13.6	---	29	162	75	0	0.25675	10^{-4}

Table 10.24. The output of approximating Borehole 25data by NovoSPT.

Depth1	Depth2	Soil type	Void Ratio	Dry Unit Weight	Saturated Unit Weight	Young's Modulus	Friction Angle	Undrained Shear strength of Clay/Silt	Shear Wave Velocity	Shear Modulus	Dilatancy Angle	Poisson Ratio	Permeability
			e	γ_{dry}	γ_{Sat}	E_s (MPa)	φ (º)	S_u (kPa)	Vs (m/s)	G_{max} (kPa)	Ψ (º)	ν	k (cm/s)
0	0.5	OS											
0.5	2.5	SM	0.79	14.5	18.9	14.8	31.2	---	174	76	1.2	0.193	10^{-3}
2.5	5.4	CL	0.77	15.4	19.7	13.6	---	29	162	44	0	0.3175	10^{-7}
5.4	11.4	ML	0.95	13.6	18.5	12.3	---	25	150	53	0	0.25675	10^{-4}
11.4	21	CH	0.95	14	18.8	17.7	---	42.33	196	81	0	0.32425	10^{-7}

Table 10.25. The output of approximating Borehole 26data by NovoSPT.

Depth1	Depth2	Soil type	Void Ratio	Dry Unit Weight	Saturated Unit Weight	Young's Modulus	Friction Angle	Undrained Shear strength of Clay/Silt	Shear Wave Velocity	Shear Modulus	Dilatancy Angle	Poisson Ratio	Permeability
			e	γ_{dry}	γ_{Sat}	E_s (MPa)	φ (°)	S_u (kPa)	V_s (m/s)	(G_{max}) kPa	Ψ (°)	ν	k (cm/s)
0	0.5	OS											
0.5	3	CH	0.77	15.4	19.7	16	---	37	184	54	0	0.3175	10^{-7}
3	4	ML	0.92	13.8	18.6	12.3	---	25	150	53	0	0.25675	10^{-4}
4	5.4	SM	0.83	14.2	18.7	14.8	31.2	---	174	76	1.2	0.193	10^{-3}
5.4	6.4	ML	0.95	13.7	18.5	9.8	---	16	123	49	0	0.25675	10^{-4}
6.4	7.4	CH	1.04	13.3	18.4	16	---	37	184	70	0	0.331	10^{-7}
7.4	9	CL	1.05	13.2	18.3	8.6	---	12	106	49	0	0.2905	10^{-7}
9	11.9	SM	0.82	14.3	18.8	21	36.3	---	221	85	6.3	0.2695	10^{-3}
11.9	18	ML	0.86	14.3	18.9	16	---	37.00	184	85	0	0.25675	10^{-4}
18	21	CH	0.95	14	18.8	14.8	---	33	174	89	0	0.3175	10^{-7}

Table 10.26. The output of approximating Borehole 27data by NovoSPT.

Depth1	Depth2	Soil type	Void Ratio	Dry Unit Weight	Saturated Unit Weight	Young's Modulus	Friction Angle	Undrained Shear strength of Clay/Silt	Shear Wave Velocity	Shear Modulus	Dilatancy Angle	Poisson Ratio	Permeability
			e	γ_{dry}	γ_{Sat}	E_s (MPa)	φ (º)	S_u (kPa)	V_s (m/s)	G_{max} (kPa)	Ψ (º)	ν	k (cm/s)
0	0.5	OS											
0.5	2.5	CL	0.98	13.7	18.6	12.3	---	25	150	73	0	0.3085	10^{-7}
2.5	6	ML	0.92	13.8	18.6	11.65	---	18.50	128	44.5	0	0.25675	10^{-4}
6	8.5	SM	0.78	14.5	18.9	16	34.6	---	184	66	4.6	0.244	10^{-3}
8.5	10	CL	0.97	13.7	18.6	16	---	20	137	60	0	0.29725	10^{-7}
10	11.1	SM	0.74	14.9	19.1	18.6	34.4	---	204	82	4.4	0.241	10^{-3}
11.1	14.5	ML	0.84	14.4	19	11	---	20	137	64	0	0.25675	10^{-4}
14.5	16	CL	0.95	13.9	18.7	8.6	---	37	184	86	0	0.286	10^{-7}
16	18	SM	0.82	14.2	18.7	18.6	34.4	---	204	82	4.4	0.241	10^{-3}
18	21	CL	0.94	14.1	18.9	21	---	53	221	106	0	0.3085	10^{-7}

Table 10.27. The output of approximating Borehole 28data by NovoSPT.

Depth1	Depth2	Soil type	Void Ratio	Dry Unit Weight	Saturated Unit Weight	Young's Modulus	Friction Angle	Undrained Shear strength of Clay/Silt	Shear Wave Velocity	Shear Modulus	Dilatancy Angle	Poisson Ratio	Permeability
			e	γ_{dry}	γ_{Sat}	E_s (MPa)	φ (°)	S_u (kPa)	V_s (m/s)	G_{max} (kPa)	Ψ (°)	ν	k (cm/s)
0	0.5	OS											
0.5	7	ML	0.78	14.9	19.3	9.2	---	14.00	114.5	40.5	0	0.25675	10^{-4}
7	8	SM	0.78	14.5	18.9	16	34.6	---	184	66	4.6	0.244	10^{-3}
8	9	CL	1.05	13.2	18.3	12.3	---	25	150	73	0	0.2905	10^{-7}
9	10	SM	0.81	14.3	18.8	18.6	34.4	---	204	82	4.4	0.241	10^{-3}
10	11.4	CL	1.02	13.4	18.4	8.6	---	12	106	52	0	0.295	10^{-7}
11.4	15	CH	0.99	13.6	18.6	16	---	37	184	80	0	0.3625	10^{-7}
15	21	CL	0.98	13.7	18.6	21	---	53.00	221	102.5	0	0.286	10^{-7}

Table 10.28. The output of approximating Borehole 29data by NovoSPT.

Depth1	Depth2	Soil type	Void Ratio	Dry Unit Weight	Saturated Unit Weight	Young's Modulus	Friction Angle	Undrained Shear strength of Clay/Silt	Shear Wave Velocity	Shear Modulus	Dilatancy Angle	Poisson Ratio	Permeability
			e	γ_{dry}	γ_{Sat}	E_s (MPa)	φ (º)	S_u (kPa)	V_s (m/s)	G_{max} (kPa)	Ψ (º)	ν	k (cm/s)
0	0.5	OS											
0.5	2.5	CL	0.86	14.6	19.2	9.8	---	16.00	150	73	0	0.2905	10^{-7}
2.5	5.5	ML	0.85	14.4	19	11.65	---	18.50	128	44.5	0	0.25675	10^{-4}
5.5	8.5	SM	0.83	14.2	18.7	11	29.8	---	137	47	0	0.172	10^{-3}
8.5	12	ML	0.93	13.8	18.6	29.8	---	82.00	137	64	0	0.25675	10^{-4}
12	14	CH	1.1	13	18.3	16	---	37.00	184	80	0	0.3085	10^{-7}
14	20	ML	0.79	14.8	19.2	21	---	53.00	137	68	0	0.25675	10^{-4}
20	25	CL	0.87	14.5	19.2	22.9	---	59.50	185.5	91.5	0	0.2815	10^{-7}

Table 10.29. The output of approximating Borehole 30data by NovoSPT.

Depth1	Depth2	Soil type	Void Ratio	Dry Unit Weight	Saturated Unit Weight	Young's Modulus	Friction Angle	Undrained Shear strength of Clay/Silt	Shear Wave Velocity	Shear Modulus	Dilatancy Angle	Poisson Ratio	Permeability
			e	γ_{dry}	γ_{Sat}	E_s (MPa)	φ (°)	S_u (kPa)	V_s (m/s)	G_{max} (kPa)	Ψ (°)	ν	k (cm/s)
0	0.5	OS											
0.5	4.5	ML	14.2	17.5	26.9	21	---	53	221	62	0	0.25675	10^{-4}
			0.84	14.5	19	21	---	53	221	62	0	0.25675	10^{-4}
4.5	5.5	SC	0.82	14.4	18.9	18.6	36.9	---	204	68	6.9	0.2785	10^{-3}
5.5	6.5	CL	0.88	14	18.6	24.15	---	63.50	240.5	76.5	0	0.304	10^{-7}
6.5	12	CH	0.86	14.7	19.3	14.77	---	32.67	169.33	70	0	0.32875	10^{-7}
12	21	CL	0.84	14.7	19.3	16	---	37.00	184	88.5	0	0.27475	10^{-7}

Table 10.30. The output of approximating Borehole 31data by NovoSPT.

Depth1	Depth2	Soil type	Void Ratio	Dry Unit Weight	Saturated Unit Weight	Young's Modulus	Friction Angle	Undrained Shear strength of Clay/Silt	Shear Wave Velocity	Shear Modulus	Dilatancy Angle	Poisson Ratio	Permeability
			e	γ_{dry}	γ_{Sat}	E_s (MPa)	φ (º)	S_u (kPa)	V_s (m/s)	G_{max} (kPa)	Ψ (º)	ν	k (cm/s)
0	0.5	OS											
0.5	3	CH	0.76	15.5	19.8	24.8	---	66.00	246	67	0	0.30625	10^{-7}
3	7.5	ML	0.86	14.3	18.9	12.3	---	25.00	150	63	0	0.25675	10^{-4}
7.5	9.5	CL	1	13.6	18.6	13.6	---	49.00	213	65	0	0.27925	10^{-7}
9.5	13	CH	1.31	11.9	17.5	12.9	---	26.50	155.5	72	0	0.32875	10^{-7}
13	14.4	SM	0.67	15.5	19.5	18.6	32.2	---	204	95	2.2	0.208	10^{-3}
14.4	15.4	CH	1	13.6	18.6	11	---	20.00	137	69	0	0.32425	10^{-7}
15.4	20.5	SM	0.67	15.5	19.5	18.6	30.4	---	204	106	0.4	0.181	10^{-3}
20.5	25	CH	0.95	14	18.8	11	---	20.00	137	65	0	0.32425	10^{-7}

Table 10.31. The output of approximating Borehole 32data by NovoSPT.

Depth1	Depth2	Soil type	Void Ratio	Dry Unit Weight	Saturated Unit Weight	Young's Modulus	Friction Angle	Undrained Shear strength of Clay/Silt	Shear Wave Velocity	Shear Modulus	Dilatancy Angle	Poisson Ratio	Permeability
			e	γ_{dry}	γ_{Sat}	E_s (MPa)	φ (º)	S_u (kPa)	V_s (m/s)	(G_{max}) kPa	Ψ (º)	ν	k (cm/s)
0	0.5	OS											
0.5	6	SM	0.78	14.5	18.9	23.85	42.15	---	238.5	61.5	12.15	0.35725	10^{-3}
6	25	CL	0.93	14.1	18.9	18.55	---	45.00	203.25	82.50	0	0.27475	10^{-7}

Table 10.32. The output of approximating Borehole 33data by NovoSPT.

Depth1	Depth2	Soil type	Void Ratio	Dry Unit Weight	Saturated Unit Weight	Young's Modulus	Friction Angle	Undrained Shear strength of Clay/Silt	Shear Wave Velocity	Shear Modulus	Dilatancy Angle	Poisson Ratio	Permeability
			e	γ_{dry}	γ_{Sat}	E_s (MPa)	φ (º)	S_u (kPa)	V_s (m/s)	(G_{max}) kPa	Ψ (º)	ν	k (cm/s)
0	0.4	OS											
0.4	2.5	CL	0.82	14.9	19.4	12.3	---	25.00	150	43	0	0.29275	10^{-7}
2.5	6.5	SM	0.8	14.4	18.8	16.7	35.80	---	187.5	61.5	5.8	0.262	10^{-3}
6.5	25	CL	0.81	15	19.5	20.67	---	52.00	218.33	91.33	0	0.29275	10^{-7}

Table 10.33. The output of approximating Borehole 34data by NovoSPT.

Depth1	Depth2	Soil type	Void Ratio	Dry Unit Weight	Saturated Unit Weight	Young's Modulus	Friction Angle	Undrained Shear Strength of Clay/Silt	Shear Wave Velocity	Shear Modulus	Dilatancy Angle	Poisson Ratio	Permeability
			e	γ_{dry}	γ_{Sat}	E_s (MPa)	φ (º)	S_u (kPa)	V_s (m/s)	(G_{max}) kPa	Ψ (º)	ν	k (cm/s)
0	0.5	OS											
0.5	6.5	SM	0.82	14.2	18.7	26.7	42.95	---	233.5	65.5	12.95	0.36925	10^{-3}
6.5	8.5	ML	0.79	14.8	19.2	9.8	---	16.00	123	140	0	0.25675	10^{-4}
8.5	13	SM	0.79	14.5	18.9	29.2	41.6	---	247	88	11.6	0.349	10^{-3}
13	15	LS	0.07	23.3	24	76.7	44.7	---	466	198	14.7	0.3955	0

Table 10.34. The output of approximating Borehole 35data by NovoSPT.

Depth1	Depth2	Soil type	Void Ratio	Dry Unit Weight	Saturated Unit Weight	Young's Modulus	Friction Angle	Undrained Shear Strength of Clay/Silt	Shear Wave Velocity	Shear Modulus	Dilatancy Angle	Poisson Ratio	Permeability
			e	γ_{dry}	γ_{Sat}	E_s (MPa)	φ (º)	S_u (kPa)	V_s (m/s)	G_{max} (kPa)	Ψ (º)	ν	k (cm/s)
0	0.4	OS											
0.4	4.5	CH	1.21	12.4	17.9	11	---	20	137	39	0	0.29275	10^{-7}
4.5	7	SC	0.97	13.3	18.2	21	39.2	---	221	68	9.2	0.313	10^{-3}
7	9	SM	0.8	14.4	18.8	16	34.2	---	184	68	4.2	0.238	10^{-3}
9	10	CL	0.8	15.1	19.5	9.8	---	16	123	55	0	0.27925	10^{-7}
10	10.5	SM	0.79	14.5	18.9	9.8	25.2	---	123	62	0	0.103	10^{-3}
10.5	11.5	SP	0.59	16.3	20	9.8	25.2	---	123	62	0	0.103	10^{-3}
11.5	14	LS	0.07	23.3	24	76.7	44.7	---	466	198	14.7	0.3955	0

Table 10.35. The output of approximating Borehole 36data by NovoSPT.

Depth1	Depth2	Soil type	Void Ratio	Dry Unit Weight	Saturated Unit Weight	Young's Modulus	Friction Angle	Undrained Shear Strength of Clay/Silt	Shear Wave Velocity	Shear Modulus	Dilatancy Angle	Poisson Ratio	Permeability
			e	γ_{dry}	γ_{Sat}	E_s (MPa)	φ (°)	S_u (kPa)	V_s (m/s)	G_{max} (kPa)	Ψ (°)	ν	k (cm/s)
0	0.5	OS											
0.5	8	CH	0.77	15.5	19.8	24.8	---	66.00	245.5	101.5	0	0.29275	10^{-3}
8	11	LS	0.07	23.3	24	76.7	44.7	---	466.00	198.00	14.7	0.3955	10^{-7}

Table 10.36. The output of approximating Borehole 37data by NovoSPT.

Depth1	Depth2	Soil type	Void Ratio	Dry Unit Weight	Saturated Unit Weight	Young's Modulus	Friction Angle	Undrained Shear Strength of Clay/Silt	Shear Wave Velocity	Shear Modulus	Dilatancy Angle	Poisson Ratio	Permeability
			e	γ_{dry}	γ_{Sat}	E_s (MPa)	φ (º)	S_u (kPa)	V_s (m/s)	G_{max} (kPa)	Ψ (º)	ν	k (cm/s)
0	0.3	OS											
0.3	3.5	CL	0.77	15.3	19.7	16	---	37	184	55	0	0.2995	10^{-7}
3.5	8.5	CH	0.79	15.3	19.7	27.6	---	75	262	84	0	0.31975	10^{-7}
8.5	11.5	ML	0.82	14.6	19.1	24.2	---	64	242	95	0	0.25675	10^{-4}
11.5	13.5	CH	0.95	14	18.9	11	---	20	137	70	0	0.313	10^{-7}
13.5	15.5	CL	0.84	14.8	19.3	22.3	---	57	230	108	0	0.27925	10^{-7}

Table 10.37. The output of approximating Borehole 38data by NovoSPT.

Depth1	Depth2	Soil type	Void Ratio	Dry Unit Weight	Saturated Unit Weight	Young's Modulus	Friction Angle	Undrained Shear Strength of Clay/Silt	Shear Wave Velocity	Shear Modulus	Dilatancy Angle	Poisson Ratio	Permeability
			e	γ_{dry}	γ_{Sat}	E_s (MPa)	φ (º)	S_u (kPa)	V_s (m/s)	G_{max} (kPa)	Ψ (º)	ν	k (cm/s)
0	0.3	OS											
0.3	5	CH	0.79	15.3	19.7	27.3	---	74	260	75	0	0.32875	10^{-7}
5	8.5	CL	0.78	15.2	19.6	21	---	53	221	78	0	0.31075	10^{-7}
8.5	15	CH	1.02	13.5	18.6	14.8	---	33	173	136.5	0	0.3445	10^{-7}

Table 10.38. The output of approximating Borehole 39data by NovoSPT.

Depth1	Depth2	Soil type	Void Ratio	Dry Unit Weight	Saturated Unit Weight	Young's Modulus	Friction Angle	Undrained Shear Strength of Clay/Silt	Shear Wave Velocity	Shear Modulus	Dilatancy Angle	Poisson Ratio	Permeability
			e	γ_{dry}	γ_{Sat}	E_s (MPa)	φ (°)	S_u (kPa)	V_s (m/s)	G_{max} (kPa)	Ψ (°)	ν	k (cm/s)
0	2.5	SP	1	13.4	18.4	49.8	45	---	368	85	15	0.4	10^{-3}
2.5	9.5	SM	1.07	13.1	18.3	26.7	35.65	---	232.5	72.5	5.65	0.25975	10^{-3}
9.5	15	CL	0.93	13.5	18.3	11	---	29.00	137	59	0	0.300445	10^{-7}

Table 10.39. The output of approximating Borehole 40data by NovoSPT.

Depth1	Depth2	Soil type	Void Ratio	Dry Unit Weight	Saturated Unit Weight	Young's Modulus	Friction Angle	Undrained Shear Strength of Clay/Silt	Shear Wave Velocity	Shear Modulus	Dilatancy Angle	Poisson Ratio	Permeability
			e	γ_{dry}	γ_{Sat}	E_s (MPa)	φ (º)	S_u (kPa)	V_s (m/s)	G_{max} (kPa)	Ψ (º)	ν	k (cm/s)
0	3	CL	0.77	15.2	19.5	7.3	---	8	87	32	0	0.2872938	10^{-7}
3	4.5	ML	1.07	13.1	18.3	11	---	20	137	19	0	0.2689	10^{-4}
4.5	12	CL	1.07	13	18.2	7.3	---	8	87	45	0	0.29185	10^{-7}

Table 10.40. The output of approximating Borehole 41data by NovoSPT.

Depth1	Depth2	Soil type	Void Ratio	Dry Unit Weight	Saturated Unit Weight	Young's Modulus	Friction Angle	Undrained Shear Strength of Clay/Silt	Shear Wave Velocity	Shear Modulus	Dilatancy Angle	Poisson Ratio	Permeability
			e	γ_{dry}	γ_{Sat}	E_s (MPa)	φ (º)	S_u (kPa)	V_s (m/s)	G_{max} (kPa)	Ψ (º)	ν	k (cm/s)
0	1	CL	0.67	16	20.1	10.7	---	10	185	161	0	0.31687	10^{-7}
1	3	CH	0.78	15	19.4	16.3	---	28	225	228	0	0.32686	10^{-7}
3	7.5	CL	0.93	14	18.8	13.1	---	18	224	195	0	0.288925	10^{-7}
7.5	8	ML	0.88	14.5	19.2	9.9	---	8	156	146	0	0.2584375	10^{-4}
8	8.5	CL	0.84	14.8	19.3	9.1	---	5	129	127	0	0.28366	10^{-7}
8.5	10.5	SM	1.07	13.4	18.5	18.7	33.4	---	270	248	3.4	0.226	10^{-3}
10.5	12	CL	0.87	14.5	19.2	10.7	---	10	163	161	0	0.2782825	10^{-7}

Table 10.41. The output of approximating Borehole 42data by NovoSPT.

Depth1	Depth2	Soil type	Void Ratio	Dry Unit Weight	Saturated Unit Weight	Young's Modulus	Friction Angle	Undrained Shear Strength of Clay/Silt	Shear Wave Velocity	Shear Modulus	Dilatancy Angle	Poisson Ratio	Permeability
			e	γ_{dry}	γ_{Sat}	E_s (MPa)	φ (°)	S_u (kPa)	V_s (m/s)	G_{max} (kPa)	Ψ (°)	ν	k (cm/s)
0	1	CL	0.77	15.1	19.5	9.8	---	16	123	37	0	0.3114925	10^{-7}
1	3	CH	0.93	14	18.8	13.6	---	29	162	61	0	0.335815	10^{-7}
3	6.5	CL	1.01	13.6	18.6	9.8	---	16	123	45	0	0.28537	10^{-7}
6.5	7	CL	0.63	16.8	20.7	8.6	---	12	106	44	0	0.264175	10^{-7}
7	8	ML	0.74	15.7	20	33.6	---	94	294	101	0	0.2572	10^{-4}
8	8.2	CL	0.65	16.4	20.3	16	---	37	184	76	0	0.29392	10^{-7}
8.2	10	CH	0.72	15.6	19.8	13.6	0	29	162	61	0	0.31993	10^{-7}

Table 10.42. The output of approximating Borehole 43data by NovoSPT.

Depth1	Depth2	Soil type	Void Ratio	Dry Unit Weight	Saturated Unit Weight	Young's Modulus	Friction Angle	Undrained Shear Strength of Clay/Silt	Shear Wave Velocity	Shear Modulus	Dilatancy Angle	Poisson Ratio	Permeability
			e	γ_{dry}	γ_{Sat}	E_s (MPa)	φ (º)	S_u (kPa)	(V_s) m/s	G_{max} (kPa)	Ψ (º)	ν	k (cm/s)
0	4	CH	0.87	14.4	19	17.3	---	41	246	62	0	0.32911	10^{-3}
4	6	CL	1.04	13.3	18.3	13.6	---	29	162	63	0	0.3016825	10^{-7}
6	14.5	CH	1.12	12.2	17.5	8.6	---	12	106	51	0	0.3228775	10^{-3}

Appendix D: Tables and Charts

Table 11.1.Calculated Settlement for Mat foundation, B=10m,D_f=0.5m .

Load (kPa)	Elastic	Consolidation in 30 days	Consolidation in 4 years	Consolidation in 10 years	Consolidation in 30 years	Consolidation in 50 years	Total in 30 days	Total in 4 years	Total in10 years	Total in 30 years	Total in50 years
10	8.1	0.24	1.59	2.24	3.11	3.38	8.34	9.69	10.34	11.21	11.48
20	11.81	0.36	2.36	3.37	4.67	5.11	12.17	14.17	15.18	16.48	16.92
30	16.08	0.6	3.87	5.21	7.38	8.22	16.68	19.95	21.29	23.46	24.3
40	21.27	0.97	6.93	9.82	14.55	16.58	22.24	28.2	31.09	35.82	37.85
50	32.95	3.75	14.97	20.33	28.71	31.43	36.7	47.92	53.28	61.66	64.38
60	61.39	10.66	32.01	40.3	56.19	53.08	72.05	93.4	101.6	117.5	114.47
69	247.32	45.23	112.29	128.14	157.9	151.37	292.5	359.6	375.4	405.2	398.69
80	Soil body collapses					Maximum of bearing capacity before collapses					69.6

Table 11.2.Calculated Settlement for Mat foundation, B=10m,D_f=1m .

Load (kPa)	Elastic	Consolidation in 30 days	Consolidation in 4 years	Consolidation in 10 years	Consolidation in 30 years	Consolidation in 50 years	Total in 30 days	Total in 4 years	Total in10 years	Total in 30year	Total in50 years
10	4.98	0.48	2.52	3.39	5.17	5.85	5.46	7.5	8.37	10.15	10.83
20	8.72	0.71	3.4	4.93	7.92	9.38	9.43	12.12	13.65	16.64	18.1
30	12.63	0.94	4.75	6.54	9.21	10.09	13.5	17.38	19.17	21.84	22.72
40	16.6	1.16	6.48	8.94	14.79	18.29	17.7	23.08	25.54	31.39	34.89
50	20.97	1.8	10.44	14.3	21.17	26.18	22.7	31.41	35.27	42.14	47.15
60	27.42	5.34	18	23.68	32.39	35.65	32.7	45.42	51.1	59.81	63.07
69	37.96	9.25	27.38	36.16	47.83	53.03	47.2	65.34	74.12	85.79	90.99
80	63.96	19.94	47.26	60.08	79.87	91.71	83.9	111.2	124.0	143.8	155.67
90	165.83	1244.17	1344.17	1374.17	1444.17	1494.17	1410	1510	1540	1610	1660
100	Soil body collapses					Maximum of bearing capacity before collapses					92

Table 11.3.Calculated Settlement for Mat foundation, B=10m,D_f=1.5m .

Load (kPa)	Elastic	Consolidation in 30 days	Consolidation in 4 years	Consolidation in 10 years	Consolidation in 30 years	Consolidation in 50 years	Total in 30 days	Total in 4 years	Total in10 years	Total in 30year	Total in50 years
	2.35	0.53	3.6	4.82	6.05	6.39	2.88	5.95	7.17	8.4	8.74
20	5.91	0.86	4.47	6.77	10.95	13.95	6.77	10.38	12.68	16.86	19.86
30	9.67	1.08	5.81	7.58	9.15	10.51	10.75	15.48	17.25	18.82	20.18
40	13.45	1.47	7.35	9.66	11.87	12.78	14.92	20.8	23.11	25.32	26.23
50	17.4	1.75	9.86	13.16	16.68	18.36	19.15	27.26	30.56	34.08	35.76
60	21.78	2.91	14.73	19.32	25.16	27.47	24.69	36.51	41.1	46.94	49.25
69	27.38	5.68	20.73	27.01	35.35	38.65	33.06	48.11	54.39	62.73	66.03
80	38.51	10.7	30.82	40.4	52.56	58.02	49.21	69.33	78.91	91.07	96.53
90	55.33	18.02	45.82	59.47	79.38	88.42	73.35	101.1	114.8	134.7	143.75
100	91.74	34.01	86.24	108.02	148.42	173.54	125.7	177.9	199.7	240.1	265.28
110	Soil body collapses					Maximum of bearing capacity before collapses					106.15

Table 11.4.Calculated Settlement for Mat foundation, B=10m,D_f=2m .

Load (kPa)	Elastic	Consolidation in 30 days	Consolidation in 4 years	Consolidation in 10 years	Consolidation in 30 years	Consolidation in 50 years	Total in 30 days	Total in 4 years	Total in10 years	Total in 30 years	Total in50 years
10	2.46	0.62	3.66	4.66	5.81	6.21	3.08	6.12	7.12	8.27	8.67
20	3.8	0.72	4.86	6.24	9.49	11.6	4.52	8.66	10.04	13.29	15.4
30	6.92	1.36	6.66	8.11	9.74	11.48	8.28	13.58	15.03	16.66	18.4
40	10.59	1.6	8.16	9.96	12.19	12.98	12.19	18.75	20.55	22.78	23.57
50	14.43	1.92	10.15	12.57	15.66	17.06	16.35	24.58	27	30.09	31.49
60	18.5	2.54	13.73	17.17	21.79	23.93	21.04	32.23	35.67	40.29	42.43
69	22.53	3.89	18.67	23.32	29.8	32.68	26.42	41.2	45.85	52.33	55.21
80	30.01	7.24	26.58	33.32	42.53	46.81	37.25	56.59	63.33	72.54	76.82
90	40.39	12.27	37.24	46.94	59.68	65.57	52.66	77.63	87.33	100.0	105.96
100	57.63	20.12	56.41	71.11	92.12	102.33	77.75	114.0	128.7	149.7	159.96
110	93.44	48.89	122.58	150.82	215.43	260.42	142.3	216.0	244.2	308.8	353.86
120	Soil body collapses						Maximum of bearing capacity before collapses				114

Table 11.5.Calculated Settlement for Mat foundation, B=14m,D_f=0.5m .

Load (kPa)	Elastic	Consolidation in 30 days	Consolidation in 4 years	Consolidation in 10 years	Consolidation in 30 years	Consolidation in 50 years	Total in 30 days	Total in 4 years	Total in10 years	Total in 30 years	Total in50 years
10	10.32	0.29	2.12	2.99	4.09	4.47	10.6	12.44	13.31	14.41	14.79
20	15.74	0.43	3.23	4.59	6.32	6.94	16.1	18.97	20.33	22.06	22.68
30	21.16	0.59	4.59	6.63	9.39	10.61	21.7	25.75	27.79	30.55	31.77
40	27.78	1.33	8.47	11.9	17.34	20.07	29.1	36.25	39.68	45.12	47.85
50	39.91	4.6	17.04	22.9	33.15	38.21	44.5	56.95	62.81	73.06	78.12
60	66.7	13.6	34.23	45.95	65.12	72.8	80.3	100.9	112.6	131.8	139.5
69	Soil body collapses						Maximum of bearing capacity before collapses				66.93

Table 11.6.Calculated Settlement for Mat foundation, B=14m,D_f=1m .

Load (kPa)	Elastic	Consolidation in 30 days	Consolidation in 4 years	Consolidation in 10 years	Consolidation in 30 years	Consolidation in 50 years	Total in 30 days	Total in 4 years	Total in10 years	Total in 30year	Total in50 years
10	6.43	0.54	3.32	4.44	6.34	7.76	6.97	9.75	10.87	12.77	14.19
20	11.7	0.72	4.61	6.22	8.22	9.91	12.42	16.31	17.92	19.92	21.61
30	16.98	0.88	5.99	8.2	12.18	14.6	17.86	22.97	25.18	29.16	31.58
40	22.4	1.16	8.14	11.41	19.17	23.68	23.56	30.54	33.81	41.57	46.08
50	29	2.25	13.1	17.87	26.79	33.79	31.25	42.1	46.87	55.79	62.79
60	39.04	5.16	21.03	28.47	39.52	43.69	44.2	60.07	67.51	78.56	82.73
69	54.09	9.86	31.48	42.69	58.58	64.87	63.95	85.57	96.78	112.6	118.96
80	100.17	31.2	74.45	112.38	190.4	234.82	131.3	174.6	212.5	290.5	334.99
90	Soil body collapses					Maximum of bearing capacity before collapses					82.8

Table 11.7.Calculated Settlement for Mat foundation, B=14m,D_f=1.5m .

Load (kPa)	Elastic	Consolidation in 30 days	Consolidation in 4 years	Consolidation in 10 years	Consolidation in 30 years	Consolidation in 50 years	Total in 30 days	Total in 4 years	Total in10 years	Total in 30year	Total in50 years
10	2.8	0.82	5.08	7.71	12.31	15.64	3.62	7.88	10.51	15.11	18.44
20	7.93	1.03	5.96	7.67	12.75	16.22	8.96	13.89	15.6	20.68	24.15
30	13.06	1.23	7.44	9.66	12.69	16.12	14.29	20.5	22.72	25.75	29.18
40	18.29	1.45	9.2	12.07	15.33	16.61	19.74	27.49	30.36	33.62	34.9
50	23.9	1.96	12.43	16.63	21.99	24.19	25.86	36.33	40.53	45.89	48.09
60	30.86	3.61	17.92	24.01	31.92	35.16	34.47	48.78	54.87	62.78	66.02
70	40.39	5.96	25.49	34.04	44.88	49.63	46.35	65.88	74.43	85.27	90.02
80	54.77	10.9	37.09	49.24	64.7	70.56	65.67	91.86	104.0	119.4	125.33
90	81.77	21.59	65.4	85.22	112.11	123.51	103.3	147.1	166.9	193.8	205.28
100	Soil body collapses						Maximum of bearing capacity before collapses				97

Table 11.8.Calculated Settlement for Mat foundation, B=14m,D_f=2m .

Load (kPa)	Elastic	Consolidation in 30 days	Consolidation in 4 years	Consolidation in 10 years	Consolidation in 30 years	Consolidation in 50 years	Total in 30 days	Total in 4 years	Total in10 years	Total in 30 years	Total in50 years
10	2.25	0.67	4.49	6.12	9.79	12.23	2.92	6.74	8.37	12.04	14.48
20	4.27	1.36	7.13	8.8	12.48	14.82	5.63	11.4	13.0	16.7	19.09
30	9.26	1.59	8.67	10.75	13.14	14.07	10.8	17.3	20.0	22.4	23.33
40	14.3	1.83	10.28	12.81	15.7	17	16.1	24.5	27.1	30	31.3
50	19.78	2.15	12.56	15.91	20.14	23.19	21.9	32.3	35.6	39.9	42.97
60	25.41	2.87	16.57	21.37	27.52	30.53	28.2	41.9	46.7	52.9	55.94
69	31.58	4.64	22.14	27.96	36.15	39.65	36.2	53.7	59.5	67.7	71.23
81	42.51	7.43	31.13	39.38	50.56	55.71	49.9	73.6	81.8	93.0	98.22
90	Soil body swelling										

Table 11.9.Calculated Settlement for Mat foundation, B=18m,D_f=0.5m .

Load (kPa)	Elastic	Consolidation in 30 days	Consolidation in 4 years	Consolidation in 10 years	Consolidation in 30 years	Consolidation in 50 years	Total in 30 days	Total in 4 years	Total in10 years	Total in 30 years	Total in50 years
10	12.44	0.46	3.08	4.27	5.74	6.25	12.9	15.52	16.71	18.1	18.69
20	18.93	0.7	4.64	6.43	8.66	9.52	19.6	23.57	25.36	27.5	28.45
30	25.46	0.99	6.56	9.16	12.74	14.36	26.4	32.02	34.62	38.2	39.82
40	33.62	2.37	10.94	14.99	21.11	24.32	35.9	44.56	48.61	54.73	57.94
50	45.61	5.46	19.58	26.05	36.86	41.66	51.0	65.19	71.66	82.4	87.27
60	69.3	12.6	34.77	45.52	60.3	68.52	81.9	104.0	114.8	129.	137.82
69	Soil body collapses					Maximum of bearing capacity before collapses					65.55

Table 11.10.Calculated Settlement for Mat foundation, B=18m,D_f=1m .

Load (kPa)	Elastic	Consolidation in 30 days	Consolidation in 4 years	Consolidation in 10 years	Consolidation in 30 years	Consolidation in 50 years	Total in 30 days	Total in 4 years	Total in10 years	Total in 30year	Total in50 years
10	7.64	0.8	4.5	5.91	7.46	7.97	8.44	12.1	13.55	15.1	15.61
20	14	1.07	6.23	8.25	10.46	11.2	15.07	20.2	22.25	24.46	25.2
30	20.36	1.34	7.93	10.58	13.72	14.69	21.7	28.2	30.94	34.08	35.05
40	27.13	1.82	10.61	14.36	20.33	25.32	28.95	37.7	41.49	47.46	52.45
50	35.16	2.94	15.89	21.34	29.79	36.62	38.1	51.0	56.5	64.95	71.78
60	46	6.06	24.03	32.35	44.35	49.14	52.06	70.0	78.35	90.35	95.14
69	60.31	9.66	34.84	46.83	63.96	70.86	69.97	95.1	107.1	124.2	131.17
80	99.39	37.5	1590.61	3950.61	11690.6	19130.6	136.8	1690	4050	11790	19230
90	Soil body collapses					Maximum of bearing capacity before collapses					81

Table 11.11.Calculated Settlement for Mat foundation, B=18m,D_f=1.5m .

Load (kPa)	Elastic	Consolidation in 30 days	Consolidation in 4 years	Consolidation in 10 years	Consolidation in 30 years	Consolidation in 50 years	Total in 30 days	Total in 4 years	Total in10 years	Total in 30year	Total in50 years
10	3.24	1.15	5.81	8.44	13.13	16.44	4.39	9.05	11.68	16.37	19.68
20	9.44	1.45	7.72	9.79	13.84	17.09	10.89	17.16	19.23	23.28	26.53
30	15.63	1.77	9.6	12.26	15.05	17.82	17.4	25.23	27.89	30.68	33.45
40	22.1	2.11	11.72	15.11	18.99	20.62	24.21	33.82	37.21	41.09	42.72
50	29.03	2.8	15.27	20.04	26.11	29.22	31.83	44.3	49.07	55.14	58.25
60	37.26	3.93	21.18	28.06	37.04	40.69	41.19	58.44	65.32	74.3	77.95
69	46.39	6.68	28.15	36.86	48.32	53.61	53.07	74.54	83.25	94.71	100
80	61.25	12	40.2	52.8	68.41	75.44	73.25	101.4	114.0	129.6	136.69
90	84.06	20.33	67.99	85.86	111.22	122.99	104.3	152.0	169.9	195.2	207.05
100	Soil body collapses					Maximum of bearing capacity before collapses					95

Table 11.12.Calculated Settlement for Mat foundation, B=18m,D_f=2m .

Load (kPa)	Elastic	Consolidation in 30 days	Consolidation in 4 years	Consolidation in 10 years	Consolidation in 30 years	Consolidation in 50 years	Total in 30 days	Total in 4 years	Total in10 years	Total in 30 years	Total in50 years
10	2.23	0.84	5.17	7.55	10.92	12.83	3.07	7.4	9.78	13.15	15.06
20	4.98	1.6	8.92	10.96	14.7	17.32	6.58	13.9	15.94	19.68	22.3
30	11.03	2.21	10.93	13.47	16.5	17.61	13.24	21.96	24.5	27.53	28.64
40	17.21	1.98	12.15	15.25	19.14	20.69	19.19	29.36	32.46	36.35	37.9
50	23.93	2.35	14.7	18.75	23.62	26.25	26.28	38.63	42.68	47.55	50.18
60	30.92	3	18.6	24.2	31.62	35.28	33.92	49.52	55.12	62.54	66.2
69	38.4	3.79	23.5	30.29	39.66	44.1	42.19	61.9	68.69	78.06	82.5
80	49.09	6.02	30.57	39.26	51.06	56.62	55.11	79.66	88.35	100.1	105.71
90	60.32	9.33	40.05	51.32	65.83	72.62	69.65	100.3	111.6	126.1	132.94
100	75.58	15.01	56.95	71.82	91.81	100.47	90.59	132.5	147.4	167.3	176.05
110	108.3	270.56	15041.7	37021.7	107232	116292	378.8	15150	37130	107340	116400
120	Soil body collapses					Maximum of bearing capacity before collapses					109.2

Table 11.13.Calculated Settlement for Mat foundation, B=22m,D_f=0.5m .

Load (kPa)	Elastic	Consolidation in 30 days	Consolidation in 4 years	Consolidation in 10 years	Consolidation in 30 years	Consolidation in 50 years	Total in 30 days	Total in 4 years	Total in10 years	Total in 30 years	Total in50 years
10	13.97	0.43	3.48	4.91	6.68	7.32	14.4	17.4	18.88	20.65	21.29
20	21.26	0.64	5.22	7.36	10.02	10.99	21.9	26.4	28.62	31.28	32.25
30	28.71	0.92	7.27	10.24	14.23	16.09	29.6	35.9	38.95	42.94	44.8
40	37.36	1.68	10.87	15.21	21.54	25.26	39.0	48.2	52.57	58.9	62.62
50	48.36	3.39	17.92	24.29	34.93	40.77	51.7	66.2	72.65	83.29	89.13
60	64.92	6.46	29.62	40.27	56.61	65.2	71.3	94.5	105.1	121.5	130.12
69	Soil body collapses					Maximum of bearing capacity before collapses					66.93

Table 11.14.Calculated Settlement for Mat foundation, B=22m,D_f=1m .

Load (kPa)	Elastic	Consolidation in 30 days	Consolidation in 4 years	Consolidation in 10 years	Consolidation in 30 years	Consolidation in 50 years	Total in 30 days	Total in 4 years	Total in10 years	Total in 30year	Total in50 years
10	8.73	0.68	4.86	6.54	8.4	9.05	9.41	13.59	15.27	17.13	17.78
20	15.85	0.92	6.8	9.2	11.87	12.8	16.77	22.65	25.05	27.72	28.65
30	22.98	1.17	8.67	11.8	15.35	16.77	24.15	31.65	34.78	38.33	39.75
40	30.74	1.6	11.51	15.7	21.03	24.61	32.34	42.25	46.44	51.77	55.35
50	39.44	2.83	15.88	21.88	31.19	35.63	42.27	55.32	61.32	70.63	75.07
60	50.29	4.04	22.53	30.69	43.76	49.71	54.33	72.82	80.98	94.05	100
69	61.7	7.17	31.02	42.51	59.27	66.27	68.87	92.72	104.2	120.9	127.97
80	83.5	22.92	66.26	86.64	119.15	140.22	106.4	149.7	170.1	202.6	223.72
90	Soil body collapses						Maximum of bearing capacity before collapses				83.7

Table 11.15.Calculated Settlement for Mat foundation, B=22m,D_f=1.5m .

Load (kPa)	Elastic	Consolidation in 30 days	Consolidation in 4 years	Consolidation in 10 years	Consolidation in 30 years	Consolidation in 50 years	Total in 30 days	Total in 4 years	Total in10 years	Total in 30year	Total in50 year
10	3.78	0.95	6.15	8.13	12.95	16.19	4.73	9.93	11.91	16.73	19.97
20	10.7	1.22	8.26	10.74	13.63	17.81	11.9	18.96	21.44	24.33	28.51
30	17.63	1.49	10.3	13.48	16.83	19.55	19.1	27.93	31.11	34.46	37.18
40	24.96	1.8	12.68	16.7	21.32	23.43	26.7	37.64	41.66	46.28	48.39
50	32.82	2.32	16.14	21.59	28.86	32.68	35.1	48.96	54.41	61.68	65.5
60	41.71	3.63	21.32	28.94	39.34	44.06	45.3	63.03	70.65	81.05	85.77
69	51.07	4.66	52.52	54.16	57.63	59.5	55.7	103.5	105.2	108.7	110.57
80	63.63	7.32	69.58	71.72	76.24	78.73	70.9	133.2	135.3	139.8	142.36
90	78.34	15.22	102.8	105.38	111.04	114.22	93.5	181.1	183.7	189.3	192.56
100	Soil body collapses					Maximum of bearing capacity before collapses					98

Table 11.16.Calculated Settlement for Mat foundation, B=22m,D_f=2m .

Load (kPa)	Elastic	Consolidation in 30 days	Consolidation in 4 years	Consolidation in 10 years	Consolidation in 30 years	Consolidation in 50 years	Total in 30 days	Total in 4 years	Total in10 years	Total in 30 years	Total in50 year
10	2.16	0.78	5.54	7.97	12.06	14.64	2.94	7.7	10.13	14.22	16.8
20	5.68	1.52	9.5	11.84	15.83	19.51	7.2	15.18	17.52	21.51	25.19
30	12.43	1.81	11.59	14.71	18.32	19.67	14.2	24.02	27.14	30.75	32.1
40	19.36	2.11	13.83	17.59	21.99	24	21.4	33.19	36.95	41.35	43.36
50	26.9	2.5	16.83	21.95	27.77	31.17	29.4	43.73	48.85	54.67	58.07
60	34.89	3.09	21.2	27.73	36.72	40.73	37.9	56.09	62.62	71.61	75.62
69	42.78	4.36	26	34.07	45.14	50.28	47.1	68.78	76.85	87.92	93.06
80	53.75	5.44	32.62	42.51	56.03	61.66	59.1	86.37	96.26	109.7	115.41
90	64	7.32	42.09	53.94	69.9	77.2	71.3	106.0	117.9	133.9	141.2
100	76.44	10.85	57.91	73.26	91.82	100.86	87.2	134.3	149.7	168.2	177.3
110	Soil body swelling										
120	Soil body collapses					Maximum of bearing capacity before collapses					110.4

Table 11.17.Calculated Settlement for Mat foundation, B=26m,D_f=0.5m .

Load (kPa)	Elastic	Consolidation in 30 days	Consolidation in 4 years	Consolidation in 10 years	Consolidation in 30 years	Consolidation in 50 years	Total in 30 days	Total in 4 years	Total in10 years	Total in 30 years	Total in50 years
10	15.29	0.49	4.12	5.84	7.99	8.79	15.78	19.4	21.1	23.28	24.08
20	23.07	0.74	6.19	8.75	11.95	13.14	23.81	29.2	31.8	35.02	36.21
30	31.14	1.04	8.6	12.1	16.67	18.78	32.18	39.7	43.2	47.81	49.92
40	40.08	1.69	12.05	16.79	23.9	28.2	41.77	52.1	56.8	63.98	68.28
50	50.49	2.74	17.25	24.27	35.68	41.97	53.23	67.7	74.7	86.17	92.46
60	62.23	4.69	25.93	35.68	52.49	60.35	66.92	88.1	97.9	114.7	122.58
69	95.47	42.39	2264.53	5704.53	17104.5	28474.5	137.8	2360	5800	17200	28570
80	Soil body collapses					Maximum of bearing capacity before collapses					69.6

Table 11.18.Calculated Settlement for Mat foundation, B=26m,D_f=1m .

Load (kPa)	Elastic	Consolidation in 30 days	Consolidation in 4 years	Consolidation in 10 years	Consolidation in 30 years	Consolidation in 50 years	Total in 30 days	Total in 4 years	Total in10 years	Total in 30year	Total in50 years
10	9.29	0.71	5.38	7.31	9.6	10.32	10	14.67	16.6	18.89	19.61
20	16.87	0.98	7.61	10.42	13.55	14.68	17.8	24.48	27.29	30.42	31.55
30	24.47	1.24	9.81	13.48	17.88	19.34	25.7	34.28	37.95	42.35	43.81
40	32.74	1.68	12.91	17.62	23.67	26.98	34.4	45.65	50.36	56.41	59.72
50	41.76	2.36	16.6	23.06	33.13	38.24	44.1	58.36	64.82	74.89	80
60	51.94	3.35	21.84	30.32	43.8	50.2	55.2	73.78	82.26	95.74	102.14
69	61.46	4.29	28.5	39.49	59.26	71.39	65.7	89.96	100.95	120.72	132.85
80	78.7	20.42	67.87	92.37	139.19	172.37	99.1	146.5	171.0	217.8	251.07
90	Soil body collapses						Maximum of bearing capacity before collapses				82.8

Table 11.19.Calculated Settlement for Mat foundation, B=26m,D_f=1.5m .

Load (kPa)	Elastic	Consolidation in 30 days	Consolidation in 4 years	Consolidation in 10 years	Consolidation in 30 years	Consolidation in 50 years	Total in 30 days	Total in 4 years	Total in10 years	Total in 30year	Total in50 years
10	4.01	0.94	6.64	8.69	13.18	16.07	4.95	10.65	12.7	17.19	20.08
20	11.39	1.23	9.04	12.01	14.98	16.37	12.6	20.43	23.4	26.37	27.76
30	18.78	1.52	11.38	15.04	19.17	20.58	20.3	30.16	33.82	37.95	39.36
40	26.55	1.86	14.1	18.75	24.17	27.06	28.4	40.65	45.3	50.72	53.61
50	34.99	2.31	17.67	23.8	32.29	36.68	37.3	52.66	58.79	67.28	71.67
60	44.04	2.98	21.94	30.48	42.24	47.52	47.0	65.98	74.52	86.28	91.56
69	52.87	3.9	26.98	37.02	50.86	57.16	56.7	79.85	89.89	103.7	110.03
80	63.66	4.96	35.49	48.42	66.23	73.93	68.6	99.15	112.0	129.8	137.59
90	75.86	10.78	54.03	72.71	96.01	105.23	86.6	129.8	148.5	171.8	181.09
100	Soil body collapses						Maximum of bearing capacity before collapses				97

Table 11.20.Calculated Settlement for Mat foundation, B=26m,D_f=2m .

Load (kPa)	Elastic	Consolidation in 30 days	Consolidation in 4 years	Consolidation in 10 years	Consolidation in 30 years	Consolidation in 50 years	Total in 30 days	Total in 4 years	Total in10 years	Total in 30 years	Total in50 years
10	2.33	0.62	5.9	9.05	12.71	14.82	2.95	8.23	11.38	15.04	17.15
20	6.02	1.47	10.17	13.09	16.37	18.62	7.49	16.19	19.11	22.39	24.64
30	13.22	1.79	12.59	16.24	20.47	22.13	15.01	25.81	29.46	33.69	35.35
40	20.53	2.12	15.13	19.62	24.84	27.48	22.65	35.66	40.15	45.37	48.01
50	28.57	2.49	18.47	24.23	31.8	35.63	31.06	47.04	52.8	60.37	64.2
60	37.13	3	22.72	30.4	41.04	46.13	40.13	59.85	67.53	78.17	83.26
69	45.2	3.58	27	36.35	49.25	55.21	48.78	72.2	81.55	94.45	100.41
80	55.76	4.6	33.29	44.64	59.99	66.42	60.36	89.05	100.4	115.7	122.18
90	65.35	5.73	41.73	55.57	72.79	80.69	71.08	107.0	120.9	138.1	146.04
100	77.08	7.35	53.73	70.04	90.28	99.24	84.43	130.8	147.1	167.6	176.32
110	96.47	29.76	117.96	138.1	190.78	227.83	126.2	214.4	234.5	287.2	324.3
120	Soil body collapses					Maximum of bearing capacity before collapses					111.6

Table 11.21.Calculated Settlement for Mat foundation, B=26m,D_f=2m .

Load (kPa)	Elastic	Consolidation in 30 days	Consolidation in 4 years	Consolidation in 10 years	Consolidation in 30 years	Consolidation in 50 years	Total in 30 days	Total in 4 years	Total in10 years	Total in 30 years	Total in50 years
10	2.33	0.62	5.9	9.05	12.71	14.82	2.95	8.23	11.38	15.04	17.15
20	6.02	1.47	10.17	13.09	16.37	18.62	7.49	16.19	19.11	22.39	24.64
30	13.22	1.79	12.59	16.24	20.47	22.13	15.01	25.81	29.46	33.69	35.35
40	20.53	2.12	15.13	19.62	24.84	27.48	22.65	35.66	40.15	45.37	48.01
50	28.57	2.49	18.47	24.23	31.8	35.63	31.06	47.04	52.8	60.37	64.2
60	37.13	3	22.72	30.4	41.04	46.13	40.13	59.85	67.53	78.17	83.26
69	45.2	3.58	27	36.35	49.25	55.21	48.78	72.2	81.55	94.45	100.41
80	55.76	4.6	33.29	44.64	59.99	66.42	60.36	89.05	100.4	115.7	122.18
90	65.35	5.73	41.73	55.57	72.79	80.69	71.08	107.0	120.9	138.1	146.04
100	77.08	7.35	53.73	70.04	90.28	99.24	84.43	130.8	147.1	167.6	176.32
110	96.47	29.76	117.96	138.1	190.78	227.83	126.2	214.4	234.5	287.2	324.3
120	Soil body collapses					Maximum of bearing capacity before collapses					111.6

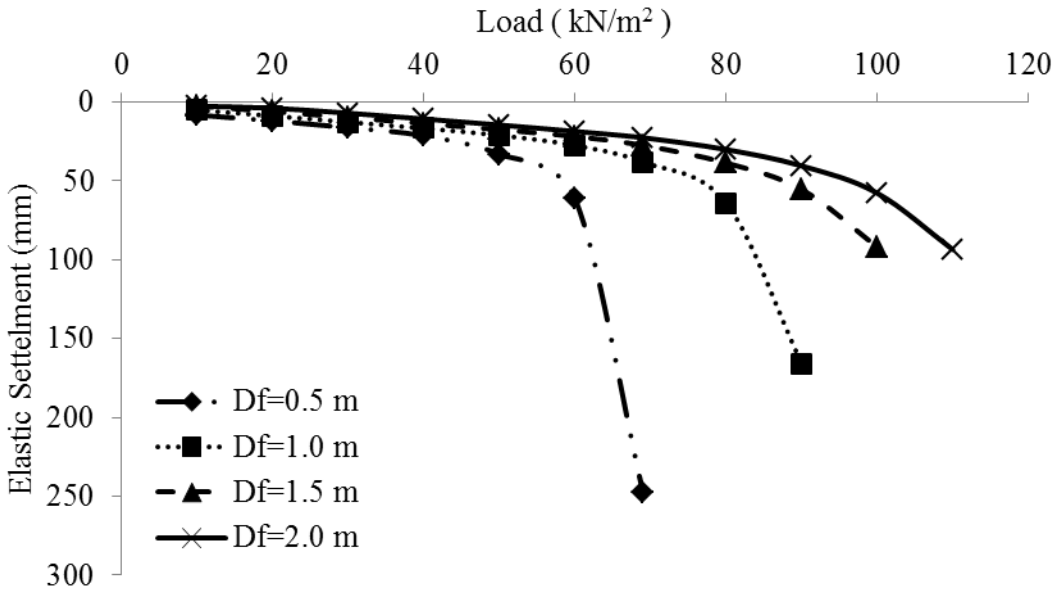

Figure 11.1.Elastic Settlement Curve for 10 m footing width.

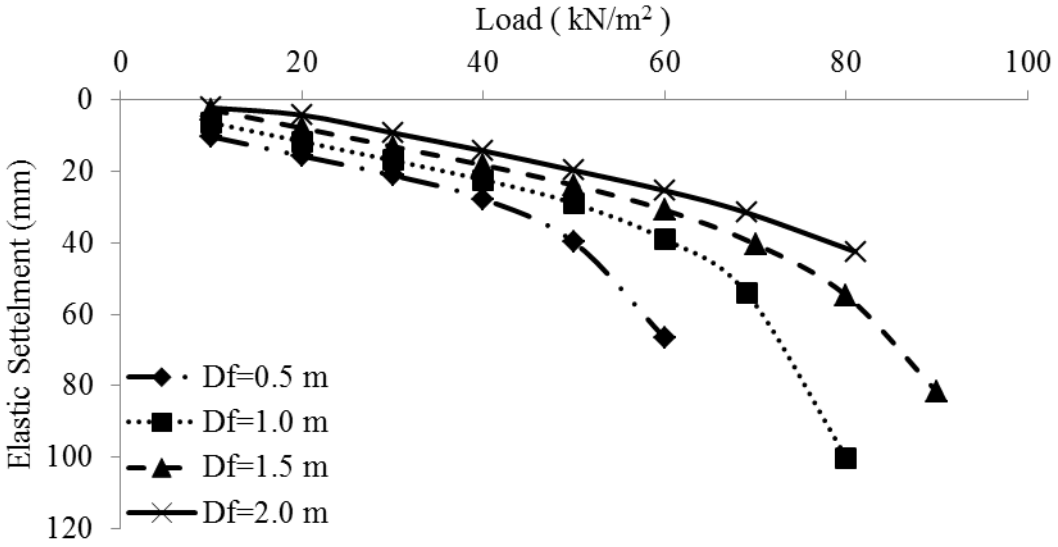

Figure 11.2.Elastic Settlement Curve for 14 m footing width.

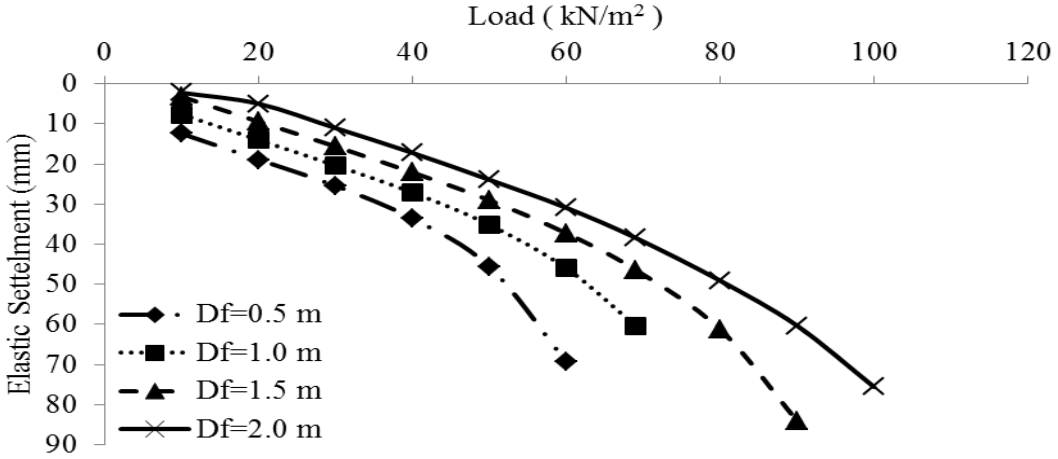

Figure 11.3.Elastic Settlement Curve for 18 m footing width.

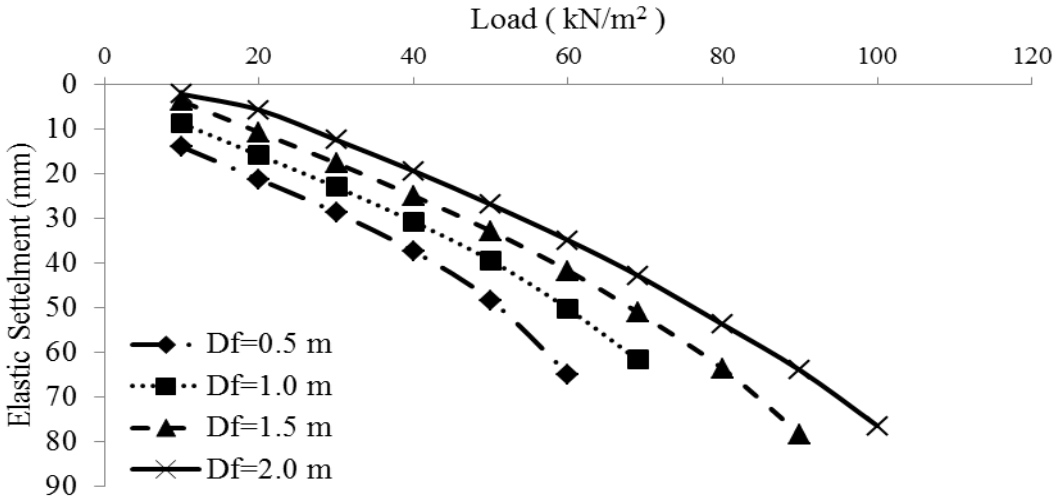

Figure 11.4.Elastic Settlement Curve for 22 m footing width.

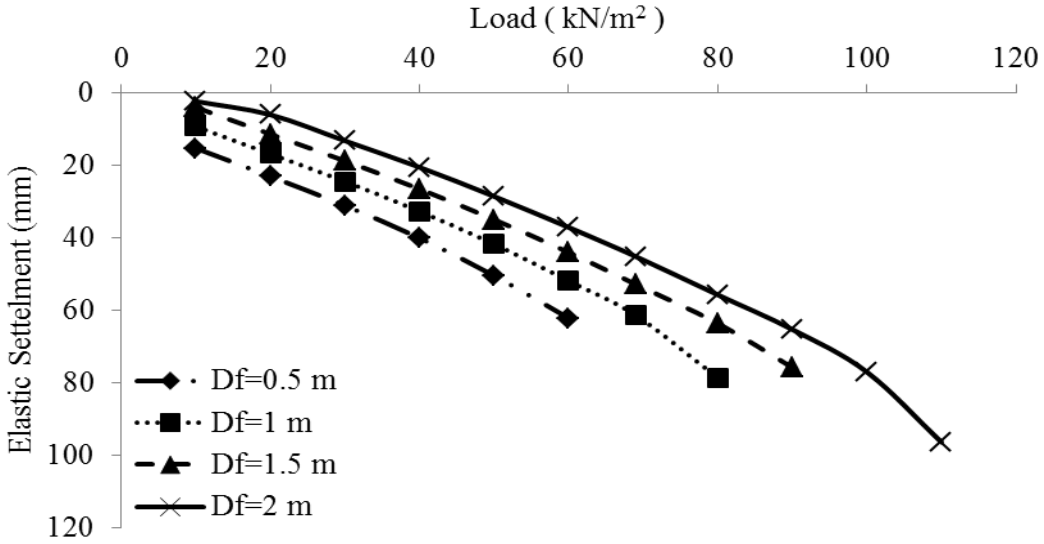

Figure 11.5.Elastic Settlement Curve for 26 m footing width.

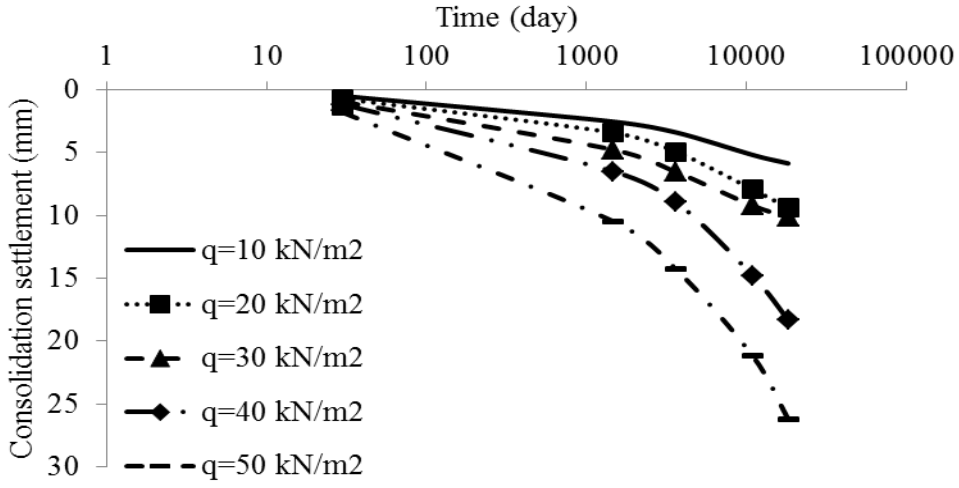

Figure 11.6.Consolidation Settlement Curve for 10 m footing width in 1 m depth.

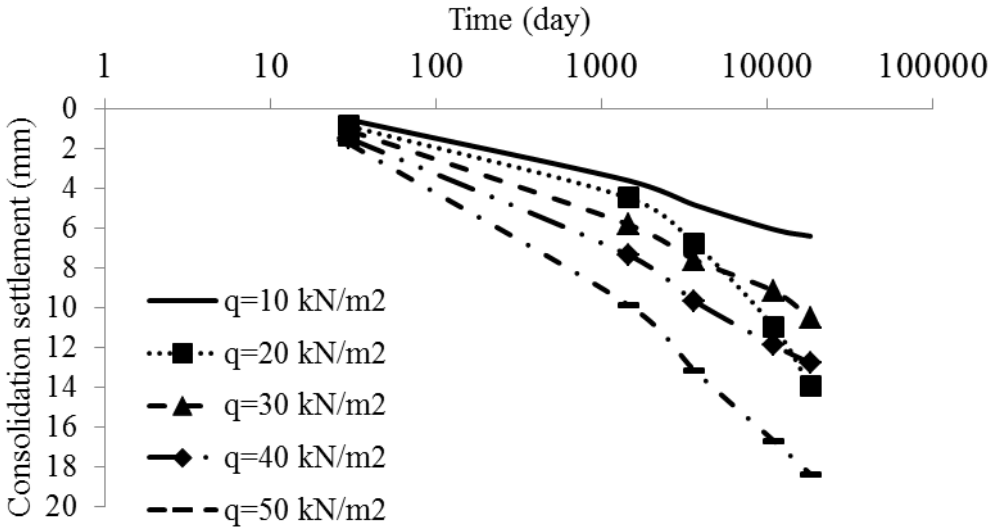

Figure 11.7.Consolidation Settlement Curve for 10 m footing width in 1.5 m depth.

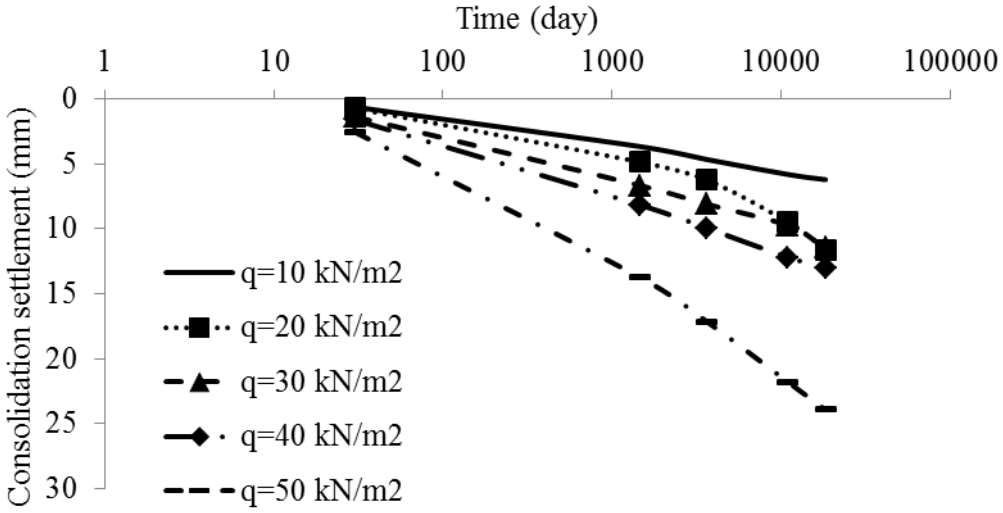

Figure 11.8.Consolidation Settlement Curve for 10 m footing width in 2 m depth.

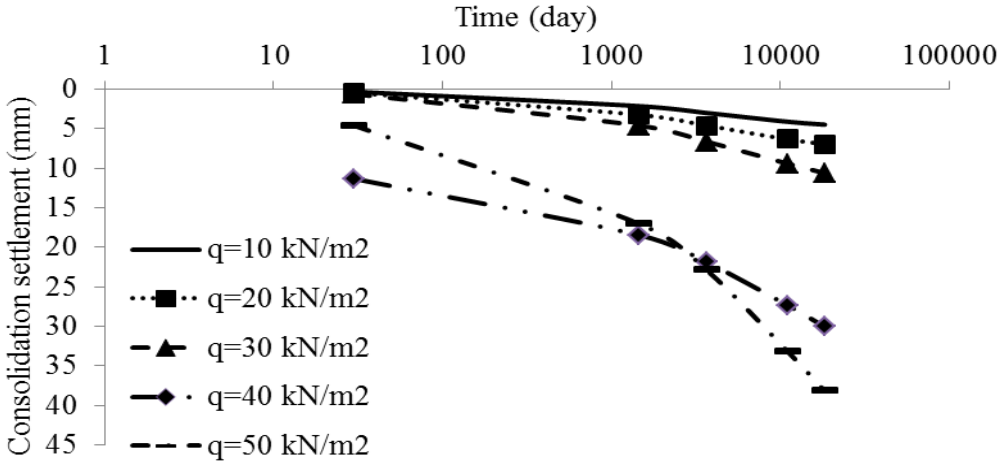

Figure 11.9.Consolidation Settlement Curve for 14 m footing width in 0.5 m depth.

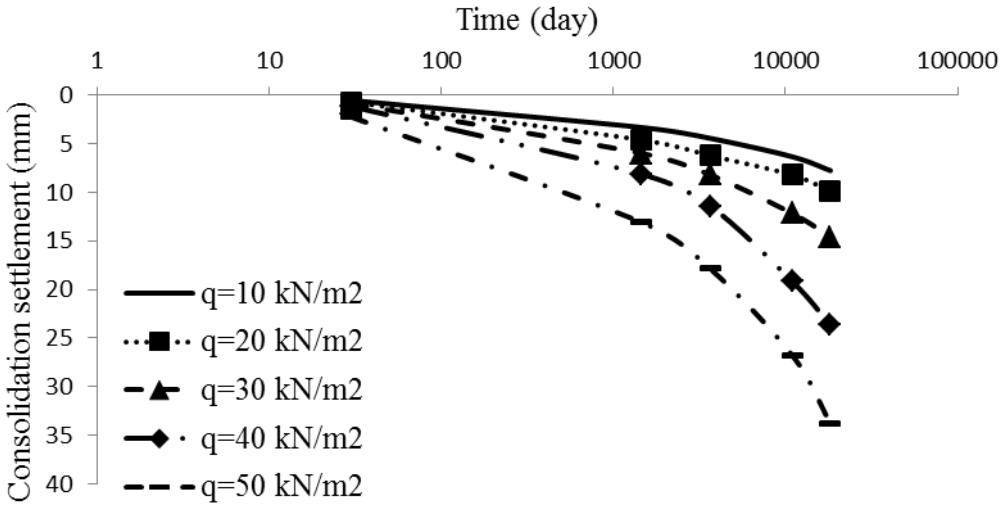

Figure 11.10.Consolidation Settlement Curve for 14 m footing width in 1 m depth.

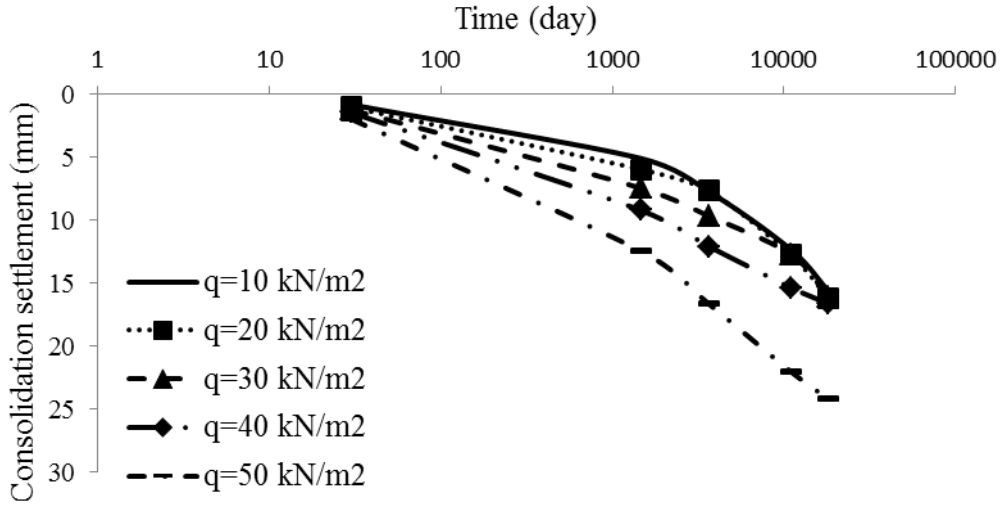

Figure 11.11.Consolidation Settlement Curve for 14 m footing width in 1.5 m depth.

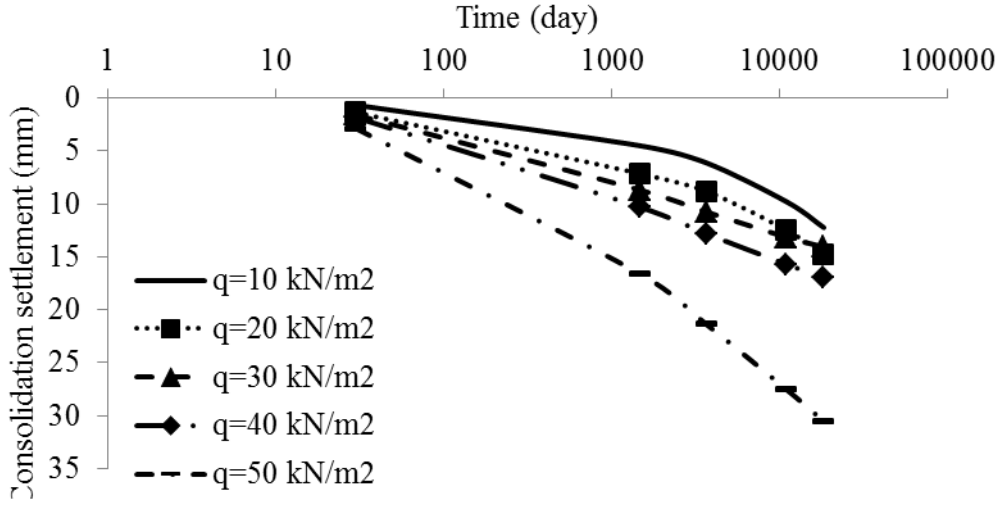

Figure 11.12.Consolidation Settlement Curve for 14 m footing width in 2 m depth.

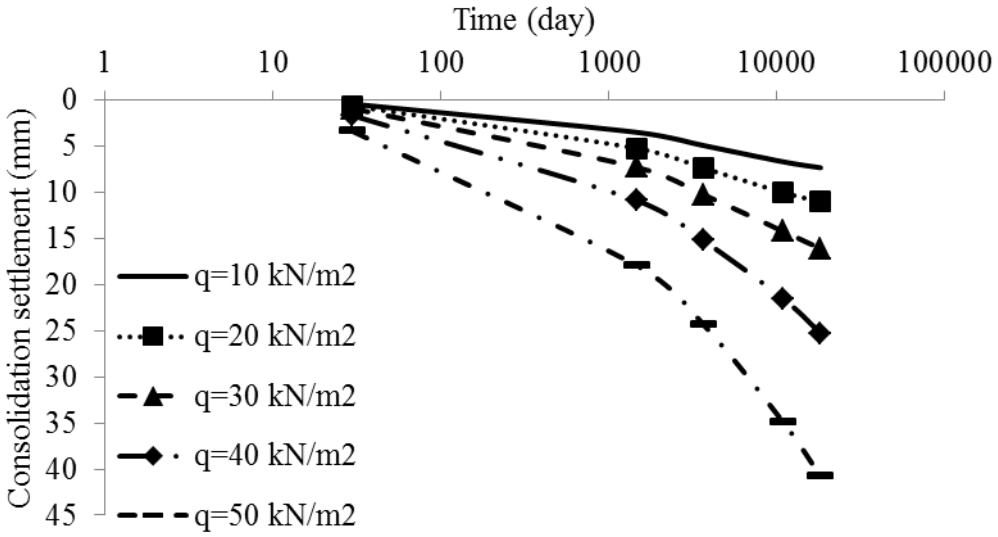

Figure 11.13.Consolidation Settlement Curve for 18m footing width in 0.5 m depth.

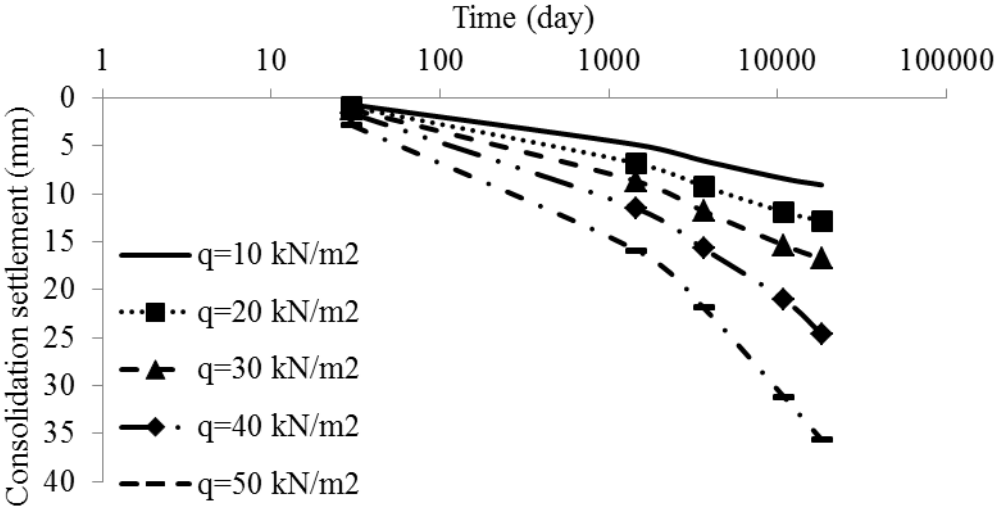

Figure 11.14.Consolidation Settlement Curve for 18m footing width in 1 m depth

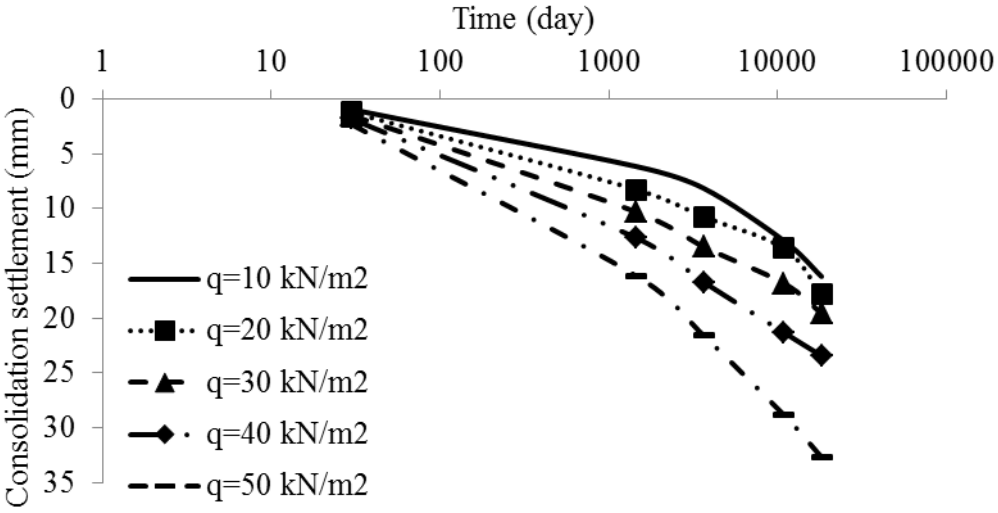

Figure 11.15.Consolidation Settlement Curve for 18m footing width in 1.5 m depth

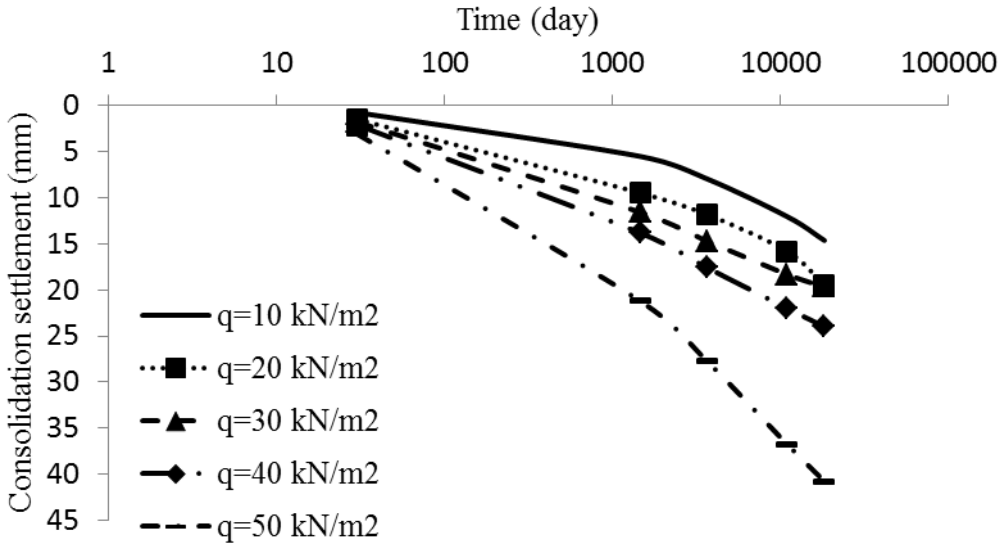

Figure 11.16.Consolidation Settlement Curve for 18m footing width in 2 m depth.

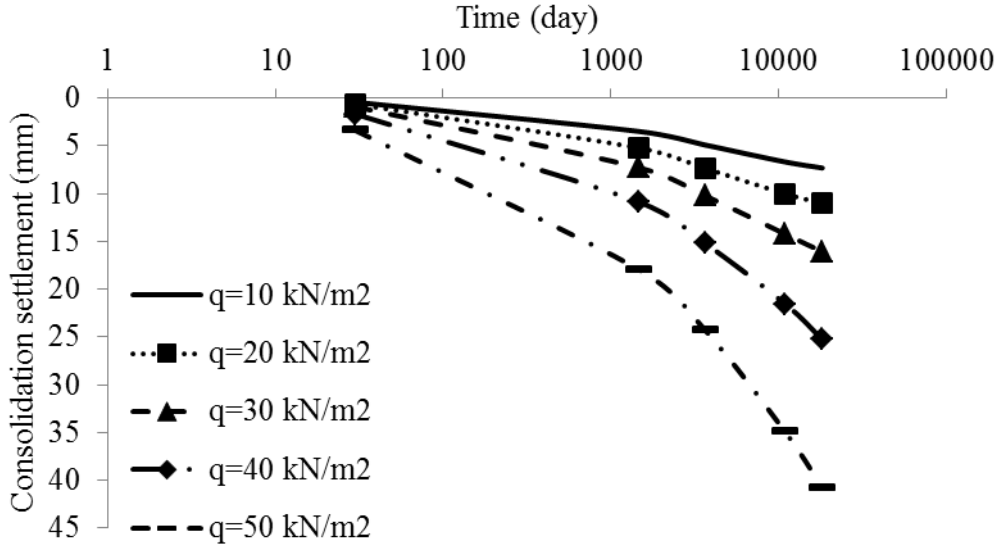

Figure 11.17.Consolidation Settlement Curve for 22 m footing width in 0.5 m depth

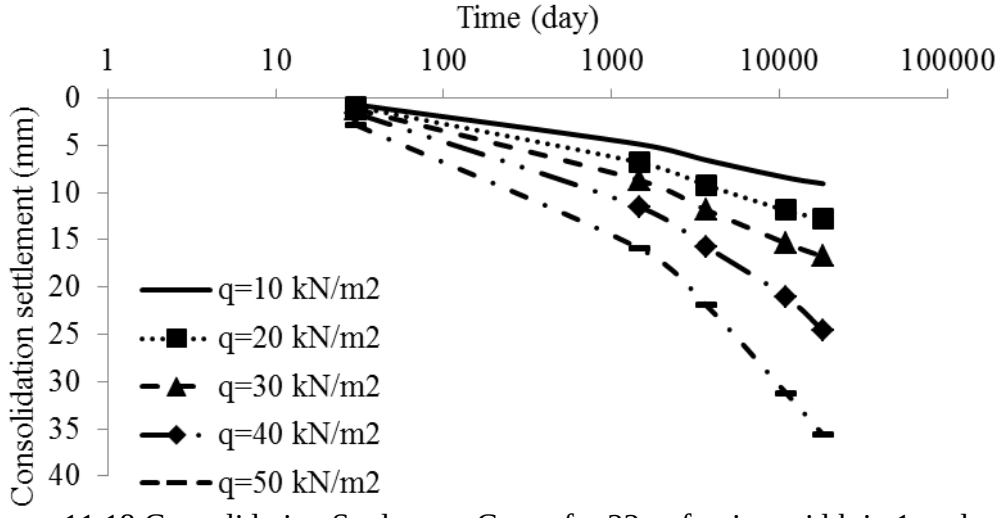

Figure 11.18.Consolidation Settlement Curve for 22 m footing width in 1 m depth

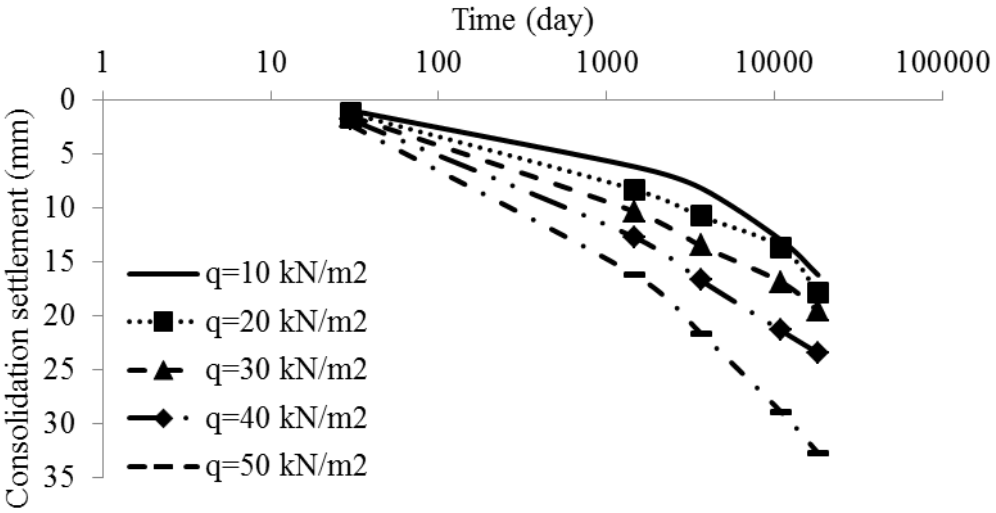

Figure 11.19.Consolidation Settlement Curve for 22 m footing width in 1.5 m depth

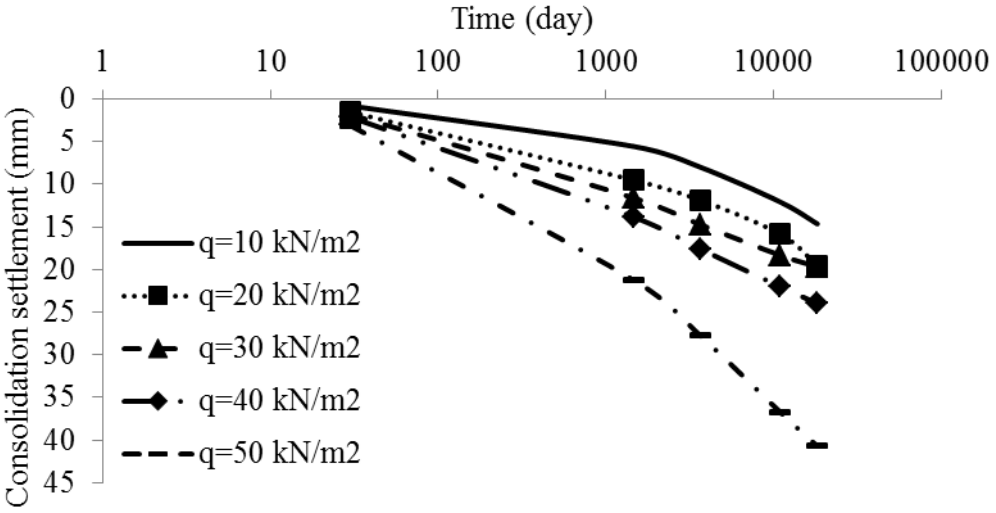

Figure 11.20.Consolidation Settlement Curve for 22 m footing width in 2 m depth

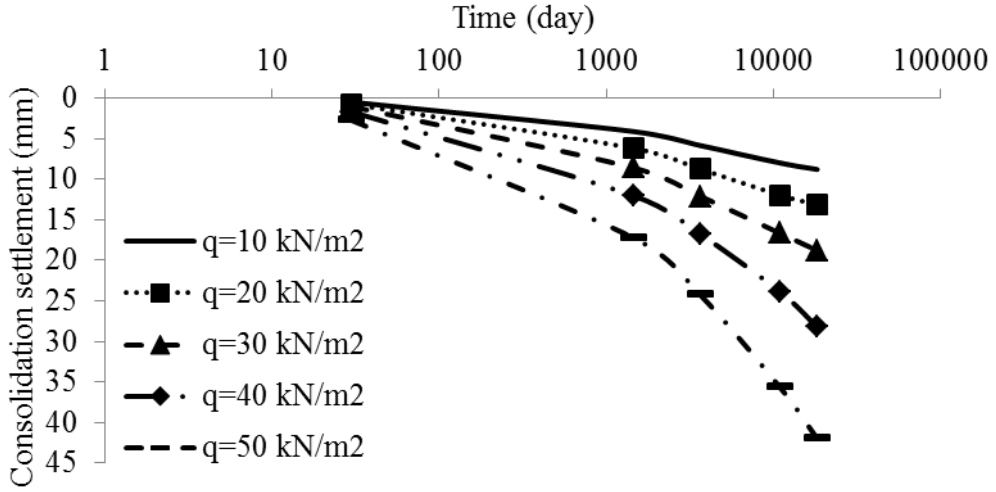

Figure 11.21.Consolidation Settlement Curve for 26 m footing width in 0.5 m depth

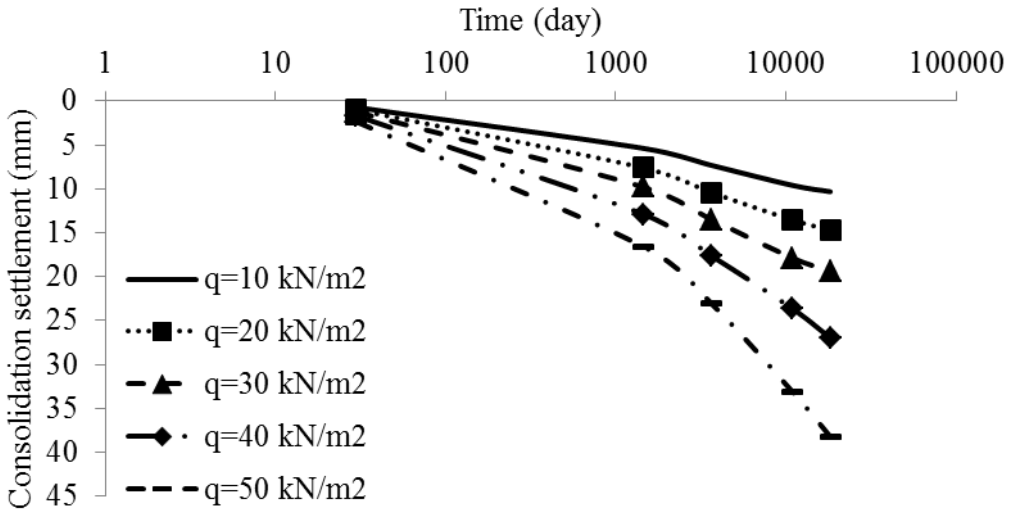

Figure 11.22.Consolidation Settlement Curve for 26 m footing width in 1 m depth

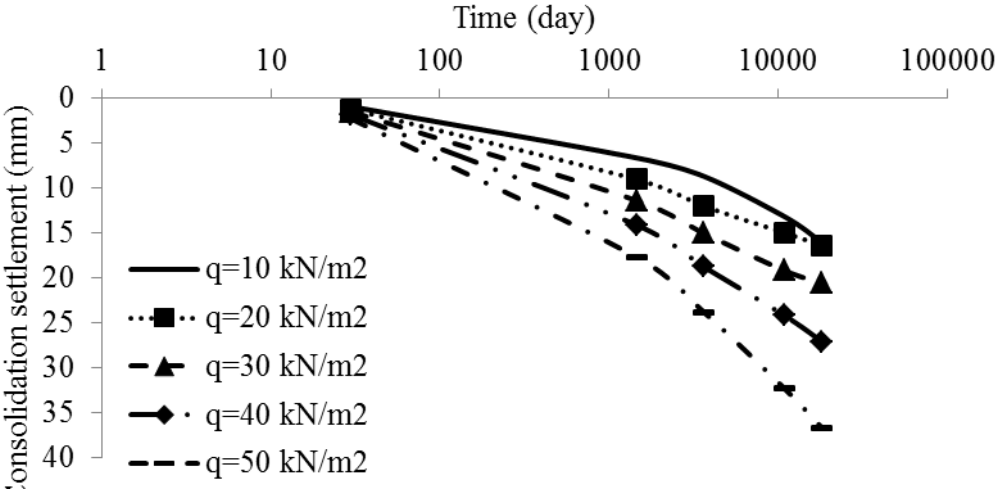

Figure 11.23.Consolidation Settlement Curve for 26 m footing width in 1.5 m depth

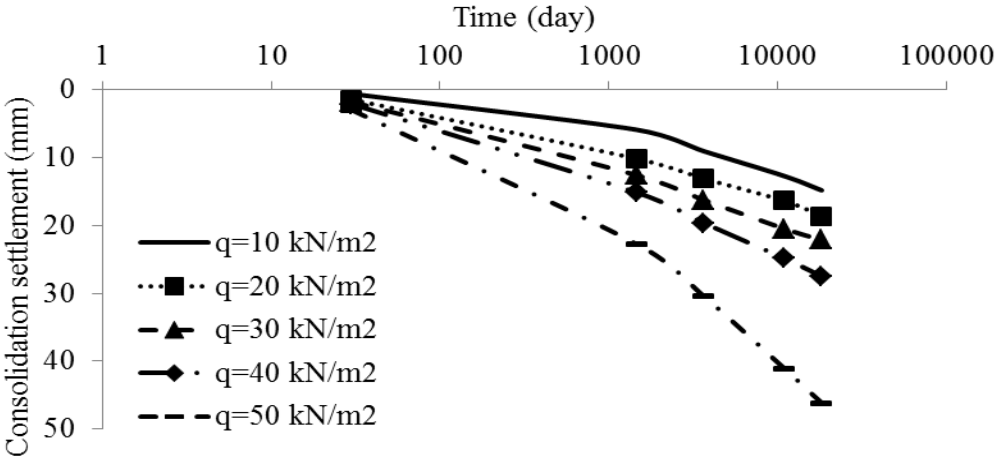

Figure 11.24.Consolidation Settlement Curve for 26 m footing width in 2 m depth